MUSCLE FORCE ESTIMATION IN CLINICAL GAIT ANALYSIS

Ursula Kathinka Trinler

Ph.D. Thesis

2016

MUSCLE FORCE ESTIMATION IN CLINICAL GAIT ANALYSIS

Ursula Kathinka Trinler

School of Health Science

University of Salford, Salford, UK

2016

Submitted in Partial Fulfilment of the Requirements of the Degree of Doctor of Philosophy, March 2016.

Table of Contents

List of Figures

List of Tables

List of Equations

Conferences and Workshops

The work was presented and discussed on following conferences and workshops:

- OpenSim workshop in Leuven, Belgium (January 2015).
- GCMAS conference in Portland, Oregon, USA (poster presentation, March 2015).
- Advanced OpenSim workshop at the University of Stanford, California, USA (March 2015).
- ISPGR conference in Seville, Spain (oral presentation, June 2015).

Acknowledgements

Firstly, I would like to express my sincere gratitude to my three supervisors Richard Baker, Kristen Hollands, and Richard Jones for their excellent support of my PhD study and related research, for their patience, their motivation, and immense knowledge they shared with me. Richard Baker, it was an honour to work with you and to be able to enter the world of mathematical modelling. One of the many highlights was the OpenSim workshop at the Stanford University where we tried to understand the secrets of OpenSim. Kristen Hollands, thank you so much for your professional support. Also, your office was always open for my worrying thoughts and fears which looked much smaller when I left your office after. Richard Jones, thank you for the support in the laboratory and the helpful comments you could give while keeping a neutral view on things. I would also like to acknowledge the contribution of the University of Salford, which provided the funding to support the project and the helpful staff at the University. Thank you Steven Horton, Laura Smith, Bernard Hoakes, and Rachel Shuttleworth for your excellent support.

Without the help of my dear friends at University, the time of the PhD would have not been the same. A big thank you goes to Carina Price and Robert Weinert-Aplin who proof-read parts of my thesis (chapter V and chapter III+IV) and for their insightful comments and discussions we had related to my work. Carina, thank you for your friendship, for giving me a roof over my head, feeding me through hard times, and just being there for me when I needed help. And then, indeed, the rest of the crew, especially Ana, Farina, and Dan, the last few month would have been really hard without you. Ponsuree, in October 2012 we started together our PhD and I am glad I had such a good friend throughout the last years, thank you for your support. Mike, thank you for being the best office mate and Matlab support.

A big thank you goes to my family and Nico. Thank you Mutti und Vati for giving me all the chances in life to be able to go to the UK and do this PhD. Thank you my Sissies for your support and your patience to cope with your sister and all her problems throughout the time in the UK. And last but not least, Nico mon coeur, thank you so much for being constantly here for me. Thank you for your amazing professional and emotional support, to cope with my craziness and to bring me down to earth when things did not look that promising anymore. You are the best thing which has happened to me here in the UK.

Declaration

I declare that this PhD thesis has been composed by myself and embodies the results of my own course of study and research whilst studying at The University of Salford from October 2012 to February 2016. All sources and material have been acknowledged.

Abstract

Neuro-musculoskeletal impairments are a substantial burden on our health care system as a consequence of disease, injury or aging. A better understanding of how such impairments influence the skeletal system through muscle force production is needed. Clinical gait analysis lacks in a sufficient estimation of individual muscle forces. To date, joint moments and EMG measurements are used to deduce on the characteristics of muscle forces, however, known limitations restrain a satisfying analysis of muscle force production. Recent developed musculoskeletal models make it possible to estimate individual muscle forces using experimental kinematic and kinetic data as input, however, are not yet implemented into a clinical gait analysis due to a wide range of different methods and models and a lack of standardised protocols which could be easily applied by clinicians in a routine processing.

This PhD thesis assessed the state of the art of mathematical modelling which enables the estimation of muscle force production during walking. This led into devising a standardised protocol which could be used to incorporate muscle force estimation into routine clinical practice. Especially the input of clinical science knowledge led to an improvement of the protocol. Static optimisation and computed muscle control, two mathematical models to estimate muscle forces, have been found to be the most suitable models for clinical purposes. OpenSim, a free available simulation tool, has been chosen as its musculoskeletal models have been already frequently used and tested. Furthermore, OpenSim provides a straight forward pipeline called SimTrack including both mathematical models. Minor and major adjustments were needed to adapt the standard pipeline for the purposes of a clinical gait analysis to be able to create a standardised protocol for gait analyses.

The developed protocol was tested on ten healthy participants walking at five different walking speeds and captured by a standard motion capture system. Muscle forces were estimated and compared to surface EMG measurements regarding activation and shape as well as their dependence on walking speed. The results showed a general agreement between static optimisation, computed muscle control

and the EMG excitations. Compared to the literature, these results show a good consistency between the modelling methods and surface EMG. However, some differences were shown between mathematical models and between models and EMG, especially fast walking speeds.

Additionally, high estimated activation peaks and uncertainties within the estimation process point out that more research needs to be undertaken to understand the mechanisms of mathematical models and the influence of different modelling parameters better (e.g. characteristics of muscle-tendon units, uncertainties of dynamic inconsistency). In conclusion, muscle force estimation with mathematical models is not yet robust enough to be able to include the protocol into a clinical gait analysis routine. It is, however, on a good way, especially slow walking speeds showed reasonable good results. Understanding the limitations and influencing factors of these models, however, may make this possible. Further steps may be the inclusion of patients to see the influence of health conditions.

CHAPTER I

1 Overview

1.1 Introduction

Human walking is driven by the muscle forces we produce. The activation of our muscular system can lead to a movement of the passive skeletal structures by achieving an imbalance of forces on the body segments (Erdemir, McLean, Herzog, & van den Bogert, 2007) and thus an acceleration of the body. This ability enables us to travel from one place to another, to manage our daily activities, and is essential for an acceptable quality of life. The development of muscle force is a complex process (Basmajian & De Luca, 1985): starting from the neuronal signal which is sent by the nervous system to the muscle fibres, leading to the mechanical output and the movement of a segment, and ending with feedback sensory signals back to the nervous system. We learn at young age to automatically use this process without the need of active interfering, the ability to walk becomes an easy task by learning and repeating the same movement (Ivanenko, Dominici, & Lacquaniti, 2007). However, if this system is disturbed at any stage of the process and the musculoskeletal system is affected, this simple task of walking can become a daily challenge.

Neuro-musculoskeletal impairments are a substantial burden on our health care system (Woolf, Erwin, & March, 2012) as a consequence of disease, injury or aging. A better understanding of how such impairments influence the musculoskeletal system is needed. Knowing the force profiles of individual muscles during walking can help to identify various musculoskeletal impairments (orthopaedic restrictions, dysfunction of the nervous system) and can give a better understanding about the underlying mechanisms and the impact of these impairments on the musculoskeletal system. Impairments like cerebral palsy or knee arthroplasty can lead for example to an overload of a joint by an imbalance of agonists to antagonists as well as spasticity of the muscles, or to a lack of joint loads through weak muscles. This can lead to secondary impairments in the bony structure and a weaken movement control, leading for example to falls in elderly people. To know the actual muscle forces helps to identify muscles responsible for such overloads or rigidness on specific joint and with the knowledge of physiological system changes by impairments and diseases, rehabilitations and treatments can be developed and

adapted which have the potential to improve the functional status of such patients and enhance their quality of life.

Insight into muscular-tendon unit function can, therefore, give crucial information about force production, tissue loading and neural control of movement, and thus help to develop an understanding how a movement is created. Existing measurements methods in the clinical gait analysis, however, lack in providing individual muscle force profiles. Modern optoelectronic measurement systems, force plates embedded in a walkway and surface electromyography can generate information about the muscle force processing during movement. Net forces and moments at specific joints can be calculated using an inverse dynamics approach by taking the segmental angular accelerations and ground reaction forces into account. Surface electromyography can additionally capture the muscular stimulation through the nerves by measuring the electrical impulse arriving at the muscle tissue. However, although both measurement techniques analyse parts of the excitation-contraction cycle of the muscle, these methods cannot account for the actual muscle activation and forces generated within individual muscles (Buchanan, Lloyd, Manal, & Besier, 2005).

Over about the last thirty years a range of computational techniques have been developed to estimate the forces produced by individual muscles for specific movements. More recently improvements in computing power and the increasing ability of specialist software have made these a practical proposition for clinical implementation. These mathematical models have already been applied in a variety of studies related to sport or for clinical interventions (Anderson & Pandy, 1999; A S Arnold, Anderson, Pandy, & Delp, 2005), however, are not yet established in a routine clinical gait analysis due to a wide range of different methods and models and a lack of a standardised protocol which could be easily applied by clinicians in a routine processing. Known limitations in the different models (sensitivity to musculoskeletal geometry, muscle-tendon complex, simplifications) and the various approaches make it difficult for the clinician to decide for the right model.

Numerous mathematical models and musculoskeletal models defining the characteristics of the bony segments and muscles-tendon complexes exists providing different approaches to the estimation of muscle forces (Anderson & Pandy, 1999, 2001b; Lin, Dorn, Schache, & Pandy, 2012). Different cost functions can be applied into the simulation to optimise the estimation by minimising a specific energetic factor (e.g. the sum of all muscle forces squared) and different experimental data (marker trajectories, ground reaction forces, or electromyography) are

frequently used as an input into these models to be able to estimate muscle forces which may alter the estimation's output. Few studies have been undertaken so far to analyse the sensitivity of the results to a range of input variables and parameters of the model, and a normative data pool for the estimation of muscle forces for specific simulation tools is still missing. Furthermore, it is not clear yet how valid these methods are for people with a range of different conditions and impairments.

This PhD thesis has been undertaken to test the possibility of incorporating a standardised protocol for the muscle activation and force estimation in clinical gait analysis. The main objectives of this work are therefore:

- To assess the state-of-the-art of mathematical modelling which enables the estimation of muscle force production during walking.
- To devise a standardised protocol which could be used to incorporate muscle force estimation into routine clinical practice.
- To analyse influences of some important input variables on the estimation's outcome such as the walking speed in comparison to surface EMG.
- To apply this protocol to generate normative reference data for a healthy adult population.
- To compare results with experimental measures of EMG activity in a range of muscles of the lower limb.

1.2 Thesis Outline

The thesis is structured in six main chapters. A thesis map which defines these chapters and their main purposes is presented in Figure 1.1. Chapter I introduces into the topic, whereas chapter II defines important background information. It includes the clinical significance of this work, the anatomical and physiological aspects of the muscle tissue, the equipment used in clinical gait analysis, the development of musculoskeletal modelling, and the description of the main mathematical models to estimate muscle activations and forces. This body of knowledge is summarised to define the goals and the scope of this thesis. The specific research question of this work is addressed at the end of chapter II.

Chapter III, the first study of this work, contains a systematic review which summarises scientific papers about the calculation of joint moments and the estimation of muscle forces in human healthy walking. Undertaking this systematic review helps to achieve the first two objectives of this work, to analyse the state-of-the-art of musculoskeletal modelling and to extract potential relevant and feasible methods for the incorporation into clinical movement analysis. The review is based on a systematic database search and a strict quality assessment scheme to identify relevant papers. These papers were restricted to those which included a graphical presentation of the joint moments or muscle forces, distributed throughout a stance phase or a whole gait cycle. By extracting these curves and digitising the patterns of joint moments and muscle forces the studies are directly compared. The agreement between studies is identified leading to a presentation of the consensus on joint moment and muscle force generation across the gait cycle during healthy adult walking.

After defining appropriate mathematical methods for the clinical gait analysis the technical background of models most suitable for the clinical gait analysis will be further presented and discussed in chapter IV. This chapter represents the second study, which includes the technical development of this work and presents a standardised protocol to estimate muscle forces. The simulation tool which has been chosen for the following experimental study will be described and areas in which further technical development was required to fully determine a clinical applicable protocol are identified.

This developed standardised protocol will be tested in study 3 (chapter V), where the muscle force estimation routine is included into a classical gait analysis. Ten healthy participants were therefore asked to walk on an instrumented walkway at five different walking speeds. The difference in speed is included as it is one of the influencing factors on the estimation's

outcome. Methods of the experimental setup as well as the validation of the estimations with surface electromyography are explained. The results of the muscle force estimations as well as the quality of the applied protocol are described and further discussed.

The last section of the thesis, chapter VI, summarises the findings of chapter III-V and gives an overall conclusion about the quality of the standardised protocol in the experimental study (study 3) and its outcomes. Finally, the novelty and original contributions of this work are stated and discussed and potential future work which could be further undertaken are defined.

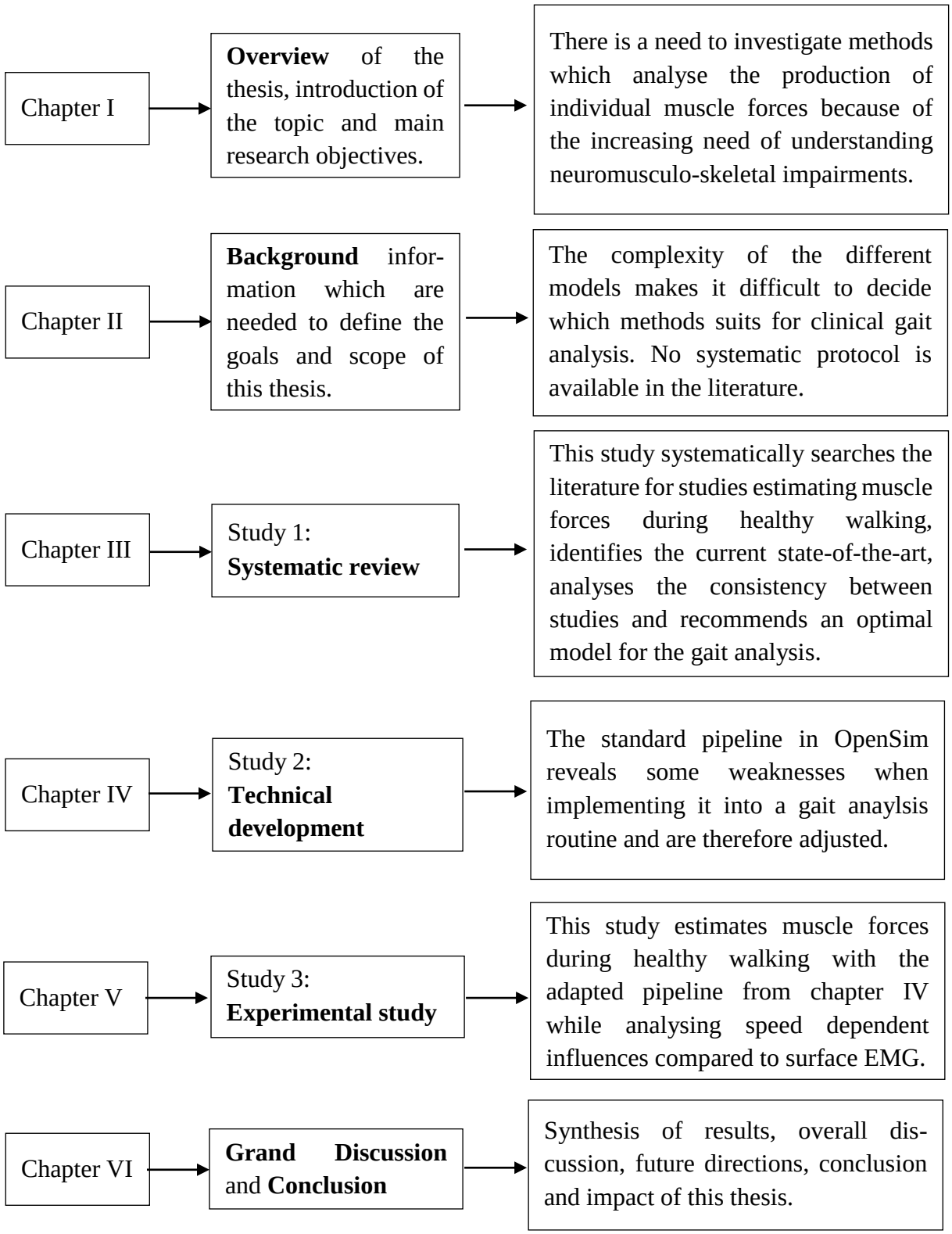

Figure 1.1. Thesis map of this work, structured in six main chapters.

CHAPTER II

2 Background Information and Main Objectives

To understand the clinical significance of muscle force analysis, it is necessary to understand the physiological principles behind muscle force generation and how measurements might be integrated into the clinical gait analysis process. This chapter gives an overview of the biological background, the limitations of different methods which have been used so far in clinical practice, and the role that new modelling techniques might have. Specific terminology which will be used throughout this work will be defined.

2.1 Clinical Significance of Musculoskeletal Analysis in Movement Science

Musculoskeletal pathologies are a growing burden on the public health care system (Woolf et al., 2012), leading to an increasing need of musculoskeletal analyses in clinical settings (Fraysse, Dumas, Cheze, & Wang, 2009). 30-35% of the population older than 60 years are estimated to suffer from gait disorders (Mahlknecht et al., 2013; Verghese et al., 2006). Sutherland (1978) explained the necessity of movement analysis to distinguish between primary abnormalities caused through the disease and compensatory gait patterns as well as the pre-/post-operative comparison to achieve objective and reliable assessments for operative treatments.

Pathologies leading to deformity of the legs and musculoskeletal disorders are of major interest (Perry & Burnfield, 2010). Fundamental work from Perry (2010), Sutherland (1978) and Gage (1994) pointed out the importance of clinical gait analysis in the field of cerebral palsy (Chris Kirtley, 2006). Elderly people (e.g. Judge, Ounpuu, & Davis, 1996; Prince, Corriveau, Hébert, & Winter, 1997) or people in need of a joint replacement at the hip or at the knee (Andriacchi, 1988) experience changes in the musculoskeletal system as well. Ensuring the longevity of implants is becoming increasingly important due to the advancing aging of the population and is dependent, in part, in understanding how the joint is exposed to load (Andriacchi, 1988). Classical gait analysis helps to analyse the functionality of these joints and, again, comparisons with pre-surgery data or those from a healthy age matched group can assist in this.

To enhance the functional outcomes of patients and therefore their quality of life it is crucial to analyse changes in the musculoskeletal system which are important for movement. The analysis of the muscles' behaviour during walking gives detailed information about the changes and adaptations in a patient's patterns which then helps to develop rehabilitation and treatments to achieve an improved functional status (Erdemir et al., 2007).

2.2 Functional Anatomy and Physiology of the Muscle Tissue

Muscles, the "active" part of the human system, have been described as one of the most challenging area of study in the field of biomechanics (Winter, 2009). The research of movement science is focused on the skeletal muscles which move the segments of the body. The morphology of a skeletal muscle is shown in Figure 2.1. The whole muscle is surrounded by a fascia, which holds the fascicles of a muscle together. These fascicles contain the muscle fibre cells, grouped together in form of bundles, and are surrounded by connective tissue sheath (perimysium) (Herzog, 1998). The muscle fibre cells are cylindrical with a diameter between 10 and 100µm (Lieber, 2010), embedded in the sarcolemma, and consist of myofibrils which are systematically ordered in parallel to each other. When looking through a microscope, these myofibrils show a striped pattern which represent the basic contractile unit called sarcomere (Herzog, 1998).

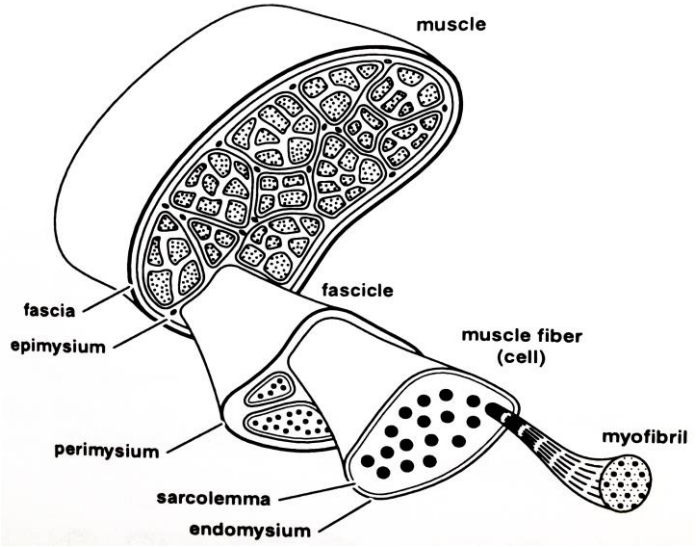

Figure 2.1. Illustration of a skeletal muscle with its sub-structures (Herzog, 1998).

The parallel ordered muscle fibres are attached and at both ends to an aponeurosis (the part of the tendon internal to the muscle) which builds up and is continuous with the external tendon (Figure 2.2). The muscle fibres are generally aligned at a specific angle to the tendon, which is called the pennation angle α. When the muscle fibres are activated, the tendons are moving along their axes while the muscle keeps its volume. As the muscle fibre shortens α generally increases by a small amount.

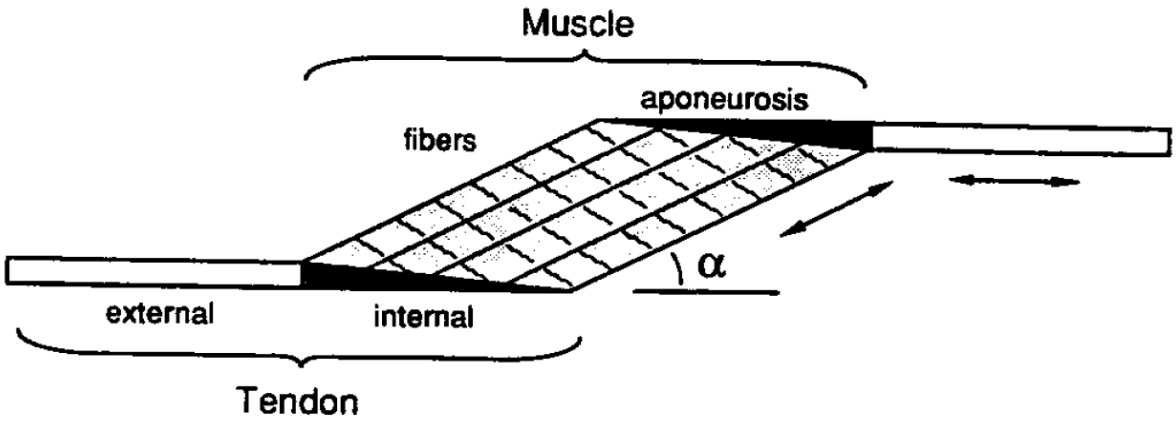

Figure 2.2. Muscle-tendon architecture and the relation of muscle fibres and attached tendons adapted from Zajac (1989). Angle α represents the pennation angle of the muscle fibres.

A muscle contracts if its fibres get excited by an action potential from a motor neuron causing an electromechanical stimuli (Herzog, 1998). Motor neurons have their origin in the spinal cord and terminate on a motor end plate on the muscle fibres (Figure 2.3) (Winter, 2009). Each motor neuron is connected to a number of muscle fibres which form a motor unit (Herzog, 1998; Winter, 2009). Dependent on the task of the muscle, these motor units contain a different number of muscle fibres: for fine control movements the motor neuron would only innervate a few muscle fibres, while for large powerful muscles and movements with less need of accuracy the number in muscle fibres is larger (MacIntosh, Gardiner, & MacComas, 2006).

The end of the motor neuron (presynaptic terminal) and the muscle fibre (postsynaptic membrane) form the neuromuscular junction (Herzog, 1998). When an action potential of a motor neuron reaches the synapse a chemical reaction is triggered and sodium ions enter the postsynaptic cell membrane. This causes an overshoot of sodium in the cell and ends in a depolarisation in form of an action potential traveling along the stimulated muscle fibre at about 5-10m/s (Herzog, 1998). This leads to the release of calcium (Ca^{2+}) ions into the sarcoplasm around the myofibrils. The increase in Ca^{2+} in the muscle fibre allows a chemical reaction which leads to the sarcomere to contract, muscle force to be generated in the muscle and the joint to move.

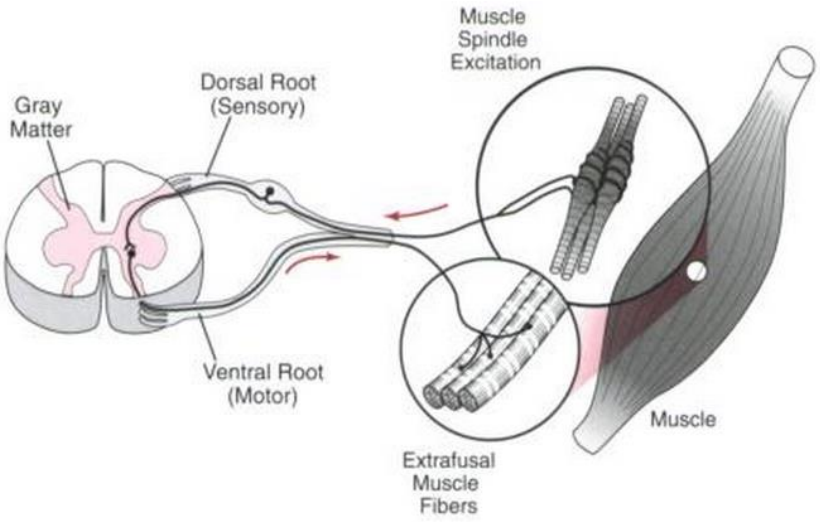

Figure 2.3. Innervation of the muscle through a motor neuron with its origin in the spinal cord, and ending with motor end plates in the muscle fibres (Lieber, 2010).

The time delay between the initial electrical stimulation of a muscle and the mechanical force output at the joints is called electromechanical delay (Yavuz, Sendemir-Urkmez, & Turker, 2010). This is dependent on the elastic properties in and around the active muscle tissue and tendon (myofilaments, tendon, and aponeuroses) as well as the electromechanical processes (Grosset, Piscione, Lambertz, & Perot, 2009; Yavuz et al., 2010). In the academic literature this delay is highly discussed (e.g. Blackburn, Bell, Norcross, Hudson, & Engstrom, 2009; Grosset et al., 2009; Knutson, 2007; Nordez et al., 2009; Rampichini, Ce, Limonta, & Esposito, 2013) and, depending on the muscle and the participants' characteristics (e.g. type of muscle fibre, age, fatigue (Yavuz et al., 2010)), it can lie between 8 and 127ms (Rampichini et al., 2013). However, it has to be kept in mind that the method with which the electromechanical delay is measured can result in different values as well (Rampichini et al., 2013; Yavuz et al., 2010).

Information about the morphology and physiology of a muscle and the muscle force generation are essential for analysing differences between individuals with a musculoskeletal disorder and a healthy group. It is important to consider the excitation of the muscle to the mechanical output of the joints as a process with multiple influencing factors which could all lead to a change between patients and control group. Simplified, this process can be divided in four main stages (Figure 2.4): the excitation of the muscle tissue through the motor neuron, the chemical activation in the muscle cell through Ca^{2+} ions, the actual mechanical force production, and the visible movement of the segments. Depending on the pathology, restrictions are originated

primarily through different systems of the body. For example cerebral palsy is primarily a restriction of the central nervous system (CNS, stage 1), whereas leg deformities are primarily a change of the skeletal system (stage 4). However, both examples can have secondary effects on other stages of the force generation which underlines the importance of understanding the whole process.

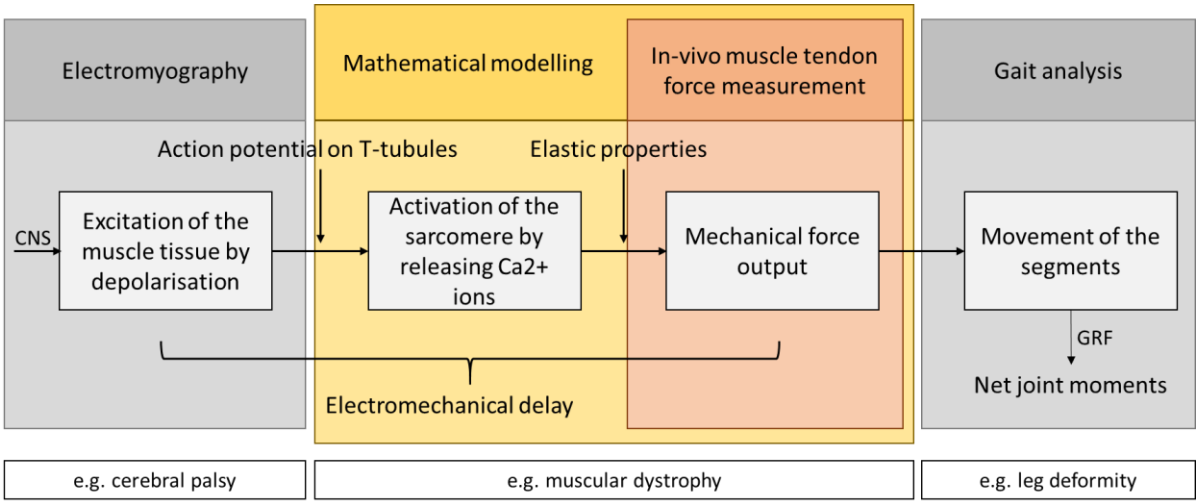

Figure 2.4. Schematic illustration of the electromechanical delay and its four main stages, including measurement methods (top) and the origin of exemplary pathologies (bottom). CNS=central nervous system, GRF=ground reaction force.

In the academic literature, the terms excitation, activation and force output can be differently defined, depending on the field of study (e.g. modelling or biology related). For this work these terms are used to describe following definition (Hicks, Uchida, Seth, Rajagopal, & Delp, 2015):

Excitation: The innervation of the muscle tissue through the motor neuron arriving at the neuromuscular junction leading to a depolarisation of the T-tubules.

Activation: The release of Ca^{2+} ions which causes the muscle to contract.

Force output: The muscle produces force, either in isometric or dynamic mode, leading to a movement or the ability to work against gravity through inertial forces or antagonistic muscle activity.

2.3 Development of the Classical Gait Analysis

Human movement is a complex topic and a growing research field. According to Baker (2007) and Kirtley (2006) Aristotle (384 until 322 BC) was one of the first known scientists to analyse human walking. It was not until the late 19th and early 20th century, however, that scientific methods started to be applied to gait analysis simulated by new measurement techniques, such as the multiple exposure camera (Muybridge, 1907). One of the first experimental studies that analysed systematically the characteristics of healthy walking was the work of Murray and colleagues (1964) using interrupted-light photography (Figure 2.5). They provided normative two-dimensional joint angles of the lower limb during walking for five different age groups while comparing different age groups as well as groups with different body heights.

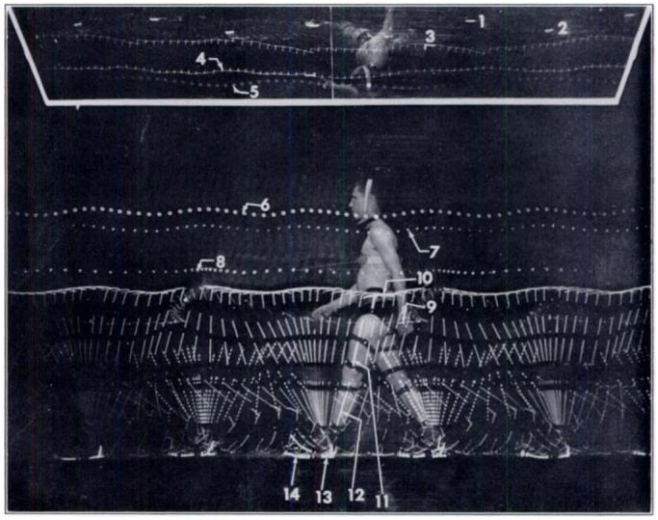

Figure 2.5. Photograph showing a participant equipped with reflecting markers which were exposed to an interrupted light flashing 20 times per second (Murray et al., 1964).

Whilst early interest focused on the analysis of healthy walking, interest in the impact of various diseases grew throughout in the 20th century, leading to the development of clinical gait analysis (Andriacchi & Alexander, 2000). Today, gait analysis is widely used in a clinical setting, where clinicians evaluate the different walking pattern of a specific patient compared to normative healthy walking (Davis III, Õunpuu, Tyburski, & Gage, 1991). In clinical movement analysis walking is a commonly used task to compare a patient with normative kinematic and kinetic data (Perry & Burnfield, 2010). It is a crucial movement impacting the quality of life (Chris

Kirtley, 2006), the independence and functional status, likely to be restricted by the consequences of various diseases.

Over 25 years ago a biomechanical model was developed known under the name of the *Helen Hayes* (Kadaba et al., 1989) or the *Newington Model* (Davis III et al., 1991). It has been integrated into the *Vicon* motion capture system (*PlugInGait*) and is known as the *Conventional Gait Model* (Baker, 2013). This biomechanical model simplifies the complex anatomical and mechanical properties of the human body and provides outputs describing the movements that occur at the different joints during walking. The conventional gait model is divided up into seven rigid segments, linked together through three degrees of freedom ball and socket joints. It includes simplified body structures of the pelvis, the femur, the tibia and the foot. Nowadays, this is the most commonly used model in clinical gait analysis.

A typical gait analysis focuses on the kinematic and kinetic data capture. Kinematic data are acquired through the recording of the trajectories of reflective markers which are placed on body landmarks of the body segments to calculate the relation of the segments in a specific coordinate system, tracked by infrared cameras (Kadaba, Ramakrishnan, & Wootten, 1990). Kinematics describe the way body segments move in space (segment kinematics) and in relation to their adjacent segments (joint kinematics). This is possible by implementing a reference coordinate system into each segment and comparing this to a global coordinate system of the space (Baker, 2013). If the segments' orientations in space are known, joint angles, velocities and accelerations can be calculated (Davis III et al., 1991).

Kinetic data include forces, moments and powers acting on the human body (Baker, 2013). Newton's laws describe how the body moves as a consequence of these factors and are representing the *equation of motions* (Winter, 2009). One force acting on the body is the ground reaction force (GRF) which is the response of the ground to the foot contact (Figure 2.6). With additional information about the kinematics, mass and moments of inertia of the body segments joint moments can be calculated by a process called inverse dynamics (Bresler & Frankel, 1950).

2.4 Classical Gait Analysis and Muscle Force

One of the easiest way to get an overview about which muscle group could be active during walking is to look at the progression of the GRF during the stance phase (Chris Kirtley, 2006). The position of the GRF in relation to the different joint centres of the lower limb indicates which muscle group must dominate to oppose the moment arising from the GRF. If the GRF passes on one side of the joint then the muscles acting across the other side of the joint are likely to be active. If the GRF passes through a joint then the moments produced by both agonist and antagonists must be equal and opposite.

Figure 2.6 shows an example for the ankle. At initial contact (A) the GRF passes behind the ankle joint and is opposed by the dorsiflexors of the ankle. At around foot flat (B) the GRF passes through the ankle joint centre indicating an equilibrium of muscle forces between the dorsi and plantarflexors. As stance progresses the GRF moves forward with respect the ankle joint centre (C) indicating increased force production of the plantarflexors. Whilst giving a broad overview of muscle activity, however, this method is quite limited. Only the stance phase of the gait cycle can be analysed, and no effects of acceleration of the body segment is taken into account.

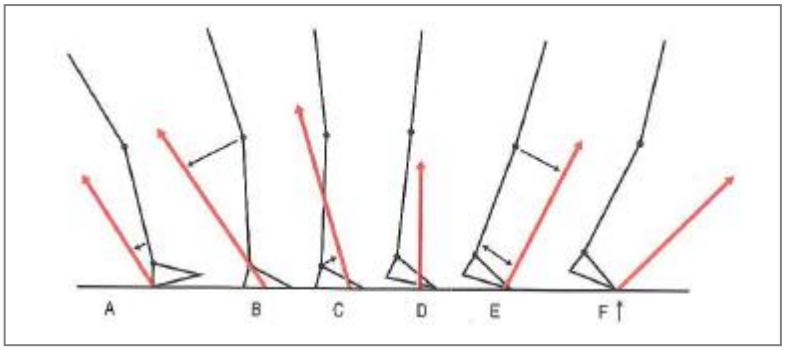

Figure 2.6. Progression of the ground reaction force vector during normal gait in stance phase (Chris Kirtley, 2006).

The calculation of joint moments using a full inverse dynamics analysis is required to give a more accurate indication of the overall net moment produced at a joint. This will arise from agonist and antagonist muscles and other passive tissues which cross the joint. Inverse dynamics, however, only indicates the overall joint forces and moments and gives no indication

of how this arises from the balance of agonists or antagonists or of which muscles within a specific muscle group are active (Buchanan et al., 2005). In general it is not possible to calculate individual muscle forces, because more muscles are acting within the body than there are degrees of freedom (rotations and translations in all three planes) in the joints (Bogey, Perry, & Gitter, 2005). This is defined as the *redundancy problem*: the same net joint moment can be achieved through many combinations of activity in the numerous muscles spanning a joint (Pandy & Andriacchi, 2010).

The absolute force of a muscle during walking can only directly be measurable with invasive methods (Figure 2.4) (Bogey, Cerny, & Mohammed, 2003). Such invasive techniques have been used in the past for human walking in a small number of studies: Komi (1990) recorded *in vivo* forces via force transducers inserted in the Achilles tendon, whereas Finni and colleagues (1998) improved this technique by using an optic fibre inserted into the tendon. Komi's technique required, however, a surgical implantation under local anaesthesia whereas Finni et al. inserted the optic fibre using a sterilised needle using only anaesthetic cream. Although they improved these techniques it is still generally assumed to be too invasive for routine clinical use.

2.5 Electromyography and Muscle Force

Another indirect method has been developed to analyse muscle excitation patterns during human movements: *electromyography* (EMG) can record the muscle action potentials which innervate the muscle (Figure 2.4) (Sutherland, 2001) thereby giving information about the activation level of a muscle (Shewman & Konrad, 2011). EMG measures muscle excitation patterns with either surface electrodes, where the electrodes are placed on the skin, or indwelling electrodes, which are inserted into the muscle (Winter, 2009). EMG is seen as the "gold standard" in clinical gait analysis to analyse muscle excitations. EMG, however, is not directly related to muscle forces (Hug, Hodges, & Tucker, 2015) as it measures the electrical rather than the mechanical activity (Whittle, 2001). The relationship between excitation and force production is complex and still unclear, leading to differing conclusions (De Luca, 1997; Pandy & Andriacchi, 2010). Some studies show a linear correlation between the amount of EMG excitation and produced muscle force in isometric (A. L. Hof & van den Berg, 1977; Johnson, 1978; Lippold, 1952), or isotonic conditions (Bigland & Lippold, 1954), whereas other studies disagree (Komi & Viitasalo, 1967) or give inconsistent findings between different muscles (Alkner, Tesch, & Berg, 2000; Woods & Bigland Ritchie, 1983). EMG measurements are also sensitive to a number of experimental factors such as skin preparation or the nature of the tissues between electrode and muscle.

Surface EMG is only applicable for larger superficial muscles. For deeper or smaller muscles it is necessary for a fine wire to be directly inserted into the muscle tissue. One of the disadvantages here lies in a small recording area in the muscle, which may not represent the whole muscle (Soderberg & Cook, 1984). It also requires specific training of a practitioner who is clinically qualified for routine clinical use.

2.6 Modelling and Simulation

A more recent way to analyse muscle physiology and, therefore, as well the force a muscle produces is the estimation of muscle forces via *mathematical models*. A *musculoskeletal model* is additionally used to present the anatomical structures while calculations and optimisation criteria simulate a specific movement. Model, simulation, and estimation are defined in detail as follows (Hicks et al., 2015):

Model: A model defines a set of mathematical equations that describe a static, physical system. This may be the human anatomy presented through a neural and muscular system acting on a rigid multibody skeletal structure.

Simulation: A simulation uses a model to be able to study a specific motion by imitating a behaviour or process. Therefore, it describes how something dynamically functions, for example how a human anatomical system is able to walk or jump.

Estimation: An estimation defines a close guess of the actual values through calculations and defines the most plausible value of a parameter.

2.6.1 Musculoskeletal Models

A musculoskeletal model is a set of mathematical equations that describe a physical system (Hicks et al., 2015), which may represent the human neuro and/or muscular system. This includes the action of this active system on the rigid multibody skeleton with interaction of the ground. It may represent, therefore, the muscular-tendon structure, the origin and insertion of this complex, and other force-dependent characteristics.

In the 60ies and 70ies, when computer programming was developing, researchers began to model human locomotion at a theoretical level by developing optimisation programmes and control theories (Chow & Jacobson, 1971). Seireg and Arivkar (1973) and Crowninshield and Brand (1981) are one of the first to implement cost functions to optimise estimated muscle forces of the lower limb. It is only relatively recent, however, that breakthroughs in the research of robotic control technique and biomechanical simulation have made musculoskeletal modelling a practical proposition for clinical gait analysis (Delp et al., 2007). Such techniques solve the redundancy problem using mathematical models to estimate muscle activations and

forces (Buchanan et al., 2005) using experimental movement analysis data as well as subject specific anthropometric data. The skeleton and the muscles are represented in form of a musculoskeletal model (Erdemir et al., 2007), which defines the number and masses of segments of the model, the degrees of freedom of the joints, and the number of muscles and their properties.

The bony structure is modelled as a number of rigid bodies articulated through joints in a 2D or 3D space. These bony segments are defined by their mass, moments of inertia, centre of mass location, and the joints by the number and nature of the degrees of freedom and permitted range of movement. These anthropometric values are taken from older cadaver studies or from the digitalisation of bony structures (Delp et al., 1990). Muscles are modelled as being attached to the segments at an origin and an insertion on specific landmarks. Straight line paths are assumed for most muscles but via points (Figure 2.7) can be included where muscles wrap around bones or other muscles or are constrained by a retinaculum (Au & Dunne, 2012; Delp, 1990).

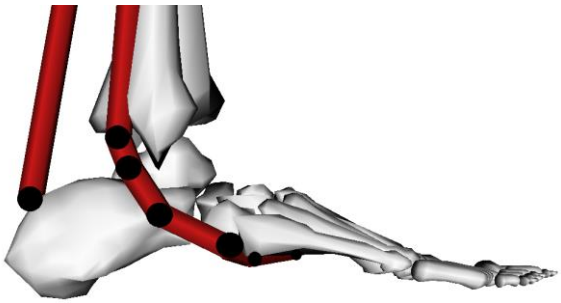

Figure 2.7. Different representation of muscles: some of the muscle patters are only defined through origin and insertion, e.g. the soleus (left muscle), others are represented through more than one line segment including via points, e.g. the peroneus longus (right muscle) (Delp et al., 1990).

Further characteristics of the muscle-tendon units are needed to create muscle-driven simulations (Delp et al., 2007) such as the optimal length of a muscle fibre (at which it produces the maximum force), the pennation angle of the muscle, the maximum force a muscle can produce, the length of a tendon where it starts to generate force (tendon slack length) and the elasticity of the tendon. The muscle activation-contraction dynamics specify how force generation within the fibres is dependent on fibre length and lengthening velocity. Arnold and colleagues (2013) define the overall muscle forces as follows,

$$F^M = F^M_{max}\,(a \times f_{AL} \times f_v + f_{PL}) \quad (1)$$

where F^M is the muscle force, F^M_{max} is the maximum isometric force, α the activation scale (0 → 1), f_{AL} is the active force-length relationship of the muscle fibre, f_{PL} the passive force-length relationship of the muscle fibre, and f_v the force-velocity relationship (E. M. Arnold et al., 2013).

Force-length relationship of a muscle

The *force-length relationship* is determined experimentally. To do this the muscle tissue has to be maximal isometrically stimulated at a variety of known fibre lengths and the force generated at these lengths is measured (Lieber, 2010). These force-length properties were first described in Hill's work (1952) on the basis of isometric measurements of frog and toad muscles (Figure 2.8). Hill included also a second curve which defines the passive muscle tension and summed both active and passive force production developments at each length of the muscle fibre.

Zajac (1989) defines that the muscle is active between 0.5 and 1.5% of the length of the fibres where the muscle force peaks. He, additionally, stated that if a muscle is not fully activated, the fibres generate proportionately less active force, but the passive force generation stays the same. This length tension relationship is a consequence of the arrangement of its actin and myosin filaments (Figure 2.8). These sets of contractile filaments overlap with each other and tension is generated by cross-bridges between the actin and myosin filaments. When the muscle is stretched, actin and myosin slide away from each other, less cross-bridges can form and, therefore, less force can be produced. During shortening the area of the overlap also reduces restricting the cross bridges and reducing the force that can be produced (Lieber, 2010). Therefore, there is an optimal sarcomere length where the muscle produces maximal isometric force, which is between 2.0 and 2.2 µm and close to the resting length of the sarcomere.

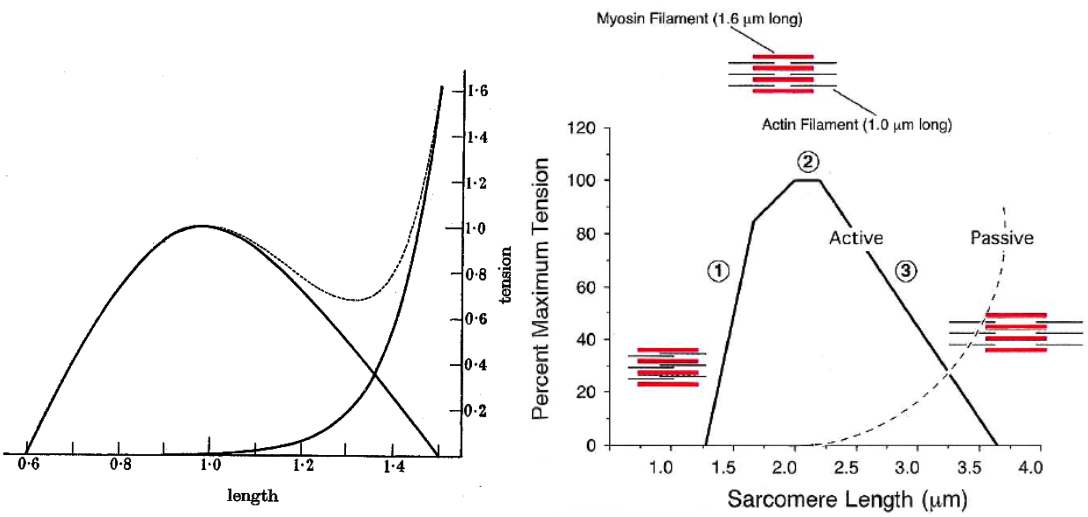

Figure 2.8. Left: force-length curve adapted from Hill (1952), right: force-sarcomeres length relationship from Lieber (2010).

It has to be kept in mind, however, that this curve is generated through isometric contractions. To understand how a muscle performs in dynamic movements the force-velocity relationship has to be taken into consideration as well (Lieber, 2010).

Force-velocity relation of the muscle

In Zajac's work (1989) the force-velocity relation of the muscle fibres is discussed and illustrated in a graph (Figure 2.9). The muscle reacts differently to velocity if the fibres getting shorten or lengthened. If the muscle shortens then the force reduces with shortening velocity until it reaches its maximum shortening velocity (v_m) after which the muscle cannot generate any fore at all. On the other side, if the muscle fibres are lengthening (which will occur if the externally applied force is greater than that which can be exerted by the muscle) then the maximum force increases quite rapidly to a value of about 1.8 of peak active isometric force (F^M_0) at optimal fibre length.

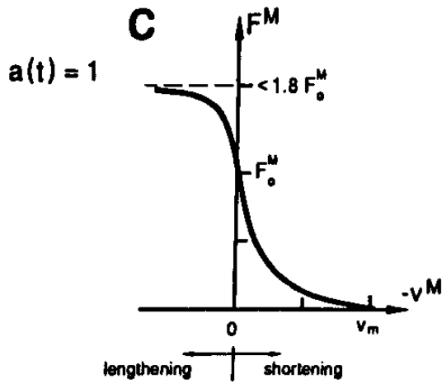

Figure 2.9: The force-velocity relation of muscle fibres adapted from Zajac (Zajac, 1989).

2.6.2 Mathematical Models: Inverse and Forward Dynamics

A mathematical model describes mathematical equations which enable the estimation of motion of a musculoskeletal model. This is operated by a simulation with which the motion and forces of a system can be analysed (Hicks et al., 2015). Biomechanical modelling to estimate muscle force generation during human movement can be done by *inverse* and *forward dynamics* (Erdemir et al., 2007). Inverse dynamics (e.g. static optimisation) calculates the forces and moments that must have acted at the joints in order to generate the measured ground reaction and body segment accelerations (Figure 2.10). This is a two-step process, as, firstly, the joint torques (e.g., moments) will be calculated with the help of Newtonian laws (equation of motions), and secondly, the muscle forces are estimated while taking the muscular-tendon properties into account. Forward dynamics, in turn, estimates the body segment accelerations that will be generated by derived muscle forces according to the equation of motions. The muscle forces have been estimated before by a given set of muscle states and the muscular-tendon properties. This whole process allows an estimation of how the body will move dependent over a particular time frame (Erdemir et al., 2007; Lin et al., 2012).

Inverse dynamics to estimate muscle forces is computationally much simpler and quicker and is known to be more robust to measurement errors (Lin et al., 2012). It, however, can only give insights into the measured movement independently at each instance in time. Forward dynamics, whilst more challenging, is able to give insights into how the body would move if different muscles had been active. Both techniques are affected by the redundancy problem (muscles spanning the joint > degrees of freedoms, chapter 3.3.6). Cost functions which minimise a specific performance criterion solving this problem by optimising the amount of each individual muscle activation (Glitsch & Baumann, 1997). For the purpose of walking a

variety of criteria such as the minimisation of the overall muscle activation, force, or power, or of energy expenditure or oxygen consumption are used (Chow & Jacobson, 1971).

One of the forward dynamic approaches is EMG-driven modelling. In this, measured EMG excitations are input into the simulation alongside one of the optimisation criteria listed in the preceding paragraph (Lloyd & Besier, 2003). This method is limited, however, both by the experimental difficulties in obtaining quantitative EMG data and by the limited understanding of the detailed relationship between the EMG signal and muscle force generation. A more detailed description of mathematical models can be found in chapter IV.

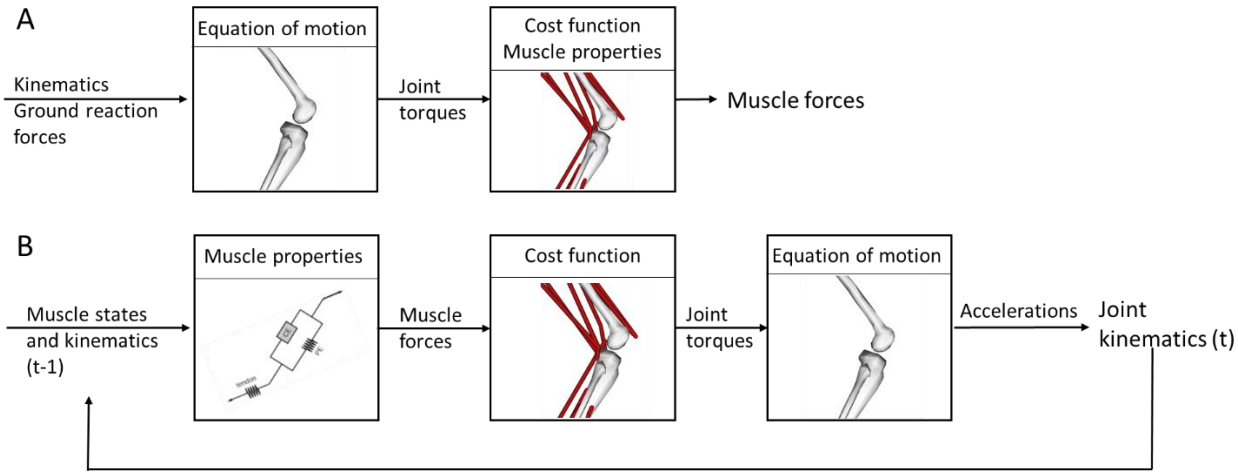

Figure 2.10. Schematic flow chart of inverse (A) and forward dynamics (B), adapted from Erdemir et al. (2007).

2.6.3 Development and Limitations of Models and Simulations

Two primary research groups have been working in the last few years on the development of a musculoskeletal model and simulations to estimate muscle activations and forces in human movement science. These are the Stanford University group with Scott Delp and the group at the University of Texas with Frank Anderson and Marcus Pandy. All three main developers are mechanical engineers, however, work in the field of movement science.

The Anderson and Pandy model started to develop in the late 80ies (Pandy & Berme, 1988a, 1988b) with the work of Pandy to create a model which simulated the movement of the human walking in stance and swing phase. In 1990, Pandy and colleagues published a paper (Pandy, Zajac, Sim, & Levine, 1990) about 2D optimal control for maximum height jumping. The

musculoskeletal model was designed as a four segment body representing one leg and the hip, which was articulated by eight Hill-type muscle-tendon units. The muscular-tendon dynamics were adapted from Zajac (1989), whereas the muscular properties (geometry, maximum isometric force…) were imported from Brand and Wickiewicz works (Brand et al., 1982; Brand, Pedersen, & Friedrich, 1986; Wickiewicz, Roy, Powell, & Edgerton, 1983). This was the ground work for the latter model of Anderson and Pandy used to estimate muscle activations and forces for a 3D maximum vertical jump (Anderson & Pandy, 1999) and during human healthy walking (Anderson & Pandy, 2001a, 2001b) while comparing different mathematical models (static optimisation, forward dynamics).

This final model of Anderson and Pandy used information about muscle parameters, especially the origin and insertion of the muscle-tendon complex, of the Delp model from 1990. Delp published through his PhD thesis a computer graphic-based musculoskeletal model which was able to be used in orthopaedic surgery simulations. This model referred as well to the muscle geometrics of Brand and Wickiewicz, however, Delp realised that especially for extreme flexions of the ankle, knee, and hip the muscles did not run around the bones but passed through the joint. This was solved by introducing points and wrapping points into the model, so that the definition of some of the muscles was not only defined by the two origin and insertion point but also by points along the muscle (Delp, 1990; Delp et al., 1990). More information about the Delp model and its enhancements can be found in chapter IV.

At the time that these models originated, the engineers were quite enthusiastic about their development of musculoskeletal models to estimate muscle forces in various movement and conditions. What, however, stayed yet in the background was the verification and especially validation of these models. Model and simulation verification and validation is crucial for implementing such musculoskeletal models into the clinical movement analysis. Today's research is aware of the important verification and validation (e.g., E. M. Arnold et al., 2013). To be able to implement these techniques into a clinical gait analysis routine the existing musculoskeletal models and simulations of the estimation of muscle forces need to be validated according to the strength and weaknesses of these models. This gets more important as musculoskeletal modelling in the field of movement science (Hicks et al., 2015) as well as in clinical gait analysis (e.g., Arch, Stanhope, & Higginson, 2015; Lerner, Board, & Browning, 2015; Skalshoi et al., 2015) is increasing. Still, the literature is lacking in a straight forward and standardised validation procedure. The first attempt to systematise a controlled verification and

validation process for musculoskeletal modellers is the work of Hicks and colleagues (2015) which will be briefly presented in chapter 2.6.3.1.

Another limitation of such models and simulations is present in the literature. A lot of different factors may influence the estimation's outcome, like the experimental data, the musculoskeletal model or the cost functions used in the optimisation process. This may result in different muscle force profiles while using different experimental or modelling and simulation protocols. For example, both studies of Glitsch and colleagues (1997) and Bogey and colleagues (2005) estimated the muscle force of the tibialis anterior during walking but resulted in different force profiles throughout the gait cycle. Several factors differ between these studies like the mathematical model used for the prediction as well as other factors related to the musculoskeletal model. Less is known about the extent of influence of individual factors which makes it hard to find the protocol most suitable for the clinical gait analysis. Also, the comparison between laboratories is impossible without a standardised protocol as too many factors may play an influencing role. To date, such protocol has not yet been developed for the clinical gait analysis.

2.6.3.1 Validation Process for Musculoskeletal Modelling and Simulations

Validation answers the question if the correct equations are being solved (Hicks et al., 2015) and, therefore, to which degree the real world is represented by the model (Thacker, 2001). Although musculoskeletal modelling and simulation have been developed over the last 25 years in the field of movement science, the approach still lacks in a good verification and validation which allows a wider implementation in the clinic and a wider impact on healthcare (Hicks et al., 2015). Important for a good validation process is the formulation of a research question which the model and simulation is able to answer. Therefore, the methods needs to be tested and a validation plan needs to be designed (Hicks et al., 2015). But also a verification of the equations is from great importance that it is sure the equations are solved correctly. In case an algorithm has been implemented wrongly this may lead to incorrect simulations.

Open source software codes can be reviewed and verified directly which makes this kind of software attractive. If a new protocol has been created to estimate muscle forces to analyse a specific pathological condition on gait pattern it is important to compare results to existing muscle force estimations in the literature. In the case this is a novel approach, it is recommended to test the protocol on healthy adults as well to be sure that similar results are received than

many other walking simulations in the literature (Hicks et al., 2015). On the contrary, if an existing protocol is chosen for a study it needs to be clarified that this protocol is suitable for the research question.

A validation process for modelling and simulations of human movement may be performed by the comparison with independent experiments or other models (Hicks et al., 2015), however, this approach is problematic (Delp, 1990). Direct validation is only possible with invasive methods and these cannot be applied in a clinical setting (Pandy & Andriacchi, 2010). With good quality experimental data joint moments as well as the kinematics and therefore the moment arms of the muscles can give first indications about which muscle must be active. This, however, does not give clear details about the exact muscles especially because of the redundancy problem and potential agonists and antagonists being active.

Although EMG excitations are not directly comparable with muscle force estimations in the magnitude of force, EMG muscle excitations provide a validation tool for the temporal characteristics of muscles estimated by mathematical models. This has been used several times in the literature (Erdemir et al., 2007), for example from Glitsch and Baumann (1997), who used a static optimisation model, where surface EMG of the lower limb was captured on the participants parallel to the experimental data capturing. Neptune and colleagues (2008) in a dynamic optimisation study even used surface activation of the muscles soleus and gastrocnemius to validate qualitatively changes in muscle force estimations throughout different walking velocities. However, when using this validation technique the limitations of EMG need to stay in mind while interpreting results.

2.7 Statement of the Problem

Summarising the above information, integrating musculoskeletal modelling into clinical gait analysis could greatly enhance its potential by improving the patient's quality of life in long term and reducing the costs for the health care system (Delp et al., 2007; Lin et al., 2012). Classical gait analysis and electromyography have two limitations which have not yet been resolved: firstly, the redundancy problem which describes the problem that more muscles spanning a joint than degrees of freedom exist as well as the existence of bi-articular muscles which cannot be solved via simple net joint moments calculations, and, secondly, the limitations of EMG measurements monitoring only the sequence and timing of muscles activities as well as to some extent a "more on" and "more off" activation but not the exact amount of individual force production (Pandy & Andriacchi, 2010).

The integration of musculoskeletal modelling could augment the classical approach in clinical gait analysis and help to enhance clinical decision making in an interdisciplinary team. By solving the redundancy problem, these models can estimate each single muscle force which completes a simple surface EMG measurement. Also, with such models, post-operative prognoses might be given which help the clinicians to decide for the right treatment. Furthermore, including mathematical models into a standardised clinical gait analysis routine can improve creating and adapting rehabilitation protocols by gaining more and better knowledge about the behaviour of the muscular system during walking. However, modelling approaches to estimate muscle activation and forces have not yet made their way into the clinical movement analysis, mainly because of two reasons: firstly, there exists a high variety of models and methods which makes the decision for a clinician hard to define the best solution; and second, a standardised protocol which can be easily implemented into a routine processing has not yet been established, also because modellers and clinicians have different approaches and foci on their studies.

Also, although musculoskeletal modelling exists for a while in the scientific literature, the validation of these methods lacks in its accuracy and quality. This, however, is crucial to be able to implement a model into a clinical setting and to widen the impact on healthcare. Therefore, it is of great interest to resolve these limitations which would make it possible for clinicians to understand and apply a protocol which includes mathematical modelling and the estimation of muscle activations and forces.

2.8 Research Question

This PhD thesis aims to develop and test a protocol to estimate muscle forces during human walking for the lower limb muscles which can be applied in the classical clinical gait analysis. The following steps need to be undertaken to understand the literature and to locate an appropriate musculoskeletal model with a mathematical model suitable for the clinical gait analysis:

1. Different mathematical modelling approaches to estimate muscle forces exist in the literature but less is known about the relation to each other and to clinical gait analysis. Therefore, a systematic review is undertaken covering academic studies estimating muscle forces in human healthy walking. It identifies the current state-of-the-art in modelling and simulation and examines how the variability between different approaches affects the consistency in estimated muscle forces. Furthermore, this review identifies the modelling approaches most likely suitable for the use in clinical gait analysis.

2. After identifying appropriate models for a potential standardised protocol with which muscle force estimations can be integrated into the clinical routine processing, musculoskeletal models need to be adapted to the clinical needs. Therefore, an adequate software needs to be selected with which these demands are possible.

3. The final step tests this musculoskeletal model as well as chosen mathematical approaches in the laboratory on a healthy population group. Static and dynamic trials are captured to collect experimental data required for the input in these models. Potential influencing factors on the estimation's outcome (e.g. experimental data, musculoskeletal model…) need to be identified and controlled that the final outcome can be drawn down to the method chosen for muscle force estimation. The results will be validated with experimental data (joint torques, EMG) to analyse the potential of these models.

Finally, these steps can help to clarify the potential of existing musculoskeletal modelling approaches related to clinical gait analysis and identify if and which further steps are needed to be undertaken to introduce these models into the clinical daily routine. Moreover, substantial body of this work can help to close the gap between modellers and clinicians and make a clear transition from the modelling approaches to the clinical needs. These results will further contribute to the current knowledge about muscle force analysis in clinical gait analysis.

Therefore, the research questions which this work will discuss are:

1. What is the state-of-the-art in movement science to estimate muscle forces and joint moments which act on the lower limb joints during walking?
2. Are there experimental parameters and/or parameters related to modelling and simulation which may affect the estimation's outcome? Which parameters need to be taken into consideration to create a standardised protocol which implements the estimation of muscle forces in the clinical gait analysis?
3. Which mathematical model, musculoskeletal model, and simulation environment to estimate muscle forces are the one most suitable for the clinical routine according to the literature?
4. Is it possible with the current facilities to estimate individual muscle forces on a human healthy population on the lower limb and are the results comparable to parallel captured surface EMG?

CHAPTER III

3 Systematic Review of Muscle Force Estimation in Gait Analysis

As described in the previous chapters, knowing the force profiles of individual muscles during walking has the potential to help to identify various musculoskeletal impairments (orthopaedic restrictions, dysfunction of the nervous system etc.) and can give a better understanding about the underlying mechanisms and the impact of these impairments on the musculoskeletal system. Currently available clinical measurement systems incorporate inverse dynamic techniques which can give insights into the net muscle forces acting across a joint but are unable to distribute these across the range of muscles. EMG measurements capture the arriving electrical impulse innervating the muscle which can give information about the muscle activation profile as well as the degree of muscle activation by normalising the signal to a maximum isometric contraction. They are, however, limited in practice to a small number of muscles and considerable assumptions are required to estimate the associated force production in the muscle. These experimental techniques are, therefore, severely limited in the information they can give us about force generation in individual muscles. In-vivo methods (e.g. force transducers, Komi, 1990) are needed to capture the muscle forces directly, but are highly invasive and not applicable in a clinical setting. Muscle force estimation with mathematical models could, therefore, fill this gap and give more detailed information about the muscle activity and the corresponding force production of a wide range of muscles.

Until now, no standardised protocol exists to estimate muscle forces as a part of routine clinical gait analysis. Before muscle force estimation can be implemented into the clinical gait analysis, it is crucial to understand the state-of-the-art of mathematical models which estimate the force characteristics of lower limb muscles during walking. Numerous musculoskeletal and mathematical models are available providing different approaches to the estimation of muscle forces (Anderson & Pandy, 1999, 2001b; Lin et al., 2012). Additionally, different experimental data (marker trajectories, ground reaction forces, or electromyography) are frequently used as an input into these models to be able to estimate muscle forces. Furthermore, different cost

functions can be applied into the simulation to optimise the estimation by minimising a range of factors (e.g. the sum of all muscle forces squared).

To be able to give an overview about these mathematical models and their underlying musculoskeletal models and principles a detailed review of the academic literature is needed. Available modelling techniques need to be analysed to identify potential mathematical approaches and musculoskeletal models which may suit the clinical gait analysis routine. Inter- and intra-model variability needs, therefore, to be investigated and factors which may influence the estimation's outcome need to be identified.

This systematic review seeks, therefore, to identify and analyse studies which have estimated muscle forces in the lower limbs during walking. Whilst the ultimate aim of clinical gait analysis is to provide such data for patients with a range of conditions, the starting point of such an analysis is an ability to generate robust data for healthy adults, which the review will focus on. The review will, thus, describe the state of the art in muscle force estimation in order to determine where consensus amongst studies exists using similar or different modelling approaches and to identify areas where these studies give different results. The overarching aim will be to identify one or more modelling approaches which could feasibly be applied in clinical gait analysis and to propose recommendations for a standardised protocol for the estimation of muscle forces during walking.

3.1 Introduction into Systematic Reviews in Movement Science

Cochrane, an independent network of scientists working in the field of health science, has defined a systematic review as follows:

> *"A systematic review attempts to collate all empirical evidence that fits pre-specified eligibility criteria in order to answer a specific research question. It uses explicit, systematic methods that are selected with a view to minimizing bias, thus providing more reliable findings from which conclusions can be drawn and decisions made."* (Higgins & Green, 2011)

In addition, five key characteristics of a systematic review have been stated as (Higgins & Green, 2011):

1. a clearly stated set of objectives with pre-defined eligibility criteria for studies;
2. an explicit, reproducible methodology;
3. a systematic search that attempts to identify all studies that would meet the eligibility criteria;
4. an assessment of the validity of the findings of the included studies, for example through the assessment of risk of bias; and
5. a systematic presentation, and synthesis, of the characteristics and findings of the included studies.

Thus, a systematic review gives an appropriate, detailed and unbiased overview about a specific topic. By rating studies and using a quality assessment tool each included paper is evaluated according to the criteria of interest. In the case of human movement analysis a systematic review can give an overview of specific biomechanical procedures and analyse the consistency of results produced by these across the literature.

Several systematic reviews in human movement science involving walking have already been published. McGinley and colleagues undertook a systematic review about inter-session and inter-assessor reliability for gait analyses (2009). They set the focus exclusively on kinematic measures of the lower limb. One year later, another systematic review about gait analysis has been published which investigated the soft tissue artefacts of the lower limb (Peters, Galna, Sangeux, Morris, & Baker, 2010). Latter study has been cited close to 100 times, whereas the

study of MyGinley et al. has been cited over 250 times (google scholar, web of science 09.01.2016), which shows the importance of such studies in the field of movement science. Good quality systematic reviews are here crucial to present the state-of-the-art as well as point out strength and weaknesses to develop the field further to ensure a high quality performance and to achieve protocols which can be applied in clinical settings.

One reason that muscle force estimations are not yet implemented into a clinical gait analysis routine is the lack of standardised protocols and processing tools. Another reason are the known limitations (e.g. sensitivity to musculoskeletal geometry, muscle and tendon characteristics and the modelling of the foot-floor interaction, see chapter II). If the effects of these limitations of musculoskeletal modelling are known, they can be taken into consideration while interpreting the results which might make these methods useful in the clinic even if the results cannot be regarded as completely robust. Such a review will also help the developers to improve the protocols according to the needs of a clinical routine so that mathematical models to estimate muscle forces may be able to be implemented in the clinic.

Factors affecting muscle force estimation are those related to the experimental and estimation's method used, to the parameters used to describe the person, and to test conditions such as the walking velocity (C Kirtley, Whittle, & Jefferson, 1985; Schwartz, Rozumalski, & Trost, 2008), or the placement of the markers (Kadaba et al., 1989; Szczerbik & Kalinowska, 2011). Additionally, there exists natural inter-subject and intra-subject variabilities in movement patterns (McGinley, Wolfe, Morris, Pandy, & Baker, 2014; Schwartz, Trost, & Wervey, 2004) which needs to be taken into account when analysing the consistency between individuals and across studies. To gain an overview across the academic literature about muscle force estimations during walking and the consistency amongst mathematical models, it is important to consider these factors in the review.

Therefore, a systematic literature database search will be undertaken to identify studies which estimate muscle forces of the lower limb during healthy adult walking. Many modelling approaches calculate net joint moments first and then apply some technique to distribute these across the various muscles crossing the joint. To give insight into whether differences in results are a consequence of the moment calculation or the force distribution stages the survey will include studies which included the calculation of joint moments on the lower limb during healthy adult walking. A customised scoring principle will be applied to qualitatively rate and

analyse the identified joint moment and muscle force studies according to their methodology and reporting of the musculoskeletal model and simulation.

Graphs presenting the joint moments and muscle forces of the lower limb will be extracted, digitised and analysed according to the variability of their profiles. Possible influencing factors on the estimation's output will be detected which will help to define parameters which are important for the creation of a standardised protocol in the clinic. The consistency between joint moment profiles compared to the profiles of estimated muscle forces will help to understand the differences between the well tested inverse dynamics method to calculate joint moments and the new approach of different mathematical models to estimate muscle forces. Inter- and intra-mathematical model force estimation variability will be compared and analysed which enables to identify the mathematical model most usable for the estimation of muscle forces in the clinical gait analysis routine and helps to give recommendations for a standardised protocol for the clinical use.

Summarised the three main aims of this systematic review are:

1. The identification and qualitative rating of studies estimating joint moments and muscle forces during human healthy adult walking.
2. The comparison of variability between joint moment and muscle force profiles of the lower limb during walking from different studies.
3. The definition of one or more mathematical model(s) most suitable for the application into clinical practise and the recommendations for a standardised protocol which includes the estimation of muscle forces.

3.2 Methods

A systematic review is bounded to specific methodical characteristics. This includes a systematic study search using topic specific databases and a systematic inclusion-exclusion procedure undertaken by more than one reviewer. In the sections of this chapter, these steps are defined and split up as follows: search strategy, selection criteria, quality assessment, and data synthesis. Selection criteria were composed along with the PICO questions (Participants, Intervention, Comparison, Outcome), which represent four main criteria defined in the Cochrane Handbook for Systematic Reviews of Interventions (Higgins & Green, 2011).

3.2.1 Literature Search

3.2.1.1 Search Strategy

To locate relevant papers, the following scientific databases were used, all associated with either mathematic modelling, biomechanics, movement science or health:

- *Ovid* including Medline (1990-Jan. 2013) and AMED (1990-Jan. 2013).
- *EBSC*O, including CINHAL (1990-Jan. 2013) and SPORTDiscus (1990-Jan. 2013).
- *Web of Knowledge* (1990-Jan. 2013).

The oldest publication year was set to 1990 corresponding to the first reports of practical mathematical modelling and simulation procedures using experimental input data (Delp et al., 1990) and the first standardised musculoskeletal models which could be applied during walking (Delp, 1990; Pandy & Berme, 1988a). A free keyword search was undertaken with additional Medical Subject Headings (MeSH). These are additional search strategies, in which the researcher has used specific medical vocabulary-based search terms (Higgins & Green, 2011).

Figure 3.1 gives an overview of the keywords which were included in the database search. They are organised in the three main categories: *gait variables*, *measurement methods* and *output variables*. These keywords cover the description of the estimation of lower limb joint moments and muscle forces of healthy human walking. Within each main category the keywords were handled as an “OR” boolean operation: at least one keyword out of this keyword group needed to appear in the title or abstract of a paper to be included. These three categories were then linked with an “AND” Boolean operation. This means that at least one keyword out of each main category had to appear. Proximity operations like “NEAR” or “NEXT” could additionally isolate terms consisting of more than one keyword. As an example the term “musculoskeletal

model" was searched using the keywords "musculoskeletal NEXT model". Hence, these two keywords were required to be located close or next to each other. This step could narrow down the database search and increase exclusion of irrelevant studies.

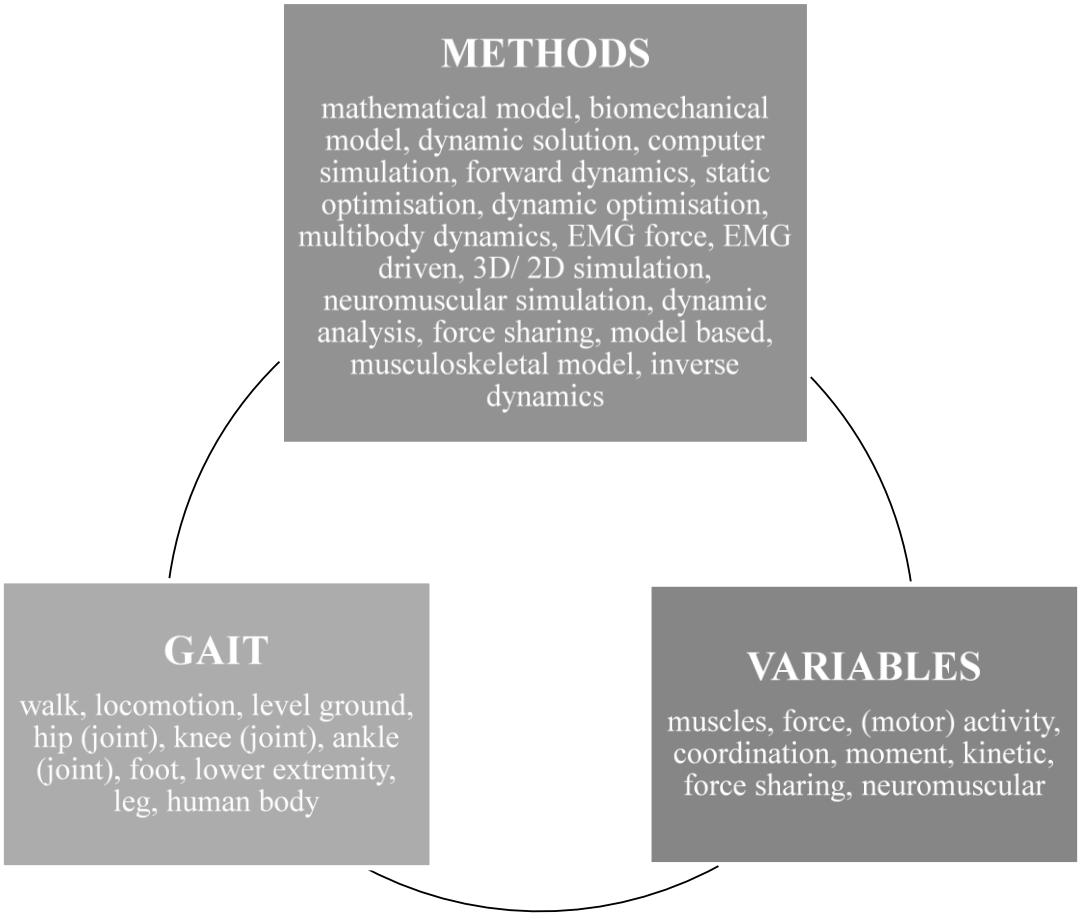

Figure 3.1. Keywords used for the systematic database search arranged in three categories GAIT, METHODS, and VARIABLES.

3.2.1.2 Selection Criteria

Only scientific studies or technical notes published in a peer-reviewed journal were included (Peters et al., 2010). In general, the systematic review process was first developed for collating information about particular interventions from clinical trials literature and inclusion criteria are often specified using PICO headings (Higgins & Green, 2011). This approach has been adopted for this study but has required some adaptation as the overall aim is not to assess intervention studies.

Participants

Studies were included if they involved healthy adult participants. Studies which included healthy participants as a control group for comparison with another patient group were included and data from healthy participants extracted. The maximum age was set to 60 years as walking kinematics (Winter, Patla, Frank, & Walt, 1990) and muscle force capacity (Hughes et al., 2001; Izquierdo, Aguado, Gonzalez, López, & Häkkinen, 1999) are known to change beyond this age.

Intervention

This study is focussing on joint moment and muscle force estimation techniques rather than a specific intervention so these criteria specify the techniques used.

Studies reporting estimates of joint moments and/or muscle forces for individual healthy humans calculated from data captured during overground walking were included. Studies presenting predictive simulations which were not based on data from individuals were excluded. No gait analyses on a treadmill were accepted as it may have changed the participants' walking pattern (S. J. Lee & Hidler, 2008). Studies were only included if experimental data, joint kinematics and kinetics data and/or EMG activations had been captured within the researchers' laboratory (no experimental data from external laboratories or previously published databases). This diminished the influence of unknown variables and allows to extract studies with a known measurement protocol.

Comparisons

This category is specific to clinical interventions and not really relevant to this review of modelling and simulation techniques. Some studies, however, do compare different combinations of models and simulations applied to the same patient data. In this results from all modelling and simulation approaches were included.

Outcome

In order to facilitate the objective of comparing time varying muscle force estimations based on different modelling approaches, only studies providing graphical or numerical data of time varying muscle force estimations over the entire gait cycle or a defined part of the gait cycle were included.

3.2.1.3 Search Process

After extracting potential studies which were located in the chosen databases, titles and abstracts of these papers were scanned on relevancy by two reviewers (Ursula Trinler, Richard Baker) and if not suitable excluded from the review. In case one of the categories could not be fulfilled, the paper was excluded. If a PICO question could not be positively or negatively answered due to missing information in the title and abstract, the study was included into the next step for clarification. After scanning title and abstracts alongside with these criteria it was then decided if these studies were included or excluded for the next step of the systematic review: the quality assessment tool. Inclusion criteria are summarised in Table 3.1. Studies which fulfilled these six essential criteria were finally included into the systematic review.

Table 3.1. Summarised inclusion criteria which decide for studies suitable for the systematic review.

	Inclusion Criteria
1	Participants had to be healthy adults.
2	The movement analysed had to be walking.
3	No treadmill was allowed to be used for experimental data collection.
4	Lower limb joint moments or muscle forces had to be included.
5	Joint moment or muscle force patterns had to be expressed in a graph normalised to a defined part of the gait cycle.
6	The inclusion or the tracking of experimental data had to be part of the modelling process. Experimental data for input into the simulation needs to be own captured data.

3.2.2 Quality Assessment Tool

Studies which passed the screening of title and abstract were fully evaluated by the same reviewers according to the criteria described above. All these included papers were subjected to a customised quality assessment carried out independently by the two reviewers. This step helped to define the state of the art of musculoskeletal modelling compared to joint moment calculations and its potential to include these existing protocols into a clinical gait routine. A

structured quality assessment tool was designed by combining items from similar tools created for kinematic quality studies (Peters et al., 2010) and randomised and non-randomised clinical interventions (Downs & Black, 1998; Ridgewell, Dobson, Bach, & Baker, 2010). Items specific to muscle modelling and simulation were created specifically for this study.

The quality assessment tool is structured to cover nine main items which were applied for all extracted studies and a further three for studies which incorporated EMG measurements. Some of the items are further divided in relevant sub-items (Figure 3.2). These items cover the structural quality of the paper, the description of the protocol and technical details as well as the presentation of the results. Sub-items' maximum scoring is defined in Figure 3.2. The score of an item and its sub-items were summed up and transformed in a percentage of the maximum possible score. The overall score was then the average of these relation scores which allows the highest score to be 100%, the lowest to be 0%.

(1) **Statement of Aims**	(2) **Descriptions of Participants**	(3) **Statement of Task**	(4) **Description of Measurement Equipment**	(5) **Inclusion of Processing and Filtering of Data**	(6) **Description of Kinematic Modelling**
Fully stated (2), partial (1), unstated (0)	1. number (1) 2. gender (1) 3. age (1), spread (1) 4. height (1), spread (1) 5. weight (1), spread (1)	1. normal gait (1) 2. walking speed (1), spread (1) 3.shod/barefoot (1)	1. capture system (1) 2. cameras (type (1)/ number (1) / Hz (1)) 3. force plates (type (1)/ Hz (1))	1. trajectories (type (1)/ Hz (1)) 1. GRF (type (1)/ Hz (1))	1. segments nr. (1), name (1), DoF (1) 2. Marker nr. (1), location (1) 3. model (IK/DK) (2) 4. IK cost function (1)

(7) **Description of Kinetic Modelling**	(8) **Description of Measurement Output**	(9) **Statement of Discussion and Conclusion**	(10) **Validation of Mathematical Model to Estimate Muscle Forces**	(11) **Statement of Musculoskeletal Model**	(12) **Description of EMG system**
1. inertia/mass of segments (1) 2. model (SO/FD) (2) 3. FD cost functions (1) 4. FD residual elimination (1)	1. units (1) 2. spread (1) 3. uncertainties (1)	Fully stated (2), partial (1), unstated (0)	Source of validation data (1)	1. nr. of muscles (1) 2. muscle model (1) 3. muscle geometry (1) 4. optimisation type (1) 5. cost function (1)	1. type of electrodes (1) 2. system (1) 3. measurement Hz (1) 4. channels (1) 3. filter types (2) and frequency (2)

Figure 3.2: Items used for the quality assessment tool, divided in main items (top rows) and sub-items (bottom rows, number in brackets indicating maximum score). Items in blue are applied to all studies, items in green are only applied to EMG or muscle force studies only; Hz=hertz, GRF=ground reaction force, DoF=degree of freedom, DK=direct kinematics, IK=inverse kinematics, SO=static optimisation, FD=forward dynamics, SD=standard deviation.

3.2.3 Data Synthesis and Analysis

The final step involved a graphical synthesis of all joint moments and muscle force profiles contained in the included studies. Estimated joint moments and muscle force profiles were extracted and automatically digitised using the programme *GetData Graph Digitiser* (version2.26, Sergei Fedorov, 2013, Russia). In case the automatic digitalisation failed due to a poor quality of the graph, the graph could be manually digitised by the operator by setting points on the pattern of the graph. For those papers which focused exclusively on the stance phase of walking without stating the stance-to-swing relation of the gait cycle a 60%-40% relation has been chosen (Fraysse 2009).

The digitised graphs were further analysed in Matlab (R2012b) by normalising then individually to the body mass (Bazett-Jones, Cobb, Joshi, Cashin, & Earl, 2011) and the joint moments additionally to the body height (Bowsher & Vaughan, 1995). Muscle force studies were grouped together according to the type of analysis used (e.g. static optimisation, forward dynamic, EMG-driven model). All joint moments and muscle force profiles were averaged across studies to gain an overall mean at each time point in the gait cycle as well as one and two standard deviation bands. In case the specification of the participants' body mass was missing the averaged body mass across all studies was used for normalisation. In cases when estimations of muscle forces were reported separately for different muscle compartments (e.g., gastrocnemius lateralis and medialis; psoas and illiacus; vastus medialis and lateralis; semitendinosus, semimembranosus and biceps femoris) the data reported were summed up across compartments to generate a force profile for the whole muscle (gastrocnemius, iliopsoas, vastii, hamstrings).

The grand mean (μ) will be presented and discussed as well as the as the standard deviation (σ) to describe the variability between studies. The simple mean has been chosen over the weighted mean (normalised to number of participants) because not the variability between participants but the differences and variability between mathematical models was the matter of interest. The standard deviation alone has no strong evidence about the variability regarding the overall mean as the same standard deviation may appear at different mean values. Therefore, the coefficient of variation (CV) will be included additionally, which is

$$CV = \frac{\sigma}{\mu} \tag{2}$$

However, with small μ or even values close to zero the CV is not applicable, as the CV approaches infinity. Winter (2009) estimated an overall CV over the whole gait cycle and not for single points in the gait cycle. However, the calculation of Winter may hide maximum CVs and may not discover differences between mathematical models as the overall CV over the whole gait cycle may be the same but not CVs of single points across the gait cycle. Therefore, the CV will not be calculated for the whole gait cycle but only for peak maxima and minima values across the gait cycle. In the academic literature, the CV has been used before for similar purposes (Kadaba et al., 1989).

3.3 Results

Figure 3.3 presents a flow chart describing the yield of the different stages of the systematic process. The electronic search identified 9870 studies. 9797 of these were excluded as having irrelevant titles in relation to the inclusion/exclusion criteria. In total, 73 studies were included and, by scanning the bibliography of these papers seven more studies were added (in total 80). However, upon review of the full papers, only 37 studies were eligible for inclusion on the basis of presenting time varying data (graphically or numerically) of joint moments and muscle force estimation over the gait cycle. 18 of these studies focused on joint moments during walking, eight on muscle forces, and eleven studies on both joint moment and muscle forces.

In total, data of 325 participants were involved in the included studies (Table 3.2). Joint moment studies included, on average, more participants than muscle force studies. Both genders were evaluated, but more males than females were included in average (79±31% male). Five studies did not define the gender of their participants (Buchanan et al., 2005; De Groote et al., 2009; Dixon, Böhm, & Döderlein, 2012; Hase & Yamazaki, 1997; J. Liu & Lockhart, 2006). Body mass and height were distributed homogeneously across all identified studies. Participants in studies estimating muscle forces with forward dynamics were slightly taller and heavier. Body mass was missing in five studies and body height in six studies.

Participants were generally asked to walk at a self-selected walking speed. Not all studies recorded the actual walking speed of their participants in quantitative units, especially muscle force studies. Walking speed was especially poorly recorded in muscle forces studies. The averaged velocity is 1.41m/s, participants included in pure muscle force studies were walking at 1.30m/s, participants in pure joint moment studies 1.45m/s. The velocity ranged between 1m/s and 2m/s.

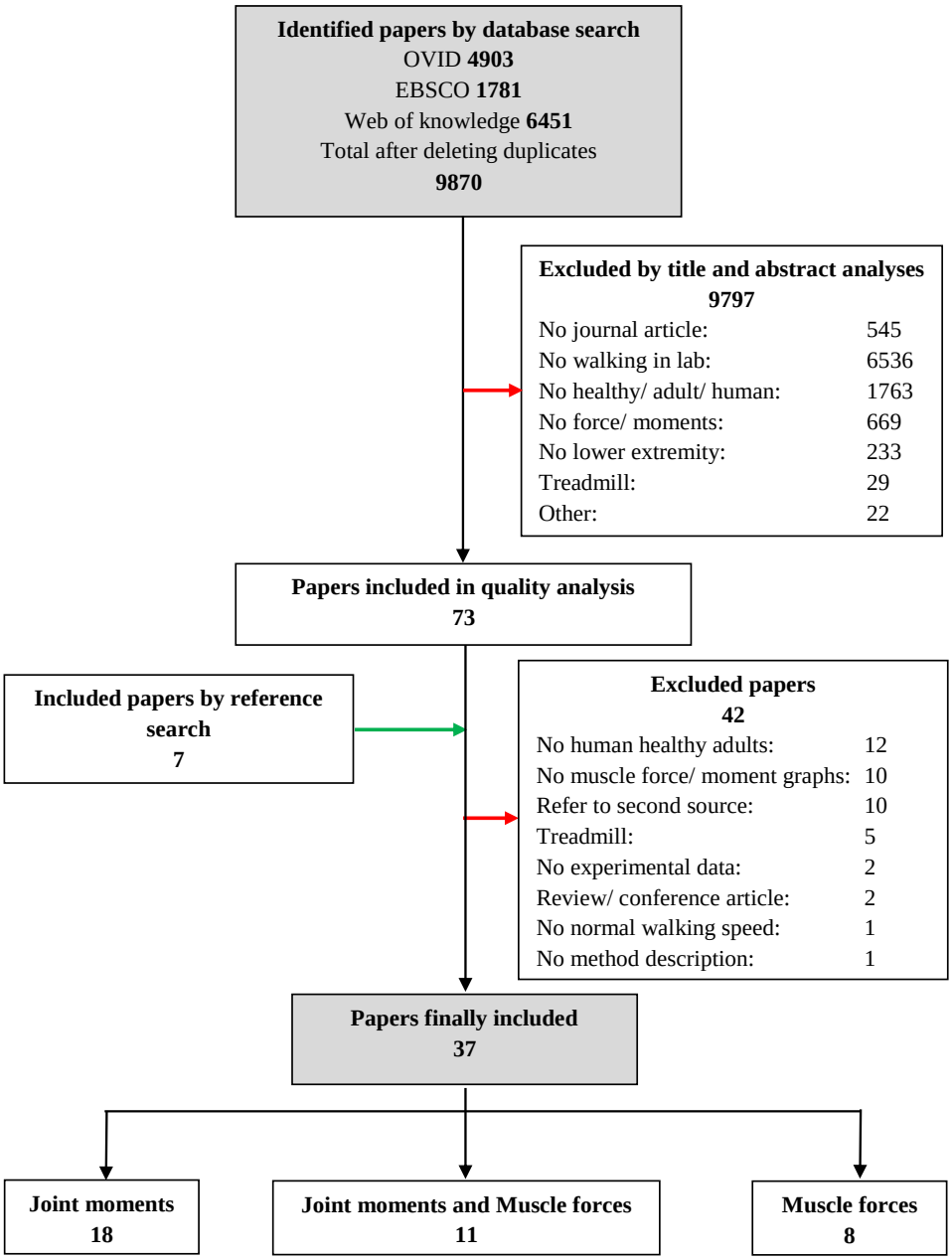

Figure 3.3. Flow chart describing the process of the systematic review. Red arrows indicate exclusion, green arrows inclusion of papers.

Seven studies focused on the stance phase of the gait cycle only (initial contact to toe off). White and Winter (1993) defined the gait cycle from toe off to toe off and attempted to transform this graph in a classical initial contact to initial contact cycle lead to scaling errors. Therefore, only the data of the stance phase from this paper were included.

Table 3.2. Average anthropometric data for all participants included in the 38 studies.

	Anthropometric data (mean, SD)					
	Nr. of participants		**% of male**	**Body mass (kg)**	**Body height (m)**	**Age (years)**
	total	**average**				
Joint moments (29)	302	10 (±19)	74 (±33)	70 (±7)	1.74 (±0.06)	28 (±6)
Muscle forces (19)	58	3 (±5)	82 (±35)	66 (±9)	1.73 (±0.05)	30 (±8)
-Static optimisation (13)	*13*	*1(±0)*	*NS*	*64 (±10)*	*1.72(±0.05)*	*31(±10)*
-Forward dynamics (3)	*3*	*1(±0)*	*NS*	*67 (±4)*	*1.77(±0.00)*	*26(±1)*
-EMG-driven (6)	*45*	*8(±7)*	*NS*	*71 (±8)*	*1.73(±0.08)*	*29(±3)*
Overall	325	9 (±17)	79 (±31)	69 (±9)	1.73 (±0.06)	29 (±8)

Note. Results are divided in a joint moment and muscle force group. Number of studies included are indicated in brackets behind the modelling technique; body mass in kilograms (kg), body height in meter (m), NS=not specified.

3.3.1 Quality Appraisal of Included Studies

The identified 37 papers were included for further analysis and rated using the quality assessment tool. Additionally, details of the biomechanical approaches to calculating joint moments and estimating muscle forces will be described.

The scoring results of identified studies are presented in Table 3.3. The overall percentage score reached in average across the 37 studies is 69% (±12%). The score ranges between 48% (Hase & Yamazaki, 1997) and 92% (Eng & Winter, 1995). For better discussion, papers where firstly divided into three groups: first and third group contain studies which present solely joint moment or muscle force graphs, the second group included papers presenting both muscle forces and joint moments. Secondly, the three main mathematical models to estimate muscle forces static optimisation, forward dynamics and EMG-driven models were further divided up to be able to compare between models. Joint moment studies achieved a higher average score of 77±10% compared to studies including both joint moments and muscle forces (62±11%) and studies focussing solely on muscle force estimations (56±10%). The scoring distribution between items slightly differ between mathematical models. Inverse dynamics studies scored better in modelling categories than both other techniques. EMG-driven models had a higher rating in the item ‘processing’ of experimental data as well as ‘task’ and ‘equipment’

description. Forward dynamics rated worse than EMG-driven and inverse dynamics studies, especially for items ‘task’, ‘equipment’, and ‘EMG’.

The overall average scoring across items was distributed between 43 and 100%. ‘Aim’ reached the highest score, as this had been clearly stated in all of the studies and, therefore, scored 100%. A high score was also achieved for ‘discussion’ which focused on the rating of the graphical or numerical analysis as well as the inclusion of description of limitations and conclusion. The item with the poorest rating was data ‘processing’ where eleven studies did not state any information about the processing tool used. The validation of the chosen mathematical models was not always included. Seven studies gave no information about any validation process whatsoever. Four studies used validation data extracted from other studies and sources, for example EMG signals (Table 3.4).

Three criteria describing the modelling techniques were included in the quality assessment tool (kinematic, kinetic and muscle modelling) which showed differences in their scoring results. The ‘kinetic modelling’ criterion was rated similar between different mathematical model groups (average values between 63-71%); the ‘kinematic modelling’, however, ranged between 55% (kinematic modelling of muscle force studies) and 76% (kinematic modelling of joint moment studies) and showed a wider distribution throughout the papers. Compared to both of these criteria, ‘muscle models’ were scored higher, with an overall average of 98% and the lowest score of 80%.

Both ‘validation’ and ‘EMG’ items were only applied for studies estimating muscle forces. Muscle force estimations in pure muscle force modelling papers were poorly validated and often compared against EMG excitations from external literature (e.g., Komura & Nagano, 2004). In average, these papers were scored with 38%. Better ratings were achieved by papers presenting both joint moments and muscle forces, with an average score of 64%. The item ‘EMG’ was rated in average with 69% and 53% for muscle force studies and studies including both inverse dynamics and muscle forces, respectively. The papers often did not state the type of filter used for the EMG signals or cut-off frequency. Only Buchanan and colleagues (2005) stated all required information.

Table 3.3. Studies which are included into the scoring process and their scoring results.

	Author	Year	Aim	Subjects	Task	Measure Equipment	Processing Filtering	Kinematic Modelling	Kinetic Modelling	Output	Validation	Muscle Models	EMG	Discussion	Score
Muscle Force	Ackland et al. [1]	2012	100	80	25	67	100	43	67	100	0	100	---	50	**67**
	Bogey et al. [2]	2010	100	60	100	92	75	29	67	50	50	100	63	50	**70**
	Fraysse et al. [1]	2009	100	80	25	67	50	71	67	75	0	100	---	100	**67**
	Glitsch& Baumann [1]	1997	100	83	100	92	0	29	100	50	100	80	75	100	**76**
	Hase& Yamazaki [3]	1997	100	17	0	33	0	43	33	50	50	100	---	100	**48**
	Komura& Nagano [1]	2004	100	100	0	17	0	43	67	50	50	100	---	100	**57**
	Komura et al. [1]	2005	100	100	0	17	0	80	67	50	50	100	---	0	**51**
	Rodrigo et al. [1]	2008	100	100	67	50	100	100	100	50	0	100	---	100	**72**
			100	**78**	**40**	**54**	**41**	**55**	**71**	**59**	**38**	**98**	**69**	**75**	**56 +/-10**
Muscle Force + Joint Moments	Anderson&Pandy [1, 3]	2001	100	33	0	0	0	43	67	50	100	100	0	100	**49**
	Besier et al. [2]	2009	100	80	75	67	100	100	60	100	0	100	94	100	**81**
	Bogey et al. [2]	2005	100	60	100	83	100	29	67	50	0	100	63	100	**71**
	Buchanan et al. [2]	2005	100	17	25	50	0	14	33	50	100	100	100	100	**57**
	Collins et al. [1]	1995	100	33	25	50	0	57	67	50	100	80	25	50	**53**
	De Groote et al. [1]	2009	100	17	0	33	0	75	100	50	100	100	25	100	**58**
	Heintz& Gutierrez-Farewik [1,2]	2007	100	100	33	50	0	86	67	50	100	100	88	100	**73**
	Leardini& O'Connor [1]	2002	100	67	0	17	0	86	0	50	0	100	63	100	**49**
	Lin et al. [1, 3]	2012	100	100	67	50	100	57	60	50	100	100	25	100	**76**
	Silva& Ambrosio [1]	2003	100	83	33	50	0	71	100	50	0	100	---	100	**62**
	White& Winter [2]	1993	100	33	25	92	50	43	67	50	100	100	50	100	**68**
			100	**57**	**35**	**49**	**32**	**60**	**63**	**55**	**64**	**98**	**53**	**95**	**62 +/-11**
Static optimisation			**100**	**75**	**29**	**43**	**27**	**65**	**71**	**56**	**54**	**97**	**43**	**85**	**62 +/-10**
Forward dynamics			**100**	**50**	**22**	**28**	**33**	**48**	**53**	**50**	**83**	**100**	**13**	**100**	**58 +/-16**
EMG-driven			**100**	**58**	**60**	**72**	**54**	**50**	**60**	**58**	**58**	**100**	**76**	**92**	**70 +/-8**

Note. [1]=static optimisation, [2]=EMG-driven models, [3]=forward dynamics.

Table 3.3. Continued.

	Author	Year	Aim	Subjects	Task	Measure Equipment	Processing Filtering	Kinematic Modelling	Kinetic Modelling	Output	Validation	Muscle Models	EMG	Discussion	Score
Joint Moments	Alkjaer et al.	2001	100	80	75	92	100	86	100	50	---	---	---	100	**87**
	Bovi et al.	2011	100	80	75	75	0	71	0	50	---	---	---	100	**61**
	Bowsher&Vaughan	1995	100	50	75	67	0	86	67	50	---	---	---	100	**66**
	DeVita et al.	2007	100	100	100	83	50	43	67	50	---	---	---	100	**77**
	Dixon et al.	2012	100	70	100	67	100	71	67	100	---	---	---	100	**86**
	Eng& Winter	1995	100	80	100	58	100	86	100	100	---	---	---	100	**92**
	Faber et al.	2010	100	83	67	75	100	86	67	50	---	---	---	100	**81**
	Fluit et al.	2012	100	67	67	0	0	86	80	50	---	---	---	100	**61**
	Frigo et al.	1996	100	33	100	50	0	86	67	100	---	---	---	100	**71**
	Ganley& Powers	2004	100	33	50	67	50	86	67	50	---	---	---	100	**67**
	Hunt et al.	2001	100	40	75	100	100	43	33	100	---	---	---	100	**77**
	Kerrigan et al.	1998	100	80	100	67	0	86	67	50	---	---	---	100	**72**
	Koopman et al.	1995	100	100	33	92	0	80	67	50	---	---	---	50	**64**
	Liu& Lockhart	2006	100	80	100	92	100	86	100	50	---	---	---	100	**90**
	Ren et al.	2008	100	33	63	67	75	100	100	100	---	---	---	100	**82**
	Riemer et al.	2008	100	80	50	75	100	43	100	100	---	---	---	50	**78**
	Schache& Baker	2007	100	80	75	75	50	86	100	100	---	---	---	100	**85**
	Stief et al.	2008	100	80	100	67	25	57	33	50	---	---	---	100	**68**
			100	**69**	**78**	**71**	**53**	**76**	**71**	**69**	---	---	---	**94**	**77 +/-10**
OVERALL SCORE ACROSS ALL STUDIES			**100**	**67**	**57**	**61**	**43**	**66**	**68**	**63**	**56**	**98**	**53**	**90**	**69 +/-12**

Note. [1]=static optimisation, [2]=EMG-driven models, [3]=forward dynamics.

3.3.2 Measurement Equipment and Data Processing

A range of measurement equipment has been used to collect experimental data (Table 3.4). Most studies used optoelectronic motion analysis capture systems of *Vicon* (n=11) to capture kinematic trajectory marker data. Koopman and colleagues (1995) used goniometers on the hip, knee and ankle to measure joint kinematics, two electrical foot contact switches under both feet defined the timing of initial contact and toe off. Eight studies have not specified which motion system they have used to collect kinematic data. The number of cameras used ranged between three and 22, with a measurement frequency between 50 and 500Hz.

All studies combined motion capture systems with force plates or pressure insoles to generate the input data needed for the muscle force estimation process. The ground reaction forces were either captured through a strain gauge system (*AMTI, Bertec, Kyowa*) or through a piezo-electronic system (*Kistler*). One study, however, used pressure insoles to capture the ground reaction forces (Faber, Kingma, Martin Schepers, Veltink, & van Dieen, 2010). Faber and colleagues (2010) used shoes provided with 3D force sensors beneath the heel and the forefoot and sampled at 50Hz. The measure frequency ranged between 60 and 2400Hz.

Three out of five studies which applied EMG data in their models used fine wire electrodes: two with bipolar 50µm wire electrodes but with an unknown system (Bogey, Gitter, & Barnes, 2010; Bogey et al., 2005). The third study (Buchanan et al., 2005) captured one muscle (soleus) with fine wire, whereas the other muscles were captured with surface electrodes (*Noraxon* 9000). No specific information about the fine wire electrode was given. Other studies used surface EMG electrodes. Heintz and Gutierrez-Farewik (2007) captured with Motion Lab System electrodes and White and Winter (1993) with a customised 16-channel PPM-FM telemetry unit. In general, the measurement frequency for EMG signals ranged between 500 to 2500Hz.

A wide range of different processing protocols have been applied in identified studies. The processing and filtering of experimental data is not always fully stated, sometimes even not mentioned at all. In general, kinematic data are filtered with a low pass 2^{nd} (n=2) or 4^{th} (n=13) order Butterworth filter which a cut-off frequency between 2 and 10Hz. Ganley and colleagues (2004) used a Woltring routine with an estimated mean square error of 20mm. Similar techniques in processing data can be found for the processing of ground reaction forces, where the range of the low pass filter lies between 2 and 60Hz.

Both studies from Bogey and colleagues do not specify the post-processing filtering of the EMG signals but define a rectification and integration through a moving integration scheme. The other three studies including EMG used following filter: low pass 8Hz cut-off 4^{th} order Butterworth (Buchanan et al., 2005), high pass 20Hz cut-off 10^{th} order Butterworth and low pass 5Hz cut-off 3^{nd} Butterworth (Heintz & Gutierrez-Farewik, 2007), and low pass 2Hz cut-off 2^{nd} order Butterworth filter (White & Winter, 1993).

Table 3.4. Parameters of the gait analysis protocol, the biomechanical model and the musculoskeletal model of included papers as well as the mathematical model description.

	Author	Year	Velocity (m/s)	Gait phase	Nr. Part-icipants	Measurement equipent	Bioemchanical model	Nr. of segments	Musculoskeletal model	Nr. of muscles	Geometric references	Model type	Input data	Cost function
Muscle Force	Ackland et al.	2012	free	S	1	Vicon (120), --, //	PiG (?)	10 (inc. trunk)	Anderson&Pandy 1999	54 bilat. (24/leg)	McConville 1980 (inertia)	SO	kinematics, GRF	∑a2
	Bogey et al.	2010	free	GC	16	Vicon 512 (100), Kistler 9281B (600), needle	Kadaba 1989	--	Delp et al. 1990	12 (ankle)	--	ED	kinematics, EMG	power
	Frayssе et al.	2009	free	GC	1	MAC (100), AMTI, (100) //	6 DoF (?)	7	Delp et al. 1990	30	Dumas 2007 (inertia) Vezin&Verriest 2005 (bone)	SO	kinematics, GRF	∑s2
	Glitsch& Baumann	1997	1.5	S	1	Selspot II (500), Kistler (500), //	Baroni 1995 (?)	7	Brand et al. 1982	47	Chandler 1975 (inertia)	SO	kinematics, GRF	∑s2
	Hase& Yamazaki	1997	1.39	GC	1	Hamasatsu Photonics PSD system C3570 (--), Kyowa Dengyo EP-386 (--), //	--	10 upper limb 9 lower limb	*own development*	44 (leg) 48 (trunk)	Chandler 1975 (inertia) Winters&Woo 1990 (muscle)	FD	kinematics, GRF	metab. energy
	Komura& Nagano	2004	--	S	1	Vicon 512 (--), --, //	PiG (?)	11	Delp et al. 1990	43	--	SO	kinematics, GRF	∑s
	Komura et al.	2005	1	GC	1	--, --, //	--	8 upper limb 13 lowerlimb	Delp et al. 1990	44	--	SO	kinematics, GRF	∑s2
	Rodrigo et al.	2008	111 st/min	GC	1	--, --, //	--	16	Delp et al. 1990 Ambrosio 1999	35	--	SO	kinematics, GRF	metab. energy
Muscle Force + Joint Moments	Anderson&Pandy	2001	1.12	GC	1	--, --, //	--	10 (inc. trunk)	Anderson&Pandy 1999	54 bilat. (24/leg)	McConville 1980 (inertia) Delp 1990 (muscle)	SO FD	kinematics, GRF	∑a2 metab. energy
	Besier et al.	2009	1.49	S	16	MAC (60), BC (2400), MLS (2400)	Kadaba 1990	--	Delp et al. 1990	10	--	ED	kinematics, EMG	moments
	Bogey et al.	2005	1.37	GC	10	Vicon 512 (100), Kistler 9281B (600), needle	PiG (?)	--	Delp et al. 1990	10 (ankle)	Dempster 1955 (bony mass)	ED	kinematics, EMG	moments
	Buchanan et al.	2005	free	S	1	Qualysis (--), AMTI (--), Noraxon 9000 (1000)	--	--	Delp et al. 1990	--	Yamaguchi 1990 (muscle)	ED	kinematics, EMG	moments
	Collins et al.	1995	--	GC	1	Vicon (50), Kistler (50), //	PiG (?)	7	*own development*	8	Winter 1979 (inertia) Friedrich 1990 (PCSA)	SO	kinematics, GRF	∑f
	De Groote et al.	2009	--	GC	1	Qualysis (--), AMTI OR6-6-2000 LG6-4-2000 (--), //	Cleveland Clinic protocol	7 exp./ 8 model	Delp et al. 1990	43	de Leva 1996 (mass, inertia)	SO phys. ID	kinematics, GRF	∑a2
	Heintz& Gutierrez-Farewik	2007	free	GC	1	Vicon (50), Kistler (--), MLS (1000)	PlugInGait, Vicon	7	Delp et al. 1990	42	--	SO ED	kinematics, GRF, EMG	∑s2 moments
	Leardini& O'Connor	2002	--	S	1	ElitePlus BTS (--), Kistler (--), //	Cappozzo 1995 Benedetti 1998	focus on ankle (1)	Leardini 1999	3 (ankle)	--	SO	kinematics, GRF	--
	Lin et al.	2012	1.61	GC	1	Vicon (250), Kistler (--), //	PiG (?)	10 (inc. trunk)	Anderson & Pandy 1999	54	--	SO,CMC FD	kinematics, GRF	∑a2 ∑a2 + ∑errors
	Silva& Ambrosio	2003	free	GC	1	--, --, //	--	16	*own development*	35	Richardson 2002, Carhart 2000, Yamaguchi 2001 (muscle)	SO	kinematics, GRF	∑s
	White& Winter	1993	--	S	1	Bolex (50+200), AMTI (1000), -- (500)	--	7	*own development*	--	--	ED	kinematics, GRF, EMG	moments

Note. --=information missing, //=not required, st=steps, S=stance, GC=gait cycle, SCS=segment coordinate system, a=activation, f=force, JM=joint moments, MF=muscle forces, SO=static optimisation, FD=forward dynamics, ED=EMG driven, phys. ID=physiological inverse dynamics, CMC=computed muscle control, SD=standard deviation, n=no, y=yes, st/min=steps per minute.

Table 3.4. Continued.

	Author	Year	Velocity (m/s)	Gait phase	Nr. of Trials	Measurement equipent	Bioemchanical model	Nr. of segments	Musculoskeletal model	Nr. of muscles	Geometric references	Model type	Input data	Cost function
Joint Moments	Alkjaer et al.	2001	1.26	S	15	Panasonic (50), AMTI (1000), //	6 DoF Vaughan 1992	7			Chandler 1975 (inertia)		kinematics, GRF	
	Bovi et al.	2011	1.22	GC	20	SMART-E (60), Kistler (960), //	LAMB marker set 6DoF Rabuffetti 2004	--					kinematics, GRF	
	Bowsher&Vaughan	1995	1.5	GC	12	MAC (60), Kistler (60), //	6 DoF Vaughan 1992	7			Vaughan 1992		kinematics, GRF	
	DeVita et al.	2007	1.52	S	34	Qualisys (120), AMTI (960), //	--	7			Havanan 1964 (mass, inertia) Dempster 1959		kinematics, GRF	
	Dixon et al.	2012	1.35	S	10	Vicon (200), Advanced Mechanical Technology (1000), //	PlugInGait vs OFM	4 (oxford foot model)			de Leva 1996 (inertia)		kinematics, GRF	
	Eng& Winter	1995	1.6	GC	9	-- (60), -- (500), //	3 DoF	7			Bell 1990 (hip joint)		kinematics, GRF	
	Faber et al.	2010	--	GC	1	Optotrak (50), Kistler (--), //	6 DoF Cappozzo 1995	--			--		kinematics, GRF	
	Fluit et al.	2012	1.27	GC	1	--, --, //	--	8 (inkl. trunk)	AnyBody (Damsgaard 2006)	--	--		kinematics, GRF	metab. energy
	Frigo et al.	1996	1.35	GC	1	Elite (50), Kistler (--), //	--	7			--		kinematics, GRF	
	Ganley& Powers	2004	free	GC	1	Vicon (60), AMTI (600), //	PiG (?)	7			DXA-derived vs Dempster 1955 (anthropometric proportions)		kinematics, GRF	
	Hunt et al.	2001	1.6	S	18	MAC (60), Kistler (960), //	6 DoF (?)	3 (leg, 2 foot)			--		kinematics, GRF	
	Kerrigan et al.	1998	1.3	GC	99	Elite (100), AMTI (100), //	Pedotti 1992 (?)	7			--		kinematics, GRF	
	Koopman et al.	1995	free	GC	1	--, --, //	--	8 (inc. Trunk)			Chandler 1975 (mass, inertia)		kinematics, GRF	
	Liu& Lockhart	2006	free	S	10	Qualisys (120), Bertec (1200), //	Lockhart 2002 (?)	7			--		kinematics, GRF	
	Ren et al.	2008	1.5	GC	1	Qualisys (100), Kistler (200), //	6 DoF Cappozzo 1995	6 upper limb 7 lower limb			de Leva 1996 (inertia)		kinematics, (GRF)	
	Riemer et al.	2008	free	GC	10	Vicon (100), AMTI (100), //	PiG (?)	6 upper limb 7 lower limb			de Leva 1996 (inertia)		kinematics, GRF	
	Schache& Baker	2007	1.2	GC	9	Vicon (120), AMTI (1080), //	adjusted PiG (?)	7			de Leva 1996 (inertia)		kinematics, GRF	
	Stief et al.	2008	2	GC	15	Vicon (200), Kistler (1000), //	adjusted PiG	8 (2 foot)			--		kinematics, GRF	

Note. --=information missing, //=not required, st=steps, S=stance, GC=gait cycle, SCS=segment coordinate system, a=activation, f=force, JM=joint moments, MF=muscle forces, SO=static optimisation, FD=forward dynamics, ED=EMG driven, phys. ID=physiological inverse dynamics, CMC=computed muscle control, SD=standard deviation, n=no, y=yes, st/min=steps per minute.

3.3.3 Biomechanical Models

As defined in chapter II the biomechanical model simplifies the complex human anatomy to define segments and joints in a way it can be applied into kinematic and kinetic calculations. Most of the studies included a reasonable description of the biomechanical model they have implemented (Table 3.3). In majority of the cases, the bony structure of the lower limbs was divided up into seven different segments, pelvis, left and right thigh, left and right shank, and left and right foot, linked together with a three-degrees-of-freedom joint over a fixed joint centre (Baker, 2013). This organisation of the bones and joints, called the *Conventional Gait Model* (Baker, 2013), is represented by most of the studies and can be found in studies referring to Kadaba and colleagues (Kadaba et al., 1989) and to the PlugInGait system of Vicon. Some of the studies using the Vicon motion system did not directly refer to the PlugInGait model, however, the description about the marker model suggests the use of the PlugInGait model.

An alternative to the Conventional Gait Model are six degrees of freedom models which assume the segments are unconstrained at joints. Most such models used the Cleveland Clinic Protocol, which was applied in the Motion Analysis Corporation's Orthotrack software (Baker, 2013), and the *Calibrated Anatomical System Technique* which was presented by Cappozzo and colleagues (1995). A six DoF system called *LAMB* was used from one of the studies (Table 3.4) which was developed (Laboratory for the Analysis of Movement in Children) from Rabuffetti and Crenna (2004) and two others used that of Vaughan and colleagues (1992).

For 11 out of 38 studies it was not possible to identify the type of biomechanical model. Glitsch and Baumann (1997) referred to an abstract from Baroni et al. presented on the XVth International Congress Biomechanics 2004. However, the abstract was not found to be able to confirm the biomechanical model used. Same problem occurred with the paper of Kerrigan and colleagues (1998) referring to a supplement from Pedotti and Frigo in Functional Neurology from 1992, and with Liu and Lockhart (2006) who referred to a study which has no additional information about the biomechanical model.

3.3.4 Musculoskeletal Models

The musculoskeletal model to estimate muscle forces describes the segments' and muscles' properties as well as the definition of the passive structures if included into a model (e.g. tendon, ligaments). Most musculoskeletal models found in identified studies are derived from the model

of Delp and colleagues (Delp, 1990; Delp et al., 1990). The basic model of one leg consists of seven rigid segments (pelvis, femur, patella, tibia/fibula, talus, foot, toes) with 43 musculotendon actuators attached to bony landmarks which were defined by digitising human bones.

These actuators were Hill-type muscle models, adapted from Zajac's work (1989), and scaled in its maximum isometric force, the optimal-muscle fibre length, the pennation angle of the muscle, and the tendon slack length (see also chapter II). The information of these scaling factors were derived from Wickiewicz and colleagues (1983) and Friedrich and Brand (1990). Most papers using the model of Delp adjusted the number of segments or the number of muscle tendon actuators depending on their focus of the study. Some included an upper limb model (Table 3.4) mostly by one segment representing the head arms and trunk (HAT) or additional segments at the foot.

Three of the identified studies refer to the musculoskeletal model of Anderson and Pandy (1999) which is modelled as a 10-segment (HAT, pelvis, left and right thigh, left and right shank, left and right hind- and forefoot) 23 degree of freedom linked model actuated by 54 muscle tendon muscles (24 muscles per leg). Muscle-tendon paths were adapted from the Delp model, the dynamics of the muscle-tendon unit from Zajac (1989). The model of Anderson and Pandy also allows to include ligaments into the model which are represented by joint torques restricting the joints in their range of motion. For all three studies there were no adjustments made regarding the number of segments or musculoskeletal actuators.

Six studies developed their own models (Table 3.4). They differ in the number of muscle-tendon actuators and in the number of segments. However, the muscles were mostly modelled based on the Hill-type muscle model. Hase and Yamazaki (1997) defined a full body 19 segments,156 muscle model which all joints modelled as ball joints. Collins (1995) modelled only in two dimensions using seven segments and eight muscles spanning the hip, knee, and ankle. Leardini and O'Conner (2002) focused only on the ankle joint which was modelled as a one degree of freedom hinge joint spanned by the tibialis anterior, the soleus and the gastrocnemius including three extensor retinaculum bands. Silva and Ambrosio (2003) defined 35 muscle actuators for one lower extremity with 16 segments of a full body model which are used to present a new solution to solve the redundant problem with mathematical modelling. The model of White and Winter (1993) was not fully described in their study as the number of muscles used for modelling and simulation are missing. The model is based on a classical seven segment

approach. Fluit and colleagues (2012) used the simulation tool *AnyBody* to implement a model into their estimation which has been developed in the Sim Mechanics toolbox of Simulink (MatLab 7.11.0, The MathWorks). Six segments are included but the number of muscles is not defined. However, this study only focused on the calculation of joint moments and not the estimation of individual muscle forces and was, therefore, only included in the joint moments group.

3.3.5 Sources of Geometric Parameters

The biomechanical models which are used for experimental data collection as well as the musculoskeletal models have to be scaled according to the subject specific anthropometric data. For the bony segments this means that the mass, the centre of gravity, and the moment of inertia are adjusted accordingly (Vaughan, Davis, & O'Connor, 1999). The values are either taken from cadaver studies, are calculated by mathematical models, are estimated by using different scan systems (e.g., magnetic resonance imaging), or can be measured by kinematic data (Table 3.4).

Identified studies often refer to cadaver studies from Dempster (1955) or Chandler and colleagues (1975) for the inertia and the bony mass of the segments. Another study referenced widely is the technical note from de Leva (1996) who adjusted the values of Zatsiorsky and colleagues (1990). Zatsiorsky estimated body segment's inertial parameters with a gamma-ray scanner of 100 male undergraduate students. Another study which was used in some of the studies is that from Havanan (1964) who used a mathematical model to estimate the inertial properties. The model needs 25 different dimensions of the whole body to be able to scale the model which includes the circumference of the ankle, knee, thigh, head, or the foot length as well as the chest depth. With the further knowledge of the body mass Havanan set calculations for every segment with which it is then possible to estimate the anthropometrics of the body segments.

Another reference for body segment scaling is the work of McConville (1980). They used a technique called stereophotometrics which implements a three dimensional photography of the participant by cameras placed around the participant. Specific coordinates of body points serve as input into calculations which reconstruct the participant. McConville used this method to determine the relationship between the body anthropometrics and its body segments mass distribution on living participants.

3.3.6 Mathematical Modelling Techniques

Three main mathematical modelling techniques which estimated muscle forces were identified across the 19 included studies: static optimisation, an inverse dynamics approach (thirteen studies), forward dynamics and EMG-driven models, two dynamic optimisation approaches (three and six studies).

Static optimisation solves the redundancy problem (more muscles spanning a joint than degrees of freedom exist) by dividing up the experimental joint moments in different muscle forces acting on that joint at each independent instant in time. In other words, this method does not optimise the estimation by considering the whole time period of a gait cycle as a whole but analysis the muscle forces for each time step with only the experimental input given for this time step. The information of the joint kinematics as well as the calculated joint moments lets the model search for the optimal muscle activations, considering for example the moment arm of the muscles as well as the muscle characteristics defined in the musculoskeletal model while solving the equation of motions of the skeletal system (derived from the Newtonian mechanics, in more detail in chapter 4.4). Output are the muscle activations as well as muscle forces at each instance in time, without taking the activation-contraction cycle into account.

Forward dynamics instead matches the desired kinematics with estimated kinematics by using generalised muscle excitations and experimental ground reaction forces which is solved time-dependent over the whole gait cycle. This means, that forward dynamics computes a set of muscle excitations by solving the equation of motions, representing the electrical stimulation arriving at the muscle, and with the information of the ground reaction forces drives the model in time forward. This results in the kinematics of the next time step which are then compared the experimental kinematics, while the error between estimated and experimental kinematics are minimised. Therefore, one time step might influence the results of the whole gait cycle as forward dynamics optimises the outcome of this whole time period. To be able to do so, this technique needs additional information like the activation-contraction cycle of the muscle (chapter 2.6.1) which enables the model to output individual muscle forces (chapter 4.4).

EMG-driven models are another dynamic optimisation approach. Instead of the computed muscle excitations, EMG-driven models use experimental EMG excitations as input in the estimations. This constrains the muscles of the model regarding their level of activation throughout the gait cycle. With this information, the model can then estimate joint moments or powers which are then compared and their error minimised to the experimental data. Two

studies presented an enhanced inverse dynamics approach called physiological inverse dynamics (De Groote et al., 2009) and computed muscle control (Lin et al., 2012), both including additionally the activation-contraction cycle to a standard static optimisation approach (for more information, please see Chapter VI).

Both static optimisation and forward dynamics models use different optimisation functions to overcome the redundancy problem (Table 3.4). These functions normally minimise a cost function, which in the case of identified studies are the sum of squared muscle activations, the sum of all muscle forces or the sum of (squared) muscle stress. Forward dynamics can use additionally cost functions which are time depended, for example the minimisation of the metabolic energy. This is an advantage for patients with diseases affecting the activation-contraction coupling like neurological disorders.

3.3.7 Validation of Estimated Muscle Forces

A direct validation of estimated muscle forces is only possible with in-vivo techniques. However, good quality EMG data can give first indications about when a muscle should be active. Twelve of the 19 muscle modelling studies compared their estimated muscle forces with EMG patterns. In most cases, on-off pattern of the muscle activity were presented and not a whole activation of EMG excitations. The researchers rarely captured EMG data on their own participants and used EMG patterns found in the literature. Only three studies compared the muscle force estimation to experimental EMG data that they had captured themselves. The other studies which used EMG as a validation tool included EMG excitations from Inman (1953), Perry (1992), Hof (2002), or Anderson and Pandy (2001b). Leardini and O'Connor (2002) do not state their source of EMG patters they use in their graph as a validation.

Another validation process is the comparison of joint moments received through the muscle force estimation process with a classical static optimisation approach using ground reaction forces. Two EMG-driven studies used experimental joint moments for the validation process (Bogey et al., 2005; Buchanan et al., 2005). A variation of this technique is shown in the second study of Bogey and colleagues (2010) who used the ankle power as a comparison. In total, four studies did not validate their muscle force estimations at all.

3.3.8 Outcome Measures

Overall, joint moments of the hip, knee and ankle in sagittal, frontal, and transverse plane were present and were included in the digitising process. Figure 3.4 to Figure 3.7 and Figure 3.8 to Figure 3.15 present single curves as well as the grand mean and one and two standard deviation bands of the joint moments and muscle forces, respectively.

Estimated force data was available for 19 individual muscles or muscle groups: gluteus maximus, medius and minimus, psoas and iliacus (or iliopsoas), rectus femoris, vastus lateralis, medialis and intermedius (or vastii), semitendinosus, semimembranosus, biceps femoris long head and short head (or hamstrings), tensor fasciae latae, gastrocnemius lateralis, medialis, soleus (or triceps surae), tibialis anterior, and tibialis posterior. These muscles are all responsible for the process of walking (M. Q. Liu, Anderson, Pandy, & Delp, 2006; Perry & Burnfield, 2010). As described in the method section, muscles were summed up if identified studies divided muscles into different compartments. This has been done for the iliopsoas (psoas, illiacus), vastii (medialis, lateralis), gastrocnemius (medialis, lateralis), and the hamstrings (semitendinosus, semimembranosus, biceps femoris long head. Number of studies presenting joint moments and muscle forces which are included into the digitising progress are listed in Table 3.5 and Table 3.6.

Table 3.5. Number of studies which present joint moments of the lower limb divided up in hip, knee and ankle in sagittal, frontal and transverse plane.

Joint moment	sagittal	frontal	transverse
Hip	19	9	7
Knee	20	6	5
Ankle	27	8	8

Table 3.6. Number of studies which included muscle forces located in relevant databases. Bold numbers indicating number of studies included in this study.

Muscle		Compartments		Total
Gluteus maximus (a, m/l)	8			**8**
Gluteus medius (a/p)	7			**7**
Iliopsoas	4	Psoas Iliacus	1	**5**
Rectus femoris	11			**11**
Vastii	4	Vastus medialis Vastus lateralis	4	**8**
Hamstrings	7	Semimembranosus Semitendinosus Long head Short head	2	**9**
Tibialis Anterior	10			**10**
Gastrocnemius	8	Gastrocnemius medialis Gastrocnemius lateralis	5	**13**
Soleus	15			**15**

Note. a=anterior, p=posterior, m=medial, l=lateral.

3.3.8.1 Digitalisation of Joint Moments

In total, 29 studies included graphical or numerical information about joint moments of the lower limb during walking. The ankle was the most frequently presented joint (27 studies), whereas the sagittal plane was the most prominent plane (sagittal=26, frontal=23, transverse=20 studies). The standard method (three-dimensional inverse dynamics using a global reference frame) was used in all studies to calculate joint moments. Some papers compared this with other methods:

Alkjaer et al. (2001)	2D vs. 3D local vs. 3D global reference frame
Bogey et al. (2005)	ID vs. EMG-driven
Buchanan et al. (2005)	ID vs. EMG-driven
Fluit et al. (2012)	ID vs. FD
Heintz & G.-F. (2007)	ID vs. EMG-driven
Kerrigan et al. (1998)	Male vs. female

Lin et al. (2012)	ID vs. SO vs. CMC vs. FD
Liu et al. (2006)	3D local vs. 3D global
Ren et al. (2008)	Force plates vs. only kinematic data to calculate joint moments
Schache et al. (2007)	Different reference frames
White et al. (1993)	ID vs. EMG-driven

The female and male joint moment curves from Kerrigan showed significant differences at the knee flexion moment in pre-swing after being normalised to body mass and height. Therefore, gender curves were averaged together before they were included in the calculation of the overall mean and standard deviation. For all other studies, only the standard approach inverse dynamics to calculate joint moments was included into the digitising process as this will give the opportunity to compare the consistency between this standard approach to the new developed models to estimate muscle forces. Single curves of extracted joint moments can be found in Figure 3.4 which are all presented as internal moments.

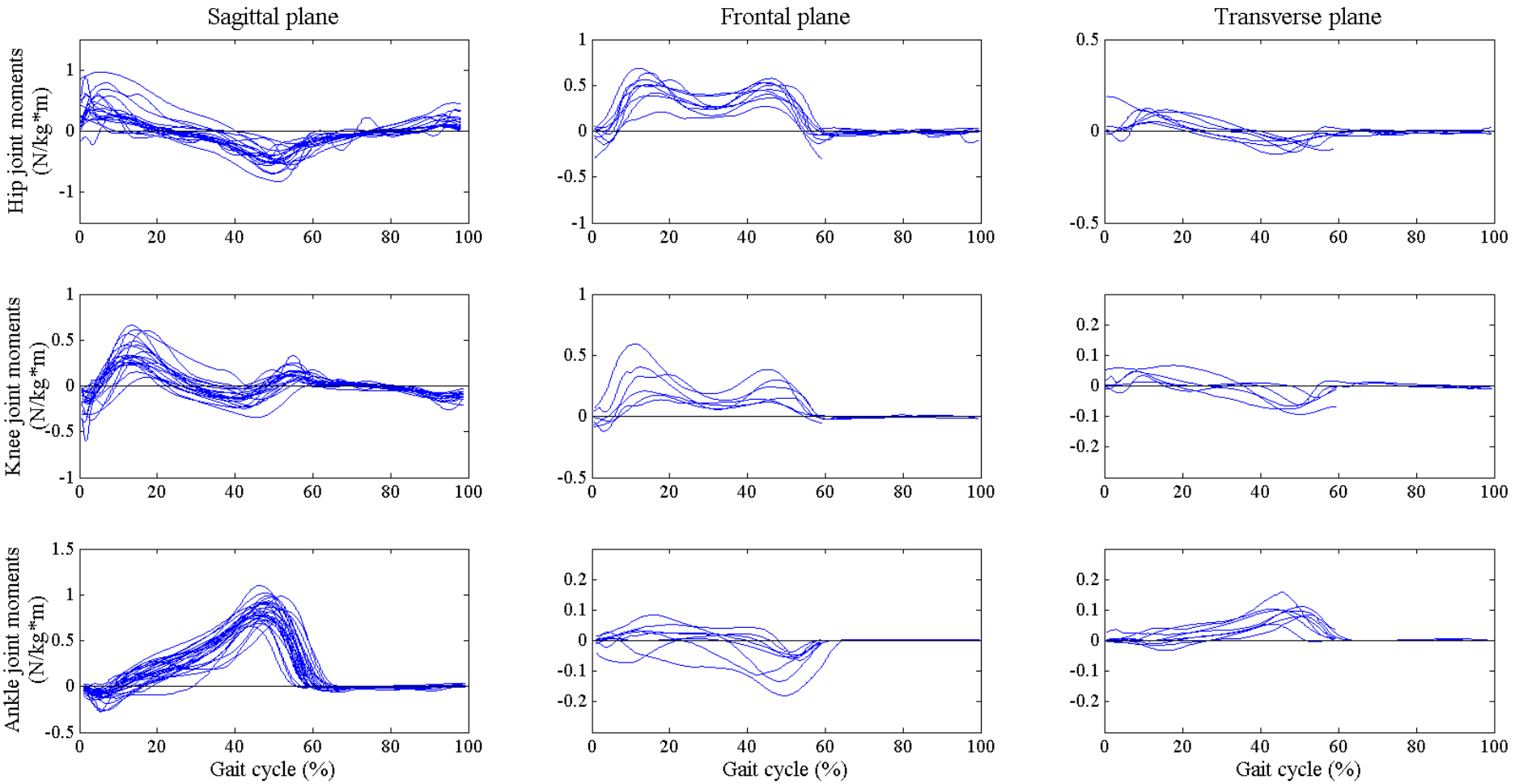

Figure 3.4. Mean joint moment profiles extracted from each identified study.

In the following paragraphs, averaged lower limb joint moment profiles are presented through a grand mean and one and two standard deviation bands over the whole gait cycle normalised to the body mass and height. All studies were ensemble averaged up to 60% of the gait cycle and is represented by a straight line in figures below. Only those providing swing phase information are presented after. Numbers in brackets indicate the number of studies included in the graph. Table 3.7 summarises the peak values of the grand mean as well as the CV of peak values.

Table 3.7. Maximum and minimum of averaged joint moments across included studies including standard deviation (SD) and coefficient of variation (CV) normalised to body mass and height. Number of joint moment profiles included are defined in brackets.

Joint Moment		Maximum (N*m/kg*m)	SD	CV	GC (%)	Minimum (N*m/kg*m)	SD	CV	GC (%)
Hip	sagittal (19)	0.38	0.23	0.6	3	-0.46	0.17	0.4	50
		0.18	0.12	0.7	96				
	frontal (9)	0.48	0.14	0.3	15	0.26	0.08	0.3	31
		0.45	0.10	0.2	45				
	transverse (7)	0.09	0.03	0.3	12	-0.07	0.03	0.5	48
Knee	Sagittal (20)	0.35	0.16	0.4	14	-0.12	0.05	0.4	42
		0.12	0.08	0.7	56	-0.13	0.05	0.4	95
	Frontal (6)	0.29	0.18	0.6	13	0.11	0.05	0.5	32
		0.22	0.11	0.5	46				
	Transverse (5)	0.04	0.02	0.4	9	-0.06	0.06	0.5	50
Ankle	Sagittal (27)	0.82	0.12	0.1	48	-0.10	0.07	0.7	5
	Frontal (8)					-0.08	0.05	0.7	51
	Transverse (8)	0.09	0.06	0.4	46				

Hip joint moments

Sagittal hip joint moments were presented in 19 studies (Figure 3.5). Highest CV was found at the end of swing (96%) with 0.7, however, with a much smaller mean value than both other peak moments. The two other peaks experienced slightly smaller CVs. Fontal and transverse joint moments, included in nine and seven studies, respectively, reached CV values up to 0.5 with the smallest CV of 0.2 at the second peak. The highest standard deviations are mostly found close to the peak values and generally in stance. Highest moments on the hip is shown

for the hip abduction moment. Almost all studies included the full gait cycle for the hip joint moments, except three studies (Alkjaer et al., 2001; DeVita, 2005; J. Liu & Lockhart, 2006).

Knee joint moments

Knee joint moments are presented in Figure 3.6. 20 studies included knee joint moments in the sagittal plane, while five of them focused on the stance phase only. Knee abduction and knee rotation moments were less present in the identified studies with six and five, respectively. The highest standard deviation at the knee extensor moment occurred during the first peak at 14% of the gait cycle. Here, the CV is the smallest at the knee with a CV of 0.4. A CV of 0.4 was also reached at the minimum peak in the sagittal plane as well as one peak in transverse plane. Highest CV occurred on the second maxima at the knee extensor moment (0.7), however, as well with a much smaller mean than other moment peaks sagittal at the knee.

Highest standard deviation bands are present for knee abduction moments in stance. The standard deviation stays high across stance but is the highest close to the peak moments. All three knee moments tend to go against zero in swing phase and also show small standard deviation bands. The highest peak is shown for the knee extensor moments with 0.388N/kg, whereas the smallest is shown in transverse plane for the knee rotation moment.

Ankle joint moments

27 studies included the plantar flexor moments, while eight studies concentrated on the stance phase only (Figure 3.7). For the frontal and sagittal plane, there are more studies including the stance phase only than the full gait cycle. All three joint moments at the ankle are close to zero in swing, whereas the standard deviation bands stay close to zero, too.

The CVs lie between 0.1 and 0.7, whereas the highest CVs occurred in the sagittal and frontal plane on the smaller peaks in stance. The standard deviation band in the sagittal plane is quite consistent throughout the stance phase. The highest joint moment throughout all joint moments is the ankle plantarflexor moment with at least two times higher moments than on the knee or hip. Ankle inversion and rotation moments are quite small compared to the other moments.

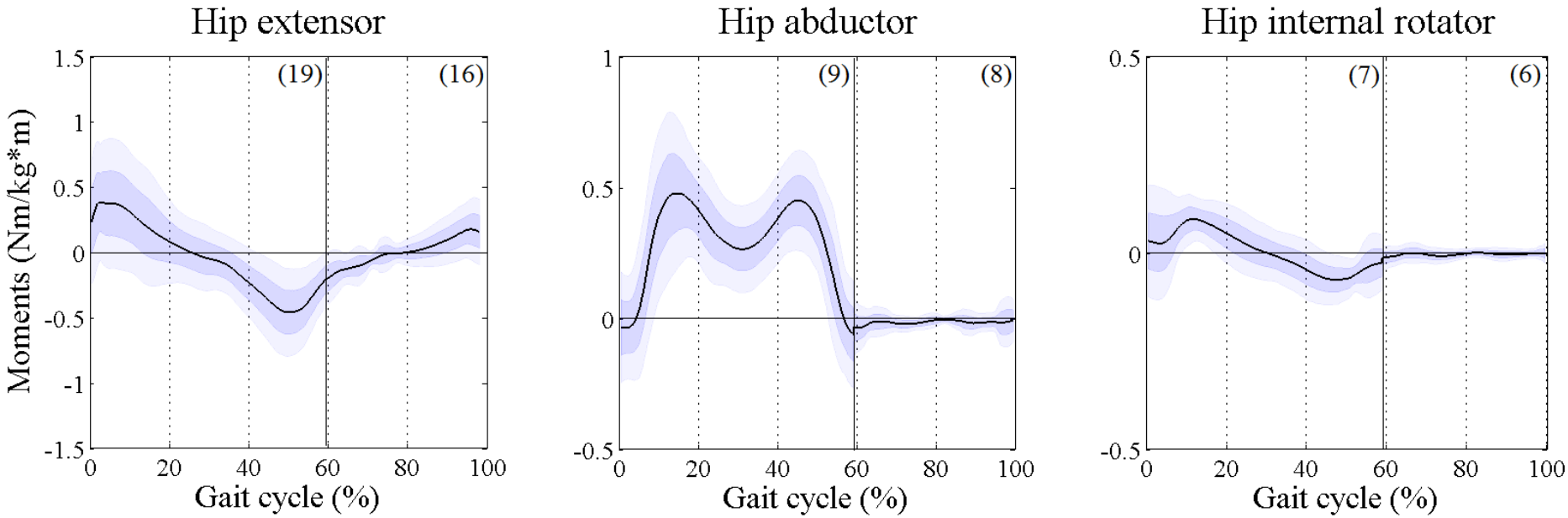

Figure 3.5. Overall mean and one and two standard deviation bands of the internal hip joint moments throughout a gait cycle, normalised to the body mass and –height. Vertical black line indicates studies which only included the stance phase of waling, number in brackets indicates number of studies.

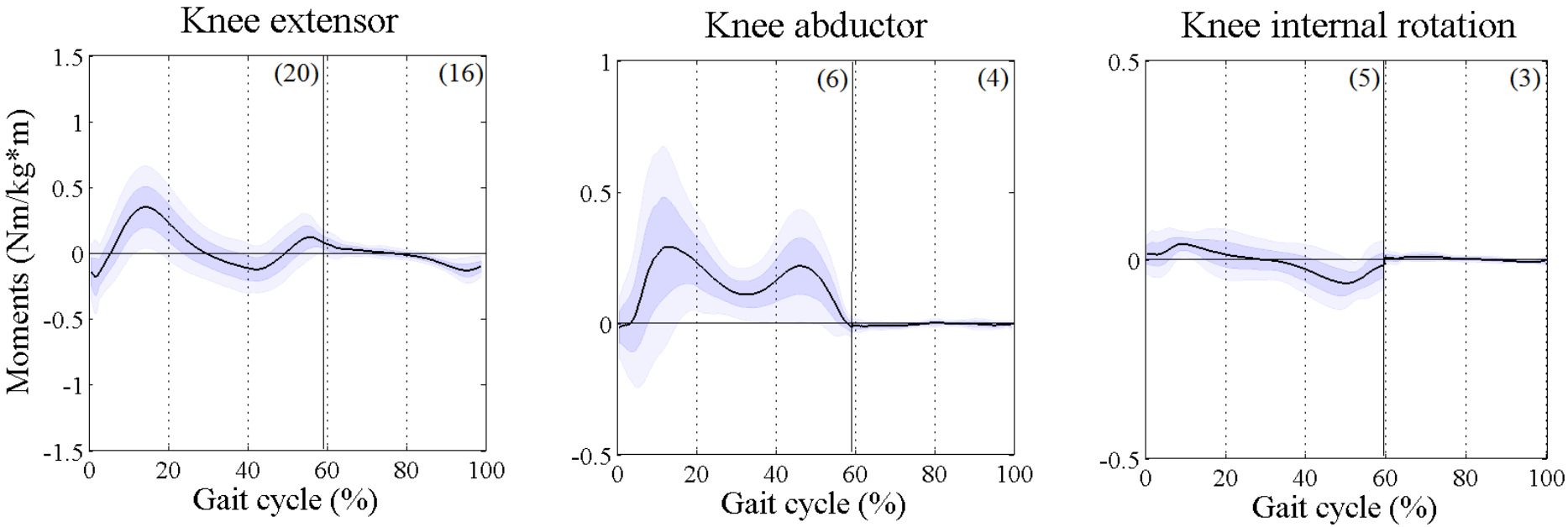

Figure 3.6. Overall mean and one and two standard deviation bands of the internal knee joint moments throughout a gait cycle, normalised to the body mass and –height. Vertical black line indicates studies which only included the stance phase of waling, number in brackets indicates number of studies.

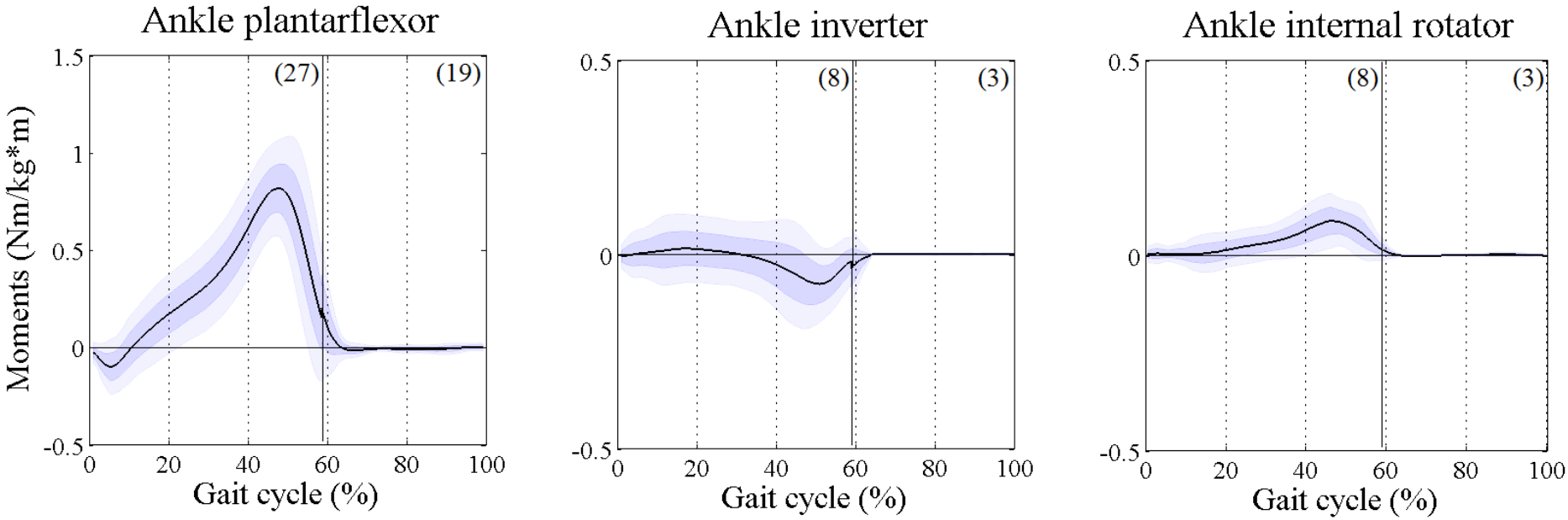

Figure 3.7. Overall mean and one and two standard deviation bands of the internal ankle joint moments throughout a gait cycle, normalised to the body mass and –height. Vertical black line indicates studies which only included the stance phase of waling, number in brackets indicates number of studies.

3.3.8.2 Digitalisation of Muscle Forces

The following section describes the muscle forces of tibialis anterior, gastrocnemius, soleus, rectus femoris, vastii, hamstrings, iliopsoas, gluteus maximus and gluteus medius across a gait cycle. The muscle forces were synthesised in three groups according to the model on which they were derived: static optimisation (SO), forward dynamics (FD) or EMG-driven models. The following studies included more than one mathematical model to estimate muscle forces and their graphical presentations were divided up according to the mathematical model used:

Anderson& Pandy (2001b)	SO physiological vs SO non-physiological vs FD
De Groote et al. (2009)	classical inverse approach vs physiological inverse approach
Heintz& G.-F. (2007)	SO vs EMG-driven
Lin et al. (2012)	SO vs CMC vs FD
Silva& Ambrosio (2003)	Two different SO types

The average across the gait cycle was taken for the two static optimisation approaches from Silva and Ambrosio (2003) and from Anderson and Pandy (2001b) as these pattern all represent an inverse dynamic approach. The three main mathematical models (static optimisation, forward dynamics, EMG-driven models) have been included in the digitalisation process, however, the physiological inverse approach from De Groote and colleagues (2009) as well as the mathematical model called computed muscle control form Lin and colleagues (2012) were neglected due to rare presence in the literature. They are, thus, discussed further in the discussion section below.

Individual profiles of muscle forces extracted out of identified studies can be found in Figure 3.8. In general, different studies show large variations between each other, however, for most of the muscles a broad agreement exists on an overall force pattern. Considerable variability can be found in minor features like smaller peaks or in magnitude. The consistency between studies seem to vary across different muscles; while studies of the hamstrings or the gastrocnemius are quite similar in their activation patterns and magnitudes, muscles like the iliopsoas or the tibialis anterior have distinctive differences in shape and magnitude between studies. Several muscles show evidence of different patterns in sub-sets of the studies especially

at gluteus maximus where two different patterns at initial contact and early stance exist. This seems not dependent on modelling approaches as both static optimisation and forward dynamics are included into both force sub-sets which suggests that other factors may be more important for differences between studies. Contrary to this, EMG-driven force patterns have mostly smaller force generations throughout the gait cycle than forward dynamics.

For some of the muscles and specific parts of the gait cycle, clear outlier can be detected. The study of Lin and colleagues (2012) (iliopsoas and gluteus medius, both static optimisation and forward dynamics), of Hase and Yamazaki (1997) (rectus femoris, forward dynamics), of Ackland and colleagues (2012) (hamstrings, static optimisation), of Heintz and Gutierrez-Farewik (2007) (rectus femoris, EMG-driven) and the study of Komura and colleagues (2005) (vastii and gastrocnemius, static optimisation) show a much higher and/or longer maximal force development than remaining studies. Other muscle force patterns like the iliopsoas from Fraysse and colleagues (2009) (static optimisation), the soleus and the tibialis anterior of Heintz and Gutierrez-Farewik (2007) (EMG-driven), the soleus of Anderson and Pandy (2001b) (static optimisation and forward dynamics) or the tibialis anterior of Glitsch and colleagues (1997) (static optimisation) show total different patterns than the rest of the studies. The results of Lin and colleagues and Anderson and Pandy suggest as well that other factors than the principles behind the mathematical models to estimate muscle forces may be influencing the differences between studies.

The most outstanding curve which has been extracted from identified studies is the hamstring estimation from Fraysse and colleagues (2009). This profile shows a completely different pattern than the rest of extracted hamstrings profiles. While other studies present the hamstrings to be active in the beginning of the stance phase and at the end of swing, the curve of Fraysse and colleagues has its maximum in mid-stance while being inactive at the start and in the end of the gait cycle. Because this pattern is totally contradictive to known EMG excitation studies, too (Perry & Burnfield, 2010; Winter, 1990), the hamstring profile of Fraysee and colleagues has been excluded.

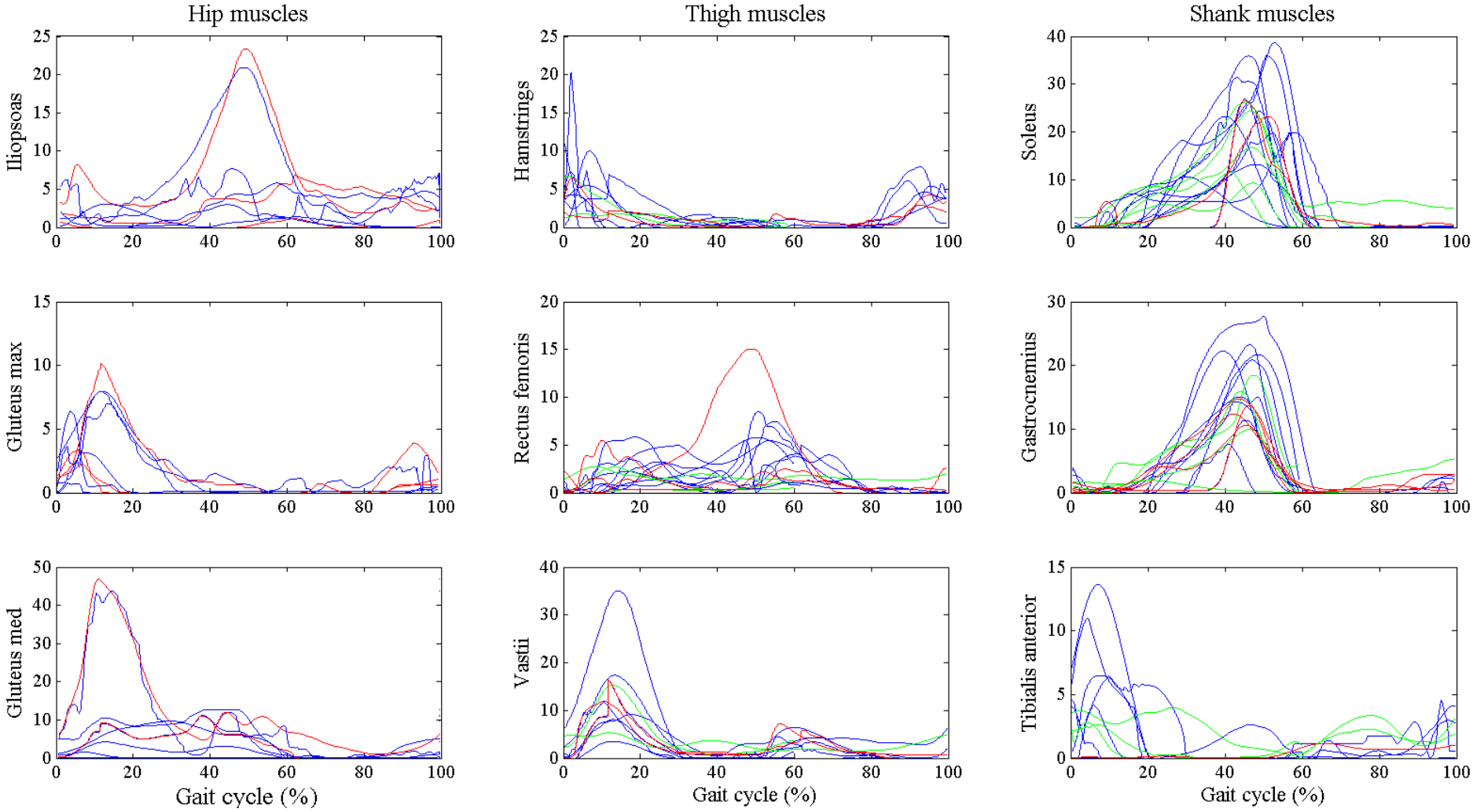

Figure 3.8. Single muscle force profiles normalised to the body mass (N/kg), extracted out of identified studies. Blue=static optimisation, red=forward dynamics, green=EMG-driven models.

Table 3.8 describes maximum peak forces and their CVs as well as the maximal standard deviation across a gait cycle, split up into different mathematical model groups. They are further described in the following paragraphs which give an overview about digitised muscle force profiles of the lower limb. Across all muscle forces, static optimisation is the most frequently used technique compared to forward dynamics and EMG-driven models. No EMG-driven model has been used to estimate muscles on the hip joint (iliopsoas, gluteus maximus and medius).

Table 3.8. Maximal standard deviation and maximal peak force of the lower limb muscles, normalised to the body mass. Number in brackets indicate number of muscle profiles included.

Muscle	type	max 1	SD	CV	GC (%)	max 2	SD	CV	GC (%)
Tibialis anterior	SO (7)	5.56	4.34	0.8	6	2.64	1.66	0.6	96
	FD (1)	1.14	--	--	64	--	--	--	--
	EMG-dr. (3)	2.98	2.79	0.9	4	2.81	1.00	0.4	78
Gastrocnemius	SO (10)	15.08	7.46	0.5	44				
	FD (2)	12.35	0.95	0.1	45				
	EMG-dr. (5)	13.53	2.88	0.2	46				
Soleus	SO (11)	20.03	9.67	0.5	47				
	FD (2)	23.12	1.58	0.1	48				
	EMG-dr. (5)	16.55	7.78	0.5	46				
Rectus femoris	SO (8)	2.71	1.58	0.6	21	4.22	2.39	0.6	54
	FD (3)	2.35	2.82	1.2	10	5.86	7.78	1.3	51
	EMG-dr. (3)	1.72	1.37	0.8	12	1.86	--	--	63
Vastii	SO (7)	13.71	9.91	0.7	12	3.07	2.41	0.8	62
	FD (2)	14.07	3.39	0.2	12	5.17	0.81	0.2	62
	EMG-dr. (2)	10.27	7.02	0.7	13	--	--	--	--
Hamstrings	SO (7)	6.78	5.79	0.9	2	4.57	1.71	0.4	94
	FD (2)	4.02	2.44	0.6	2	3.46	0.72	0.2	94
	EMG-dr. (2)	4.05	2.55	0.6	2	--	--	--	--
Iliopsoas	SO (5)	7.17	7.93	1.1	48				
	FD (3)	8.97	12.55	1.4	50				
	EMG-dr. (-)	--	--	--	--	--	--	--	--
Gluteus max	SO (6)	4.21	3.67	0.9	12				
	FD (4)	4.75	4.87	1	12				
	EMG-dr. (-)	--	--	--	--	--	--	--	--
Gluteus med	SO (7)	10.60	15.04	1.4	14				
	FD (2)	27.94	26.36	0.9	12				
	EMG-dr. (-)	--	--	--	--	--	--	--	--

Note. GC=gait cycle, SD=standard deviation, CV=coefficient of variation, EMG-dr.=EMG-driven.

Tibialis anterior

Ten studies included the tibialis anterior (eleven curves), whereas only one study used forward dynamics. There is considerable variability between studies estimating tibialis anterior force generation (Figure 3.8). In most cases, studies suggest peak activity in early stance but show considerable variation on the magnitude. Most also suggest activation in swing which is lower and also shows considerable variability in magnitude. Collated data (Figure 3.9) from both static optimisation and EMG-driven analyses confirms activation in late swing rising to a peak in first double support (6% gait cycle) but high SD and CV confirm considerable variability concerning the magnitude of these peaks. Force generation is low in second half of stance. EMG driven studies show increased activation in the first half of swing (peaking at 78% gait cycle with reasonably good repeatability) which is not present in any of the static optimisation studies. Data from the one forward dynamics study is quite different to the other two with minimal force generation in stance but a low level of activation through swing.

Soleus

With 18 curves extracted out of 15 studies, soleus is the most frequently estimated muscle. There exist a considerable variability between studies in magnitude and timing of maximal muscle force production (Figure 3.8). Peak forces lie between 30 and 60% of the gait cycle and are about 10 to 40N/kg high. Except one study (EMG-driven model of Heintz & Gutierrez-Farewik, 2007), studies suggest no force development in swing. Averaged profiles confirm maximum forces to be around 50% with high SD bands and CVs showing a high variability between studies (Figure 3.10). Averaged maximum force from all three mathematical models are similar in timing and magnitude. EMG-driven in swing phase and forward dynamics at first double support (8%) show different patterns compared to static optimisation which may be triggered through outliers described above. Forward dynamics CV is much smaller than for static optimisation or EMG-driven models which is confirmed through the standard deviation bands.

Gastrocnemius

17 curves from 13 studies define the muscle forces progression of the gastrocnemius during walking. There exists a general agreement between studies about the activation profile (Figure

3.8). After forces stay close to zero until 10-15% of the gait cycle, studies suggest a rise in force up to 50% of the gait cycle leading onto a rapid fall down close to zero at about 60% of the gait cycle. At initial foot contact and at the end of swing studies agree in a small force development. Considerable differences are shown in the magnitude of the maximum muscle force which lies around 10 to 30 N/kg. Peak forces and profiles are similar between mathematical models (Figure 3.11). The standard deviation for static optimisation is much higher than for forward dynamics and EMG-driven curves. Static optimisation and forward dynamics show the same patterns of late swing phase force generation which is completely lacking with EMG-driven models. Static optimisation's CV is as for the soleus much greater than for forward dynamics, but also for EMG-driven approaches.

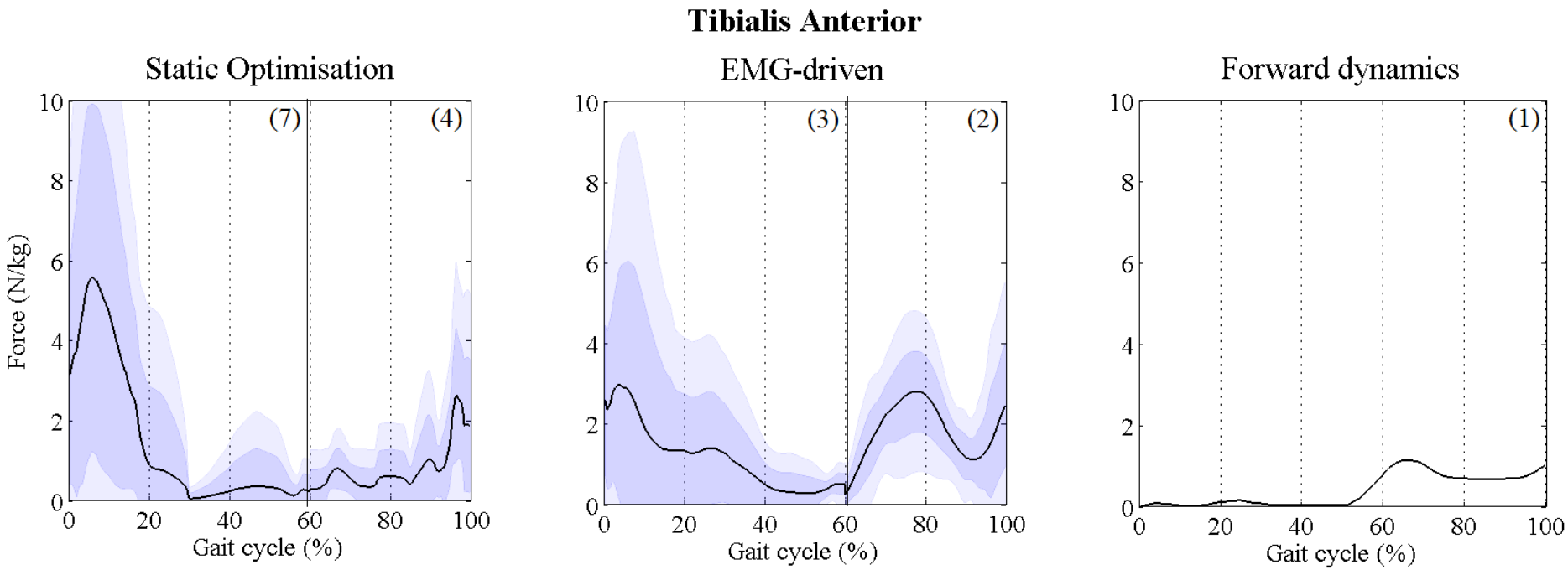

Figure 3.9. Overall mean and one and two standard deviation bands of the tibialis anterior throughout a gait cycle, normalised to the body mass, divided up into three mathematical models static optimisation., EMG-driven, and forward dynamics. Vertical black line indicates studies which only included the stance phase of walking, number in brackets indicates number of studies.

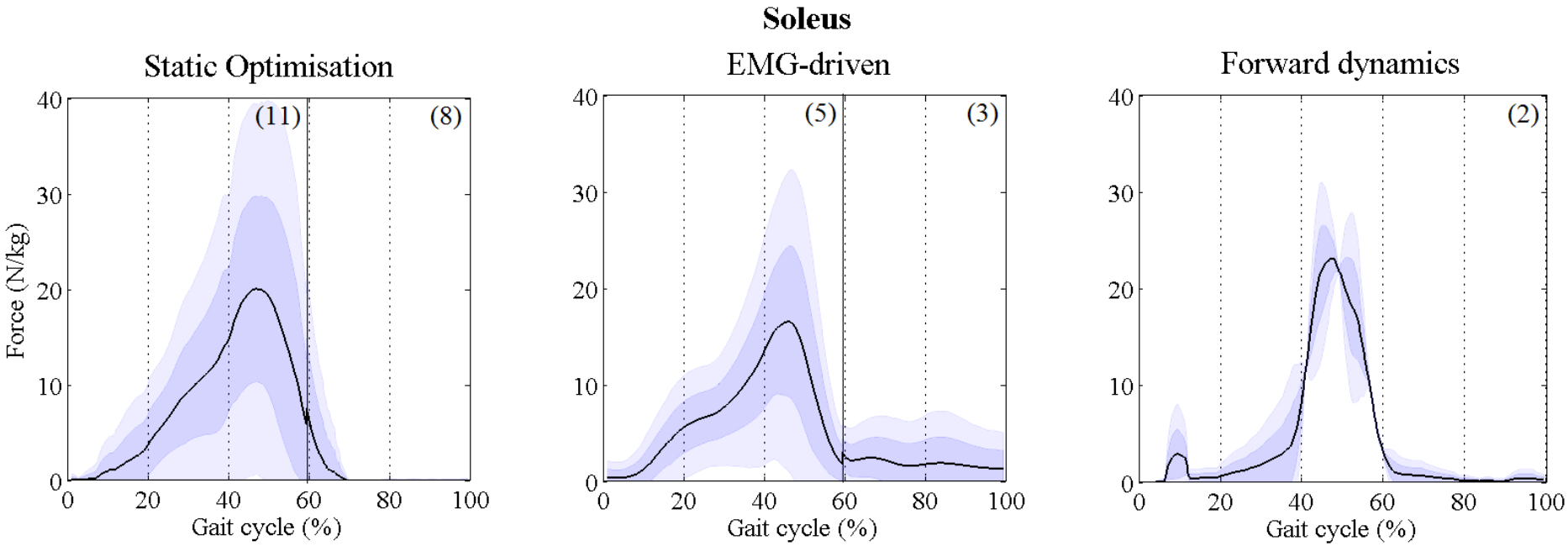

Figure 3.10. Overall mean and one and two standard deviation bands of the soleus throughout a gait cycle, normalised to the body mass, divided up into three mathematical models static optimisation., EMG-driven, and forward dynamics. Vertical black line indicates studies which only included the stance phase of walking, number in brackets indicates number of studies.

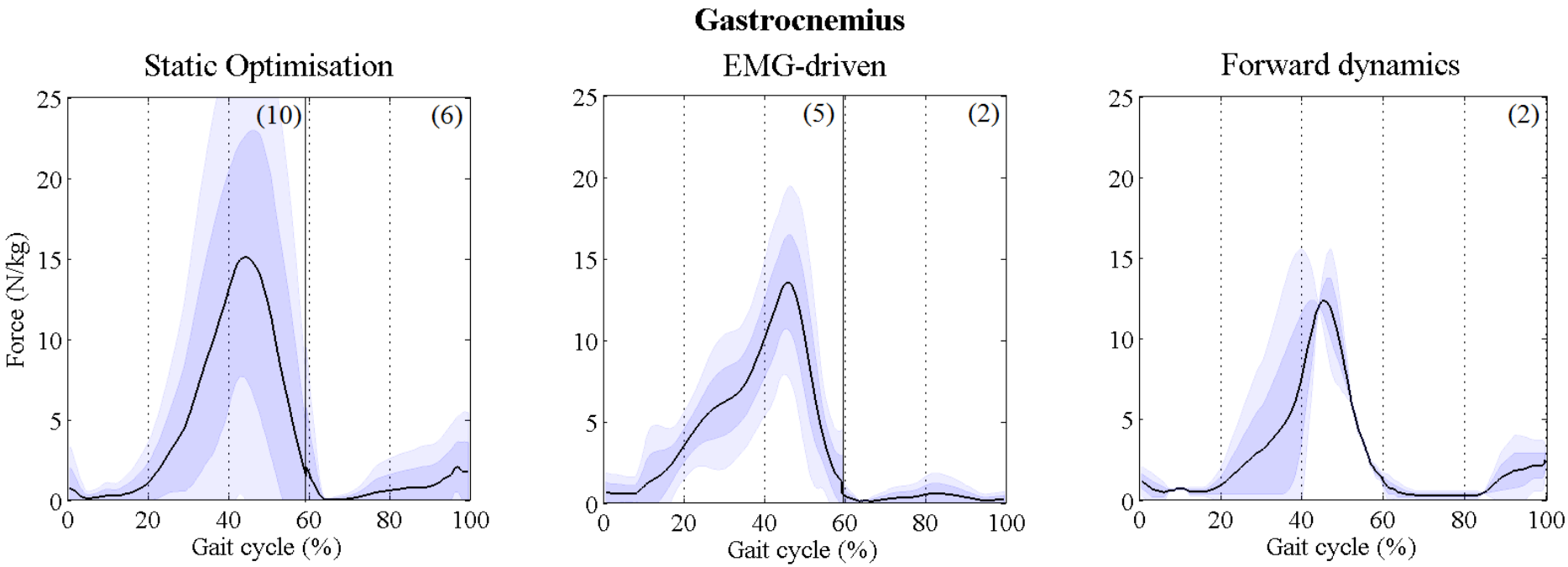

Figure 3.11. Overall mean and one and two standard deviation bands of the gastrocnemius throughout a gait cycle, normalised to the body mass, divided up into three mathematical models static optimisation., EMG-driven, and forward dynamics. Vertical black line indicates studies which only included the stance phase of walking, number in brackets indicates number of studies.

Hamstrings

Nine studies included muscle force estimations of the hamstrings (eleven curves). There is considerable consistency in profile and magnitude between these studies estimating hamstrings force production except for the force magnitude during initial contact (Figure 3.8). At this point of the gait cycle studies suggest a peak activation which decreases to zero at 20% of the gait cycle. After this first maximum hamstrings' forces stay close to zero until mid-swing at 80% of the gait cycle when the second maximum appears (90-95% of the gait cycle). Two slight different patterns are shown at the second maximum peak by two static optimisation curves being different to the rest of the curves (Collins, 1995; Rodrigo, Ambrósio, Tavares da Silva, & Penisi, 2008). First maximum peak between EMG-driven and forward dynamic approaches are similar with high standard deviation bands and CVs (Figure 3.12). Static optimisation shows here a greater maximum as well as higher standard deviation bands and CVs which, however, may result out of the heavy influence of one outlier (Ackland et al., 2012). Static optimisation and forward dynamics agree in the force production during swing but with a higher standard deviation and CV for static optimisation; EMG-driven models did not include the swing phase.

Rectus femoris

Recuts femoris has been presented in eleven studies which included in total 14 curves. There exists considerable variability between studies in rectus femoris force pattern and magnitude (Figure 3.8). An overall agreement is suggested by two peak forces during the first half of stance and during the second half of stance with decreasing force in swing down to zero. Static optimisation and forward dynamics suggest overall similar patterns with a small difference at the end of swing (Figure 3.13). Big differences in variability exist due to higher standard deviation bands and CVs for forward dynamics during the second peak. These differences may occur through the highly influence of one outlier (Hase & Yamazaki, 1997). EMG-driven analyses are different compared to others between 40-100% of the gait cycle. In this part of the gait cycle, the second peak does not occur and a constant force production in swing exists which is not shown for static optimisation and forward dynamics. However, only one study has estimated rectus femoris forces during swing with an EMG-driven approach which may represent the force production of an outlier (Heintz & Gutierrez-Farewik, 2007).

Vastii

Graphical presentation of eleven curves have been detected in eight studies presenting the muscle force generation of the vastii muscle group. There exists an overall agreement in the pattern of vastii muscle forces but with high variability in magnitude for the maximum peak at 10-15% of the gait cycle (Figure 3.8). Second smaller peak occurs at transition from stance to swing. Between first and second peak as well as after the second peak until the end of swing studies suggest minimal forces close to zero, except two outliers (Heintz & Gutierrez-Farewik, 2007; Komura et al., 2005). These may be responsible for the difference in force pattern and variability between mathematical models (Figure 3.14). Static optimisation and forward dynamics show similar patterns but different CVs during the first maximum peak. Furthermore, there exists different standard deviations between static optimisation and forward dynamics during the swing phase caused through the static optimisation outlier of Komura and colleagues (Table 3.8). Forward dynamics shows a steep peak force development at about 10% of the gait cycle, which reflects the heavy influence of the curve of Anderson and Pandy (2001b). Compared to static optimisation and forward dynamics, EMG-driven analyses present one curve with a different pattern during the swing phase which reflects the pattern of the outlier of Hientz and Gutierrez-Farewik (Figure 3.8). Both outliers cause the higher standard deviation bands for static optimisation and EMG-driven approaches compared to forward dynamics (Table 3.8).

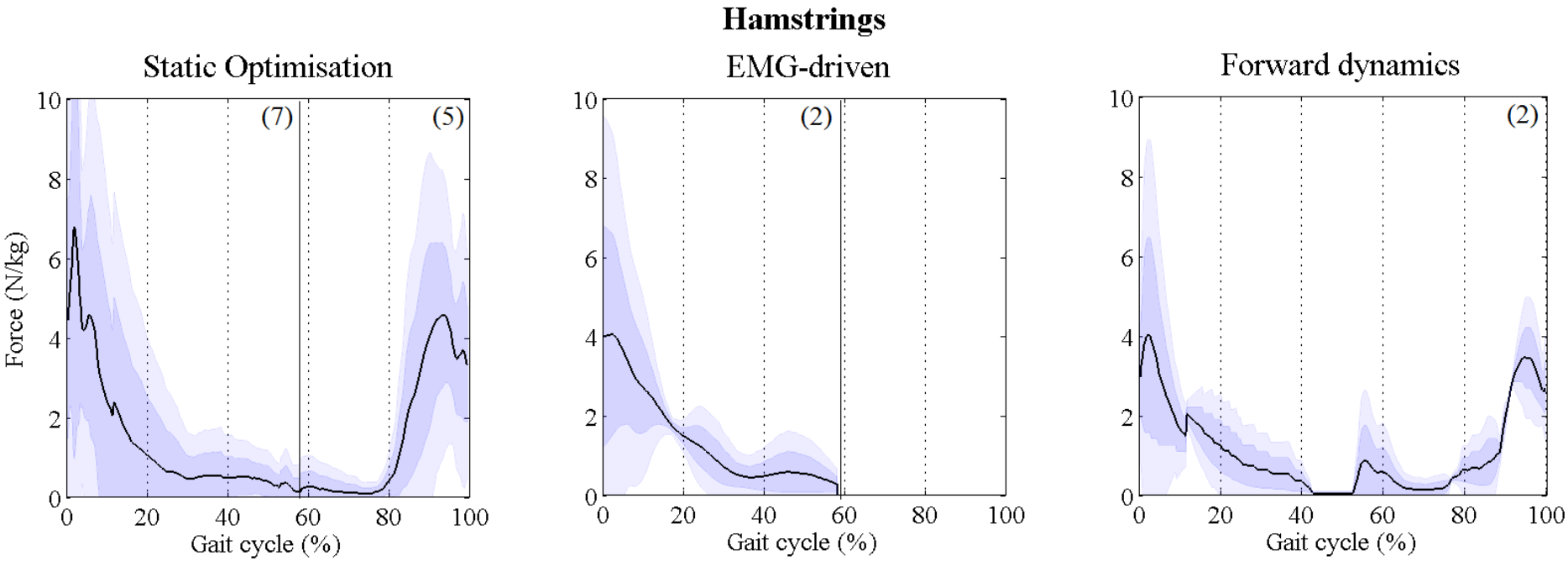

Figure 3.12. Overall mean and one and two standard deviation bands of the hamstrings throughout a gait cycle, normalised to the body mass, divided up into three mathematical models static optimisation., EMG-driven, and forward dynamics. Vertical black line indicates studies which only included the stance phase of walking, number in brackets indicates number of studies.

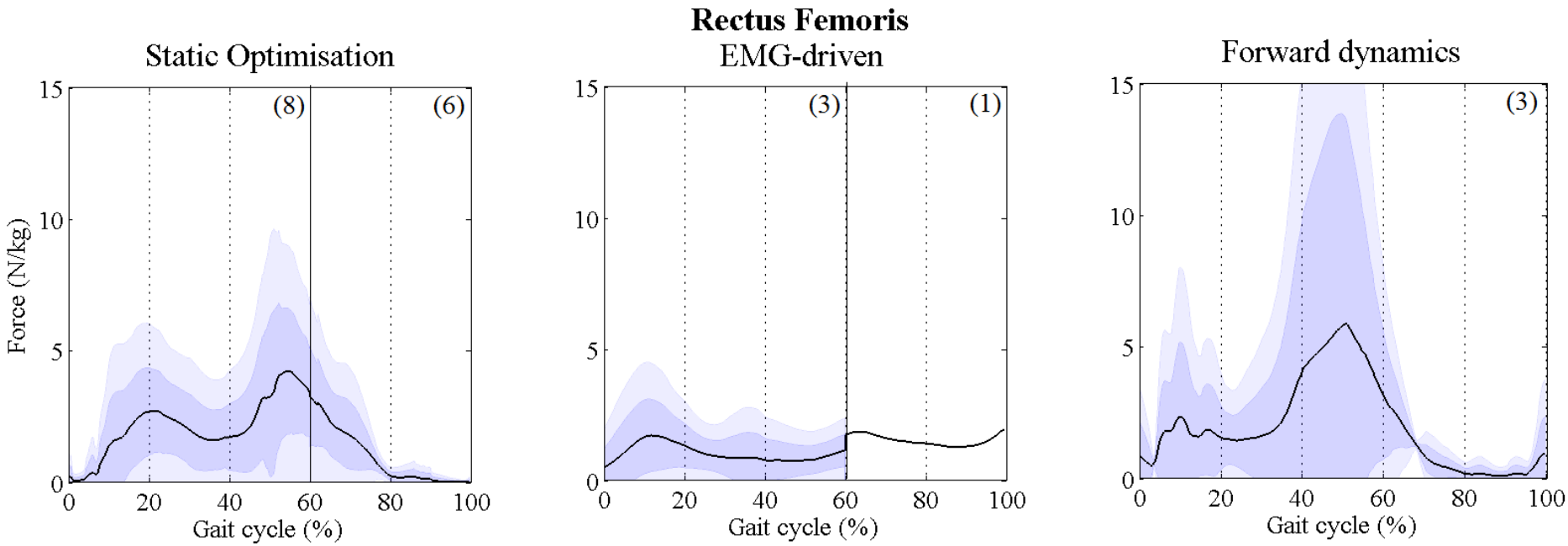

Figure 3.13. Overall mean and one and two standard deviation bands of the rectus femoris throughout a gait cycle, normalised to the body mass, divided up into three mathematical models static optimisation., EMG-driven, and forward dynamics. Vertical black line indicates studies which only included the stance phase of walking, number in brackets indicates number of studies.

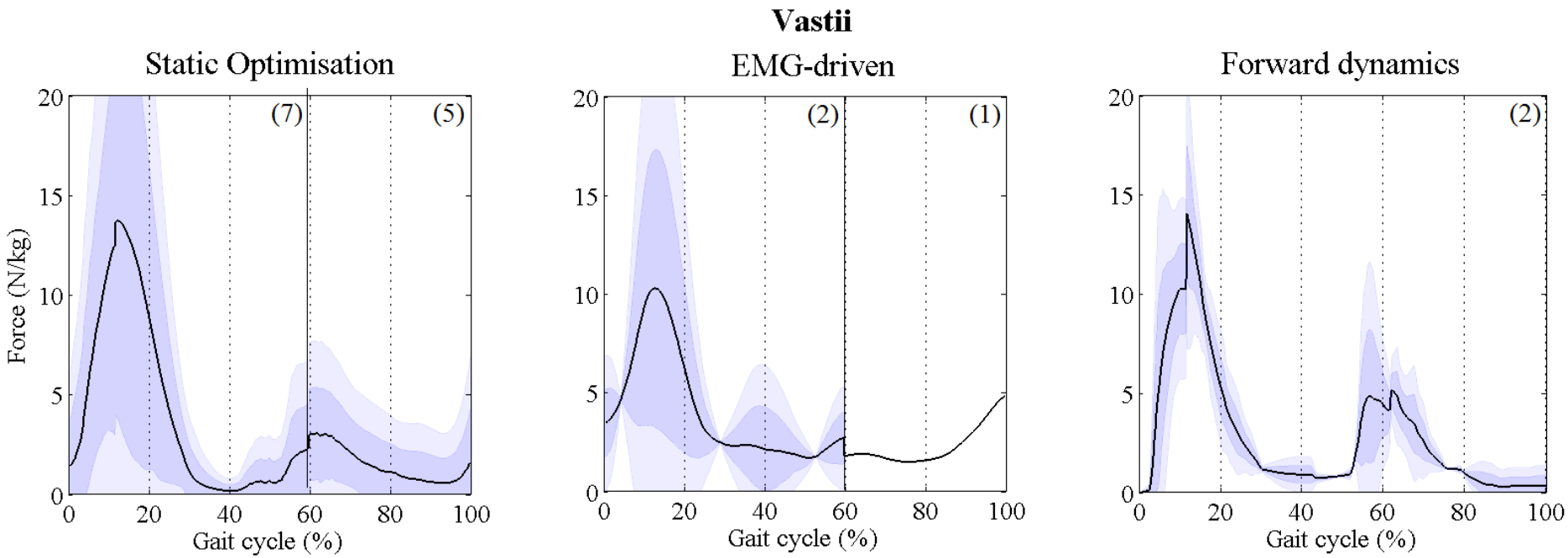

Figure 3.14. Overall mean and one and two standard deviation bands of the vastii throughout a gait cycle, normalised to the body mass, divided up into three mathematical models static optimisation., EMG-driven, and forward dynamics. Vertical black line indicates studies which only included the stance phase of walking, number in brackets indicates number of studies.

Iliopsoas

As described above, all three hip muscles (iliopsoas, gluteus maximus and medius) have not been included in an EMG-driven approach. Five studies and eight force profile curves in total presented the force production of the iliopsoas during walking. All curves included the whole gait cycle. Figure 3.8 shows very poor agreement between studies. Shapes in force production as well as magnitudes differs greatly between studies. The averaged curves in Figure 3.15 presenting static optimisation and forward dynamics are similar in shape and magnitude but seem heavily influenced through two outliers from Lin and colleagues (2012). After a small force generation during initial contact the force rises up to 50% of the gait cycle where it decreases again to a smaller force similar to forces appearing during initial contact. Throughout the gait cycle, high standard deviation bands exist which maximise around peak force and represent the great variability between curves. Both mathematical models have CVs over 1 (Table 3.8).

Gluteus maximus

Ten curves showing the gluteus maximus forces could be extracted which were presented in eight studies. The studies suggest two sub-sets in shape during initial contact until 40% of the gait cycle (Figure 3.8). One sub-set has a peak force close to initial contact which quickly decreases close to zero until 20% of the gait cycle, whereas the other pattern shows small forces during initial foot contact, which rises to its maximum at 20% of the gait cycle and decreases again until 40% of the gait cycle. Both sub-groups have curves from both static optimisation and forward dynamics. Studies suggest as well a small force production of the gluteus maximus close to zero except two studies which are slightly activated until the end of swing (Hase & Yamazaki, 1997; Lin et al., 2012). Both outliers, however, are not from the same sub-group. The average force profile of mathematical models is similar between each other. The slight difference of the forward dynamics curve of Hase and colleagues at the end of swing is represented through a small differences between the average profiles of static optimisation and forward dynamics. Standard deviation bands and CVs are similar between mathematical models (Table 3.8).

Gluteus medius

Seven studies with nine curves in total have been extracted showing the gluteus medius force generation. A considerable variability between studies is shown, whereas two different sub-sets can be defined (Figure 3.8). One sub-group, however, are two curves from the same study (Lin et al., 2012). This study shows a high peak at 18% of the gait cycle, and a decrease up to 40% with a second small peak at 50% of of the the gait cycle, whereas other studies are in general agreement with each other showing a slow rise in force to a much smaller force between 20-50% of the gait cycle compared to the curves of Lin and colleagues. Except the forward dynamics curve of Lin and colleagues, studies agree in a small force until the end of swing. Averaged curves of static optimisation and forward dynamics show similar patterns but great differences in magnitude for the peak at about 15% of the gait cycle. This may represent the outliers of Lin and colleagues and a different number of other studies of the second sub-group with which they are combined to form the average force profile (Figure 3.15). This also may be reflected in the higher standard deviations and CV of forward dynamics compared to static optimisation (Table 3.8).

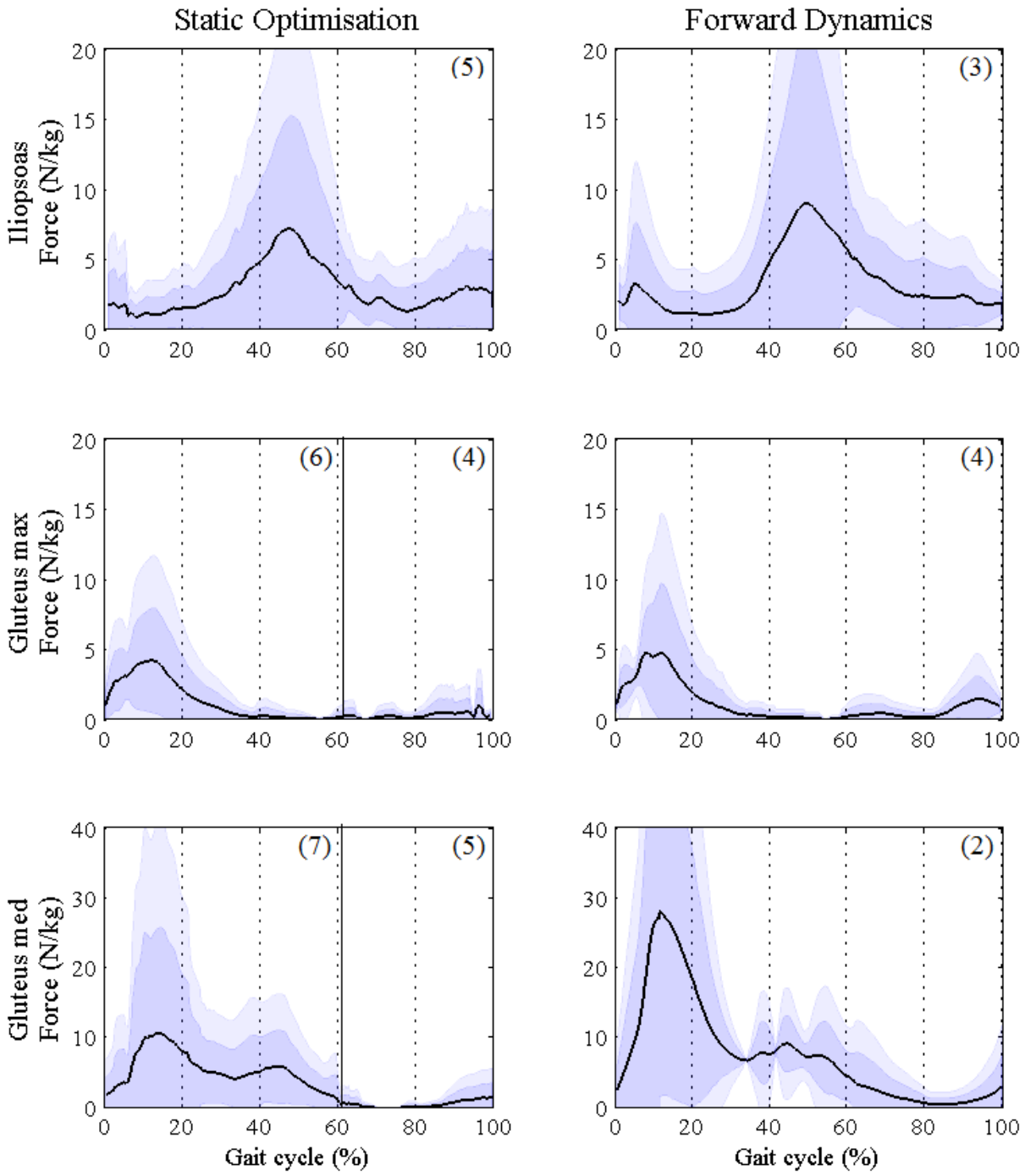

Figure 3.15. Overall mean and one and two standard deviation bands of the iliopsoas (top), gluteus maximus (mid),and gluteus medius (rear) throughout a gait cycle, normalised to the body mass, divided up into three mathematical models static optimisation., EMG-driven, and forward dynamics. Vertical black line indicates studies which only included the stance phase of walking, number in brackets indicates number of studies.

3.4 Discussion

This systematic review aimed to analyse existing estimated muscle force profiles of the lower limb during human healthy walking which were published in the academic literature. The objective was to be able to analyse the state-of-the-art of musculoskeletal modelling related to walking, to define the best mathematical method for the clinical gait analysis routine and to formulate recommendations for a standardised protocol. Joint moment profiles were included in the systematic review, too, which serve as a comparison in variability as well as a first indicator for the quality of the muscle force estimations.

The systematic review identified 9870 studies through initial electronic screening of relevant databases resulting in a much higher number than in comparable earlier reviews (e.g., Hollands, Pelton, Tyson, Hollands, & van Vliet, 2012; McGinley et al., 2009; Peters et al., 2010; Ridgewell et al., 2010, between 374 and 1132 studies). The cause for this may be that this systematic review is a "sensitive" rather than a "selective" search. This is driven by the need to identify a small number of studies which can be described using a wide variety of terms covering multiple research areas.

The results between joint moments and muscle force studies differ in their quality reporting and numerical or graphical moment and force presentation. A first quality distinction between muscle force and joint moment studies was made through the scoring principle. Studies focussing solely on the estimation of joint moments had a 20% higher overall score (77±10%) in comparison to muscle force studies (56±10%). Muscle force studies reached a smaller rating especially in the items 'task' description and 'measurement equipment' compared to joint moment studies. This may be due to a different interest of muscle force modelling studies as they often focus solely on the presentation of their mathematical model and underlying processes, which is reflected by a high rating of item 'muscle models'. The focus on the practical and clinical details seems often secondary. However, experimental data collection is crucial and should be presented in more detail. Joint moment studies, on the other side, are mostly based on a clinical background or focus on parameters related to the experimental data processing.

The quality assessment tool showed an overall higher score for EMG-driven models estimating muscle forces than static optimisation and, especially, forward dynamics. Forward dynamics papers scored worse than both other techniques in all items except 'muscle models', 'validation' and 'discussion'. Especially studies involving forward dynamics are focused on the description

of the musculoskeletal model and scored lower in other items. EMG-driven models scored higher in items related to the experimental data collection but showed deficits in presenting other items. All three modelling techniques have, therefore, significant limitations in presenting and describing the techniques and protocols they have used but inverse dynamics and EMG-driven models are achieving overall better results than forward dynamics. These scores, however, do not reflect the quality of the actual research of the studies. Missing information make it harder to compare the quality between studies and mathematical models with each other.

Another difference between joint moments and muscle force studies were the number of participants involved. Studies analysing joint moments included in average more participants than muscle force studies (10±19 vs 3±5, respectively). Most mathematical modelling studies estimating muscle forces included only a single participant (n=16 out of 19 studies). This may result of the fact that these studies simply presented their model technique on one participant (e.g., Anderson & Pandy, 2001b). Only three EMG-driven studies presented more than one participant (Besier, Fredericson, Gold, Beaupre, & Delp, 2009; Bogey et al., 2010; Bogey et al., 2005). In some studies, although more than one participant has been included, only one representative participant has been numerical or graphical presented (e.g., Ganley & Powers, 2004). To be able to include mathematical modelling into a clinical gait analysis routine, adequate data of a normative population is needed. To date, however, such a data pool has not been published.

3.4.1 Joint Moments and Muscle Force Profiles

Individual joint moment profiles are in broad agreement with each other. The pattern across a gait cycle is in general similar between studies, except the ankle joint moment in the frontal plane. This may occur because of the different foot models used across studies (Ferrari et al., 2008). This shape similarity between joint moment profiles is not present for the muscle forces which resulted in considerable differences between studies. A general agreement exists during maximum peak forces, however, with different levels of agreement for different muscles. For some of the muscle peak forces, the on-off pattern is similar but the force peak is shifted, for example the soleus where the peak forces of individual studies can be found between 30-60% of the gait cycle. The results of the CVs confirm a higher consistency for joint moments than for muscle forces, although the CV distribution between muscles is not homogenous. Most CVs

for joint moment peaks are saying under 0.5. For muscle force peaks, however, the CV range from 0.1 up to 1.4. Especially muscles acting on the hip (iliopsoas, gluteus maximus and medius) reach CV values over 1. Two muscles experience smaller CVs which are the soleus and gastrocnemius on the shank.

Distinctive outliers or sub-groups were detected for almost all muscle forces. Sub-groups were, however, not dependent on mathematical models. Individual outliers came from eight different studies which included curves of all three different mathematical models. For almost all of these studies, only one of their presented muscle was detected as an outlier; all other estimated muscle forces were in the range or had no abnormal force profile compared to the others. Quality assessment analysis results of studies including these outliers ranged from very low to high quality scores. Other possible factors which may have affected the outliers to be different to the others, may be the mathematical model or the cost function for optimisation. However, studies with outliers vary between all these factors, which may suggest a multifactorial influence on the estimation of muscle forces. As not all studies have reported clear information about their experimental data collection it may also result out of different protocols and poor experimental data.

The process of muscle force prediction can be simply divided in two main parts, the experimental protocol and its data as well as the actual modelling and simulation process. This "decoupling" of the experimental and modelling/simulation part is useful as different factors may influence the outcome of muscle force estimation. These are defined in the following chapters.

3.4.1.1 Influences on the Output through the Experimental Protocol and Data

Variability in joint moments and muscle force profiles may occur because of different reasons affecting the experimental data. A change in magnitude around a peak moment or peak force may occur because of different walking speeds (Schwartz et al., 2008). Schwarz and colleagues (2008) and Lelas and colleagues (2003) analysed the dependence of speed on kinematics, kinetics, and EMG excitations and show that speed has a significant influence on these parameters and that especially peak values increased or decreased with walking speed. This may be also partially the case for time shifts as the stance-to-swing relation changes with walking speed (Schwartz et al., 2008).

Other factors related to experimental data collection may have influenced the differences between studies. The filtering of experimental data which has been undertaken before the data was used in the calculations to receive joint moments and muscle forces could have influenced the output. For example the cut off frequency has an influence on the kinematics data which is used for both inverse dynamics and muscle force estimation as an input (Sinclair, Taylor, & Hobbs, 2013). But also the filtering of the ground reaction force could have changed the estimations' output (van den Bogert & De Koning, 1996). The reference frame in which moments referring to may change the kinematics as well (J. Liu & Lockhart, 2006; Schache, Baker, & Vaughan, 2007). Finally, the applied biomechanical model contains parameters which influence the calculation of kinematics and kinetics. Ferrari and colleagues (2008) compared five different biomechanical protocols with each other, including the PlugInGait model, the LAMB model and the CAST model (6-degree-of-freedom model). They placed 60 markers on three participants so that they were able to use the same trials for comparison. There result showed that (although intra-protocol variability was small) inter-protocol variability revealed high variability between protocols. Especially in the frontal and transverse plane the correlations were poor for the knee and ankle. The authors conclude, that comparing results from different protocols should be carefully undertaken.

Interestingly, one of the studies which was excluded from this systematic review compared the influence of different body segments' parameter estimation techniques, including the model of Havanan, the cadaver studies from Dempster and Chandler, and the in vivo body mass scan technique from Zatsiorski and colleagues and de Leva (Rao, Amarantini, Berton, & Favier, 2006). They observed that when applied to the classical gait analysis the body segment parameters were highly sensitive to the different techniques applied and received great differences during the swing phase. Furthermore, the study from Ren and colleagues (2008) claims that the mass properties of body segments can affect the estimated joint forces and moments. On top of this, a third study from Ganley and colleagues (2004) focused on lower limb anthropometry and compared a method using dual energy X-ray absorptiometry with the values of Chandler's work. They concluded that especially in swing phase joint moments could be influenced by using different anthropometric measures as the ground reaction force is zero.

3.4.1.2 Influences on the Output through Modelling and Simulation Processes

The higher consistency of joint moment profiles compared to profiles of estimated muscle forces may indicate that irregularities between muscle force estimations may not only result out of differences in experimental input but also through other factors related to the mathematical muscle force modelling and simulation. Three main mathematical models were identified (static optimisation, forward dynamics, EMG-driven). In general, no mathematical method has been found to result in more consistent results than others. Static optimisation was the most frequently applied method compared to the others and often used as a reference model to compare to other mathematical models. Static optimisation seems to be seen as the most widely accepted approach in the literature.

Some differences were detected in the magnitude of the peaks as well as some steeper or flatter rise in force production. Particular the profiles of forward dynamics experienced quite steep force developments which even could reach discontinuities (e.g., vastii). In some cases the magnitude differs (e.g. the hamstrings). Additionally, smaller peaks occurred for some of the muscles especially with forward dynamics which were not shown for the other mathematical models. EMG-driven models stayed for some of the muscles active across the whole gait cycle whereas other modelling techniques had phases where there was no force production at all.

Some identified studies compared mathematical models with each other. Anderson and colleagues (2001b) compared static optimisation with forward dynamics during healthy walking. They showed a general agreement between models, but some smaller differences for some of the muscles could also be detected. They concluded that static and dynamic optimisation should be seen as "complementary approaches". However, their comparison may have been biased by the fact that they used the joint moments estimated through the dynamic optimisation technique as an input in the static optimisation pipeline.

Heintz and Gutierrez-Farewik (2007) compared a static optimisation approach with an EMG-driven approach. The paper focused on the different energetic performance criteria while using the sum of muscle stress squared in the static optimisation approach and the product of maximal isometric muscle force in the EMG-driven approach. The maximal isometric forces used for the definition of the muscles as well as to normalise EMG excitations were the same. Results showed big differences between some of the muscles analysed. Lin and colleagues (2012) compared a static optimisation approach with computed muscle control (CMC) and a forward dynamics method adapted from Seth and Pandy (2007). Their results showed similar patterns

of muscle forces estimated by the three approaches for both walking and running in healthy adults as well. However, the data is only based on one participant. Furthermore, they used two different musculoskeletal models and simulation environments (Matlab and OpenSim) for different mathematical approaches which may have influenced the simulations' output. To verify both musculoskeletal models they run static optimisation though both simulation environments. Although an overall similarity could be shown some differences in magnitude and shape between both static optimisation solutions can especially be seen for muscles on the thigh and hip.

These results of Lin et al. have shown that using two different musculoskeletal models in two different simulation environments may change the estimation's output. Ten of the 19 muscle modelling studies used the musculoskeletal model of Delp and either applied it in the standard version or changed the number of muscles or number of segments (Delp, 1990; Delp et al., 1990). It is the model which is used regularly for muscle force modelling purposes in the academic literature. Other musculoskeletal models applied in identified studies were for example the musculoskeletal model developed by Anderson and Pandy (1999). However, as described in chapter II, they implemented parts of the Delp model, especially the geometric information for most of the muscles.

As discussed before, anthropometric differences and differences in the geometry of the musculoskeletal model can lead to differences in the modelling output. The degrees-of freedom of a model (Sartori, Reggiani, Farina, & Lloyd, 2012), the geometric properties of the segments, the number of the muscles, the geometries of the muscles, and the activation-contractions of the muscle-tendon properties influence the calculations' outcome. Although the Delp model has been used in more than 50% of the studies it has been adapted to the needs of the studies which may have led as well to the inconsistency between studies. Body segments parameters like the segments' mass or inertia and the source of lower limb anthropometry may also influence the estimations' outcome (Ganley & Powers, 2004; Rao et al., 2006; Ren et al., 2008). Some studies model muscles as one single line, whereas others represent a muscle by more than one compartment, especially when muscles fulfil more than one task. For example the gluteus maximus is a wide muscle which is involved with the extension, adduction and rotation of the leg. One of the developed models of Delp and colleagues (1990) represents this muscle with three different compartments.

Another factor which could have influenced the output of muscle force estimations are the different cost functions which were applied in identified studies. Monaco and colleagues (2011) changed the exponent of the muscle power from n=2 up to n=100 and compared their results to surface EMG excitations. They concluded that the exponent factor can have a significant influence on the final results. Collins (Collins, 1995) compared different optimisation techniques with each other, including the minimisation of the total muscle force, the total muscle force squared, total muscle stress, total ligament force, total contact force inter-articular, and instantaneous muscle power. Their result showed differences between minimisation principles and that the minimisation of total ligament force was the less successful method when compared to surface EMG excitations.

3.4.1.3 Muscle Force Estimation Compared to Experimental EMG

Experimental EMG excitations can either be used as an input into the estimation of muscle forces (EMG-driven models) or may be used as an indirect validation to get a first impression about the validity of the estimated muscle forces. A limitation of many identified studies estimating muscle forces was that, although muscle force studies frequently compared their estimations against EMG excitations they often did not comment on differences between mathematical model estimation and EMG or defined a "general agreement" between estimation and EMG excitations. For example Anderson and Pandy (2001b) experienced a great jump in their muscle force estimation of some of the muscles which they did not comment on in detail. Rodrigo and colleagues (2008) presented a much earlier maximum peak using static optimisation, still in the double support phase of the gait cycle, as the other studies show a burst in the single support phase.

But not all studies were ignoring differences occurring between estimation and EMG excitation. The EMG-driven estimation of Heintz and Gutierrez-Farewick (2007) shows the soleus especially in swing a totally different pattern than all the other studies. They conclude that it may indicate noise from the soleus' EMG signal. They further discuss that differences may result out of a failure to properly normalise the soleus to a known maximum force. They also criticise surface EMG in general that especially in the swing phase EMG excitations may reduce the quality of the estimation of muscle forces due to known limitations (electrical disturbances, electrode misplacement, intra-subject variation).

To get a first indication about the validity of the averaged digitised curves of identified studies they can be compared to the EMG excitations of Winter (1990). The patterns of averaged muscle forces are in a general agreement with Winter's EMG excitations. However, mathematical models differ for some of the muscles. For example, muscle force estimations of tibialis anterior are in their profile very similar to Winter's work, however forward dynamics shows a complete different activation in stance. Same results are found for the hamstrings, where static optimisation and EMG-driven models have similar patterns to Winter's EMG excitations of medial and lateral hamstrings, but forward dynamics shows an additional small activation around stance-to-swing transition which is not shown in Winter's EMG work. Gluteus maximus shows two different sub-sets of estimated muscle forces during the first 20% of the gait cycle. Winter's data supports the sub-set with the later peak, however, different sub-sets may also indicate different activation profiles between participants.

Extracted profiles from identified studies of the rectus femoris revealed interesting findings. The studies mainly agree on a peak activation at about 50% of the gait cycle. However, Winter's EMG pattern shows two additionally peak forces at beginning and at the end of the gait cycle. The study of Nene and colleagues (2004) investigated this behaviour and realised that these additional activations are crosstalk from the vastii muscle group which are captured with surface EMG equipment. They compared surface EMG to indwelling fine-wire EMG and could show that rectus femoris is only active at about 50% of the gait cycle. This information is an indication that the quality of the estimation of muscle forces may be good and that the mathematical models do work. It is important that in cases where muscle forces have been estimated with the help of EMG to careful interpret these results because of the known limitations of EMG and the differences between excitation and force production of a muscle.

When comparing the results to Winter's work the results show that not all outliers are totally off the muscle activation pattern. For example the force estimation of the gluteus medius in Lin and colleagues work shows a total different force profile than the other studies, but is the one closest pattern to the EMG gluteus medius from Winter. However, most of the outliers differ to the EMG activations of Winter, like the two outliers on the tibialis anterior. This shows the broad variability between studies and the difficulty in defining the "correct" muscle force estimation pattern. It is also important to keep in mind while comparing estimated muscle force data to experimental EMG excitation that muscle forces are not equal to muscle excitations. This means that although differences may exist between estimated muscle forces and

experimental EMG profiles that this is not a measurement or estimation error but simply the natural differences between the excitation of the muscle and the latter muscle force production.

3.4.1.4 Recommendations for a Protocol Suitable for the Clinical Gait Analysis

Summarised, significant limitations were shown for all three mathematical models, but the approach most promising for the clinical gait analysis is static optimisation as this method has already been widely used and tested in the literature. Furthermore, the summarised data presented in chapter 3.3 suggests that static optimisation produces results that are at least as consistent as shown for the other modelling techniques. Also, this method is much more time efficient compared to forward dynamic methods (Anderson & Pandy, 2001b) and is independent of EMG measures. An advantage of static optimisation to the models using experimental EMG excitations is the limitation of EMG-driven models reflected by the missing estimated forces of muscle at the hip (e.g. iliopsoas, glutei) which shows the restrictive access to specific muscles. Therefore, the robustness, its efficiency, the independence from experimental EMG excitations, as well as the summarised results of the literature makes static optimisation the most attractive model to be included into a clinical routine to estimate muscle forces (Lin et al., 2012).

The limitation of this approach compared to the others is that it does not take the muscle activation dynamics into account (Lin et al., 2012). This might be a limitation for patients with disorders affecting the activation-contraction cycle. A new developed technique called computed muscle control (CMC) which was presented in the identified study of Lin and colleagues (2012) promises to keep the computational time low while including the activation-contraction cycle by combining an inverse and a forward method. It was developed in cooperation with two main research groups involved in musculoskeletal modelling (Thelen, Anderson, & Delp, 2003) and is already implied in simulation environments like OpenSim. This approach, however, has not yet been widely tested in the literature and needs detailed testing and comparison with static optimisation.

Many influencing factors related to the experimental data collection or the modelling and simulation process were detected. It is important to understand the influence of these factors to be able to analyse estimated muscle forces. Known limitations resulting out of these factors can be taken into account to be able to use muscle force estimation in a clinical environment. However, more research needs to be undertaken to understand better the individual influences

of these factors. Also, to be able to compare between gait laboratories, it is either important to know the different protocols and the resulting changes in muscle force estimation profiles, or a standardised and free available protocol needs to be developed which can be used by every gait laboratory.

The validation of estimated muscle forces is crucial, however, to date only indirect methods are applicable in the clinic. Numerical or graphical presentation of muscle forces were often indirectly validated with experimental EMG excitations. Frequently, however, studies used EMG data from other studies or only compared to EMG on-off bars. Best validation with EMG excitations are experimental data of the same participant and same trial which has been used for the estimation of muscle forces. By doing so, individual differences as well as trial-to-trial differences can be eliminated. This is also important for EMG-driven estimations of muscle forces. It is crucial for these models to use high quality EMG excitations into the calculation of these models as this data are used to define the activation pattern of a muscle. EMG-driven models are, therefore, highly dependent on the operators knowledge and experience.

To be able to create a standardised and free available protocol a simulation tool needs to be included which fulfil these needs. The simulation tool OpenSim is a free available tool in the internet and already frequently used in the literature. This simulation environment has been also used in one of the included studies (Lin et al., 2012). Some of the mathematical models provided by OpenSim were already tested in the literature which makes this programme attractive to include into a standardised protocol. OpenSim has some other advantages compared to other programmes, which is that it gives access to detailed information about the musculoskeletal models. Furthermore, it provides a pipeline called SimTrack which gives the operator the possibility to estimate muscle forces in a routine processing (Delp et al., 2007). Also, the musculoskeletal models are based on the model from Delp which has been used and tested several times in the academic literature. Finally, it offers a wide range of different mathematical models, including the classical inverse dynamics approach (static optimisation) and the new developed technique CMC.

3.4.2 Limitations

Some limitations of this systematic review need to be discussed. To normalise the extracted joint moments and muscle force graphs the averaged body mass and body height across all included studies has been estimated to be used for studies which have not included this

information. This may have slightly altered the graphical presentation of joint moment and muscle force profiles. Also the stance phase was normalised to 60% in relation to swing in case this relation was not mentioned in the study. Another factor which may have influenced the consistency of muscle force profiles are the different walking speeds of the participants in identified studies (R.R. Neptune et al., 2008). Because not all studies mentioned the exact walking speed it was not possible to normalise against speed.

Furthermore, the process of digitising caused some issues for some of the joint moment and muscle force curves. Due to factors like the differences in the quality of colours, overlaying curves, or the graphs' differences in resolution, the digitising process could have caused some inaccuracies. Overlying curves resulted in manual digitising and guessing of the right rack of the curve, and different line widths, especially thick lines could have lead to errors. However, it was always attempted to approach the middle of these lines when they needed to be manually digitised.

3.5 Conclusion

This is the first study which thoughtfully summarised the knowledge about muscle force estimation during walking. Also, it is the first time that experimental data from the literature has been digitised and a huge amount of data has been merged together to be able to judge the variability which exists in the literature regarding joint moments and muscle forces of the lower limb in healthy adults.

Therefore, the results of the systematic review give a summary of what is known about muscle force estimation during human normal walking in the academic literature. Joint moment profiles were more consistent than muscle force profiles which showed that work needs to be done to conduct a standardised protocol to estimate muscle forces to eliminate influencing factors which may affects results. The well-established estimation of joint moments have been tested several times in the academic literature which makes a clinical interpretation of these possible. Limiting factors are known which can be taken into consideration. To be able to reach a similar standard for muscle force estimations, limiting factors need to be tested. This needs to be done on more than one participant to account for individual differences which may be otherwise interpreted as indication for another influencing factor. Direct validation of the estimation of muscle forces is not yet possible, however, the comparison to EMG excitation gives first indication when a muscle should produce force.

This standardised protocol needs to close the gap between a classical engineering and clinical approach. Both, the quality of the musculoskeletal model and the mathematical model to estimate muscle forces needs to be tested but also the application and understanding in a clinical setting needs to be given. According to the results of this systematic review, static optimisation is the model most suitable for the clinical but new developed techniques like computed muscle control may have potential to be used in the clinic, too. These models, however, need to be tested and implemented into a classical gait analysis routine to be able to judge their potential to be included into a standardised protocol. The dominance of OpenSim and its advantages compared to other simulation tools make it attractive to be included in such a standardised clinical routine. It provides the musculoskeletal models and mathematical approaches of interest to estimate muscle forces while the operator can customise the models according to the needs.

Therefore, the following chapter will test OpenSim's potential to be included into a standardised protocol using static optimisation and computed muscle control which then will be used in

praxis on a healthy population of ten participants. This will help to understand the clinical evidence of the estimation of muscle forces and may provide additional steps to be undertaken before the protocol can be used on patients in a clinical gait analysis routine.

CHAPTER IV

4 Technical Development of the Modelling and Simulation Protocol

A standardised protocol for the clinical gait analysis which includes muscle force estimation must be easy applicable and understandable. The systematic review has shown that to-date static optimisation, an inverse dynamics approach, may be the mathematical model most suitable for the clinic. Compared to forward dynamics or EMG-driven models it has a lower calculation time, is independent of EMG, and more robust than forward dynamics. However, static optimisation does not include the muscle activation-contraction dynamics in the estimation of muscle forces. Other limitations of these models are that they are essentially an optimisation technique optimising for example the overall muscle activation which may be not valid in conditions with disrupted neurological control. However, these techniques are to-date the best way which can be achieved to estimate muscle forces at the current state-of-the-art. The new developed method computed muscle control (CMC) pledges to combine both a low computational cost and the activation-contraction dynamics of the muscle. This technique has not been widely tested but first results show promising results (Lin et al., 2012) with potential advantages. Therefore, additional to static optimisation CMC is proposed to be tested for the use in clinical gait analysis.

To estimate muscle forces as a part of routine clinical gait analysis a simulation tool which can be incorporated into routine data processing is required. OpenSim is a freely available simulation tool which incorporates both static optimisation and CMC. The operator has the possibility to modify parameters in the musculoskeletal model OpenSim is supplied with or to create their own musculoskeletal model. One of the OpenSim models, *gait2392*, is the most frequently used in the literature to analyse muscle forces in the lower limb during walking and seems the most suitable model for this study (chapter III). Another advantage of OpenSim is that it provides additionally a standardised pipeline called *SimTrack* with, which the kinematics and kinetics as well as muscle forces can be estimated. At the start of this PhD project, OpenSim's SimTrack pipeline was planned to be used as a tool in its standard configuration while applying the musculoskeletal model *gait2392* in its standard form. After running some

pilot studies it became clear, however, that some minor and major adjustments were required to make the protocol suited to the requirements of clinical gait analysis.

This chapter, thus, describes the simulation tool OpenSim and its musculoskeletal model *gait2392* and the SimTrack pipeline and how these have been adapted in the light of these requirements. The standard package is described first followed by a number of separate adaptations that were undertaken. In the end a standardised protocol for gait analysis which includes the estimation of muscle forces during walking will be proposed which will be tested in the following chapter (chapter V).

4.1 Introduction to OpenSim

OpenSim is a simulation tool already frequently used in various research fields. OpenSim arose out of SIMM (Software for Interactive Musculoskeletal Modelling), a commercial tool which is used for biomechanical modelling, surgical planning, and ergonomic analysis (Delp et al., 2007). With SIMM it has been possible to create, alter, and evaluate different models of a wide range of musculoskeletal structures which have then been used to simulate different movements. Some are walking, running, cycling or stair climbing, or the consequences of different surgical implementations in joint mechanics or muscle function (R. R. Neptune & Hull, 1999; R. R. Neptune, Kautz, & Zajac, 2001; Thelen & Anderson, 2006; Thelen et al., 2005). SIMM, however, is essentially a modelling package and has very limited support for the simulation of movement using those models. Particular disadvantage is that it does not provide any assistance with the computation of muscle excitations for coordinated movements and only limited tools to analyse the estimated results (Delp et al., 2007). On top of that, the user does not have full access to the source code, which leads to difficulties in developing the researcher's skills and reproduce results achieved by other laboratories. As a consequence, OpenSim was developed by Delp and colleagues (2007) as an open source project allowing operators full access to all codes and models and incorporating a repository for the sharing of newly developed code and models.

The OpenSim programme is, therefore, a free simulation tool with which it is possible to create, exchange and analyse mathematical models and dynamic simulations of different kind of movements (Delp et al., 2007). The core is programmed in C^{++}, the graphical user interface (GUI) is written in Java (Hicks, 2013). The first version 1.0 was presented at the American Society of Biomechanics Conference in 2007. Since then, the programme has been used by many researcher and scientists based in different research fields, including sport science, computer animation, biomechanics research, robotics research medical device design, orthopaedics, and many more (Arch et al., 2015; Holloway et al., 2015; Miller Buffinton, Buffinton, Bieryla, & Pratt, 2016; Skalshoi et al., 2015).

The systematic review of this PhD has shown that OpenSim is already in use for the analysis of human walking. Besides different other models which are applicable for a variety of body parts involved in different movements, developed and shared either through the OpenSim group or developed by other users, OpenSim provides also musculoskeletal models for the purpose of human gait analysis. Because of its features OpenSim has, therefore, been chosen for this study

to estimate muscle forces during walking compared to experimental surface EMG which is described in chapter V.

4.2 Musculoskeletal Model gait2392

Most of the models which are available in OpenSim are based on the musculoskeletal model of Delp and colleagues (Delp, 1990; Delp et al., 1990). This model, in turn, was based on a model developed at the VA Rehabilitation R&D Centre on Palo Alto, California, and includes 43 muscle-tendon actuators of the lower limb. Delp enhanced the model and developed a graphics-based lower limb model to study the results of the musculoskeletal reconstructions on the function of muscles and resulting movement. It can be used for surgery simulations to enable an analysis and sttimation of surgical reconstructions of the muscles and bones of the lower limb.

Since then, the model has been widely used for different purposes and has been tested and adapted to present variations at a range of anatomical locations. For example Delp and Maloney (1993) changed the hip centre position to analyse the effect on the capacity of the muscles of generating forces and moments. They concluded that maximal muscle forces and moments are sensitive to the location of the hip joint centre. Another study from Gonzales and colleagues (1997) analysed the influence of muscle architecture and moment arms on the wrist flexion-extension moments. The motivation of the work was to study the different contributions of single muscles which span the wrist and to overcome the redundancy problem with this simulation. One of the first publications in a human walking related study involving the Delp model was from Piazza and Delp (1996), who analysed the role of muscles on sagittal knee flexion during the swing phase of walking. In the same year Delp and colleagues (1996) studied the length of the hamstrings and psoas during crouch gait in cerebral palsy compared to normal walking and discussed the implications for a muscle-tendon surgery.

In OpenSim, musculoskeletal models are defined in an .osim file format using eXtended Mark-up Language (XML). It is essentially a collection of rigid segments (bones) which are linked by joints with a range of different degrees-of-freedom. Muscles are defined as acting in a straight line between an origin on one segment and insertion on another. In some cases, intermediate via points are included to represent wrapping around other structures like bones, other muscles or retinacula. A model of the physiology of the muscles' excitation, activation, and contraction is incorporated to define the forces the muscles generate in response to a given neurological impulse. Each of the different components is described by a number of parameters (e.g., maximum isometric force, position of a joint centre, axial orientation…) which can be modified by the user. Lower limb models also generally include a representation of how the

foot interacts with the ground (Hicks, 2012b). For the purpose of gait analysis a model including the lower limb and the torso is mainly sufficient while considering the aim of the study. For a standard gait analysis with interest on the lower limb no upper extremities are needed, as it has been shown that the arm swing has a small influence on walking parameters (Umberger, 2008). However, for some of the models a torso segment is included which presents to upper body mass and is required for some of the calculations to estimate muscle forces.

The most frequently used model for gait simulations in OpenSim is a three-dimensional model called *gait2392*, one of the core models in OpenSim. It has been adopted from the Delp model (1990) and was designed for simulations of movements which are leg dominated (Au & Dunne, 2012). Main developers of the model were Darryl Thelen from the University of Wisconsin-Madison and Ajay Seth, Frank C. Anderson and Scott L. Delp from the University of Stanford. This model represents the segments torso (including the head), pelvis, femur, tibia, fibula, talus, foot (including calcaneus, navicular, cuboid, cuneiforms, metatarsals) and toes (Figure 4.1).

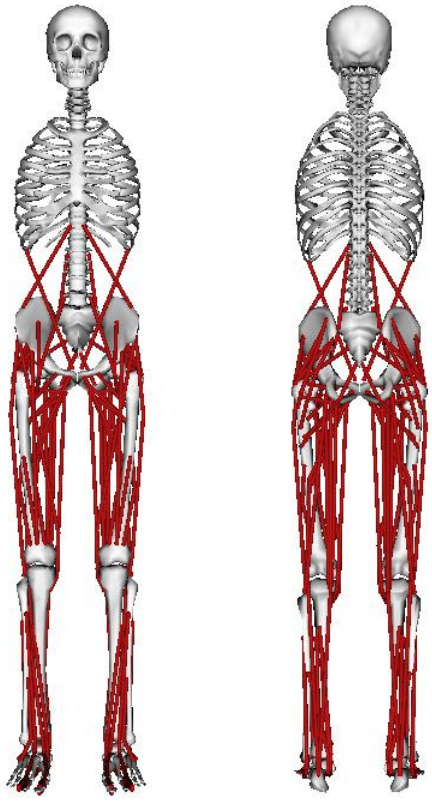

Figure 4.1. OpenSim's musculoskeletal model gait2392, with twelve segments, 23 degrees of freedom and 92 muscle-tendon actuators.

The name of the model gives the degrees of freedom (23) and the number of muscle-tendon actuators (92) of the model. The actuators can be summed up to 72 muscles, as some of the larger muscles are represented through more than one muscle-tendon compartment depending on their anatomy. For example, if a muscle is widely diversified and acts in more than one direction like the gluteus then it may be modelled as a number of essentially independent muscle elements (Figure 4.2). More information and a list of all actuators can be found in appendix A1.

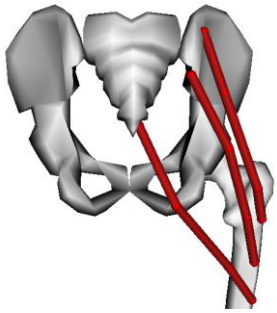

Figure 4.2. Representation of the gluteus maximus in the OpenSim model gait2392. Three musculo-tendon compartments define the whole muscle.

The generic model of *gait2392* describes a male subject with a body height of 1.80m and a body mass of 75.16kg. The bone geometry data of the pelvis and the femur are acquired by marking the surface of bones with a mesh of polygons which were then digitised to determine the coordinates of the vertices (Delp, 1990). Geometry data for the bones of the shank and the foot have been adopted from a Master thesis of D.L. Stredney from the Ohio State University from 1982 (Au & Dunne, 2012). These coordinates of the bones are then used in a file to set the bone geometries for the musculoskeletal model.

All segments are modelled as rigid-bodies, with each corresponding reference frame fixed inside each segment (Figure 4.3). The axes are defined as x-axis to represent the anterior-posterior direction, y-axis the proximal-distal direction, and z-axis the medio-lateral direction. This stays constant for all reference frames and coordinate systems in this study. The relative motion of the segments to each other are defined by the following joints: lumbar joint, hip, knee, ankle, subtalar, and metatarsophalangeal (MTP) joint (Delp et al., 1990). The coordinate frame of the pelvis is modelled parallel to the ground midway between the anterior superior iliac spines (ASIS), meaning that in neutral position there exists a zero pelvic tilt with respect

to the laboratory's ground. This is important to take into consideration, because many biomechanical models used in clinical gait analysis use the pelvic tilt in neutral position (i.e. location of ASIS and PSIS) as a zero reference and this is thus anteriorly tilted by an average of 14° with respect to the *gait2392* pelvis.

The length of the segments of the generic model gait2392 were extracted from Delp's model (1990). The anthropometric details of the segments including the mass and inertial properties are adapted from Anderson and Pandy's work (1999), who modelled a 10-segment, 23 degree-of-freedom model. They based the inertial properties as well as the mass of the segments on the average anthropometric data from five healthy participants (26 ± 3 age, 1.77 ± 0.03m, 70.1 ± 7.8kg) using the method of McConville (1980). For the model gait2392 these properties are then multiplied by a factor of 1.05626 (Au & Dunne, 2012) which is defined in the OpenSim user guide. This number, however, has not been verified by the developers of OpenSim and reasons for the scaling to this factor are unclear. The centre of mass and inertia characteristics for the hindfoot and the toes have been found by measuring the surface of a tennis shoe size 10 (Au & Dunne, 2012). The density is then divided up in separate foot segments while assuming a uniform density of the foot with 1.1 g/cm^3. All mass and inertial properties of the gait2392 model can be found in appendix A2.

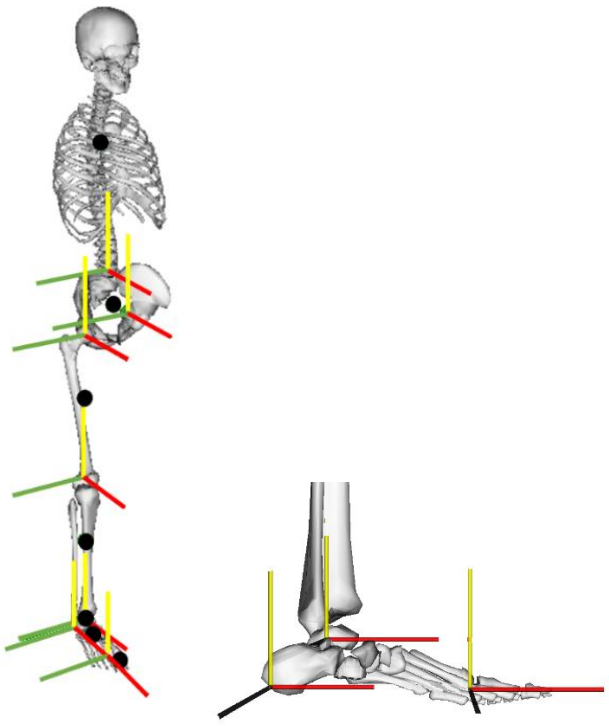

Figure 4.3. Coordinate frames and centre of mass for each segment of the gait2392 model in OpenSim. Red lines represents the x-axis, yellow lines represent the y-axis, and black lines represent the z-axis.

The characteristics of the lumbar joint are taken from the work of Anderson and Pandy (1999). The trunk segment is articulated with the pelvis through a three degree-of-freedom ball and socket joint which is located at the third lumbar vertebra. The hip joint is characterised as the same type of joint as the trunk-pelvis joint, the femur head is fixed in the acetabulum of the pelvis, whereas no translations between segments are possible.

The modelling of the knee joint is more complicated than the hip joint due to its multi-bone and ligament structure. The knee joint properties are implemented from Yamaguchi and Zajac (1989). They designed a one-degree of freedom model which includes both the tibio-femoral and the patella-femoral joint. Additionally, it accounts for the levering mechanism of the patellar. For the model *gait2392* the patellar has been excluded to simplify the kinematic constraints. The femoral condyles, modelled as ellipses, can move on the tibia plateau, with the contact point of being a function of the knee angle (Nisell, Németh, & Ohlsén, 1986). Examples of the segmental parameters defined in the .osim file of the *gait2392* model can be found in appending A3.

4.2.1 Muscle-tendon Properties

The geometry for the 92 muscle-tendon actuators from model *gait2392* are, firstly, adapted from the Delp model, who specified 43 muscles of one leg, and, secondly, from the work of Anderson and colleagues' model (Anderson & Pandy, 1999, 2001a) from which six of the lumbar muscles were included. The lines of action of the muscles are defined using the anatomical landmarks of the bony segments of the model (Anderson & Pandy, 1999; Au & Dunne, 2012; Delp, 1990). These are represented either by one or more line segments called actuators of the muscles. Mostly, the definition of the muscle's origin and insertion is sufficient to describe the line of action. However for some muscles, especially muscles spanning over more than one joint or muscles which wrap over a bone (e.g., the muscles of the quadriceps) a single line segment would lead to a wrong muscle path which might pass though the bones and deeper muscles at specific angles of the joint (Delp et al., 1990). Therefore, intermediate via points are included to prevent this happening (see chapter II).

Both the musculoskeletal model of Delp (1990) and Anderson and Pandy (1999) define the muscle-tendon units with a Hill model type (Figure 4.4). The muscle fibres are modelled as a

contractile element (CE) in parallel with an elastic element (parallel elastic element, PE) which represents all passive structures in and around the muscle. These are arranged in series with the series elastic element (SE) which represents the tendon. Each muscle-tendon actuator is characterised by a number of five parameters listed in the *gait2392* .osim file.

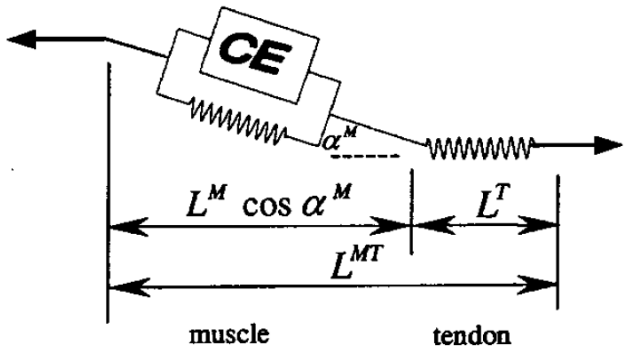

Figure 4.4. Graphical presentation of the Hill-type muscle tendon model adapted from Thelen et al. (2003) dividing the musculotendon complex into a contractile element (CE) and two elastic elements PE and SE. The elastic elements are parallel to the CE (PE) and in series with the CE (SE).

Three of these parameters describe the muscle, the muscle *maximum isometric force*, the *optimal muscle-fibre length* and the *pennation angle* to account for specific muscle characteristics. The maximum isometric force of each muscle has been adapted from the Delp model and has been calculated from the muscle's measured cross-sectional area (Spector, Gardiner, Zernicke, Roy, & Edgerton, 1980). It is assumed that the cross-sectional area and the muscle volume are constant throughout the movement (Hoy, Zajac, & Gordon, 1990). The cross-sectional area values have been taken from Friederich and Brand (1990) and Wickiewicz and colleagues (1983). The maximal isometric forces stated in the ground work of Delp and colleagues (1990) were scaled according to a specific individual factor, as the developers while designing the gait2392 model, realised that the Delp model was too weak (Au & Dunne, 2012). Appendix A1 defines the maximum isometric forces of all included muscles in gait2392.

The optimal muscle fibre length defines the length of the muscle fibre at which it can generate the greatest force in isometric condition. Values describing the optimal muscle-fibre length and the pennation angle of the muscle have been taken from the work of Wickiewicz and colleagues (1983) and Friederich and Brand (1990). The values have been scaled with a factor of 2.8/2.2, as 2.2μm are the initial values of the study but 2.8μm is the actual length of a sarcomere at

which the fibres can produce maximum force according to the sliding filament theory (Gordon, Huxley, & Julian, 1966).

The other two parameters describe the tendon. The tendon elasticity has an effect on the muscle force generation, which has been recognised by Hill (1938). The tendon can store energy while being extended either actively through a concentric muscle contraction or passively by eccentric movement. However, when Delp designed his model no experimental data existed about the characteristics of the tendon length; the knowledge about the length of the tendon at which it starts to store energy when stretched (tendon slack length) was missing. The solution was to estimate the tendon slack length for each muscle-tendon actuator accounting for the optimal muscle fibre length and the joint angle at which the muscle-tendon unit can generate the most force in isometric contraction. Detailed description can be found in the dissertation of Delp (Delp).

OpenSim provides a number of different muscle models which define the activation-dynamics parameters of the muscle-tendon units. The standard model implemented in the gait2392 model is the *Thelen 2003 Muscle Model* (Thelen, 2003). Three curves define parts of the individual characteristics of the muscle-tendon units (Figure 4.5) which are the active and passive force-length and force-velocity relationships of the muscle and the normalised force-length relationship of the tendon.

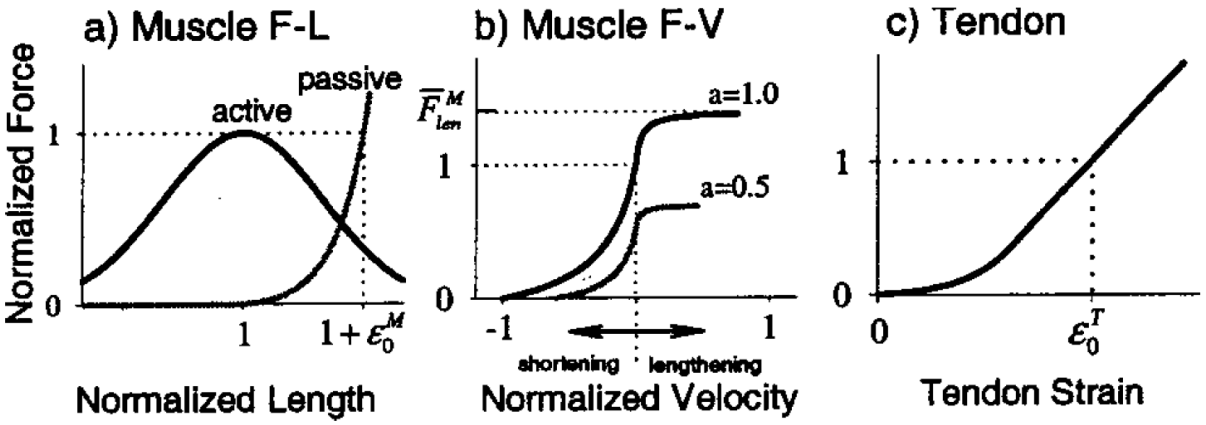

Figure 4.5. a) Gaussian curve showing a muscle force-length relationship, normalised to the maximal isometric force of the muscle and the optimal fibre length; b) Muscle force-velocity relationship, a describing the activation of the muscle; c) Tendon force-strain relationship; adapted from Thelen (2003) who refers to Zajac (1989).

Muscle force production starts with the innervation of the muscle fibres. The *neural excitation* represents the firing rate of motor units which innervate the muscle tissue and causes the calcium release from the sarcoplasmic reticulum. The *muscle activation* represents the calcium concentration within the muscle which initiates the cross-bridges of myosin and, therefore, the contraction of the muscle (Lieber, 2010). This leads into the muscle force production, until the calcium concentration decreases again (see chapter II). Between the neural excitation of the muscle and the actual force output a time delay exists with is defined in the literature between 8 and 127ms (Rampichini et al., 2013), also depending on the muscle. Similar process applies for the deactivation of the muscle, where the calcium ions are returned into the sarcoplasmic reticulum, which is a slower process than the release into the muscle (OpenSim, 2013). In OpenSim the activation time constant is set to 10ms, whereas the deactivation is defined as 40ms (OpenSim, 2013).

4.2.2 Limitations of the Model

Although the model *gait2392* is one of the most widely used models in the literature some limitations exist. As mentioned above, the muscular characteristics including maximal isometric force of each muscles is not automatically adjusted according to the characteristic of the individual participant. However, for patient groups or athletes these values may be far off from the generic values assumed by the models. The muscle architecture is derived from cadaver studies or from anthropometrics of a small number of healthy participants (of typically men) (E. M. Arnold, Ward, Lieber, & Delp, 2010) and may not represent the exact muscle-tendon architecture of every individual participant either. Newer studies like those of Arnold and colleagues (E. M. Arnold et al., 2013; E. M. Arnold et al., 2010), question the accuracy of these models and identify influencing factors which may affect the muscle force production. Newer models, however, have not yet been widely tested. Furthermore, the goal of this PhD thesis is to test the applicability of OpenSim in a "standard" configuration and *gait2392* is the model that most obviously fits that objective.

4.2.3 Adjustments to Model gait2392

To take the flexibility of the foot into account, the structure has been divided into three segments. These are linked to the tibia and each other by the ankle joint, subtalar joint and MTP

joint which are all defined as frictionless revolute joints (Delp et al., 1990). This structure, however, led to problems when using CMC to estimate muscle forces. While testing the standard approach with some pilot data, the foot would not stick to its physiological boundaries but would go into extreme positions, especially in swing (Figure 4.6). In stance, the toes were sometimes additional over-flexed. After discussing this behaviour with some members of the OpenSim team during a OpenSim workshop (2015 enhanced OpenSim workshop Stanford University, California, USA) and with other OpenSim users, it was decided to lock the subtalar and MTP joint, which seemed a normal procedure for similar cases as the foot segments with a small mass compared to other segments were too sensitive against errors in the muscle force estimation.

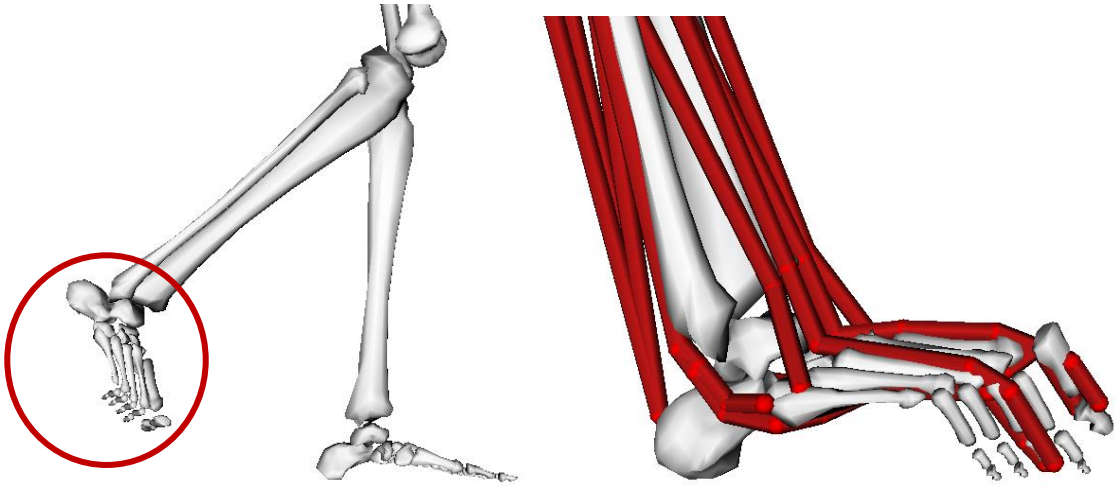

Figure 4.6. Subtalar and MTP joint of the foot here in the swing phase of the gait cycle (left) and at initial contact (right) during the estimation of muscle forces with CMC are out of the physiological boundaries.

4.3 Experimental Data Preparation

To run a simulation in OpenSim successfully it is important to have high quality experimental data: if the data used for the input into the simulation lacks in accuracy, the experimental error will have a major input on the calculations and, therefore, on the output of the simulation. Thus, the first step of capturing and preparing experimental data is crucial and should not be neglected. OpenSim needs the experimental data in specific file formats, .trc (Track Row Column, adapted from Motion Analysis Corporation) for marker files and .mot (Motion, adapted from SIMM) for ground reaction forces or joint angles. The information in these files has a specific structure which is compulsory.

To create these experimental files, additional tools are provided from OpenSim to convert an output file of a motion capture system, e.g. Vicon, into a .trc and a .mot file. For the purpose of this study a toolbox created from S. Lee and J. Son (2010) has been chosen and has been downloaded from the OpenSim internet platform. This tool needs a motion capture ASCII file which includes the information of the marker trajectory and the ground reaction forces. After aligning the coordinate system of the motion capture system to the one of OpenSim a .trc and a .mot file are being created which then will be needed to scale a generic musculoskeletal model. The kinematic data can be filtered in OpenSim, however, not the GRF data. While running some pilot data through OpenSim, a non-filtering of the GRFs led to spiky muscle forces, or the muscle force estimation could not be successfully run as the calculation crashed in between the calculation process and failed. Therefore, the filtering of these need to be performed beforehand. As it is also not possible to filter the raw analogue data of the ground reaction force directly in Vicon, MATLAB was used as a pre-step between the experimental data collection and the estimation in OpenSim.

For adequate results OpenSim recommends the placement of three markers or more to define each segment. The marker model can be either defined in the chosen model's .osim file itself or in a separate .xml file. OpenSim provides an own marker set which is presented in some of the example data enclosed to the download of the programme (Figure 4.7). It is defined as a modified Cleveland Clinic marker set (39 markers), and includes additionally markers on the medial and lateral ankle and knee which are used to determine the joint centres of both joints (Chand, Hammer, & Hicks, 2012). This marker set defines twelve segments (torso, pelvis, right and left thigh, right and left shank, right and left talus, right and left calcaneus, right and left toes). However, for the following experimental study some adjustments to the placement of the

markers and segments' definition were made due to a better scaling of the segments' parameters which is discussed in the section below.

OpenSim Marker model	
Sternum	Acromium L/R
TopHead	ASIS L/R
V.Sacral	Thigh.Upper L/R
Thigh.Front L/R	Thigh.Rear L/R
Knee.Lat L/R	Knee.Med L/R
Shank.Upper L/R	Shank.Front L/R
Shank.Rear L/R	Ankle.Lat L/R
Ankle.Med L/R	Heel L/R
Midfoot.Sup L/R	Midfoot.Lat L/R
Toe.Lat L/R	Toe.Med L/R
Toe.Tip L/R	

Figure 4.7. OpenSim' standard marker model; L=left, R=right, ASIS=anterior superior iliac spine, med=medial, lat=lateral, tip=tip toe, sup=superior.

4.4 Pipeline SimTrack

OpenSim is a modelling and simulation framework that allows the user to estimate muscle forces using a range of built-in sub-routines or by developing own routines. The developers of OpenSim provide a standardised pipeline called SimTrack which enables the user to generate dynamic simulations of human movements using experimental data as an input into the calculations to estimate muscle forces (Delp et al., 1990). Several steps need to be undertaken to be able to estimate muscle forces during a movement (Figure 4.8). Firstly, the generic model (i.e. gait2392) is scaled according to the participant's anthropometrics using an experimental static trial. Secondly, with the use of inverse kinematics and an experimental dynamical trial the joint kinematics can be calculated. And thirdly, either an inverse dynamics or a forward dynamic approach is used to estimate muscle forces. For the following experimental study static optimisation and computed muscle control will be chosen as discussed in chapter III. After every step the simulation tool outputs a .log file which includes all the processes undertaken during a specific step of the pipeline as well as, in case the pipeline could not be successfully run, indications of reasons of failing.

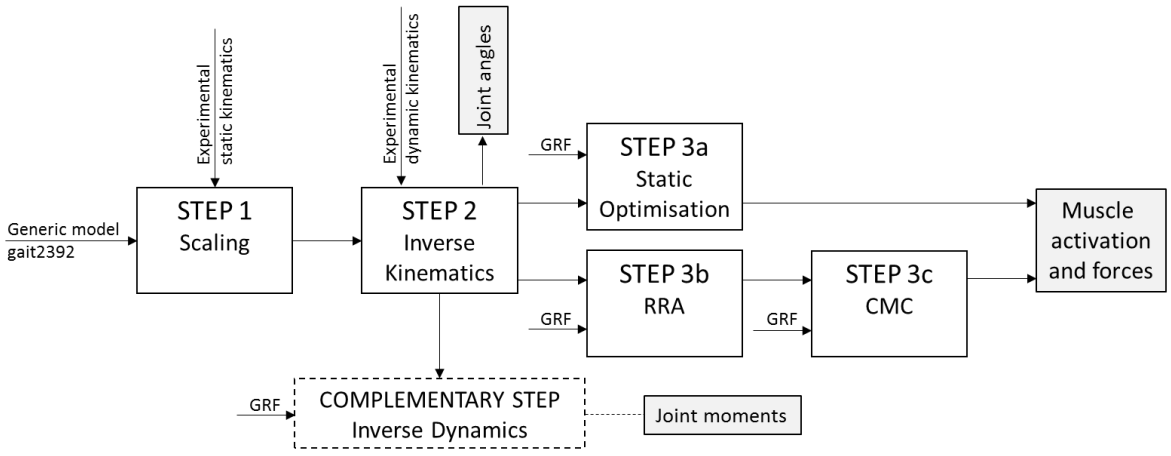

Figure 4.8. SimTrack pipeline from OpenSim, adapted from Delp and colleagues (Delp et al., 1990).

Before the actual experimental study has been conducted, every step of the SimTrack pipeline has been tested regarding its practicality for incorporation within routine clinical gait analysis. In the following sections, each step as recommended in the standard SimTrack pipeline will be

explained, its limitations in the context of clinical goat analysis discussed and the adaptions which have been implemented to address these will be described.

4.4.1 Step 1: Scaling in SimTrack

The OpenSim Scaling Tool scales and fits the generic model to the anthropometrics of the participant using the body mass and the experimental marker trajectories as captured during a static trial with the participant standing upright. The mass and inertia as well as the dimensions of the unscaled model segments and the tendon slack length and optimal muscle fibre length are adjusted to fit the participant (Hicks & Dunne, 2012).

OpenSim provides two options for scaling, firstly, by a measurement-based scaling where distances between markers measured during a static standing trial are compared to the equivalent distances between marker pairs on the model (virtual markers), and secondly, by manual scaling in case segment length are known from medical imaging information such as MRI or CT scans. Given that MRI or CT information cannot be guaranteed in routine clinical testing only measurement based scaling has been considered.

The key to the implementation of measurement based scaling in the Scaling Tool is that virtual markers are specified in the model at locations which are assumed to represent the placement of actual markers in relation to palpable anatomical landmarks. The calibration marker pairs which define a scaling factor *s* for a segment are defined in a participant's specific .xml setup file. To minimise scaling errors it is recommended to use markers placed on clearly defined anatomical bony landmarks, for example the anterior superior iliac spine on the pelvis. The scaling factor for each segment is calculated by dividing the distance of the experimental marker pair (*e*) through the distance of the virtual, unscaled marker pair (*m*):

$$s_1 = e_1/m_1 \tag{3}$$

If a segment's dimension is scaled by more than one marker pair the average of these pairs is taken while summing the scaling factors and dividing through the number of scaling pairs:

$$s = (s_1 + s_2 + \cdots + s_n)/n \tag{4}$$

In principal different scaling factors could be used to scale segments differently along any of the three axes x,y,z. In the standard approach, however, one scaling factor is used for an isometric scaling in all three directions. Left and right segments have the same scaling factor in the standard settings, which means that thigh, shank and segments on the foot have the same dimension after scaling while using the left and right marker pair to calculate one scaling factor for both sides.

The mass and inertia of the segments get scaled as well after the dimension of the segments are known, while the scaled total mass of all segments should be equal to the experimental body mass of the participant. This can either be achieved through keeping the mass distributions throughout segments the same than defined in the generic model, which allows to scale the masses independently to the dimensional scale factors, or the dimensional scale factors are used to adjust the mass distributions between the segments, which can scale the model closer to the participant but can lead into a body mass difference compared to the one experimental value. Finally, the inertia tensor of each segment is adjusted as well using the new dimension and mass (Hicks & Dunne, 2012). For this work, option one has been chosen as for option two detailed measurement techniques like MRI are needed to define different masses between segments.

Not all markers are involved in the scaling process. The *calibration marker* pairs used for the scaling are a sub-set of the entire marker set which also includes *tracking markers*. During movement trials the pose of the model is adjusted so that the position of virtual tracking markers within the model is fitted to the measured position of the actual markers. In the last step of the Scaling Tool the position of all the virtual markers on the model are calculated to match the experimental data from the static pose. Because the alignment of the segments during standing is unknown this must be estimated using a weighted “best fit” to the experimental marker positions (Hicks & Dembia, 2012). For the standard approach all markers are weight with 1, except the calibration markers on the pelvis, the knee and ankle markers and the heel markers which are weighted with 1000.

After running the Scaling Tool in OpenSim the overall RMS marker error as well as the maximum marker error are calculated. This indicates how much the experimental markers differ to the virtual markers and are an indication for the quality of the scaling process. OpenSim recommends a maximum marker error less than 2cm, and a RMS error less than 1cm for gait analysis. If RMS scaling errors are too large it is recommended that manual adjustments are made to the virtual marker positions within the model in an iterative manner to improve the

performance of the Scaling Tool. After running the scaling tool a new participant adapted .osim model file is created where the participant specific data is included and segments and muscle-tendon complexes are accordingly adjusted.

Limitations of scaling within SimTrack

After testing the standard scaling approach of OpenSim with experimental pilot data the RMS and maximal marker errors were too big to be included into a clinical gait analysis according to the recommendations of OpenSim. Therefore, the scaling protocol was analysed step by step, starting with the placement of the markers. The first requirement for correct scaling is a musculoskeletal model which has the position of virtual calibration markers specified correctly in relation to the anatomical landmarks. In case this requirement is not fulfilled the segments are scaled wrongly which will lead to errors in the following steps of the SimTrack pipeline. Having a closer look on the graphical presentation of the model gait2392 in the GUI of OpenSim there were clear discrepancies between the position of virtual markers in the relation to the bone meshes and were actual markers are placed in relation to the anatomical landmarks.

Another factor which restrains the process to be systematically correct is the subjective influence of the operator. The scaling tool allows the operator to intervene into the model if the errors between experimental and virtual markers are too big. OpenSim then recommends to undergo the step “preview the static pose” where the inverse kinematics solution for the static pose before adjusting the positions of the model markers is shown compared to the experimental markers. This helps the operator to analyse which marker is not in agreement between experimental marker placement and markers on the model. The operator can then adjust the markers on the model to fit the placement of the experimental static trial, or to exclude this markers from the inverse kinematics solution. This process, however, is highly subjective regarding the operators decisions.

If not manually changed by the operator the maximum isometric forces stay the same before and after scaling as these values are not automatically scaled according to the participants’ characteristics. But each individual muscle of the model can be manually strengthened and weakened by the operator. It is important to mention that if a muscle gets strengthened and the maximum isometric force will be enhanced, the relation to the tendon stiffness stays the same. In other words, if the maximum isometric force of a muscle increases the stiffness of its tendon rises, too. This shall keep the muscle fibre force-length-velocity curve consistent (E. M. Arnold

et al., 2013). A great enhancement in maximum isometric force of a muscle means unrealistic tendon stiffness and is not physiological anymore. Also, a systematic approach needs to be defined to adjust the maximum isometric force individually for every participant which may represent a distinctive work on its own. To first understand, however, the standard approach of SimTrack, it has been decided to accept these standard settings as a limitation of this model.

Adjustments to the SimTrack Scaling Tool

The exact placement of the markers on the defined anatomical points is crucial to result in adequate data (Xu, Merryweather, Bloswick, Mao, & Wang, 2015). The following virtual marker positions were adjusted according to the definition of the experimental marker model as these deviate from the anatomical landmarks (Figure 4.9) and are not in agreement in the literature (Schuenke, Schulte, Ross, Schumacher, & Lamperti, 2006):

- The anterior pelvis marker were placed too high and not directly on the anterior superior iliac spine (ASIS). They were moved more distal in front of the bony mesh landmarks which represents the ASIS (3cm distal).
- The shoulder markers were adjusted as they were too dorsal and as well as too high (1cm ventral, 2cm distal).
- The marker on the tip of the big toe was slightly too lateral and was shifted medial on top of the big toe (1.5cm medial).

Additionally to the adjustment of these markers, an error in the bony mesh of the tibia on the right side was detected, as it was placed in the same directions than the left side. In other words, the medial malleolus of the right tibia was pointing in direction of the distal fibula. Therefore, this bone was rotated 180° around the y-axis so that the medial malleolus was pointing in direction of the left foot. With this change, the medial ankle marker was shifted 1.5cm distal compared to the original position as the true medial malleolus was found to be more distal than the original position of the marker.

Some of the standard gait 2392 virtual markers were also fully excluded from the marker set as they did not further enhance the model. Firstly, the head marker was removed, as the torso in the model gait2392 is represented by one segment and therefore does not account for the individual differences between shoulder-head distance. This resulted in large scaling errors which reduced the accuracy of the scaling. Secondly, both midfoot markers were excluded in

the marker set of the following experimental study as both the MTP and subtalar joint were locked (Figure 4.9).

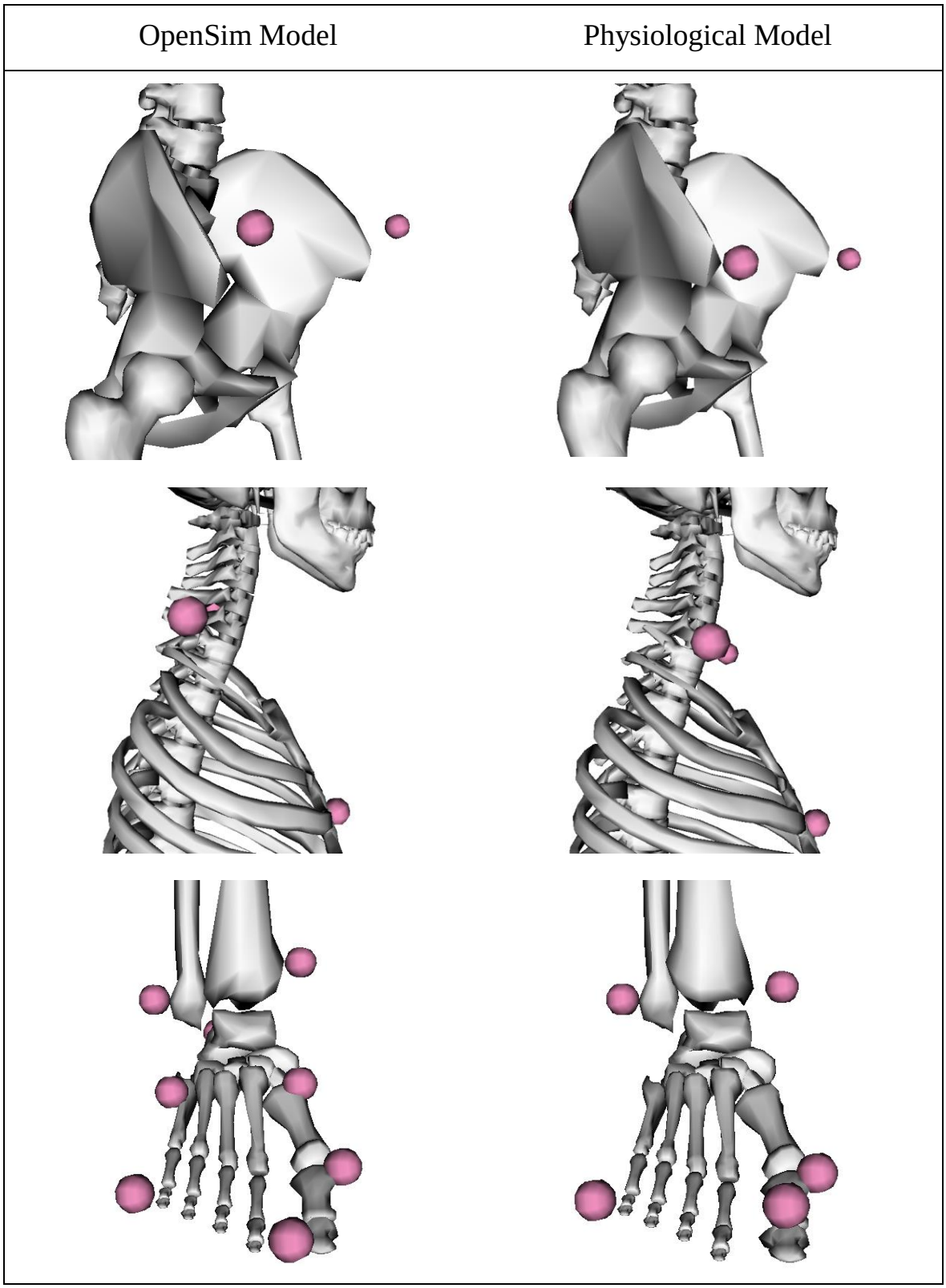

Figure 4.9. Standard OpenSim model (left) and adjustments on the marker model to account for placement errors.

The recommendation of OpenSim to subjectively interfere by “preview static pose” is not applicable in a clinical gait analysis routine as individual decisions may have an influence on the estimation’s outcome. Therefore, another approach has been developed for scaling the model. Markers which were chosen to scale the segments of the model were changed and, if needed, virtually reconstructed. This was done according to the principle of axis alignment: the line between the scaling markers should be as parallel to the axis to which the segment should be scaled to (Baker, 2011) to decrease errors in the scaling of the segments. This also means that, for a better scaling, the segments were not anymore scaled isometric, but separately and independently in the x,y, and z directions using different marker pairs and, therefore, scaling factors.

To enhance the scaling according to the principle of axis alignment it was decided to use experimental marker locations to estimate the position of joint centres and bony anatomical landmarks which lie directly on the bone in such a way that scaling and fitting can be performed simultaneously in a manner that is consistent with the biomechanical model. The anatomical landmarks are estimated on the basis of the measured experimentally calibration marker positions, the known dimensions of the markers and an estimate of the soft tissue thickness. Thus, for example, the lateral femoral epicondyle landmark is estimated to be offset by the marker radius, the thickness of the base plate and the estimated soft tissue artefact from the measured centre of the marker in the direction of the measured centre of the medial epicondyle marker. Joint centres are then estimated in relation to these landmarks, for example the knee joint (in standing) is the mid-point of the medial and lateral epicondyle markers.

During the experimental data collection and processing, marker locations are reconstructed within Nexus (Nexus 1.8.5, Vicon, T40S cameras). The estimated anatomical landmarks and joint centres for static trail data are calculated using a customised BodyLanguage model (Vicon, Oxford, UK) running within Nexus (see appendix A4). In OpenSim, the same bony landmarks and joint centres were defined as additionally virtual markers in the model for the static trial. This was done by estimating the locations of the key anatomical landmarks within their respective coordinate systems from the bony meshes and of the joint centres from the model. Only these estimated anatomical landmarks and joint centres were then used for the scaling and fitting of the model (Table 4.1). A weighting of 3:1 in favour of the joint centres biased the fitting of the principal axes to the joint centres leaving the landmark information to determine the rotation of segments about those axes. A more detailed description of the adapted scaling can be found in appendix A5.

This process includes an additional step into the standardised pipeline. However, it is structured in such a way that the interacting elements of scaling, fitting and model marker alignment are automatically satisfied without the requirement for any interaction from the operator. The calculation of additional anatomical landmarks and joint centres can be easily implemented in the experimental routine processing of capturing and processing experimental data. Therefore, for the following experimental study this step will be included into the routine processing and into the standardised pipeline.

Table 4.1. Anatomical landmarks and joint centres which are additional included for the static scaling of the model.

Landmark	Derivation
Anterior superior iliac spine (ASIS)	Marker radius[1] and ASIS soft tissue thickness (STT) behind ASIS marker centre in a direction parallel to the line between the mid-point of the ASIS markers and the sacral marker.
Sacrum	Marker radius and PSIS STT in front of marker centre in a direction parallel to the line between the mid-point of the ASIS markers and the sacral marker.
Lateral epicondyle	Marker radius and knee STT from the marker centre in the direction of the medial epicondyle marker.
Medial epicondyle	Marker radius and knee STT from the marker centre in the direction of the lateral epicondyle marker.
Lateral malleolus	Marker radius and knee STT from the marker centre in the direction of the medial malleolus marker.
Medial malleolus	Marker radius and knee STT from the marker centre in the direction of the lateral malleolus marker.
Posterior calcaneus	Marker radius and heel STT from the marker centre in the direction of the hallux marker.
Ankle floor	Projection of ankle joint centre onto floor.
Posterior calcaneus floor	Projection of posterior calcaneus marker onto floor (to ensure plantar surface of foot is positioned flat on the floor).
Hallux floor	Projection of hallux marker centre onto floor.
1st metatarsal phalangeal joint floor	Projection of 1first metatarsal phalangeal joint marker centre onto floor.
5th metatarsal phalangeal joint floor	Projection of fifth metatarsal phalangeal joint marker centre onto floor.
Joint Centre	
Hip joint centre	Scaled in the sagittal plane to the distance between mid-point of ASIS landmarks and mid-point of PSIS landmarks and in medio-lateral direction to distance between the ASIS landmarks.
Lumbar sacral joint centre	Scaled in the sagittal plane to the distance between mid-point of ASIS landmarks and mid-point of PSIS landmarks.
Knee joint centre	Mid-point of lateral and medial epicondyle landmarks.
Ankle joint centre	Mid-point of lateral and medial malleolus landmarks.
Mid-acromion point	Mid-point of acromion markers.

Note. STT=soft tissue thickness, ASIS=anterior superior iliac spine, PSIS=posterior superior iliac spince.

4.4.2 Step 2: Inverse Kinematics in SimTrack

In movement science there exists two different ways of calculating joint angles, either through direct kinematics or inverse kinematics. Direct kinematics is frequently used in gait analysis (e.g., PlugInGait) where marker trajectories are measured through time and an algorithm is applied to calculate the positions of the segments and the kinematics of the joints. Inverse kinematics uses an optimisation approach to adjust the joint angles in order to fit the trajectory of virtual markers defined within the model to experimental marker trajectories (Kainz, Modenese, Carty, & Lloyd, 2014). OpenSim uses the second method in its SimTrack pipeline. The inverse kinematics tool positions the model in every time frame into a pose which best matches the experimental marker data by minimising a sum of weight squared marker errors (equation 5). Additionally, experimental joint coordinates (which can be joint angles) can be included into this calculation, too, which, however, has not been done for the present study, as only the experimental marker trajectories were used as the kinematic input. OpenSim recommends maximum marker errors to be less than 2-4cm, the RMS under 2cm.

Like the static scaling, markers can be weighted which specifies how strongly the error of a marker should be minimised. The least squares equation which is solved by the inverse kinematics pipeline is

$$\min_{\mathbf{q}} \left[\sum_{i \in \text{markers}} w_i \left\| \mathbf{x}_i^{\text{exp}} - \mathbf{x}_i(\mathbf{q}) \right\|^2 \right] \tag{5}$$

where q is the vector of the generalised coordinates (i.e., joint angles), x_i^{exp} is the vector of the position of the experimental marker i and $x_i(q)$ is the vector of the position of the corresponding virtual marker on the model output depending on the generalised coordinates of the model q (Hicks & Dembia, 2012). The constant w_i describes the weightings of the markers. These weights are defined in the participant's inverse kinematics setup file and can be changed manually through the operator. In the standard approach, the pelvis markers as well as the heel and tip toe markers are rated with 10, whereas all other markers are rated with 1, except the acromion markers (weight of 0.5) and the head marker (weight of 0.1). Further setting definitions in the .xml setup file are the time range of the gait cycle, the participant's adapted model, and the experimental marker trajectory file.

The output file of inverse kinematics is a .mot file where following coordinates over the gait cycle are defined: pelvis tilt, pelvis list, pelvis rotation, hip flexion, hip adduction, hip rotation, knee flexion, and ankle dorsiflexion. Furthermore, subtalar and MTP angle are defined, too; however, as both joints are locked for this study they are set to zero. Pelvis tilt describes how much the pelvis is tilted forward or backward in relation to the sagittal plane, pelvis list describes the angle of the pelvis in frontal plane.

Adjustments to the SimTrack Inverse Kinematics Tool

The only adjustment to the standard approach is a different weighting of the tracking markers for the least squared error calculation. With the settings in the standard approach, the marker errors were too high regarding the guidelines of OpenSim (chapter 5.3.2). Also, the rationale behind the OpenSim standard weighting of the markers has not been explained in the user guides or anywhere else. Except the markers on the pelvis (RASIS, LASIS, VSacral) and the heel markers which were weighted 10 times higher than all other markers, no other marker was favoured in its weighting. Shank and thigh markers or any other foot marker were not defined for a higher rating, which, therefore, might lead to bigger tracking errors in the kinematics of the knee.

This standard weighting has no clinical or anatomical rational for walking purposes, whatsoever. Tracking markers are important for defining the orientation of the coordinate reference frame and the position of the segment in space during the movement. Therefore, markers were weighted as defined in Table 4.2. A weighting of 1 or 2 was chosen, to keep the weighting throughout tracking markers more homogeneous but also to be able to set the focus on markers important to define the segments of the lower limb. With this standardised approach the Inverse Kinematics tool resulted in smaller marker errors (chapter). Besides this change, the pipeline inverse kinematics is kept on standard settings.

Table 4.2. Weighting of the tracker markers for a dynamic trial.

Weighting of 1	Weighting of 2
Sternum	RASIS, LASIS
R+L Acromium	VSacral
R+L ThighUpper and ThighRear	R+L ThighFront
R+L ShankUpper and ShankRear	R+L ShankFront
R+L ToeLat and ToeMed	R+L Heel
	R+L ToeTip

4.4.3 Complementary Step: Inverse Dynamics

Inverse Dynamics is an essential step for the estimation of muscle forces via estimating the joint moments and using them further for static optimisation or RRA. However, the estimated joint moments are not given as an output and a complementary step besides SimTrack needs to be undertaken to receive these. Inverse dynamics calculates the joint moments at the joints from the joint angles of the inverse kinematics pipeline and the experimental, filtered GRF which will be both used in static optimisation and CMC and is therefore useful to validate the input data. The outputs are also useful in routine clinical gait analysis and including this step allows OpenSim to be used to generate all the outputs and ensure that they are mutually compatible. Inputs into this step of the pipeline are the .mot file of the inverse kinematics solution, a .xml file which defines the GRFs, and the participant specific model file. Parameters of the inverse dynamics pipeline are defined in a setup .xml file.

As in the setup file of inverse kinematics, the time of the gait cycle needs to be defined for the calculation. The .xml setup file refers to the .xml GRF file where, firstly, left and right foot contacts of the force plates are defined and, secondly, the body parts to which the GRFs are applied to are specified. In the standard settings the GRFs are applied to the left and right calcaneus during initial contact. Thirdly, the kinematics of the inverse kinematics solution can be lowpass filtered and the cut-off frequency in the standard settings is set to 6Hz.

The following equation is presented on the OpenSim user guides which calculates the joint moments (Hicks, 2012a):

$$\tau = M(q)\ddot{q} + C(q,\dot{q}) + G(q) \tag{6}$$

where q,$\dot{q}$, and $\ddot{q}$ are the vectors of generalised positions, velocities and accelerations, *M(q)* is the system matrix, *C(q,$\dot{q}$)* is the vector representing the Coriolis and centrifugal forces, *G(q)* are the gravitational vector forces, and τ is the vector of the generalised forces on the joints. No adjustments compared to the standard approach were made for the following experimental study.

4.4.4 Step 3a: Static Optimisation in SimTrack

The first mathematical model which has been chosen to estimate muscle activations and forces in the following experimental study is static optimisation. It is an inverse dynamics approach that attributes the net joint moments to moments arising from a number of individual muscle forces at each independent instant in time (Hicks & Dembia, 2014). Inputs into the calculations are the generalised coordinates from the inverse kinematics pipeline (i.e., joint angles) and the experimental and filtered GRF.

Static optimisation is divided up in two main steps, firstly, the calculation of joint moments which includes the equation of motions and the experimental input, and secondly, the estimation of muscle activation and forces via using the characteristics of the musculoskeletal model as well as a cost function to minimise estimation errors. Therefore, the static optimisation tool needs the participant's adjusted .osim model which is the output of the scaling tool, the time specification of the walking trial, the results of the Inverse Kinematics Tool, the GRFs, and the specification about the low pass cut-off filter for the kinematic data. In the static optimisation setup .xml file it can be specified if the muscle force-length curve is included while running the static optimisation tool, which is set to 'true' in the standard approach. The standard objective function which is used to optimise the muscle force estimation is the overall sum of muscle activations squared. The exponent of the optimisation criterion can be changed if needed, however, for the following experimental study the settings were kept on following optimisation criteria:

$$\sum_{m=1}^{n} (a_m)^2 \tag{7}$$

where *n* is the number of muscles of the model and a_m the activation level of the muscle *m* at a discrete time step. The ideal force generators constrained by the force-length-velocity properties of *m* muscle are defined with following formula:

$$\tau_j = \sum_{m=1}^{n} [a_m f(F_m^0, l_m, v_m)] r_{m,j} \tag{8}$$

where F_m^0 is the maximum isometric force, l_m the length, and v_m the shortening velocity of the muscle. $r_{m,j}$ defines the moment arm about the j^{th} joint axis and τ_j is the generalised force which acts about the j^{th} joint axis. As static optimisation is a time independent solution and does not takes the activation-contraction dynamics into account, the force-length-velocity complex $f(F_m^0, l_m, v_m)$ does not take the contributions from the parallel elastic element into account and assumes the tendon to be inextensible (Hicks & Dembia, 2014).

For the following experimental study, the static optimisation tool was applied without any changes to the standard approach. The cut-off frequency of 6Hz for the kinematic input data as well as the exponent of 2 for the optimisation criterion were kept the same. The static optimisation tool outputs the estimated muscle activations which define the amount of the activation of the muscles between a scale of 0 and 1 and the estimated muscles forces.

4.4.5 Step 3b: Residual Reduction Algorithm in SimTrack

The second mathematical model which has been chosen for the estimation of muscle forces is the method *computed muscle control* (CMC). However, to be able to use this technique a preliminary step is required to minimise discrepancies between the dynamics of the system based on the kinematic analysis and the experimental GRFs. This is called residual reduction algorithm (RRA). Dynamic inconsistencies are removed by applying nonphysical compensatory forces and moments known as residuals, while this process also modifies the kinematics to minimise the size of these (Thelen & Anderson, 2006).

After locking the subtalar and MTP joints, the model has 19 degree of freedoms, each characterised by a generalised coordinate and actuated by a single actuator. Most of the coordinates represent joint angles with the actuators representing the action of the muscles around the relevant axis. Six of the model's degree of freedom, however, represent the translation and rotations of the pelvis relative to the ground in all three planes and are actuated

by actuators representing the nonphysical compensatory forces and moments. These are the residual actuators providing the residual forces F_x (anterior-posterior), F_y (proximal-distal), and F_z (medial-lateral), and the residual moments M_x (sagittal), M_y (frontal), and M_z (transverse) (Hicks & Uchida, 2013b).

These six residual actuators account for the errors occurring through the experimental data collection (e.g., noises) and modelling assumptions (e.g., HAT segment) and, therefore, for the dynamic inconsistency, by adding a new force to the equations. This force balances Newton's second law by changing

$$F = m * a \tag{9}$$

to

$$F + F_{residual} = m * a$$

$F_{residual}$ represents the overall force by the six actuators on the six degrees of freedom on the pelvis to the ground. The lower these values the less the dynamic inconsistency.

After running the RRA pipeline, the average value for each of the residual actuators is computed (Fx, Fy, Fz, Mx, My, Mz), and averaged. M_x and M_z are then used to adjust the torso's centre of mass to account for an excessive 'leaning' of the model (Hicks & Uchida, 2013b) which can occur by inaccuracies in the segment's mass distribution or the geometry of the segment. Furthermore, the RRA outputs recommendations for segments' mass adjustments of all segments of the model. This is done by using the averaged value of F_y and dividing it proportionally up among the model's segments. It is worth noting that the model's segments masses are not adjusted automatically and are only output as a recommendation to the user. Unfortunately, OpenSim does not provide a pipeline which would include this step into a routine processing. However, a manual adjustment for every participant and every trial would be time costly in a clinical gait analysis. As these segment adjustments are highly recommended in OpenSim a MATLAB script has been used which automatically adjusts the mass of the segments in the .osim file.

A last step of RRA is to rerun the tracking algorithm that was used to calculate the residuals based on the original kinematics of the dynamic walking trial. This time the model with adjusted masses and centres is used and the cost function is modified so that the motion defined throughout the desired kinematics is generated purely by the internal joint moments.

4.4.6 Step 3c: Computed Muscle Control in SimTrack

The RRA pipeline outputs the adjusted joint kinematics which are then used for the estimation of muscle forces in the CMC pipeline. CMC tries to track these set of desired kinematics by computing a set of muscle excitations that will drive the generalised kinematics of the musculoskeletal model towards the experimental kinematics (Figure 4.10) (Hicks & Uchida, 2013a). For each time step t CMC loops the process forward to the next time step t+T. Therefore, the process is a pseudo-forward-dynamics process as not the whole time instant but only the time steps before and after a specific time step are dependent on each other.

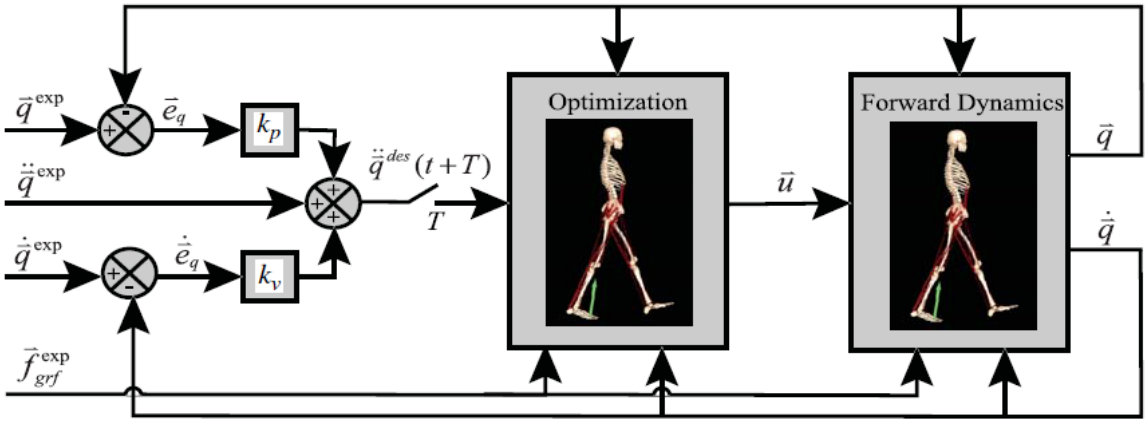

Figure 4.10. Schematic presentation of the CMC pipeline, adapted from Thelen and Anderson (2006). $\vec{q}_{exp}$, $\dot{\vec{q}}_{exp}$, $\ddot{\vec{q}}_{exp}$ *are positions, velocities, and accelerations of experimental kinematics, respectively,* $\vec{f}_{grf}^{exp}$ *is the GRF vector,* k_v *and* k_p *are feedback gains which weight the current velocity and position errors* $\dot{\vec{e}}_q$ *and* $\vec{e}_q$ *to compute a set of desired accelerations* $\ddot{\vec{q}}^{des}$. $\vec{u}$ *are the muscle excitations, whereas* $\vec{q}$ *and* $\dot{\vec{q}}$ *are the generalised coordinates and speeds of the model which are driven towards the experimental ones.*

The first step in CMC is to compute initial states for the model to be able to create initial values for the muscle states like the muscle activation levels and the muscle fibre length. CMC is therefore applied to the first 0.03 seconds. However, these 0.03 seconds should be prior to the desired movement time as during that period the forces can change dramatically until they are balanced for the actual walking trial (Hicks & Uchida, 2013a). This also allows generalised coordinates and speeds (joint angles and joint angular velocities) to be computed for the initial states of the walking trial.

The second step is the computation of a set of desired accelerations $\ddot{\vec{q}}^{des}$ which will drive the model coordinates $\vec{q}$ and speeds $\dot{\vec{q}}$ towards the experimental coordinates $\vec{q}_{exp}$ and experimental speeds $\dot{\vec{q}}_{exp}$ (Hicks & Uchida, 2013a). This is done by using a proportional-derivative control (PD) law, with the following calculation:

$$\ddot{\vec{q}}^{des}(t+T) = \ddot{\vec{q}}_{exp}(t+T) + \vec{k}_v\left[\dot{\vec{q}}_{exp}(t) - \dot{\vec{q}}(t)\right] + \vec{k}_p\left[\vec{q}_{exp}(t) - \vec{q}(t)\right] \tag{10}$$

where $\vec{k}_v$ and $\vec{k}_p$ are feedback gains for the speed and position errors between experimental and generalised kinematics, respectively, where the standard settings for these gains are set to 20 for $\vec{k}_v$ and 100 for $\vec{k}_p$. The desired accelerations are computed in a small time step T in the future, as the muscle forces which are applied to the body cannot change instantaneously. In standard settings this time interval T is set to 0.01 seconds. The errors between experimental and generalised coordinates will be driven to zero.

Third step of the CMC pipeline is to compute the muscle excitations, or actuator controls, which will achieve the desired acceleration $\ddot{\vec{q}}^{des}$. A static optimisation routine distributes the joint moments, calculated by a classical inverse dynamics routine, across the muscles involved, implementing the Newtonian equation of motions. An optimisation criteria called the *fast target*, which is set in the standard approach (Hicks & Uchida, 2013a), is used as a cost function to optimise the muscle excitations. Following formulation defines the fast target in OpenSim:

$$J = \sum_{i=1}^{nu} u_i^2 \qquad ; C_j = (\ddot{\vec{q}}_j^{des} - \ddot{\vec{q}}_j)^2 \tag{11}$$

While the performance criterion *J* is driven to zero and the additional constraint C_j needs to be within a tolerance set through the optimiser, with u_i^2 being the estimated muscle excitations, $\ddot{\vec{q}}_j$ being the experimental accelerations and $\ddot{\vec{q}}_j^{des}$the desired accelerations and from the model.

In case a muscle shows strength deficiencies, *reserve actuators* are added to the model, so that the fast target is prevented from failing. These reserve actuators have a very low optimal force, which means, that they need a high excitation to be able to apply more force to the model. This means, that the reserve actuators are a good indicator for which joints and muscles defined in the musculoskeletal model are not strong enough. A model strong enough for the movement of interest shows, therefore, very small reserve actuators.

The last step of CMC is a forward dynamics solution advancing forward in time T to compute the generalised kinematics of time t+T by using the computed muscles excitations *u* while considering the equations of motion. Furthermore, with the knowledge of the muscular-tendon characteristics of the musculoskeletal model, muscle activations and forces are estimated for the time step t+T. The three steps consisting of computing the desired accelerations, the static optimisation routine, and the forward dynamics simulation are driving the CMC forward in T time steps until the end of the walking trial is reached. The upper and lower bounds for muscle excitations are set to 1 (maximum excitation) and 0.02 (minimum excitation) in the standard settings. They cannot reach zero because, as defined in the OpenSim user guides (Hicks & Uchida, 2013a), musculoskeletal models do often not behave according to the physiological pattern if they are able to switch the excitation totally off.

Adjustments to the SimTrack Computed Muscle Control Tool

Most of the standard settings in CMC are kept the same. However, one main change has been undertaken which, in the end, enhanced the muscle force estimation output. The standard time steps of CMC are set to 0.01 seconds. With this setting, especially in swing, the estimated muscle excitations and forces were unstable (Figure 4.11). However, with changing the time steps from 0.01 to the half of 0.005 seconds, the muscle forces were much smoother. Figure 4.11 shows estimated muscle forces of five normal walking trials throughout a gait cycle of one typical participant for a standard 0.01 seconds time step CMC calculation and with changed time steps to 0.005 seconds. Reason for this smoothening from 0.01 to 0.005 seconds might be the shorter time frame in which CMC can adjust the muscle excitations to the new acceleration conditions of the segments. This process is time-independent, i.e. each time step is handled independently in relation to the adjacent time frames, which might initiate a greater change with bigger time frames. However, an adjustment in dividing the time steps in half means a double as long estimation time for CMC. The 0.005 seconds have been chosen after balancing accuracy and time efficiency and discussing this issue with several OpenSim researchers as well as researchers who applied OpenSim during walking and experienced the same problem.

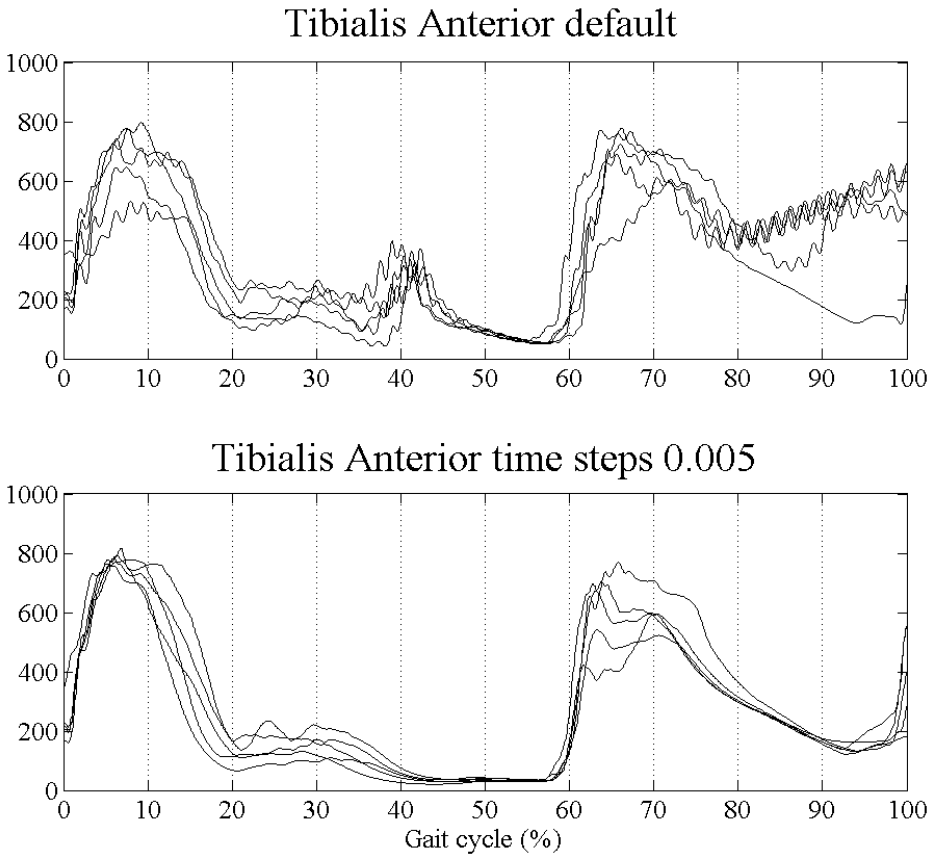

Figure 4.11. Estimated tibialis anterior muscle forces with CMC for five normal walking trials of a typical participant while keeping the standard settings by 0.01 seconds per time step (above) and changing the time steps to 0.005 seconds (below).

4.4.7 Final Structure of the OpenSim Pipeline for the Experimental Study

This Chapter could improve the standard pipeline SimTrack of OpenSim while adjusting it to a more physiological and clinical approach which is needed for the purpose of this study. Especially the scaling approach is novel compared to OpenSim's standard settings, as the model can be scaled individually along the axes of the system and not isometric in all three directions.

Table 4.3 summarises adjustments which have been undertaken in the different steps of OpenSim's SimTrack to estimate muscle forces during healthy walking. Summarised, some adjustments were undertaken to make the standard SimTrack more applicable for the clinical gait analysis. Firstly, the markers on the musculoskeletal model were adjusted according to the placement in the clinic and a more physiological definition (e.g., the ASIS marker), secondly, additional joint centres and anatomical landmarks were calculated to be able to scale the segments closer to the principle of axis alignment, thirdly, segments were scaled non-isometric

and independently in all three directions, fourthly, the marker weighting for the static inverse kinematics pipeline were changed according to the calibration markers, fifthly, the subtalar and the MTP angle were locked due to high errors with CMC, sixthly, the marker weighting for the dynamic trial were adapted, too, seventhly, the experimental GRFs were filtered before to input into any of the pipelines, and eighthly, the calculation time steps of CMC was changed from 0.01 to 0.005 seconds per time step.

These adjustments were all tested beforehand by small pilot studies; however, the whole adjusted OpenSim pipeline to estimate muscle forces needs to be tested now for a larger population. This will be presented in the next chapter (chapter V), where ten healthy participants were tested in a VICON motion system while walking at five different speeds to be able to systematically control the results of the estimation while changing the known influencing parameter speed. The muscle force estimations will be compared to parallel captured surface EMG of some of the muscles of the lower limb for validation. Furthermore, static optimisation and computed muscle control are analysed and compared to each other to possible find the best estimation technique for the clinical gait analysis routine.

Table 4.3. Summarised adaptations which have been undertaken on the standard SimTrack pipeline for the implementation into a routine clinical gait analysis.

Steps	Changes to the standard SimTrack pipeline
1	- Additional calculation of joint centres and anatomical landmarks - Adapted marker weighting and adapted segment scaling
2	- Adapted marker weighting
3a	*No changes*
3b	*No changes*
3c	- Changed calculation time steps (0.005)

CHAPTER V

5 Experimental Implication of a Standardised Protocol to Estimate Muscle Forces for Routine Clinical Gait Analysis

5.1 Introduction

OpenSim and its implemented musculoskeletal model from Delp and colleagues (1990) represents an attractive modelling and simulation tool to be applied into clinical gait analysis. The operator has access to the source code of the musculoskeletal model and this allows the operator to adjust this model to suit the purposes of the study (see chapter IV). With the adjustments undertaken in chapter IV on the provided pipeline SimTrack in OpenSim the operator does not need to interfere with any step of the process anymore. All virtual markers have been placed on the correct anatomical landmarks within the musculoskeletal model. The developed enhanced scaling approach enables a systematic and physiological scaling of the model.

This chapter will test this developed standardised pipeline by implementing it into a classical gait analysis routine. This will facilitate an analysis of the robustness of the pipeline while controlling some of the factors which influence the estimation of muscle activations and forces. Currently, no gold standard relating to muscle force estimation is available; thus other ways of validating estimated muscle forces are needed. In their recent work Hicks and colleagues (2015) point out the importance of validating the estimations output to independent experiments or other models. They suggest EMG data as a validation tool to determine if the muscle coordination of the estimated muscle forces correlates to the experimental captured EMG activity.

Important, however, is a validation tool independent to the estimation process (Hicks et al., 2015). As chapter III showed, most studies using EMG as a validation tool also incorporated EMG data into their estimation process to define the neural input (Bogey et al., 2005) or applied constraints to prevent what are perceived as non-physiological activations (Collins, 1995). To

date, the literature lacks a detailed validation of estimated muscle activations and forces with independent EMG measurements. A key focus of this research is to assess the match of non-EMG constrained; OpenSim derived activation and force estimations with independent EMG data. Surface EMG will be simultaneously captured during the experimental data acquisition of kinematics and kinetics, on the same participants and trials. This will minimise inter- and intra-variability between participants and trials while keeping EMG independent from the estimation process.

Walking speed is one of the main factors influencing experimental outputs. Differences in walking speed result in changes in joint angles, ground reaction forces (Lelas et al., 2003) and EMG (Schwartz et al., 2008). The change in joint kinematics can lead to differences in the contractile state (fibre length, velocity) of each muscle and, therefore, lead to differences in the generation of muscle forces (R.R. Neptune et al., 2008). This information is important, especially in a clinical gait analysis routine when comparing a patient group with the healthy population. Differences caused by factors such as walking speed need to be known to exclude them from other changes initiated by the impairment of the patient. Therefore, this experimental study will systematically control the walking speed to analyse speed-dependent changes on muscle force estimation.

One of the studies using EMG excitations as a comparison tool in relation with speed dependence is the study of Neptune and colleagues (R.R. Neptune et al., 2008). Nonetheless, they used these experimental EMG excitations within their estimation process to define the muscle excitation patterns, causing a bias of their validation technique. Also, they only presented the EMG speed changes for the soleus and medial gastrocnemius. Additionally, the estimated muscle force of the gastrocnemius has been defined by summating the medial and lateral modelling compartments together, whereas only the EMG excitations of the medial gastrocnemius were used for comparison. Their data show the changes caused by different walking speeds averaged across all participants, but individual muscle force estimations compared with individual EMG excitations were not presented. This may underestimate individual differences as well as inter-subject variability due to missing standard deviation bands. Lastly, it is also not clear how many trials for each participant were included into the estimation and graphical representation.

Another study has been undertaken by Liu and colleagues (M. Q. Liu, Anderson, Schwartz, & Delp, 2008) who used OpenSim to provide reference data about muscle contributions to the support and progression of locomotion across different walking speeds of eight children

(12.9±3.3 years). The musculoskeletal model gait2392 was used in a computed muscle control (CMC) estimation. Again, differences in muscle forces caused by different walking speeds were detected. However, the number of experimental trials included is unclear and cited as “at least one double-stance phase on the force plates at each walking speed”. Only muscle force data of children were provided, kinematic and kinetic input data were extracted from the data pool of Schwartz and colleagues (2008). The graphs show averaged curves of the estimated muscle forces with underlined EMG standard deviation bands. These EMG signals, however, show only the average excitation of all eight participants, but do not include individual comparison of muscle estimations and EMG excitations. The study also merely used EMG excitation data for the whole quadriceps and the plantarflexors and not for single muscles.

In summary, the literature is lacking comprehensive analyses of muscle force estimations on both healthy and pathological adults and, additionally, the dependence of walking speeds compared to individual EMG excitations. The first stage of implementing such standardised measurement protocol into the clinic is to provide and validate normative reference data. Therefore, this study will estimate muscle forces of the lower limb in a healthy adult population while walking at different speeds using the developed standardised protocol (chapter IV). Static optimisation and CMC which are both most suitable for the clinical daily routine (chapter III) will be both tested and applied in OpenSim. Both approaches will be validated against individual surface EMG measurements and compared in reference to the shape and speed-dependent changes.

The pipeline SimTrack additionally provides joint angles through the Inverse Kinematics Tool and joint moments through the complementary tool Inverse Dynamics. To be able to implement the whole pipeline clinically it would be useful to know the compatibility of OpenSim’s joint angles and moments compared to current clinical models like the Conventional Gait Model. Therefore, as a subsidiary step, joint angles and moments are additionally calculated in Vicon Nexus with the use of the PlugInGait model to analyse the usefulness of OpenSim as a whole package for the implementation onto the routine clinical gait analysis.

The results of the study will provide information about the robustness of the developed standardised protocol and about the potential to implement this protocol into the clinical gait analysis. This study aims to provide a base for a normative data pool for subsequent clinical trials. Furthermore, it will distinguish between the two estimation methods to define the model most suitable for a clinical use.

5.2 Methods

This chapter will define the methods used to conduct the experimental study to implement the developed protocol to estimate muscle forces. Participants' characteristics and experimental data collection as well as the processing of experimental and estimated data are explained. Detailed information about the OpenSim modelling process can be found in chapter IV. Ethical approval for the experimental study was granted by the College of Health and Social Care Ethics Panel (appendix A6).

5.2.1 Participants

Ten healthy adults, five male and five female, were recruited from the University of Salford student and employee population and participated in this study. The population group has been restricted to healthy adults to avoid influences caused by different age groups or disabilities (Winter et al., 1990). Participants received an information sheet beforehand (appendix A7) and filled out a research consent form (appendix A8) after being introduced to the purpose, the procedure and potential risk of the study. It was clearly indicated to the participants that they are able to interrupt or stop the participation at any time without explanation.

5.2.2 Laboratory Set-up and Calibration

The study has been undertaken in the movement laboratory of the University of Salford. The laboratory is equipped with a Vicon motion analysis system including ten infra-red cameras (Vicon 1.8.5, 100Hz, T40S cameras) and four force plates mounted into the walkway to capture the ground reaction forces (Kistler, 1000Hz, 2x 9286A, 2x 9253A) (Figure 5.1). The origin of the global reference frame was set on one of the corners of the first force plate. The surface EMG excitations were collected in parallel with a wireless 16 channel Noraxon system using an in-built low pass filter of 500Hz (DTS receiver, 1000Hz). Data from the following muscles were collected on both legs: rectus femoris, vastus medials and lateralis, semitendinosus, tibialis anterior, soleus, gastrocnemius medialis and lateralis (Table 5.1).

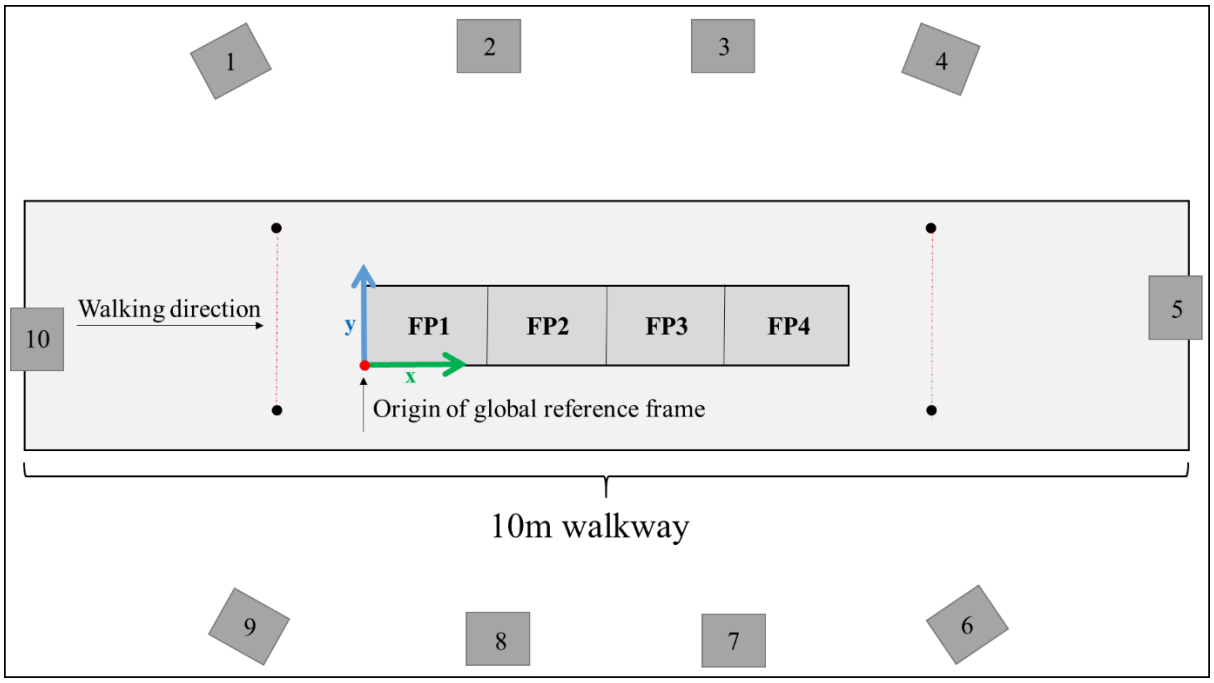

Figure 5.1. Set-up of the movement laboratory at the University of Salford showing four force plates implemented into a ten meter long walkway, including the origin of the global reference system (red dot), surrounded by ten infra-red cameras. The black dots linked with a dashed red line represent the timing gates. Figure's layout is not to scale of the laboratory.

Table 5.1. Electrode placements on the lower limb muscles, adopted from the SENIAM guidelines (Hermens, Freriks, Disselhorst-Klug, & Rau, 2000).

Muscle	Electrode placement
Tibialis anterior	1/3 of the line between the tip of the fibula and the tip of the medial malleolus
Soleus	2/3 of the line between the medial condylis of the femur to the medial malleolus
Gastrocnemius medialis	On the most prominent bulge of the muscle, in direction of the leg
Gastrocnemius lateralis	1/3 of the line between the head of the fibula and the heel
Rectus femoris	50% of the line from the anterior spina iliaca superior to the superior part of the patella
Vastus medialis	80% of the line between the anterior spina iliaca superior and the joint space in front of the anterior border of the medial ligament
Vastus lateralis	2/3 of the line from the anterior spina iliaca superior to the lateral side of the patella
Semitendinosus	50% of the line between the ischial tuberosity and the medial epicondyle of the tibia

Before starting the measurement, the capture volume was calibrated with a calibration wand so that the infra-red cameras were calibrated according to the origin of the global measurement volume and the position of the force plates. Furthermore, the force plates' centre of pressure (CoP) and the direction of the GRF vector of each force plate were tested using the so-called *CalTester* method (Figure 5.2) (Goldberg, Kepple, & Stanhope, 2009), where a metal plate was temporarily placed on top of each force plate and fixed with double sided tape. This plate was provided with a small notch where a metal rod equipped with five reflecting markers could be inserted. This ensured that the CoP on the force plate and the tip of the metal rod stayed consistent throughout the testing and prevent that a moment is created. One trial per force plate was captured while the metal rod was placed onto the notch. The rod was then moved in circles around the notch while keeping pressure on the metal rod. To ensure that during the trial the force was consistently passing through the rod, a metal bar could be placed on top of the rod so that the operator was able to apply a consistent force. The orientation of the tip position of the rod and the CoP could then be calculated by the force platform data and be compared with the orientation and position of the notch delivered by the motion system.

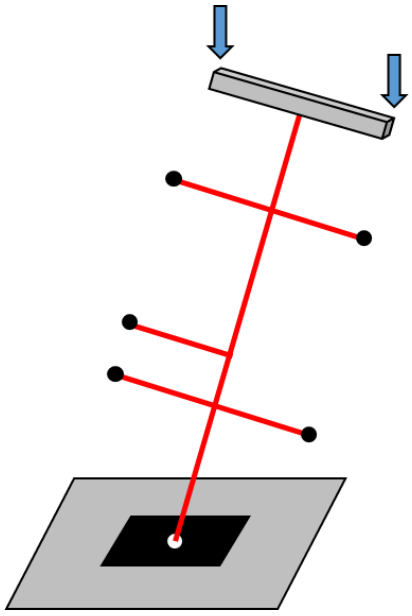

Figure 5.2. Principle of the CalTester. A rod is placed onto a small notch provided on a metal plate (black square) which is temporarily placed on the force plate (grey square) and fixed with double sided tape. Another metal bar can be placed on top of the rod, again provided with a small notch, to ensure that the force vector is passing through the rod. Five markers are placed alongside the rod. The arrows define where the operator should place pressure on the rod while moving the rod in circles.

5.2.3 Participant Preparation

To place the electrodes onto the skin the SENIAM (Surface Electromyography for the Non-Invasive Assessment of Muscles) guidelines were applied (Hermens & Freriks; Merletti & Hermens, 2000). After gently shaving the skin to ensure a minimisation of artefacts resulting out of small hairs between the skin and the electrodes, the skin was prepared with an abrasive paste. This insures a lower impedance between electrode and skin and a good fixation of the electrodes, which also reduces the risk of artefacts (Hermens et al., 2000). The skin was then gently cleaned with disinfectant pads before the electrodes were placed along the muscle fibres as defined by the SENIAM guidelines. The reflective marker set which has been described in detail in chapter IV was placed. Additional markers were placed on the right and left posterior iliac spine and on top of the tarso-metatarsal joint to allow parallel use of the Conventional Gait Model which is used in Vicon (PlugInGait) (Baker, 2013). The same experimenter positioned the reflective markers as well as the wireless EMG sensors, which were fixed with double sided tape and placed on the required positions and landmarks. To minimise skin movement artefacts the markers were placed on bony landmarks or on a part of the segment with less skin movement.

5.2.4 Data Collection

After taking required anthropometric data from the participant (height, mass, knee and ankle width) the participant was asked to stand stationary on one of the force plates while the operator captured a static trial. This enables the musculoskeletal model in OpenSim to be scaled as well as the joint centre locations in Vicon to be calculated relative to the local coordinate systems of the segments (Davis III et al., 1991). The participant stood still with the arms gently crossed in front of the chest so that all markers were visible with the shoulders still in a neutral position. This trial was also used to measure the body mass of the participant for the OpenSim pipeline. After the representative static trial had been captured, the participant walked at his/her self-selected speed straight over the force plates on a ten meter walkway. The participant was asked to continue walking until five gait cycles each starting with the right and left foot were recorded.

All trials required that both feet during the foot contact phase were fully placed on top of one of the force plates so that the whole GRF related to the body mass could be captured. To be sure that the participants walked in their most normal walking pattern, targeting was not allowed. Although some studies have shown that variations to spatiotemporal patterns (Verniba,

Vergara, & Gage, 2015) and ground reaction forces (Grabiner, Feuerbach, Lundin, & Davis, 1995) may not be significant, it is generally assumed that visual targeting of the force plates should be avoided due to the risk of an unnatural walking pattern (Oggero, Pagnacco, Morr, Simon, & Berme, 1998; Perry & Burnfield, 2010).

This procedure was repeated for 20% and 40% slower and faster walking speeds. This was monitored with timing gates placed five meters apart the start and end of the force plates alongside the plane of progression. Participants were given feedback on their speed to guide them to walk at the prescribed speed to within 1%. The faster walking trials were set to the end of the testing session to prevent the participant of an early stage of fatigue. Therefore, the walking protocol was arranged in following order with the inclusion of at least five right and five left valid walking trials each: 1. Self-selected walking speed, 2. 20% slower, 3. 40% slower, 4. 20% faster, 5. 40% faster.

The EMG excitations were recorded with Vicon Nexus and synchronised with the motion capture system. However, a time delay of 312ms of the wireless EMG system needed to be taken into account resulting from the wireless settings of the system. Before the actual start of the measurement and after placing the EMG electrodes a cross-talk check of all the EMG muscle excitations was undertaken by asking the participant to activate separately the muscles of interest. During the measurement session some of the trials were pre-processed to ensure the quality of the EMG excitations. Also, during the measurement the force plates were regularly reset to zero to receive accurate ground reaction force data.

5.2.5 Data processing

After the data collection procedure, the raw marker trajectories were pre-processed in Vicon by a customised pipeline to calculate a number of virtual landmarks and joint centres (see chapter IV.4.1 for more details) and then, including the raw ground reaction force data, exported in an ASCII file for further processing. The ground reaction forces were filtered in MATLAB (2012b) with a 6Hz low-pass 2^{nd} order Butterworth filter and automatically replaced in the ASCII file. All these files were then imported into an OpenSim tool called *Lee-Son's Toolbox* (S. Lee & Son, 2010). This tool re-formats the data to be compatible with OpenSim. Raw marker trajectory data in Vicon for the Conventional Gait Model (which is used for comparison) were filtered with a Woltering routine including a mean standard error of 10.

The surface EMG signals were separately exported out of Vicon into .c3d files and further processed in MATLAB (2012b) by using an EMG analyser tool which has been developed from the University of Salford (version 1.3, Phil Tresadern). This tool contains a two stage process where, firstly, the .c3d files are converted into MATLAB files which, secondly, are further used to process and filter the EMG excitations. By defining the gait cycle prior in Vicon the trial can be automatically cut to the time of interest. EMG signals are then high-pass filtered with a 20Hz Fast Fourier transform filter in addition to the 500Hz low-pass filter of the NORAXON system. To create a linear envelope of the muscle excitations the signals are finally filtered with a 6Hz low-pass 2nd order Butterworth filter and then finally exported into an ASCII file.

To be able to compare the surface EMG patterns to the estimations of muscle activations and forces the magnitude of the signals need to be normalised (Burden, 2010). To date, normalisation of EMG excitations are highly discussed in the literature, but no gold standard has been defined yet (Perry & Burnfield, 2010). Pilot work suggests that attempts to normalise the EMG excitations using maximum voluntary contraction tests on a dynamometer (KinCom) led to excessive inter-participant variability (in agreement with Clarys, 2000). The results of the pilot data of this study showed that normalising to the average muscle EMG excitation across the gait cycle is a more time efficient but still reliable technique. Therefore, the average excitation value across a typical gait cycle at very fast walking speed has been chosen for normalisation.

As described in chapter IV of this work, the simulation tool OpenSim has been chosen for this study to estimate the muscle activations and forces during healthy walking. The adapted musculoskeletal model gait2392 was implemented using the adjusted pipeline defined in chapter IV for the estimation process. This includes the scaling of the musculoskeletal model, the calculation of the joint angles using inverse kinematics, and the calculation of joint moments using inverse dynamics. Furthermore, both optimisation methods static optimisation and CMC including the pre-step residual reduction algorithm (RRA) were selected (chapter IV) and used to estimate muscle activation and forces. For the comparison with surface EMG the estimated excitations (actuator controls) of CMC were used and not the latter calculated activations as the CMC excitations are closer to the experimental surface EMG excitations (chapter IV). Static optimisation provides only the muscle activations which were chosen for comparison with surface EMG.

5.2.6 Data Analysis

To analyse the quality of the Scaling Tool the overall mean as well as maximal RMS marker errors across all ten participants will be stated and discussed and compared to OpenSim's recommendations. Also, scaling factors of individual segments are averaged across participants and presented. Marker fitting errors of the Inverse Kinematics Tool will be averaged and the overall mean and maximal RMS errors across all ten participants will be presented. Furthermore, estimated joint angles with OpenSim will be descriptively compared to joint angles which were calculated with the standard Conventional Gait Model (PlugInGait) in Vicon while taking the average for self-selected walking speed. The same comparison will be undertaken with estimated joint moments.

RMS values for the Scaling Tool and the Inverse Kinematics Tool were calculated as follows: firstly, a RMS value for each participant was calculated separately by taking the RMS value for each gait cycle which then is averaged to gain a mean RMS value for that participant; secondly, the overall mean and maximal RMS value are calculated across all ten participants by using the calculated individual mean RMS values of each participant.

The body mass adjustment within RRA is presented for each participant and walking speed separately, whereas the torso's centre of mass adjustment is averaged across participants and its distribution presented across walking speeds. Additionally, adjusted joint angles with RRA are compared to results of the Inverse Kinematics Tool. Averaged ground reaction force and moment residuals of RRA and CMC's reserve actuators of the hip, knee and ankle moments across participants are presented for each walking speed and compared to the recommendations of OpenSim.

The activation/excitations and forces which have been estimated with static optimisation and CMC are presented and descriptively analysed for the tibialis anterior, gastrocnemius medialis and lateralis, soleus, semitendinosus, rectus femoris, and vastus medialis and lateralis. Estimated muscle activation/excitation are compared to surface EMG for each walking speed averaged across corresponding walking trials to validate estimations in shape and speed-dependence. Estimated muscle forces are compared to corresponding activation/excitations of static optimisation/CMC. Additionally, results of three participants are exemplarily presented to demonstrate individual differences.

5.3 Results

The measurement duration for a testing session took in average approximately two and a half hours. Participants walked at a self-selected walking speed of 1.28±0.12m/s which lies within the values in the literature (Bohannon & Williams Andrews, 2011). Participants' characteristics are displayed in Table 5.2.

Table 5.2. Participants' characteristics, including age, gender, height in meter, and mass in kilograms.

Participant	Age	Gender	Height (m)	Mass (kg)
P01	29	F	1.62	55.80
P02	24	M	1.81	95.21
P03	41	M	1.73	65.00
P04	27	M	1.83	74.31
P05	23	F	1.69	70.95
P06	28	M	1.69	61.88
P07	29	F	1.63	65.75
P08	30	F	1.68	57.80
P09	26	M	1.84	72.99
P10	27	F	1.72	61.57
Average	28.40	5M:5F	1.72	68.13
SD	4.95		0.08	11.35

The following results were achieved for the calibration of the measurement system: the standard wand calibration of the Vicon system resulted in an average camera image error of 0.103±0.007mm, whereas the results of the caltester revealed an average force orientation error of 1.9±1.5° and an displacement vector between the centre of pressure (CoP) location estimated by the force plate and the endpoint of the caltester of -1.99±2.41mm in direction of progression (x-axis), 8.03±5.74mm in the vertical direction (y-axis), and -0.32±0.91mm in the lateral-medial direction (z-axis).

For two participants, one EMG sensor was not functioning throughout the measurement session through an unexplained error. It was decided to not interrupt and stop the session but to go on as planned taking the not functioning EMG sensor into account.

5.3.1 Scaling

The developed scaling pipeline (chapter IV) was running successfully for all ten participants. Table 5.3 summarises the mean and maximal RMS marker fitting errors between experimental and virtual calibration markers for static scaling. The overall RMS fitting error of the participants' static trials is 0.83cm. The highest RMS fitting error is presented on the lateral and medial epicondyles (lateral left=2.98cm and right=2.61cm, medial left=2.75cm and right=2.15cm) and on the fifth metatarsals (left=2.67cm, right=3.14cm). In the online user guide OpenSim recommends a mean RMS fitting error of less than 1cm and a maximum fitting error of 2cm. The epicondyle markers as well as the marker on the fifth metatarsal lie, therefore, over the recommendations of OpenSim's. All other markers are within the recommended marker error range. The smallest maximal RMS values can be found on the trunk, pelvis and hip.

Table 5.3. Mean and maximal RMS marker fitting error of the calibration markers used for static scaling in centimetre.

Static Trial (overall RMS = 0.83)						
Marker	**MidAcromium**	**LASIS**	**RASIS**	**Sacrum**	**L HJC**	**R HJC**
Mean	0.15	0.27	0.27	0.32	0.21	0.22
SD	0.04	0.17	0.13	0.12	0.15	0.15
Max	0.22	0.61	0.50	0.58	0.48	0.50
Marker	**L KJC**	**R KJC**	**L Epicondyle l**	**R Epicondyle l**	**L Epicondyle m**	**R Epicondyle m**
Mean	0.78	0.65	2.05	1.95	1.35	1.17
SD	0.46	0.40	0.46	0.57	0.60	0.51
Max	1.81	1.56	2.98	2.61	2.75	2.15
Marker	**L AJC**	**R AJC**	**L Malleolus l**	**R Malleolus l**	**L Malleolus m**	**R Malleolus m**
Mean	0.43	0.46	0.98	0.78	0.66	0.61
SD	0.15	0.22	0.27	0.18	0.20	0.18
Max	0.65	0.76	1.41	1.10	0.95	0.85
Marker	**L 5MTP**	**R 5MTP**				
Mean	2.21	2.33				
SD	0.38	0.51				
Max	2.67	3.14				

Note. LASIS=left anterior superior iliac spine, RASIS=right anterior superior iliac spine, L=left, R=right, l=lateral, m=medial, HJC=hip joint centre, KJC=knee joint centre, 5MTP=fifth metatarsal joint.

Bony segments of the generic musculoskeletal model were scaled independently in its principle axis (proximal-distal P-D) compared to both other axis (anterior-posterior A-P, medial-lateral M-L). Scaling factors differ slightly between segments as well as between different dimensions (Figure 5.3). The biggest discrepancy was within the femur, with the transverse plane scaling factors about 40% larger than those for the primary axis and showing most variability as well (as represented by standard deviation bars). By contrast, the tibia was scaled about 20% less in the transverse plane than along its primary axis. All other scaling factors were similar.

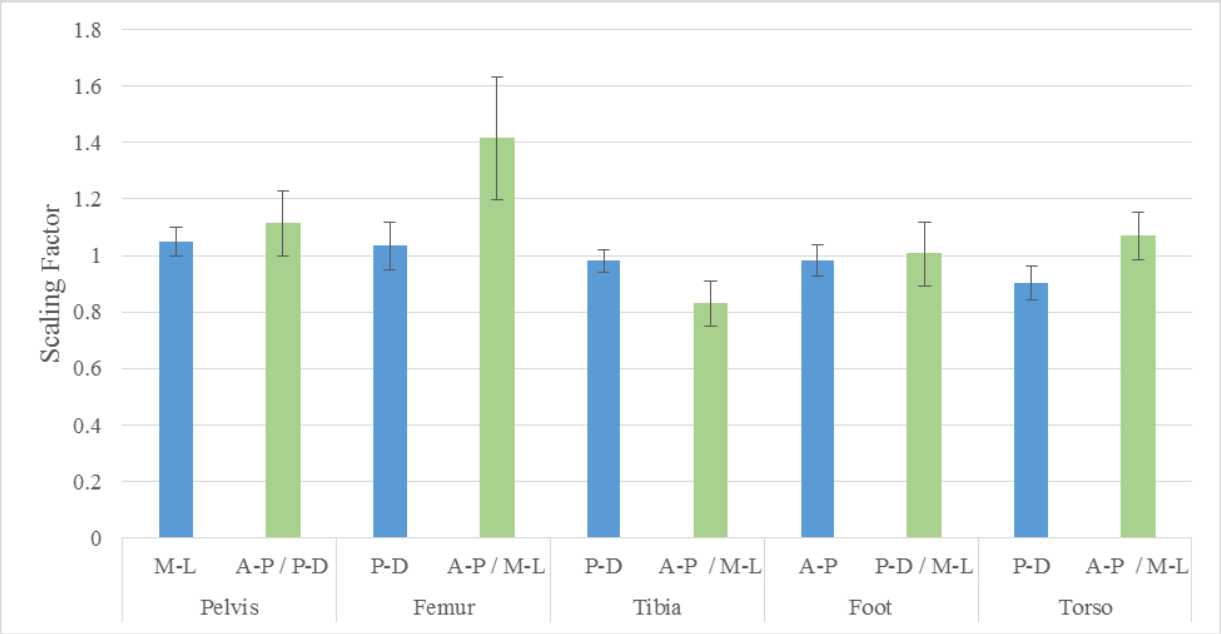

Figure 5.3. Mean and one standard deviation bars representing the scaling factors of the bony segments of the generic musculoskeletal model gait2392 in all three directions anterior-posterior (A-P), medial-lateral (M-L), and proximal-distal (P-D). Blue indicates the primary axis, green both other axes.

5.3.2 Inverse Kinematics

The results of the least square error problem which has been solved during inverse kinematics are listed in Table 5.4. This table includes one typical self-selected walking trial per participant and presents the tracking markers. The overall mean RMS error reached 0.91cm which lies within the recommended OpenSim user guidelines for dynamic fitting (<2cm). None of the markers exceeded the recommended mean RMS value; the highest mean fitting error is shown on the thigh markers and on the tip toe marker. It is further recommended that the maximum fitting errors should not exceed 4cm. This only occurs on the right medial toe marker with an error of 6.82cm.

Table 5.4. Mean and maximal RMS marker fitting error in centimetre of the tracking markers used for one typical walking trial during inverse kinematics.

Dynamic Trial (overall RMS = 0.91)						
Marker	**LAcromium**	**RAcromium**	**Sternum**	**LASIS**	**RASIS**	**VSacral**
Mean	0. 82	0.75	0.85	0.86	0.81	0.65
SD	0.32	0.24	0.44	0.23	0.22	0.21
Max	2.36	2.17	2.29	2.33	2.32	1.89
Marker	**RThighFront**	**RThighUpper**	**RThighRear**	**RShankFront**	**RShankUpper**	**RShankRear**
Mean	1.07	1.14	1.00	0.76	0.87	0.79
SD	0.20	0.22	0.20	0.12	0.19	0.16
Max	2.69	2.75	3.25	3.94	3.50	3.42
Marker	**LThighFront**	**LThighUpper**	**LThighRear**	**LShankFront**	**LShankUpper**	**LShankRear**
Mean	1.14	1.18	1.02	0.82	0.88	0.75
SD	0.16	0.29	0.26	0.20	0.40	0.35
Max	2.61	2.93	2.32	2.14	2.79	2.61
Marker	**LHeel**	**RHeel**	**LToeTip**	**RToeTip**	**LToeLat**	**RToeLat**
Mean	0.85	0.82	1.12	1.14	1.01	0.98
SD	0.18	0.16	0.26	0.17	0.16	0.16
Max	2.97	3.39	3.71	3.83	3.55	3.00
Marker	**LToeMed**	**RToeMed**				
Mean	0.76	0.83				
SD	0.21	0.21				
Max	1.89	6.82				

Note. L=left, R=right, LASIS=left anterior superior iliac spine, RASIS=right anterior superior iliac spine, lat=lateral, med=medial.

In general, estimated joint angles are comparable with results in the literature (for example Perry & Burnfield, 2010). In this study, the experimental data have also been fully processed using the Conventional Gait Model PlugInGait in Vicon to compare them with the results in OpenSim. A typical comparison of the joint angles of participant P02 can be found in Figure 5.4. The patterns for both the joint angles of the OpenSim solution and the PlugInGait solution are overall similar to each other. However, some differences are detected. Firstly, the pelvis tilt and hip flexion are slightly higher for the results of PlugInGait than for OpenSim. Secondly, the hip abduction's pattern in swing phase is different between the two approaches. Thirdly, both the knee flexion peak values are higher with the OpenSim approach than with PlugInGait. And, fourthly, the ankle dorsiflexion for the results received with PlugInGait shows, especially in swing, a higher plantar flexion. Furthermore, the dorsiflexion in OpenSim is earlier and increased in swing.

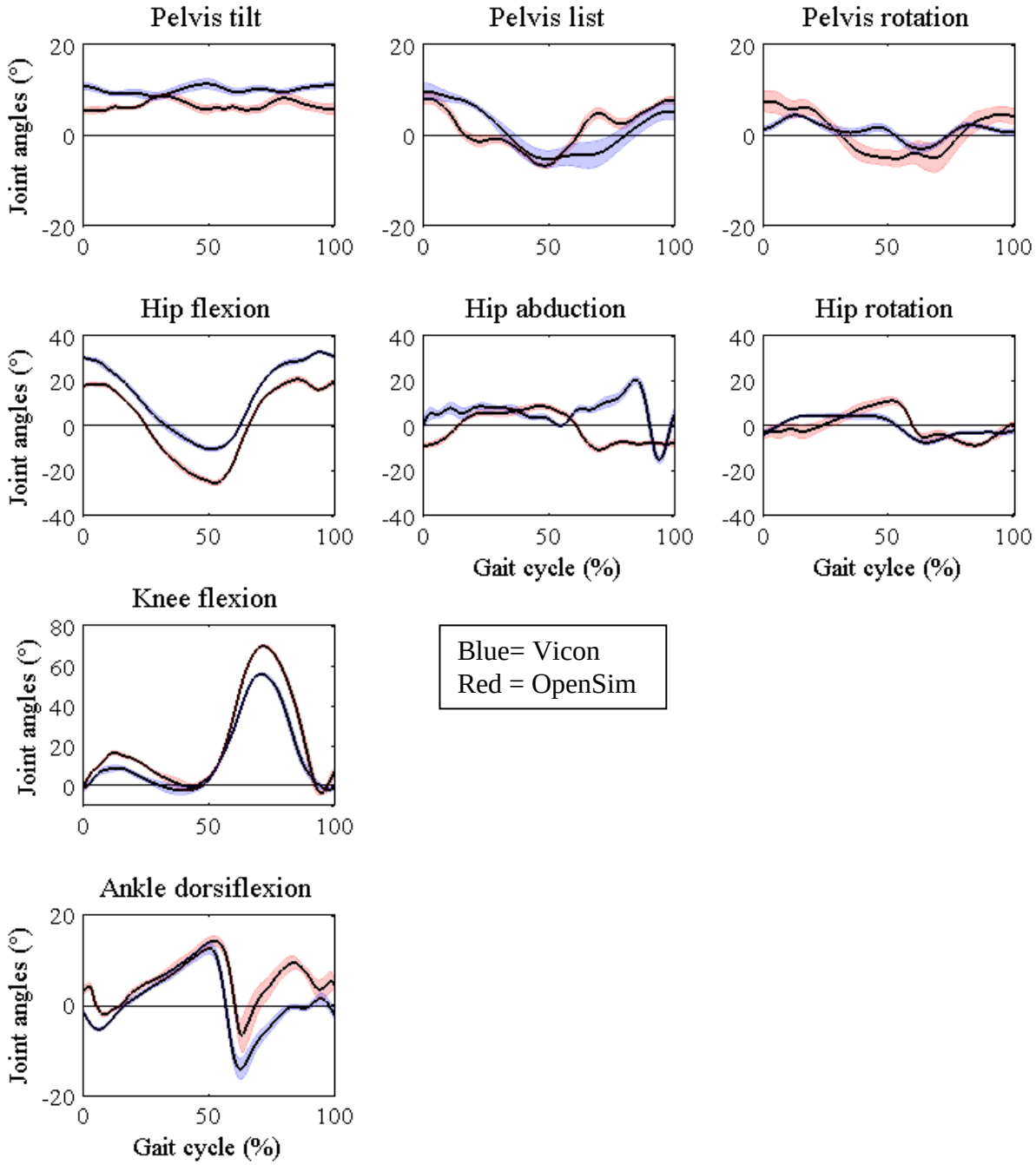

Figure 5.4. Mean and one standard deviation of joint angles calculated in OpenSim (red) and Vicon Nexus (blue) for five right walking trials of one typical participant (P02) during self-selected walking speed.

Averaged joint angles estimated with OpenSim for all ten participants at their self-selected walking speed including both the right and left gait cycle are shown in Figure 5.5. In general, there exists a low variability between participants; however, a high standard deviation band is shown around the mean for pelvic tilt and, therefore, a higher variability than in the other planes

of the pelvis (pelvis list, pelvis rotation). Additionally, knee flexion in stance phase shows an increased standard deviation at the first peak. This variability, however, has also been shown previously in the literature (Kadaba et al., 1989; Winter, 1990).

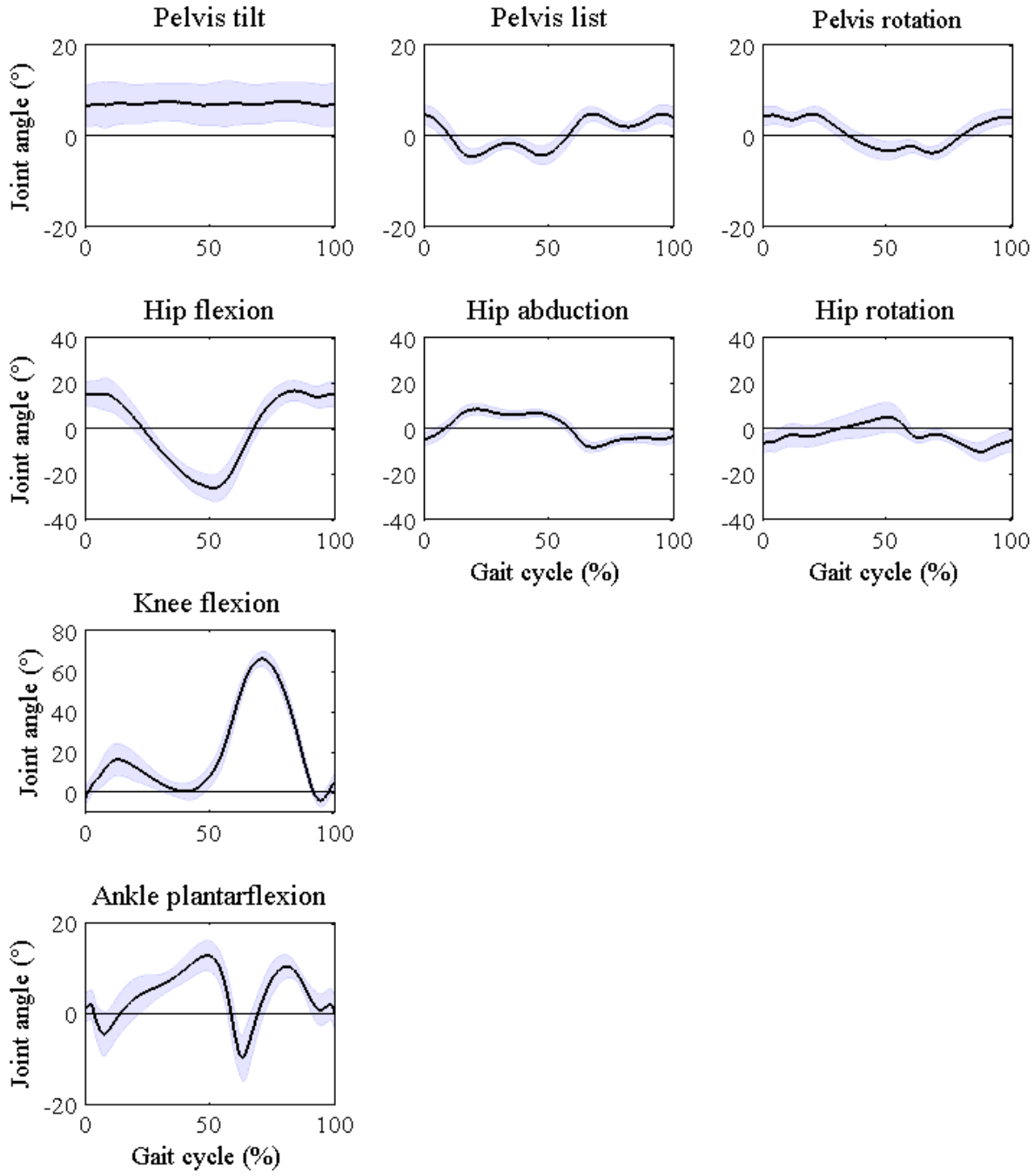

Figure 5.5. Average joint angles of OpenSim across five right and five left walking trials of all ten participants during self-selected walking speed.

5.3.3 Joint Moments

Estimated joint moments are not used as an input in the muscle force estimation pipeline but are a good indicator of the quality of kinematic and kinetic modelling. They, however, are frequently discussed in clinical gait analysis and thus are of interest in their own right. Figure 5.6 shows the internal joint moments of the hip, knee and ankle during self-selected walking speeds for one typical participant calculated with OpenSim and compared with the results from Vicon.

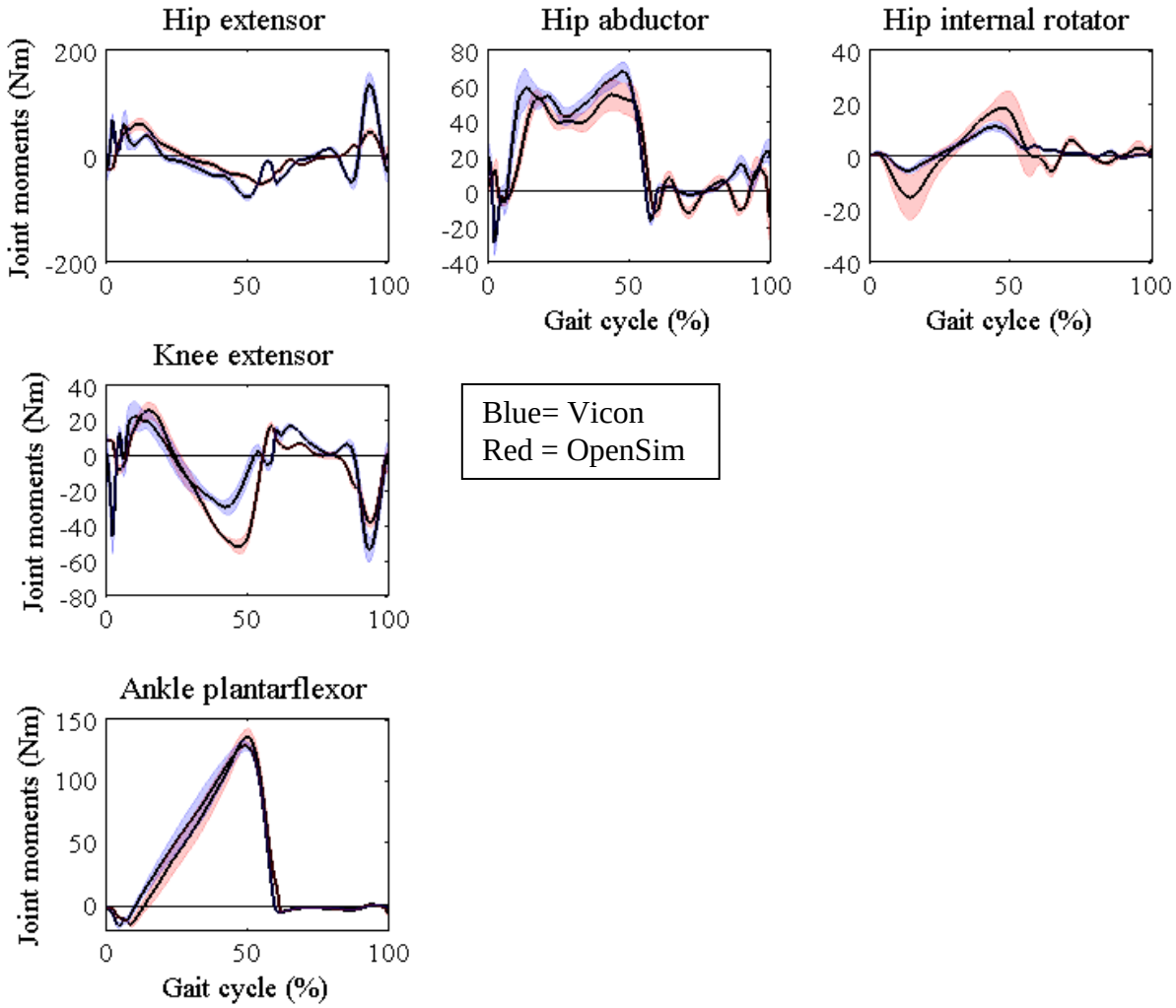

Figure 5.6. Mean and one standard deviation internal joint moments (Nm) calculated in OpenSim (red) and Vicon (blue) for five trials each of one typical participant during normal walking.

Like the findings for the joint kinematics, an overall agreement between the results of PlugInGait and OpenSim is shown. However, some small differences can be detected as well: the hip flexion moment has more prominent peaks for the PlugInGait solution than for the

results of OpenSim; however, for the frontal and transverse plane it is the other way round. Also, the magnitude as well as the standard deviation band of the hip rotation moment is smaller with PlugInGait than with OpenSim. The magnitude during mid stance of the knee flexion moment is higher with OpenSim than with Vicon. Compared to the hip and knee joint moments, the ankle plantar flexion moment is consistent between Vicon and OpenSim.

Figure 5.7 presents the average internal joint moments including the right and left gait cycle for all ten participants for self-selected walking speeds. The consistency between participants is again high; increased standard deviation bands can be found at peak joint moments and at the ankle during 20 to 30% of the gait cycle.

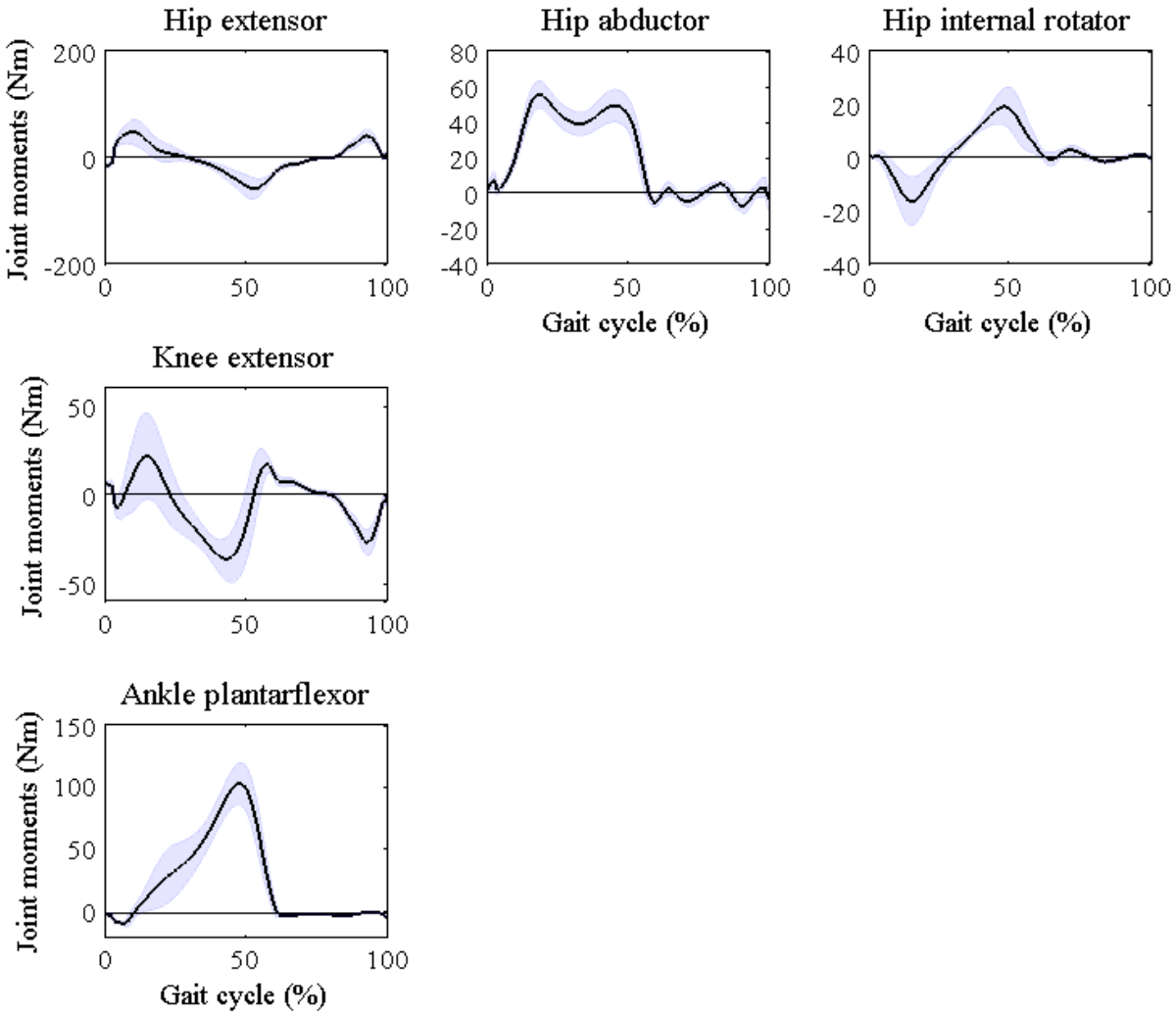

Figure 5.7. Average internal joint moments of OpenSim (Nm) for ten participants including five right and left gait cycles for self-selected walking speeds.

5.3.4 Muscle Activations/Excitations and Force Estimations

The results of estimated muscle activations of static optimisation and the excitations of CMC are compared to surface EMG. The estimation's pattern as well as speed-dependent changes will be evaluated and individual results of three participants additionally presented in his section. Furthermore, estimated muscle forces will be compared to corresponding activations/excitations including speed-dependent and participant specific evaluations of the results.

The computational time which was needed to successfully run muscle force estimation for one trial were about one minute for static optimisation and 30 minutes for CMC. Before presenting the muscle activations and forces the results of CMC's pre-step RRA will be presented.

5.3.4.1 Results of the Residual Reduction Algorithm

In general, the residual reduction algorithm ran successfully. However, for some of the walking trials RRA crashed during processing. This affected walking trials from six out of the ten participants (P02-P04, P06, P09, P10). Fast (8 trials) and very fast (13 trials) walking trials failed most commonly. Additionally, the left very fast walking trials of participant P06 and the right fast walking trials of P09 were crashing throughout with RRA. Apart from the faster walking speeds, only one trial for slow and one for very slow walking failed (P03). The OpenSim output file which is given after every step of the OpenSim pipeline defines the failure of RRA as follows:

> *CMC.computeControls: ERROR- Optimizer could not find a solution.*
> *Unable to find a feasible solution at time = 2.857.*
> *Model cannot generate the forces necessary to achieve the target acceleration.*
> *Possible issues: 1. not all model degrees-of-freedom are actuated,*
> *2. there are tracking tasks for locked coordinates, and/or*
> *3. there are unnecessary control constraints on reserve/residual actuators.*

Table 5.5 presents the body mass adjustments, relatively distributed across all segments, which were carried out by the RRA Tool to adjust the kinematics to be more consistent with the experimental ground reaction forces (chapter IV). The biggest change in participants' body mass is shown for the very fast walking trials, where the average mass adjustment is -1.69±1.10kg with the smallest and greatest individual mass adjustment of -0.29kg and -3.31kg,

respectively. The body mass during very fast walking speeds have, therefore, been all corrected in negative direction, resulting in a smaller body mass than before. However, for the other walking speeds some of the participants' body masses have been adjusted slightly upwards towards a greater body mass, with 0.67kg for participant P04 while walking at self-selected walking speed.

Table 5.5. Overall adjusted mass (kg) through RRA for all ten participants divided up in five walking speeds, averaged across all ten trials.

Participant		Walking speed				
		Very slow	Slow	Self-selected	Fast	Very fast
P01		0.01	0.07	0.16	0.40	-0.29
P02		-1.59	-1.39	-0.23	-0.60	-1.42
P03		-1.60	-1.41	-0.48	-1.24	-3.31
P04		-0.11	0.18	0.67	-0.25	-0.94
P05		-1.27	-1.05	-1.35	-1.88	-2.61
P06		0.32	0.50	0.57	0.57	-2.10
P07		0.12	-0.04	-0.20	-0.16	-3.25
P08		-0.32	-0.23	-0.32	-0.10	-0.34
P09		-0.25	-0.30	0.12	-0.65	-1.56
P10		-0.17	-0.17	-0.10	0.00	-1.09
Average	Mean	-0.49	-0.38	-0.12	-0.39	-1.69
	SD	(0.72)	(0.67)	(0.57)	(0.74)	(1.10)

The walking speed with the smallest averaged mass adjustment is the self-selected walking speed with -0.12±0.57kg. During this speed all participants show a mass adjustment under ±0.5kg, except two participants who are slightly over (0.57kg, 0.67kg) and one participant who is clearly over ±0.5kg (-1.35kg). However, the latter represents a participant with a general mass adjustment of 1kg or more throughout all walking trials.

Another parameter which is adjusted while running RRA is the torso's centre of mass (CoM) in medial-lateral as well as anterior-posterior direction which leads into a better consistency between kinematics and experimental GRFs. Average adjustments across all ten participants can be found in Figure 5.8. The torso CoM is moved anterior closer to the sternum compared to its original position across all walking speeds. However, from very fast (1.64cm) to very slow walking (3.88cm) a slight increase in the amount of adjustments in anterior-posterior direction can be detected. Here, the standard deviations stays similar across speeds. Different

results are shown for the adjustments in medial-lateral direction as the amount the CoM is shifted stays similar across different speeds (2.90-3.18cm), which is also reflected in its standard deviation bands (±1.19-1.38cm). This means, however, that the CoM of the torso independent of participant and trial is shifted in average about 3cm to the same lateral side.

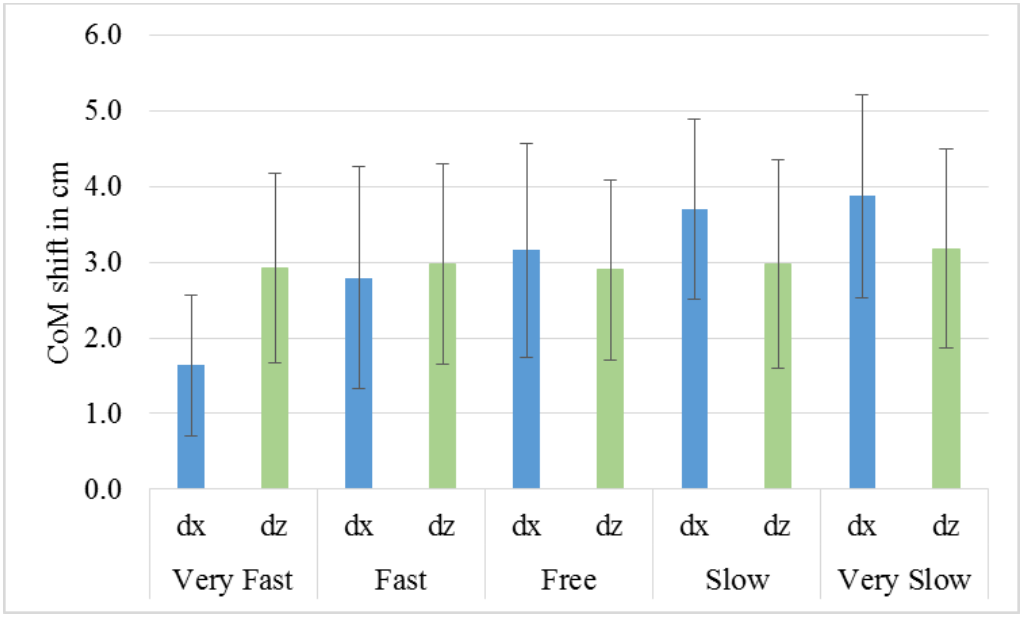

Figure 5.8. Histogram showing the torso centre of mass adjustments in centimetres for all five walking speeds after running RRA in OpenSim. The bars indicate the mean adjustment across all ten participants, the error bars show one standard deviation; dx=anterior-posterior direction, dz=medial-lateral direction.

RRA residuals account for the measurement errors between experimental ground reaction forces and estimated joint angles (chapter IV). The average and standard deviation of the RRA residuals across all participants are presented in Table 5.6. The user guide of OpenSim recommends residual thresholds for average residual forces up to ±5N (good) and ±5-10N (okay) and defines more than ±10N as too high. For the residual moments the recommended values are defined up to ±30Nm (good), ±30-50Nm (okay) and trials including residual moments above ±50Nm should not be used for further processing (Lund & Hicks, 2013).

Highest average residual forces which could be found for this study occurred during very fast walking with 5.35±12.29N (F_y) and -5.02±3.48N (F_x). These are also the only force residuals exceeding the good quality level set by OpenSim. However, when reviewing the peak maximum and minimum residual forces both F_x and F_y show high residuals which exceed the

limit of 10N. The highest residual force occurs again during very fast walking with 80.18N. The residual moments stay all under the recommended level, with the highest average and standard deviation of 5.50±4.84Nm at M_y and the highest maximum residual of 26.41Nm at M_z during very fast walking.

Table 5.6. Mean, standard deviations and the range of averaged residuals across the gait cycle after running RRA including five left and five right walking trials for each participant and walking speed.

Residuals			Walking speed				
			Very fast	Fast	Self-selected	Slow	Very slow
F_x	(N)	Mean	-5.02	-4.82	-4.07	-3.47	-2.85
		SD	(3.48)	(3.53)	(3.73)	(3.75)	(4.65)
		Range	-12.09/2.79	-15.95/2.45	-12.71/3.81	-13.54/3.84	-15.32/15.98
F_y		Mean	5.35	-1.16	-1.80	1.13	2.48
		SD	(12.29)	(6.99)	(5.89)	(6.31)	(6.72)
		Range	-14.06/80.18	-21.02/14.98	-14.74/18.45	-11.50/19.22	-8.09/21.46
F_z		Mean	0.59	0.33	-0.09	-0.18	-0.38
		SD	(1.67)	(1.12)	(0.82)	(0.78)	(1.01)
		Range	-3.39/7.35	-1.92/3.55	-2.24/2.15	-2.30/1.43	-3.65/1.85
M_x	(Nm)	Mean	1.10	0.47	0.37	0.54	0.57
		SD	(3.69)	(1.12)	(1.13)	(1.32)	(1.30)
		Range	-2.62/26.41	-2.16/3.98	-2.96/3.05	-3.09/3.28	-3.65/1.85
M_y		Mean	5.50	2.42	1.14	1.57	1.69
		SD	(4.84)	(3.12)	(1.75)	(1.28)	(1.22)
		Range	-3.70/20.38	-3.50/13.55	-4.92/4.96	-2.75/4.38	-2.73/4.25
M_z		Mean	0.56	0.55	0.59	0.53	0.43
		SD	(2.15)	(2.24)	(2.00)	(2.03)	(1.80)
		Range	-3.81/11.67	-4.15/8.76	-5.13/7.32	-4.34/8.98	-3.44/6.64

The RRA pipeline adjusts the estimated joint kinematics to a better fit closer to the experimental ground reaction forces. These adjustments are presented in Figure 5.9, which shows the average joint angles of RRA for normal walking overlaid over the results which were achieved running the inverse kinematics. The adjustments are minimal as for all joint angles both the inverse kinematics and the RRA solution are lying neatly on top of each other; however, ankle plantar flexion shows slight differences between RRA and inverse kinematics, especially during heel strike and at the end of the swing phase.

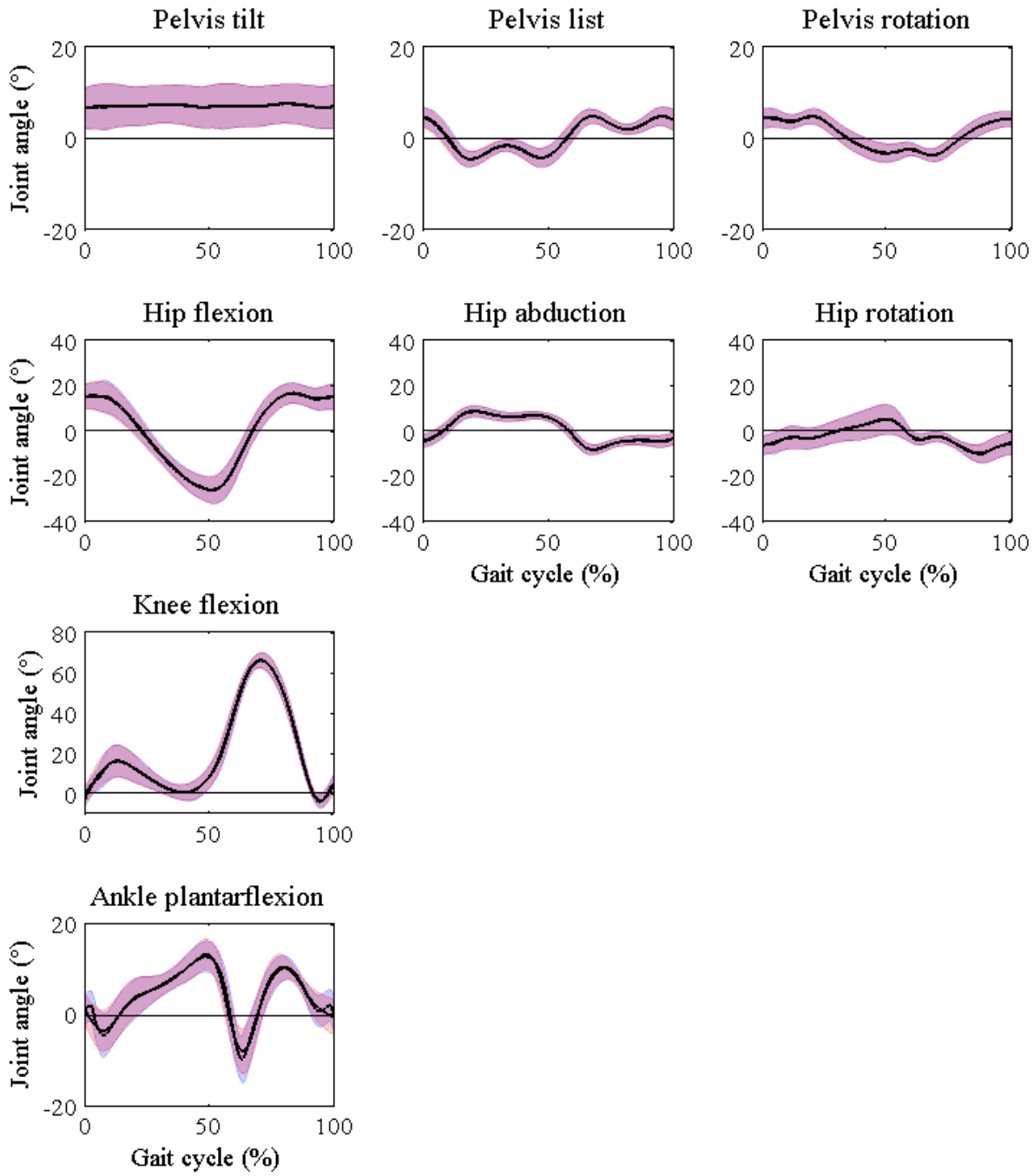

Figure 5.9. Adjusted kinematics through the pipeline RRA (red) compared to the results of inverse kinematics (blue) during normal walking, averaged across all 10 participants including both right and left.

5.3.4.2 Results of Estimated Muscle Excitations and Activations Compared to EMG

Static optimisation ran successfully for all ten participants. However, like with RRA CMC crashed for some of the walking trials as well. None of the participants had a success rate of 100% with CMC. The highest failure rate occurred during trials for very fast walking (14 trials out of overall 100 very fast walking trials), but all walking speeds were affected. Slow and very slow were, however, the walking speeds with the least failures (three trials each). Normal and fast walking speeds resulted in nine and six unsuccessful trials, respectively. In case CMC failed and crashed during the calculation process, the same output message then with RRA was specified.

As explained in chapter IV, reserve actuators are applied in CMC to make up for possible strength deficiencies in muscles. Because these reserve moments have, by definition, a very low optimal force and thus require very high excitations to apply substantial forces they are an indicator of muscles that are too weak as specified in the musculoskeletal model (Hicks & Uchida, 2013a). OpenSim recommends average reserves under 10Nm and peak reserves under 25Nm (good) or between 25-50Nm (okay). Average reserves on the hip, knee, and ankle joints across all ten participants are presented in Table 5.7, including the maximal and minimal reserve actuator which occurred across all trials. The mean and standard deviation of all joint moment reserves do not exceed OpenSim's recommendations. However, in some cases participant specific maximal and minimal values are greater than 50Nm, especially for the ankle plantarflexors. Highest peak reserve actuator can be detected at the knee flexors with -147Nm. With decreasing walking speeds the number of reserve actuators which lie within the recommendations increases. Furthermore, average reserve values are generally smaller with slower walking speeds than with faster walking speeds.

Table 5.7. Average, standard deviations, maximum and minimum reserve actuators of the hip, knee, and ankle joints for CMC.

		Walking Speeds				
		Very Fast	Fast	Self-selected	Slow	Very Slow
Hip flexion	Mean	0.227	0.077	0.016	0.011	0.007
	SD	0.263	0.119	0.063	0.026	0.008
	MAX	35.952	35.466	28.352	29.675	32.389
	MIN	-11.457	-7.846	-8.392	-2.020	-2.157
Hip adduction	Mean	-0.279	-0.113	-0.036	-0.018	-0.015
	SD	0.276	0.110	0.035	0.024	0.010
	MAX	7.113	7.407	0.977	0.480	0.033
	MIN	-34.963	-13.874	-12.192	-8.217	-15.257
Hip rotation	Mean	0.374	0.234	0.102	0.025	0.017
	SD	0.426	0.286	0.134	0.064	0.022
	MAX	34.707	35.349	32.512	9.198	3.744
	MIN	-19.701	-6.583	-6.725	-2.501	-4.622
Knee flexion	Mean	-0.277	-0.135	-0.068	-0.038	-0.029
	SD	0.250	0.152	0.125	0.047	0.030
	MAX	59.007	50.298	40.347	38.991	81.657
	MIN	-94.260	-71.520	-146.766	-105.631	-77.137
Ankle plantar flexion	Mean	1.305	0.761	0.438	0.251	0.197
	SD	0.718	0.395	0.260	0.128	0.084
	MAX	127.837	106.229	109.396	88.271	118.406
	MIN	-41.611	-43.890	-27.733	-29.252	-23.819

Note. SD=standard deviation, MAX=maximum, MIN=minimum.

By using a static optimisation procedure, CMC calculates muscle excitations called actuator controls which are further processed to estimate muscle forces. However, for this study the CMC excitations resulted in heavily noisy patterns (Figure 5.10). To be able to compare the CMC excitations in its shape and speed-dependence with surface EMG, it has been decided that these estimated excitations were filtered with the same 6Hz low-pass 2^{nd} order Butterworth filter which has been applied to create a linear envelope over the muscle EMG excitations. To be consistent while validating estimated data with surface EMG, activations of static optimisation were also filtered with the same 6Hz low-pass filter.

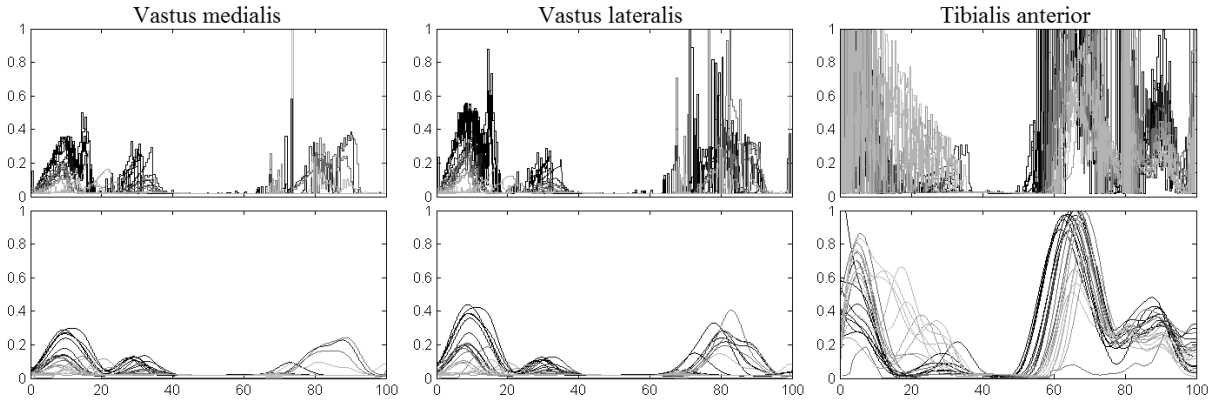

Figure 5.10. Example data of estimated muscle excitations with CMC of the tibialis anterior, vastus medialis and lateralis, non-filtered (above) and filtered with a 6Hz low pass 2nd order Butterworth filter (below) for walking trials of all speeds (light grey to dark grey=very slow to very fast) for one participant (P01).

Averaged static optimisation's muscle activations, CMC's muscle excitation and surface EMG excitations including one standard deviation across all ten participants for the self-selected walking speed are presented in Figure 5.11. Estimated peak values range between less than 0.2 (semitendinosus, vastus medialis) up to 1 (tibialis anterior, soleus). Normalised peak surface EMG excitations' range between 2.5 and 4.5 times an average EMG excitation across a typical walking trial.

The shapes and magnitudes between CMC and static optimisation are similar for all muscles except for the tibialis anterior. Here, CMC results in relatively high excitation patterns close to an activation of 1 which occur during the stance-swing transition, whereas static optimisation stays below an activation of 0.3. Another difference between CMC and static optimisation is the second peak of vastus medialis and lateralis around 80% of the gait cycle which is nearly not present for static optimisation but quite dominant for CMC. Small differences can be also found for the semitendinosus, where a third peak around 60% of the gait cycle occurs with CMC but is nearly not visible for static optimisation, and for the rectus femoris, where the peak value is slightly shifted between CMC and static optimisation (75% to 55%). Furthermore, for some of the muscle excitations of CMC a sharp and high peak is presented for the first percentage of the gait cycle. However, this may be due to the first 0.03 seconds which are used for the initial states needed for the CMC pipeline and are prone to be unstable.

The pattern of most estimated muscle excitations/activations are in general agreement with the surface EMG excitations. However, four main differences could be detected. Firstly, the peak

close to the stance-swing transition which has been estimated for the semitendinosus has not been captured with surface EMG as the EMG signal stays silent during this period. Secondly, rectus femoris estimation during heel strike and at the end of stance is relatively small or totally absent with the use of CMC and static optimisation compared to surface EMG. On the other side, between 30-70% of the gait cycle, the muscle estimations peak, whereas surface EMG shows only a small peak compared to the peak at heel strike and at the end of swing. Thirdly, the dominant peak for vastus lateralis and medialis at the end of swing is missing when using static optimisation, and peaks earlier with CMC. And fourthly, estimated results for the gastrocnemius lateralis and medials show both a second smaller peak at the end of the gait cycle which is not present with EMG.

The participants' inter-variability is mostly similar between static optimisation, CMC, and surface EMG as the standard deviation bands are comparable with each other compared to the mean. However, CMC excitations of the gastrocnemius medialis have a slight higher standard deviation for the descending activation after the peak around 40-50% of the gait cycle compared to static optimisation and surface EMG. Similar results occur for the tibialis anterior, where the standard deviation band of CMC at the end of swing is higher than with static optimisation or EMG.

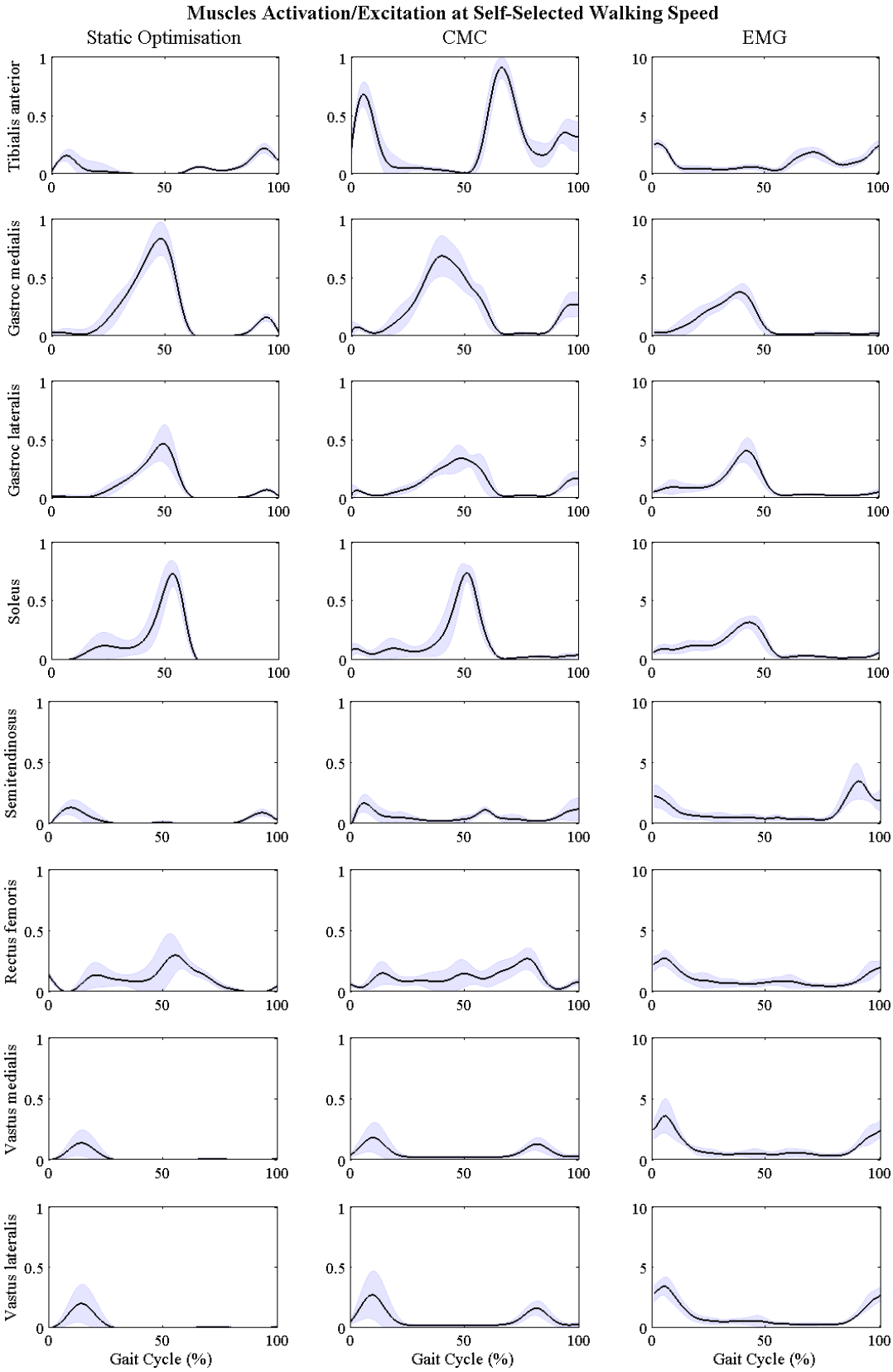

Figure 5.11. Mean and one standard deviation bands for static optimisation's muscle activation and CMC's muscle excitation (0= no activation, 1=full activation) compared to surface EMG (normalised to average signal across gait cycle) across all ten participants during self-selected walking speed.

Figure 5.12 to Figure 5.19 show the averaged muscle excitation of CMC compared to the activation of static optimisation and to surface EMG across all five walking speeds. Each figure presents the dependence of walking speed of one single muscle.

Tibialis anterior

Both estimation methods show nearly no speed-dependent influence on the tibialis anterior (Figure 5.12) which is comparable with the results of EMG. The average activation of static optimisation and CMC' excitation stay similar across walking speeds, except a longer activation after the first peak with slower walking speeds is evident for both mathematical models (10-50% of the gait cycle). The peak values in swing are slightly increasing with speed but stay within the range of the standard deviation bands. This difference with speed is not shown for EMG. Here, the only speed-dependent difference is a small increase of the whole signal during very fast walking compared to the other walking speeds. Again, however, the change stays within the standard deviation bands. In general, the standard deviation bands increase from very slow to very fast for both mathematical models and EMG.

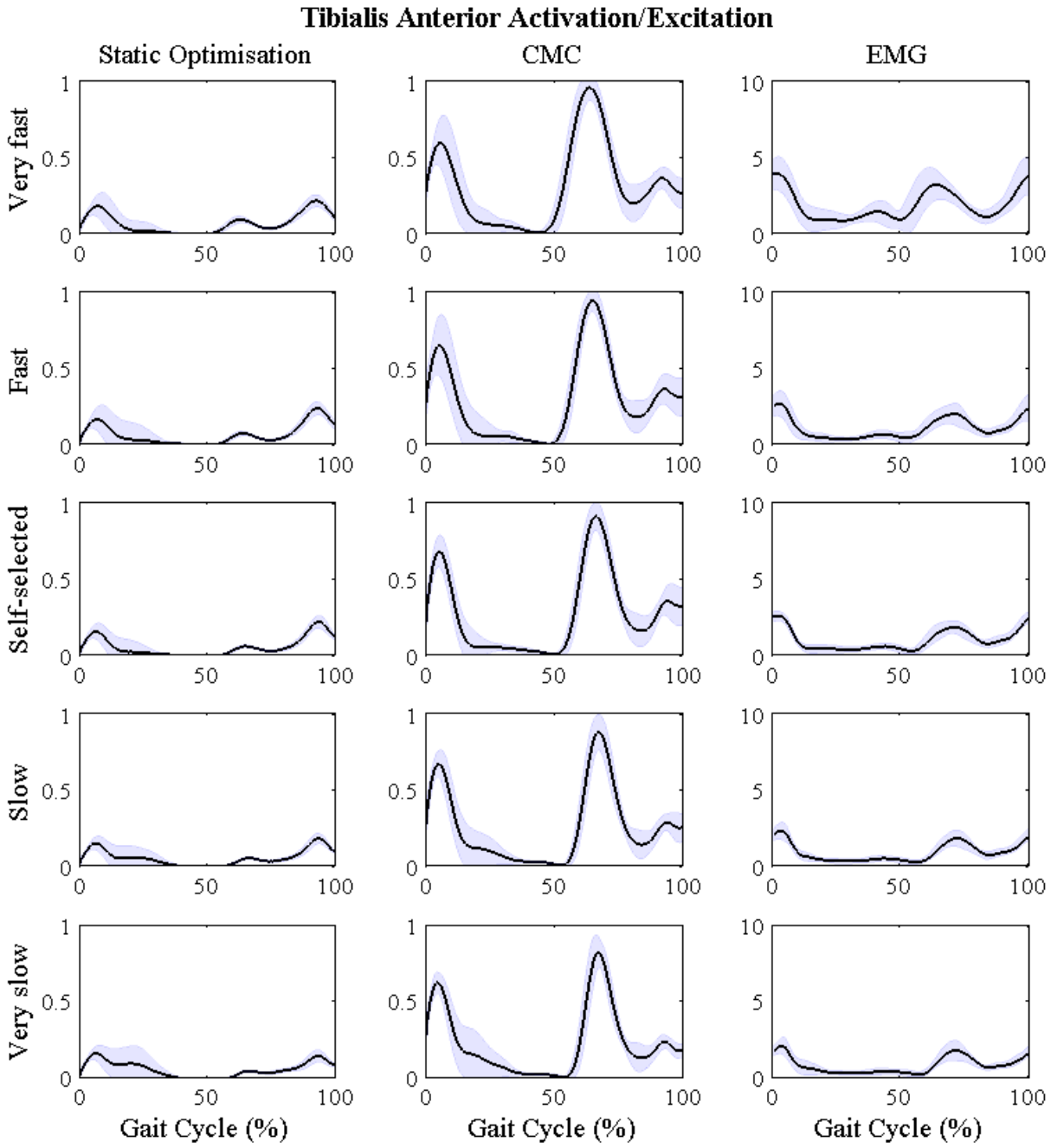

Figure 5.12. Mean and one standard deviation bands for static optimisation's muscle activation and CMC's muscle excitation of the tibialis anterior compared to surface EMG across five walking speeds including all ten participants.

Gastrocnemius medialis and lateralis

Both muscles of the gastrocnemius show in general dependence in speed (Figure 5.13 and Figure 5.14). The maximum peak increases with speed around 45-50% of the gait cycle as well as the small peak at the end of swing. Gastrocnemius medialis reaches slightly higher estimation values than lateralis of up to 1 during very fast walking. CMC estimations show additionally a second smaller peak during descending form the first peak at about 55% of the gait cycle for very slow and slow walking which is not shown for static optimisation. This is also shown for gastrocnemius lateralis, however, to a lesser extent. The estimations of CMC show another small peak after foot contact (5% of the gait cycle) for both gastrocnemius lateralis and medialis which is not shown for the estimation of static optimisation.

The different patterns of CMC are also not shown for surface EMG, except for very fast walking, where a small peak occurs during the first 10% of the gait cycle. Another difference between mathematical models and EMG is the peak at the end of swing which is not present with EMG. EMG, however, shows similar speed-dependent results than CMC and static optimisation, although an increased rise between fast and very fast walking is seen which is not seen to such an extent with both modelling techniques. The standard deviation bands of the gastrocnemius medialis for all three techniques stay the same throughout walking speeds except EMG's very fast walking, whereas gastrocnemius lateralis shows increasing standard deviation bands with faster walking speeds for both modelling techniques and EMG.

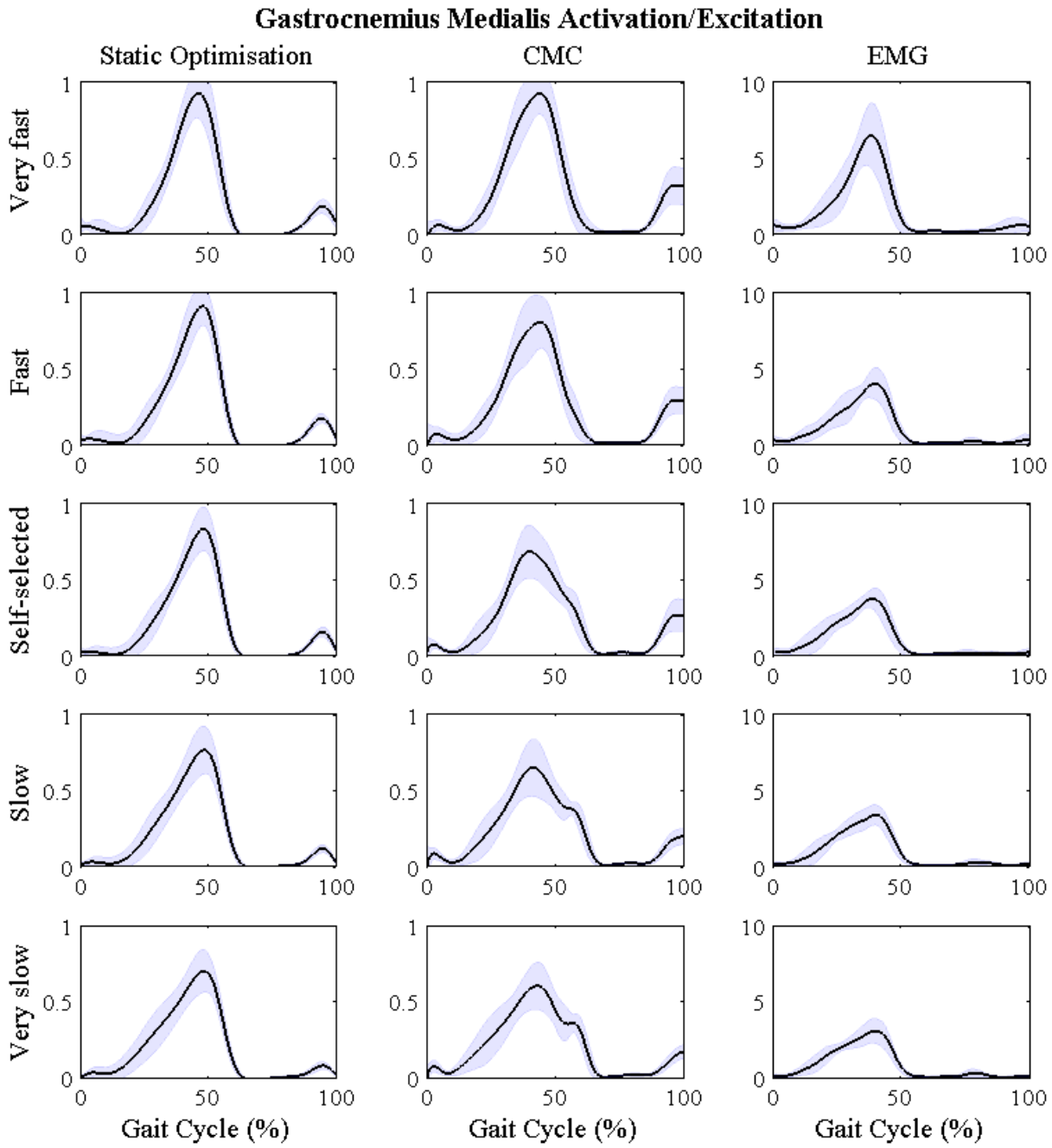

Figure 5.13. Estimated activation/excitation of the gastrocnemius medialis compared to surface EMG throughout walking speeds.

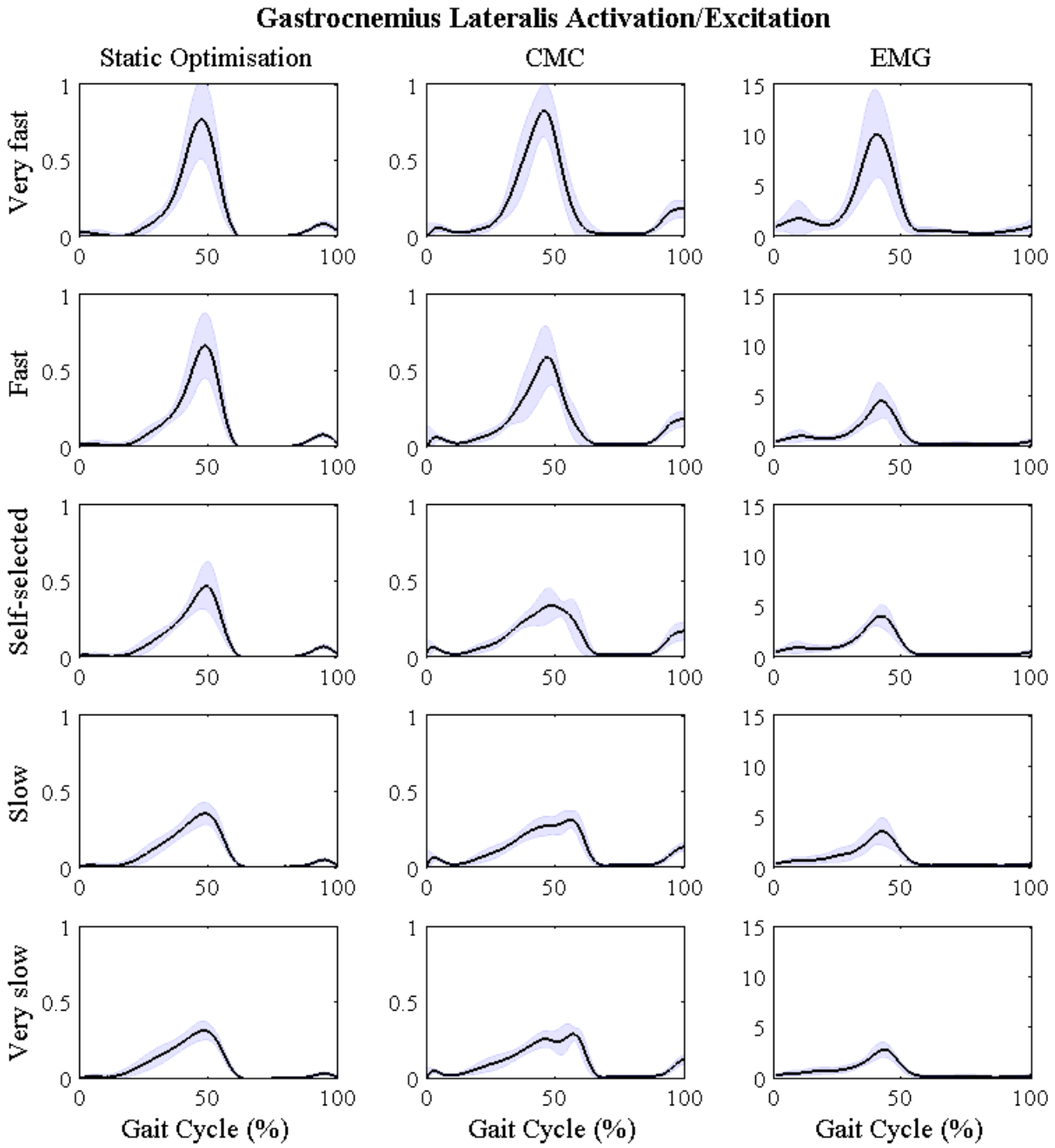

Figure 5.14. Estimated activation/excitation of the gastrocnemius lateralis compared to surface EMG throughout walking speeds.

Soleus

Like the gastrocnemius, the soleus shows dependence with different walking speeds for static optimisation and CMC (Figure 5.15). The maximal peak around 50% of the gait cycle increases and occurs slightly earlier with faster speeds. Static optimisation additionally shows an increase of the small activation plateau between 20-30% of the gait cycle which develops into a small peak for fast and very fast walking. This is not shown in such an extent for CMC. EMG shows as well an increase from very slow to very fast with the same increased rise between fast and very fast than with the gastrocnemius. The small activation plateau between 0-30% of the gait cycle rises, too, but does not develop into a peak. The standard deviation bands do not change greatly between speeds, only EMG shows a great increase for very fast walking.

Semitendinosus

The estimations of the semitendinosus for both static optimisation and CMC are changing with walking speed (Figure 5.16). Especially the first peak after initial foot contact (about 5-10% of the gait cycle) rises with increased speed. The second peak at the end of the gait cycle changes to a lesser extent for static optimisation and stays the same throughout speeds for CMC which is also true for the third peak of CMC. Only CMC's estimation during very fast walking shows a general rise in excitation in stance. Static optimisation develops a third peak with increasing walking speeds, too, which occurs a bit earlier than for CMC (45% of the gait cycle) and is shown for fast and very fast walking.

Compared to the mathematical models, EMG shows no great speed-dependence between very slow and fast walking; only the second peak at the end of swing is increasing with speed. Contrary to this, EMG's very fast walking shows a general increase and additionally smaller peaks between 40-60% of the gait cycle which is accomplished by an increase in the standard deviation band. In general, the standard deviation band increases with speed for static optimisation and CMC but stays the same for EMG except very fast walking.

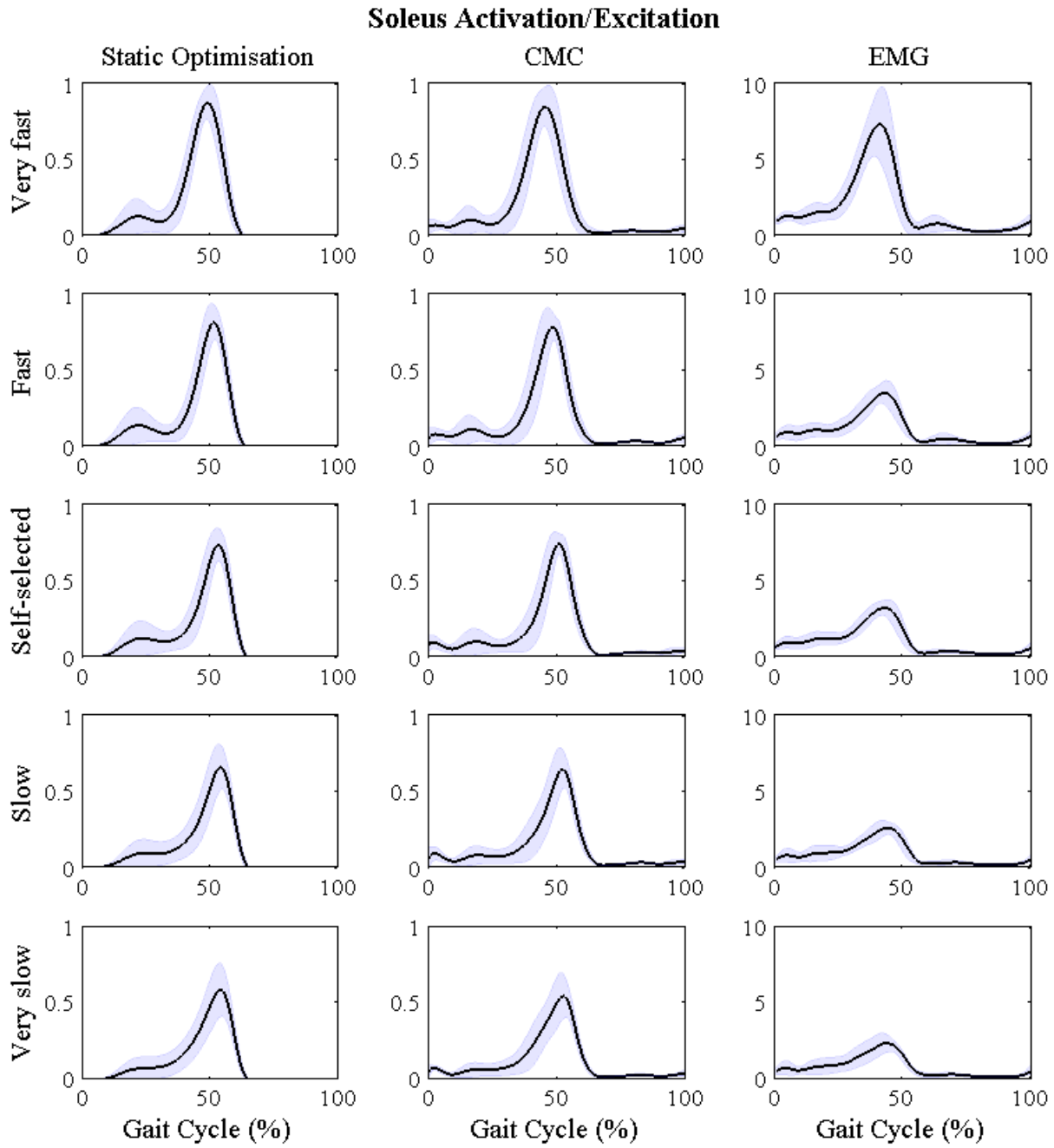

Figure 5.15. Estimated activation/excitation of the soleus compared to surface EMG throughout walking speeds.

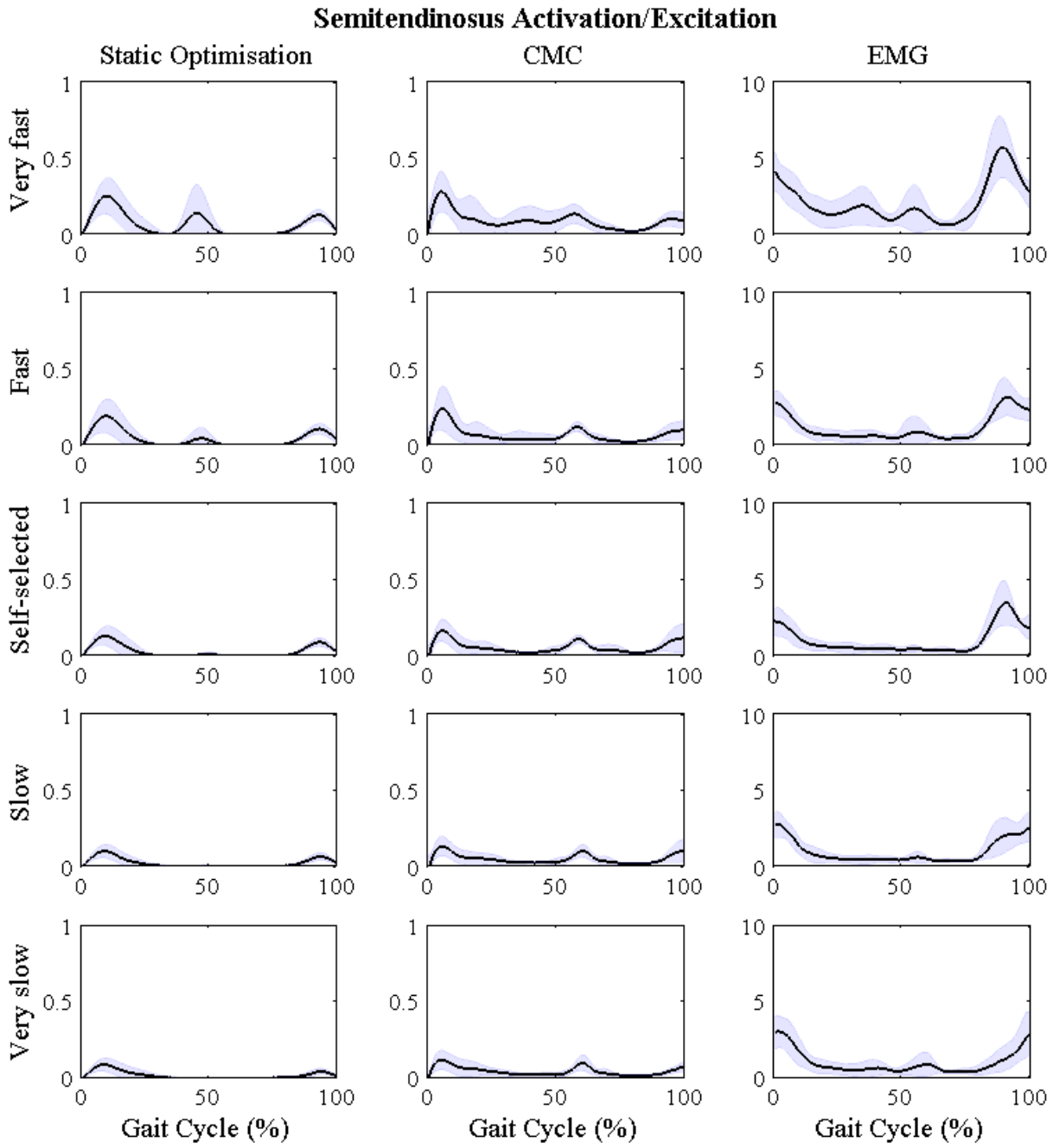

Figure 5.16. Estimated activation/excitation of the semitendinosus compared to surface EMG throughout walking speeds.

Rectus femoris

All three techniques static optimisation, CMC, and EMG increase in their magnitude with speed (Figure 5.17). However, the shapes of them differ between each other. Static optimisation has throughout walking speeds a peak at about 55% of the gait cycle which is accomplished by a small activation plateau between 20-75% of the gait cycle. The peak as well as the plateau to a lesser extent increase with walking speeds. A small activation at the start of the gait cycle is present throughout walking speeds but does not change greatly. A second small activation at the end of the gait cycle is developed for fast and very fast walking. CMC on the other side presents a small excitation plateau from 10-90% of the gait cycle with a small peak at the end of swing for very slow walking. With faster walking speeds the plateau increases and develops first a peak at about 80% of the gait cycle which is then followed by a second higher peak for fast and very fast walking at about 50% of the gait cycle.

Surface EMG when compared to the modelling techniques shows a different change throughout walking speeds. The peak at the start and at the end of the gait cycle increasing while the EMG signal stays low between 20-90% of the gait cycle. This changes with fast and very fast speeds where a third peak occurs at about 45% of the gait cycle. All three techniques show increased standard deviation bands with increasing speed.

Vastus medialis and lateralis

Both compartments of the vastus which are included in this study (medialis, lateralis) behave similarly for both mathematical models and EMG, while vastus lateralis has higher estimations than medialis (Figure 5.18 and Figure 5.19). In general, a speed-dependence for all three techniques can be detected. The peak at about 20% of the gait cycle is increasing with walking speed for static optimisation and CMC. This is also shown for the results of the EMG measurements with a slightly earlier peak than the modelling techniques. CMC's second peak about 80% of the gait cycle increases with speed, too, and occurs slightly earlier with faster walking speeds. This second peak is not shown for all walking speeds with static optimisation. EMG develops a third peak about 45% of the gait cycle during very fast walking. Again, EMG's very fast walking results have an increased rise in activation to all the other speeds. The standard deviation bands for static optimisation and CMC increase slightly with walking speeds for both vastus medialis and lateralis which is also shown for the EMG measurements.

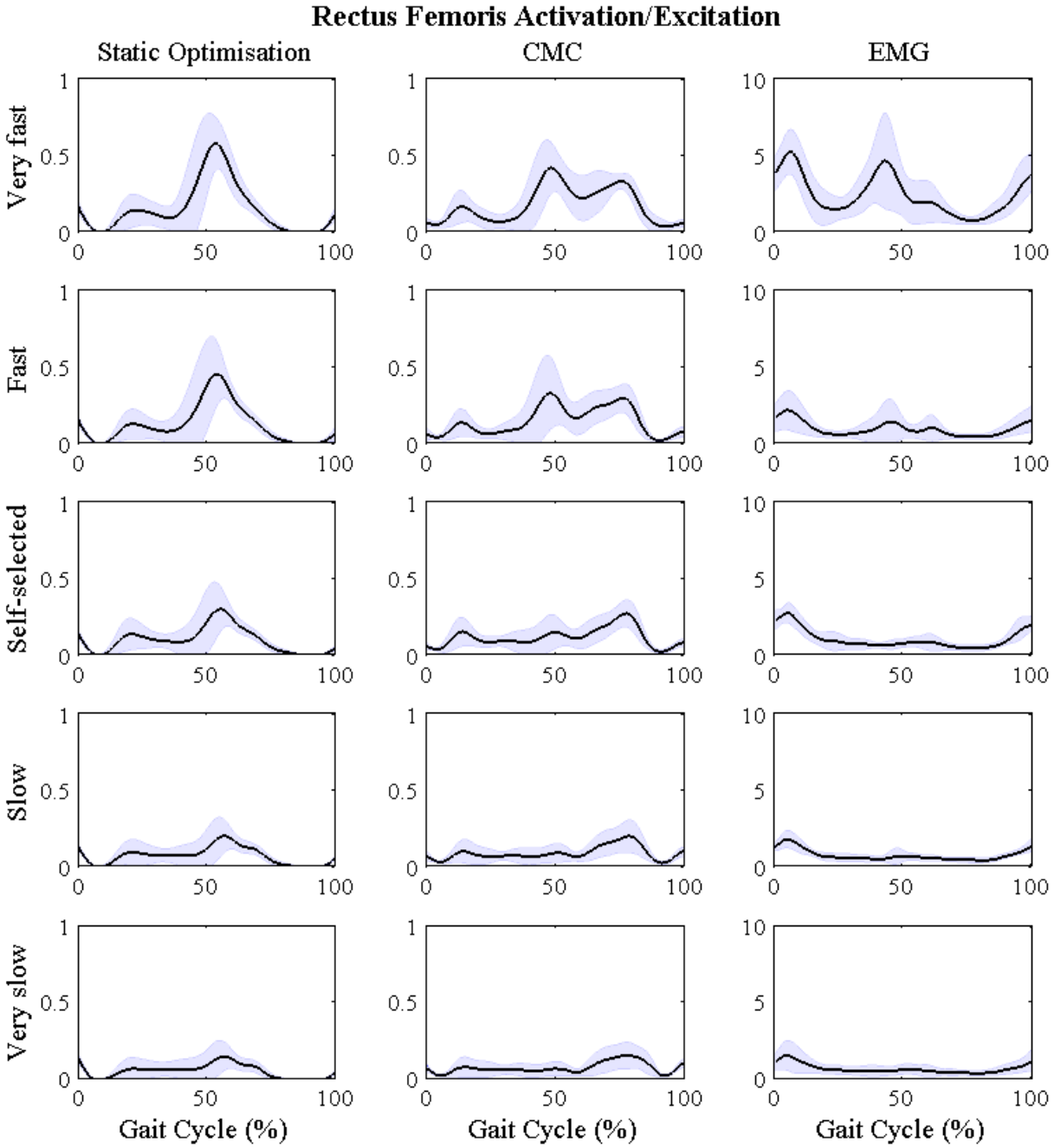

Figure 5.17. Estimated activation/excitation of the rectus femoris compared to surface EMG throughout walking speeds.

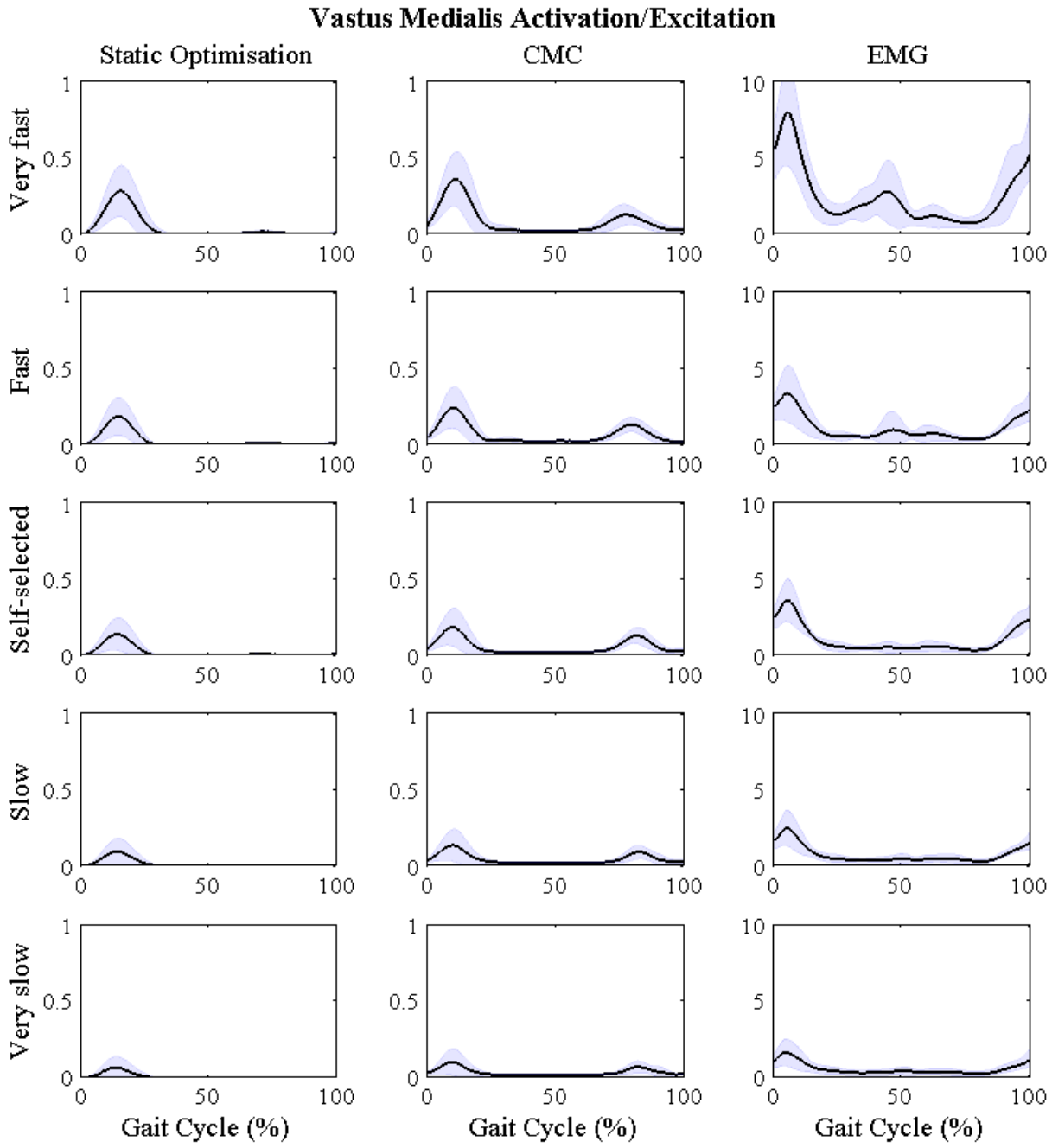

Figure 5.18. Estimated activation/excitation of the vastus medialis compared to surface EMG throughout walking speeds.

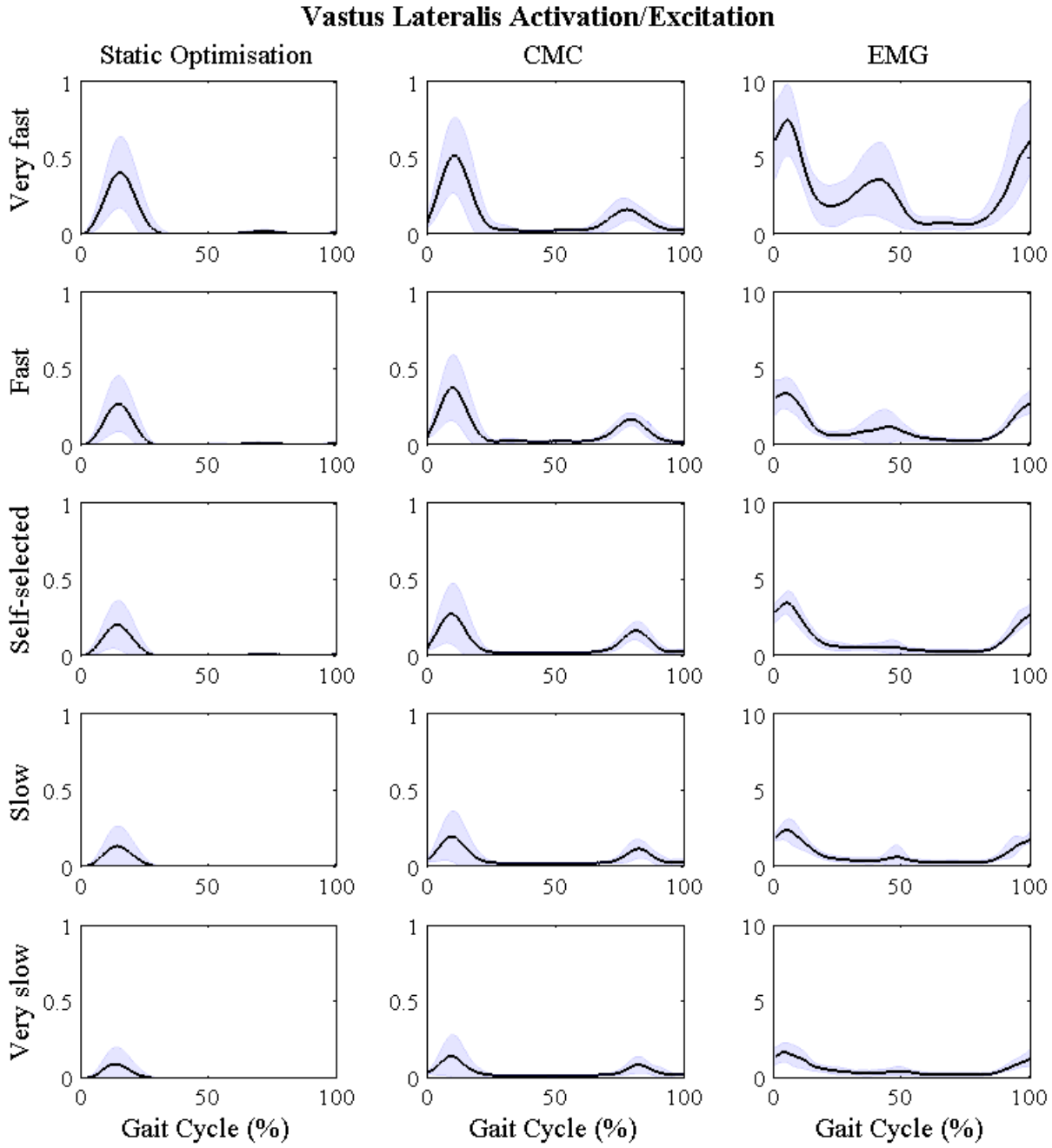

Figure 5.19. Estimated activation/excitation of the vastus lateralis compared to surface EMG throughout walking speeds.

The following figures (Figure 5.20 to Figure 5.22) show exemplary individual results of three participants' estimated muscle activation (static optimisation) and muscle excitation (CMC) patterns for all five walking speeds compared to surface EMG. Light blue represents very slow which increases to dark blue for very fast walking. The three participants which were chosen differ in their body mass, body height, and gender. P02 (1.81m, 95.21kg) and P04 (1.83m, 74.31kg) are male, whereas P04 is additionally close to the anthropometrics of the generic model of gait2392 (1.80m, 75.16kg). P08 (1.68m, 57.8kg) is female, and represents one of the smallest and lightest participants which were included into the study.

Participant P02

Figure 5.20 presents the results of participant P02. In general, the muscle excitations of CMC and muscle activations of static optimisation show an increase in the magnitude with faster speeds which is also shown with surface EMG. Some muscles show a nice speed-dependent pattern change for all three techniques, like for the gastrocnemius medialis, where after initial contact the force raises later as faster the speed is, but then develops a steeper curve and higher peak for the fast speeds compared to the slow speeds. Faster speeds can reach an activation level of 1 for the triceps surae muscles for both static optimisation and CMC. This is also present for the tibialis anterior of CMC, however, not with static optimisation where the activation stays under 0.5.

Some of the muscles show a speed-dependent change between very slow and slow walking speeds with the mathematical model estimations, which is different for EMG where no change between very slow and slow across all muscles can be seen. Especially fast and very fast walking speeds experience a great rise in activation for both the modelling techniques and EMG. The tibialis anterior of the CMC estimation shows two different pattern between the slow walking speeds compared to self-selected and fast walking speeds at the end of the gait cycle, where the excitation decreases for slower walking speeds after 90% of the gait cycle and further rises for the faster walking speeds until the end of the gait cycle. The surface EMG excitation changes slightly its pattern for some of the muscles for very fast walking. For the muscles on the thigh additional surface EMG peaks occur which are not present for the other walking speeds. For example a peak at 40% of the gait cycle occurs for vastus medialis and lateralis, whereas the muscle is inactive for the rest of the walking speeds. This behaviour is not shown with the mathematical models.

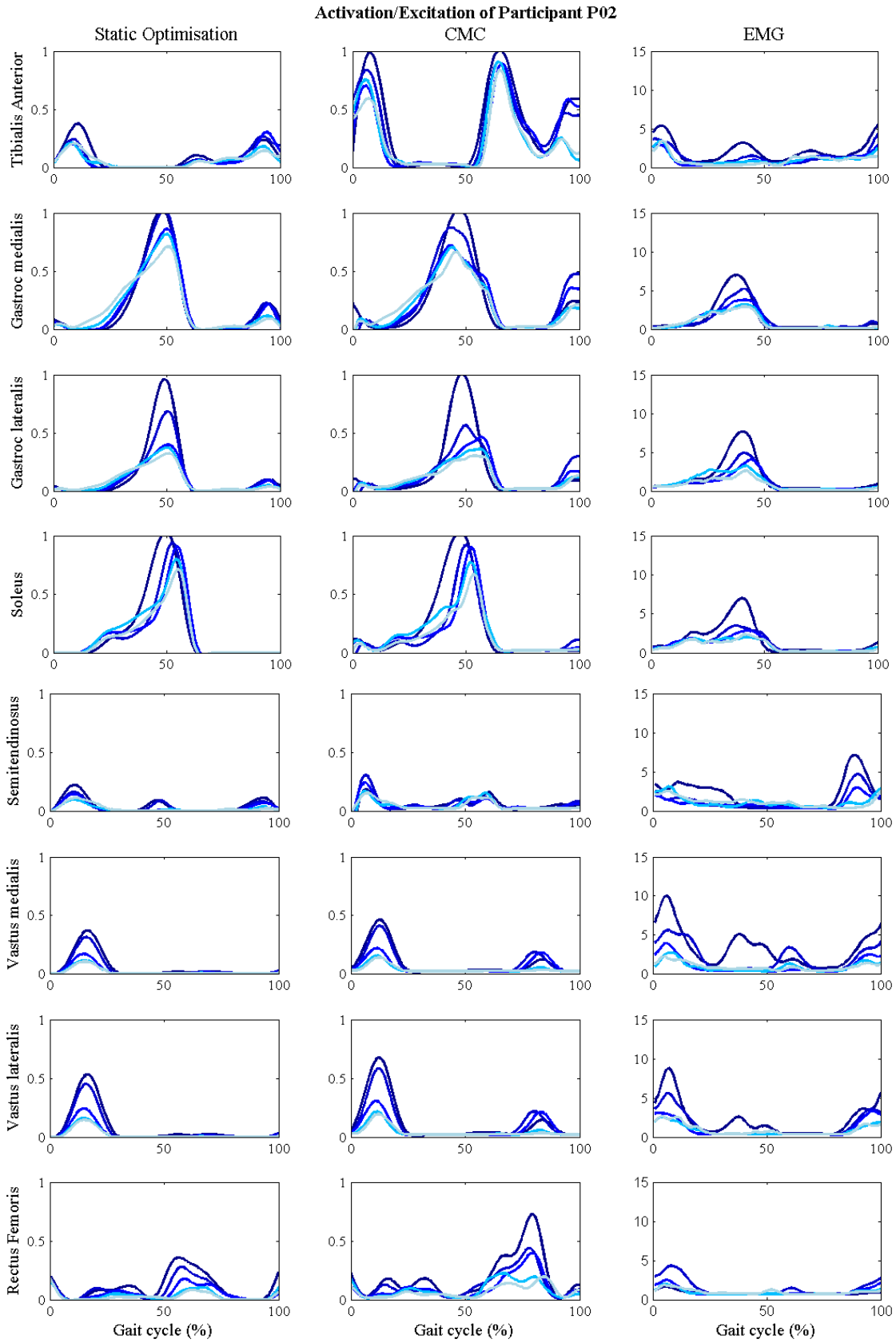

Figure 5.20. Single graphs of participant P02 (95.21kg) showing static optimisation's muscle activations, CMC's muscle excitations compared to surface EMG excitations for five different walking speeds; dark blue=very fast to light blue=very slow.

Participant P04

Participant P04 (Figure 5.21) shows a similar pattern to participant P02, however, some individual differences exist. For the static optimisation solution of P04 the soleus shows a more distinctive peak around 20% of the gait cycle, especially for the very fast walking speeds which ends in a decrease of activation until 40% of the gait cycle for fast and very fast walking. This pattern is partially reflected by the EMG excitations, although not to the same extent.

All three triceps surae muscles (soleus, gastrocnemius lateralis and medialis) and the rectus femoris show two slight different patterns between the fast walking speeds (fast, very fast) and the self-selected and slow walking speeds (slow, very slow) which is also shown with surface EMG. Additionally, the semitendinosus of CMC shows as well two patterns for the fast compared to the slow walking speeds, as fast and very fast walking experience the highest excitation at about 40% of the gait cycle where the other speeds are close to zero. This is partially shown with EMG but not with static optimisation.

Throughout the walking speeds, tibialis anterior shows no great change in activation. The estimations for very fast walking with static optimisation show a slight higher activation pattern at around 5% of the gait cycle and with the solution of fast walking of CMC an earlier rise around 60% of the gait cycle in relation to different walking speeds. Interestingly, the first peak of tibialis anterior with CMC shows a decrease in excitation with increasing speeds. A similarity between CMC and surface EMG is a small burst of tibialis anterior at around 30-40% of the gait cycle, which occurs a bit earlier with CMC compared to EMG. This small bust is shown for the fast walking speeds but not or the slower walking speeds. Static optimisation shows only a hint of activation around 40% of the gait cycle which can barely be defined as a true activation.

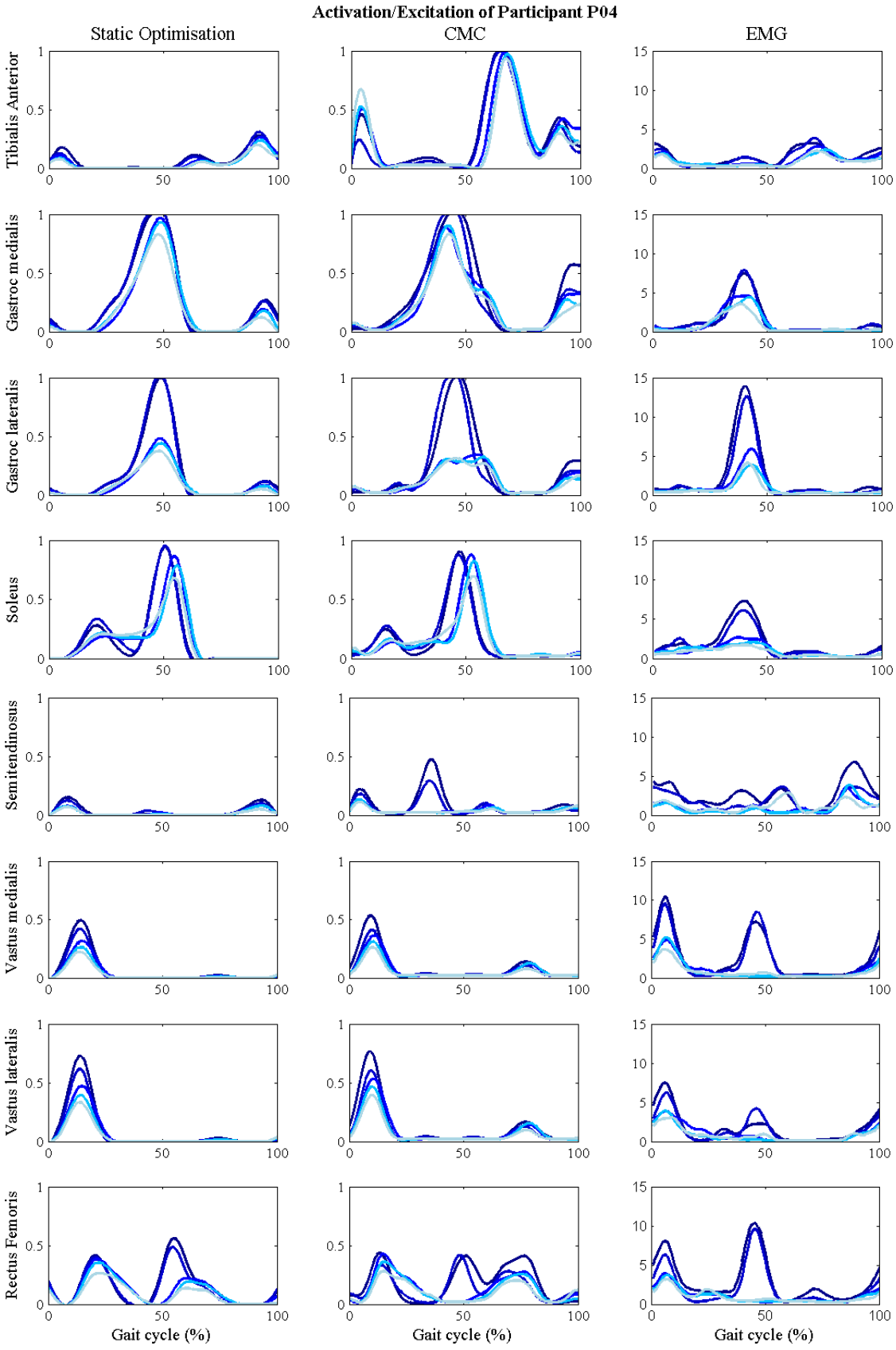

Figure 5.21. Single graphs of participant P04 (74.31kg) showing static optimisation's muscle activations, CMC's muscle excitations compared to surface EMG excitations for five different walking speeds; dark blue=very fast to light blue=very slow.

Participant P08

P08 (Figure 5.22), in contrast to the other participants, has nearly no soleus activation around 20% with the mathematical models static optimisation and CMC. This is again reflected in the EMG excitations with reduced activation until 20% of the gait cycle compared to the other participants. The soleus additionally shows an increase in activation with increasing speed which is accomplished by an earlier and steeper rise and an earlier peak. The fast speeds but especially very fast behaves slightly different at the first 20% of the gait cycle and during peak activation at 50% of the gait cycle compared to other speeds for both compartments of the gastrocnemius.

As shown for P02 and P04 the activation between static optimisation and CMC for the tibialis anterior are different. CMC reaches excitations levels up to 1 whereas the activation of the tibialis anterior stays under 0.3 for all walking speeds. No systematic speed difference can be shown for static optimisation or CMC, except for the first CMC excitation peak during very fast walking. This speed-independence is not reflected by surface EMG which shows an increase in peak activations for very fast at initial foot contact and self-selected, fast and very fast walking speeds at around 60% of the gait cycle where the peak rises additionally quicker and stays elevated for a longer duartion than slower walking speeds.

Static optimisation's activations for vastus medialis and lateralis are very small and ranging around 0-0.1. Only activations for fast and very fast walking speeds are detectable which are the highest around 55% of the gait cycle. CMC has slight higher excitations up to 0.4 and around 85% of the gait cycle its highest peak. A slight speed dependence can be here detected which is also shown for the EMG data. However, EMG shows a totally different pattern compared to CMC and static optimisation. The EMG electrode of vastus medialis was non-functioned and resulted in no useful information.

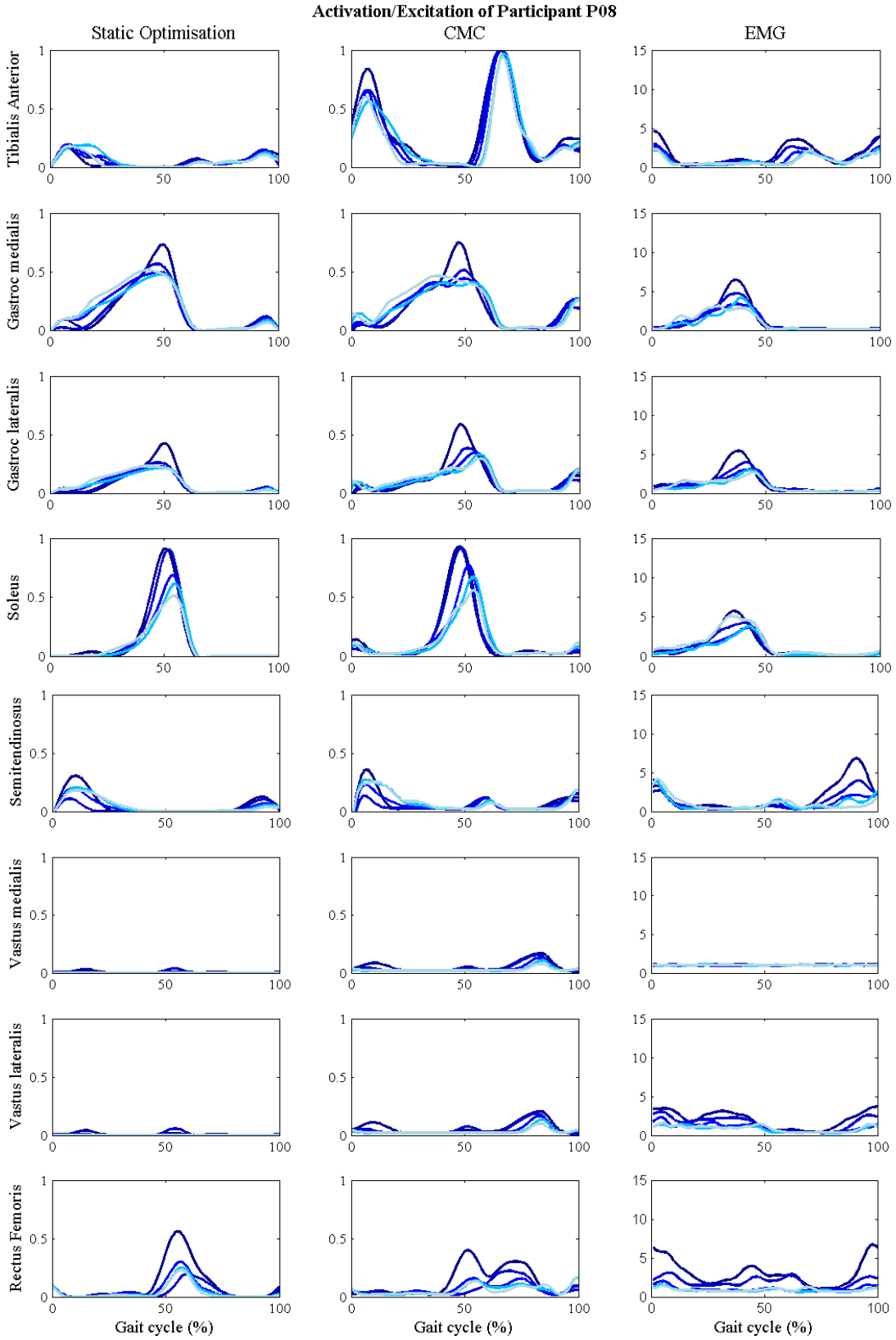

Figure 5.22. Single graphs of participant P08 (57.8kg) showing static optimisation's muscle activations, CMC's muscle excitations compared to surface EMG excitations for five different walking speeds; dark blue=very fast to light blue=very slow.

P02 compared to P04 and P08

All three participants show a muscle activation speed-dependence for all three techniques, however, not for all muscles and to a different extent. For example the gastrocnemius medialis, which shows an increase from very slow to self-selected walking speed for P02, but not for P08. P04 has, except for very slow, a peak activation of 1, but the activation of P08 stays under or around 0.5 except for very fast walking. In general, however, the activation of the three triceps surae muscles is maximised for the very fast walking speeds and, for S02 and S04 for the fast speed, too. Different behaviour compared to the triceps surae is shown by the tibialis anterior which shows for P04 and P08 nearly no speed dependent change and for P02 solely for the very fast walking speed. Also, static optimisation is far less activated than CMC which reaches full excitation for all three participants.

The behaviour of the muscles on the thigh regarding changes in walking speeds are comparable between participants. However, the magnitude of the vastii muscles differs between P02 and P08 as there is a maximal CMC excitation under 0.3 and for static optimisation even under 0.2 for P08 which is at least three times as high for the first peak at about 10% of the gait cycle for P02. The changes of the semitendinosus across different walking speeds differs as well between participants. Compared to the results of P02, P08 shows no activation around 50% of the gait cycle with static optimisation and less spiky excitation patterns for CMC between 40-60% of the gait cycle. However, P04 does have the activation for both static optimisation and CMC and shows a much greater peak at about 30-40% of the gait cycle compared to P02.

Interestingly, the surface EMG excitation patterns of rectus femoris, vastus medialis and laterals for fast and especially very fast walking speeds behave slightly differently for all three participants between 20-60% of the gait cycle.

5.3.4.3 Results of Estimated Muscle Forces compared to Estimated Activations/Excitations

Figure 5.23 presents mean and one standard deviation of the estimated muscle forces for self-selected walking speeds with static optimisation and CMC compared corresponding estimated activations/excitations, averaged across all ten participants. Estimated activations of static optimisation and excitations of CMC are in this section presented without the applied filter of 6Hz to see the actual data which has been used to estimate the muscle forces. The upper bound

of each muscle force estimation graph is the muscle specific maximum isometric force defined in the musculoskeletal model. These settings are kept for this whole section.

The muscle which produces the greatest force during self-selected walking is the soleus muscle with about 1500N for both static optimisation and CMC, whereas the muscle with the least peak force is the semitendinosus with less than 100N. The results for muscle force estimations are in general similar in the shape compared to the estimated CMC muscle excitations and static optimisation muscle activations; however some differences exist especially in the magnitude when comparing the force boundaries defined through the maximal isometric forces to the activation/excitation boundaries of 1. Static optimisation shows here a smaller force for the gastrocnemius medialis and lateralis and the soleus, CMC for the tibialis anterior and the soleus. Contrary to this, the rectus femoris has a slight higher magnitude with static optimisation. All other muscles are comparable in their magnitude between activation/excitation and estimated force production.

The only difference in the shape between estimated activations/excitations and forces is the second peak during the swing phase of the gait cycle for the vastus medialis and lateralis CMC excitation which nearly disappears for the CMC muscle force estimations and has now much closer similarity with the solution of static optimisation. The sharp CMC peak excitations of the semitendinosus during 60% of the gait cycle is with the estimation of muscle forces smoothened and extended and does not fully decrease anymore after rising at about 60% of the gait cycle.

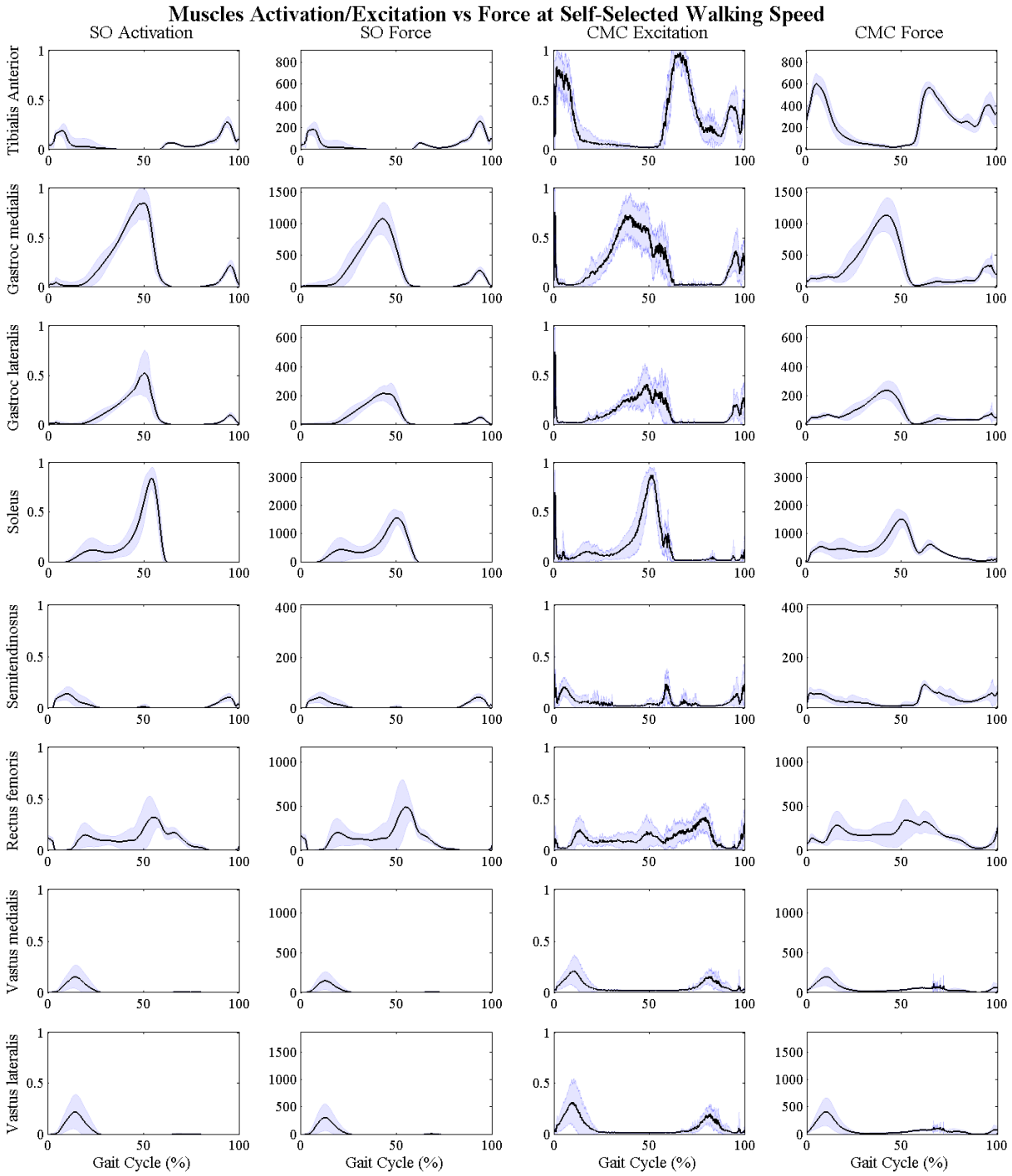

Figure 5.23. Mean and one standard deviation bands for static optimisation's and CMC's muscle forces compared to the activations of static optimisation and the excitations of CMC across all ten participants during self-selected walking speed.

Figure 5.24 to Figure 5.31 present speed-dependent differences in force production for each individual muscle compared to corresponding activations/estimations, averaged across ten participants. Then mean as well as one standard deviation across the gait cycle are presented.

Tibialis Anterior

Both mathematical models show in general no speed-dependent differences in the muscle force production which is comparable with the corresponding activations/excitations (Figure 5.24). The only difference is the swing phase of CMC, where a small increase after the peak at 60% of the gait cycle is seen. This corresponds well with a slight increase of CMC's excitation at the end of swing. The mean force peak at about 10% of the gait cycle is slightly decreasing for very fast walking, however, stays in the standard deviation bands. A small increase in the standard deviation bands may be detected for fast and very fast compared to self-selected and slow walking. Very slow, however, shows similar standard deviation bands than the fast speeds.

CMC's force production stays much smaller than the estimated CMC excitations throughout speeds. The highest force of CMC stays around 500N, whereas static optimisation stays around 250N.

Gastrocnemius medialis and lateralis

Like the estimated activations/excitations, the muscle force production of the gastrocnemius medialis and lateralis rise slightly for static optimisation and CMC with faster walking speeds, however, to a lesser extent (Figure 5.25 and Figure 5.26). The forces of gastrocnemius lateralis are becoming sharper with increasing speeds for both static optimisation and CMC which results in spikes for static optimisation's fast and very fast walking speed. Additionally, the standard deviation increases with speed. This is not the case for the CMC results of gastrocnemius lateralis where the mean force and standard deviation stay similar across walking speeds.

Both gastrocnemius medialis and lateralis experience spiky raw CMC excitations at initial foot contact which are not shown for CMC forces. Additionally, the excitation at the end of swing is greatly decreased.

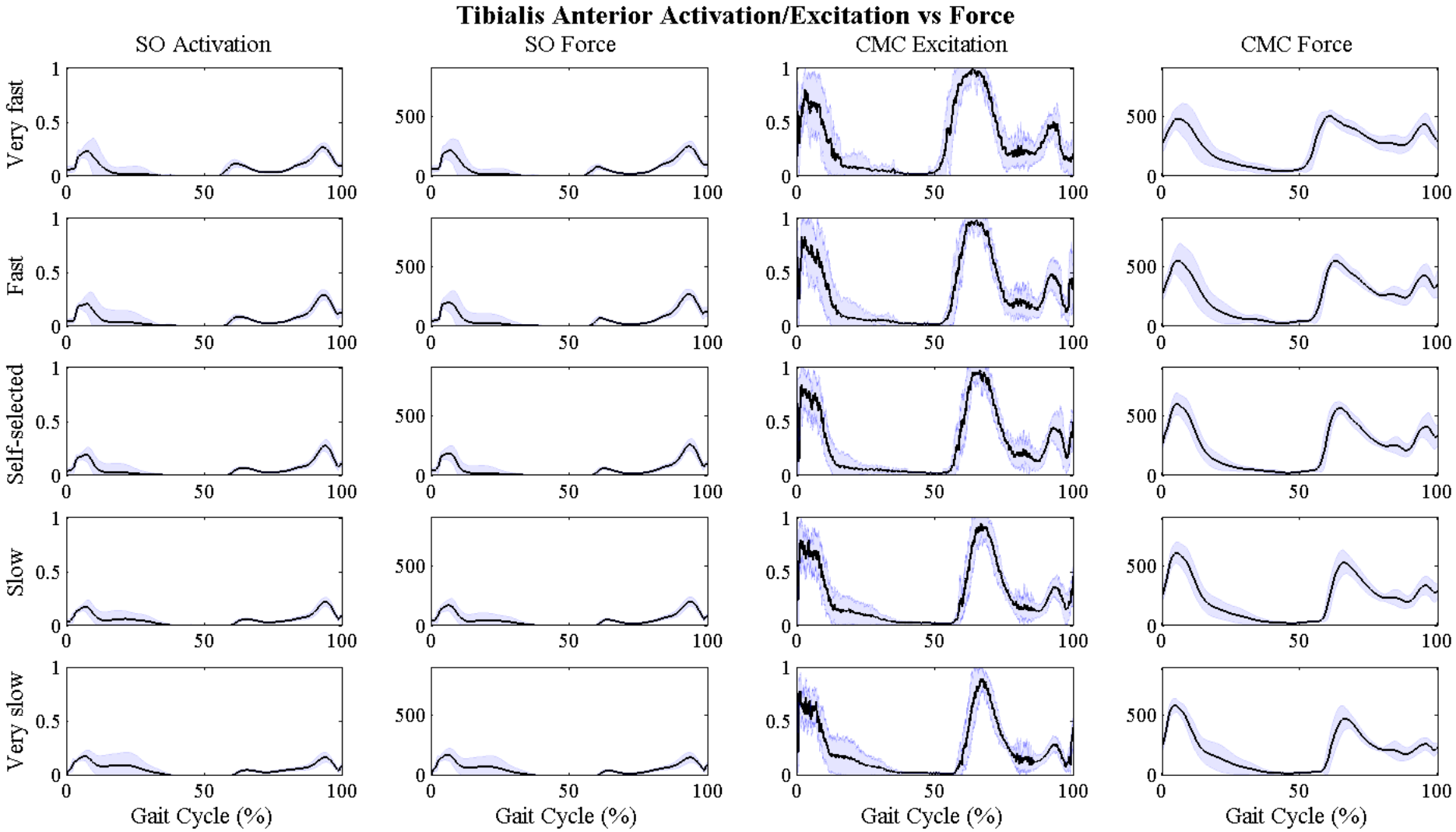

Figure 5.24. Mean force production and one standard deviation bands for static optimisation's and CMC's muscle forces of the tibialis anterior compared to estimated activations of static optimisation and excitations of CMC across all ten participants during very slow walking.

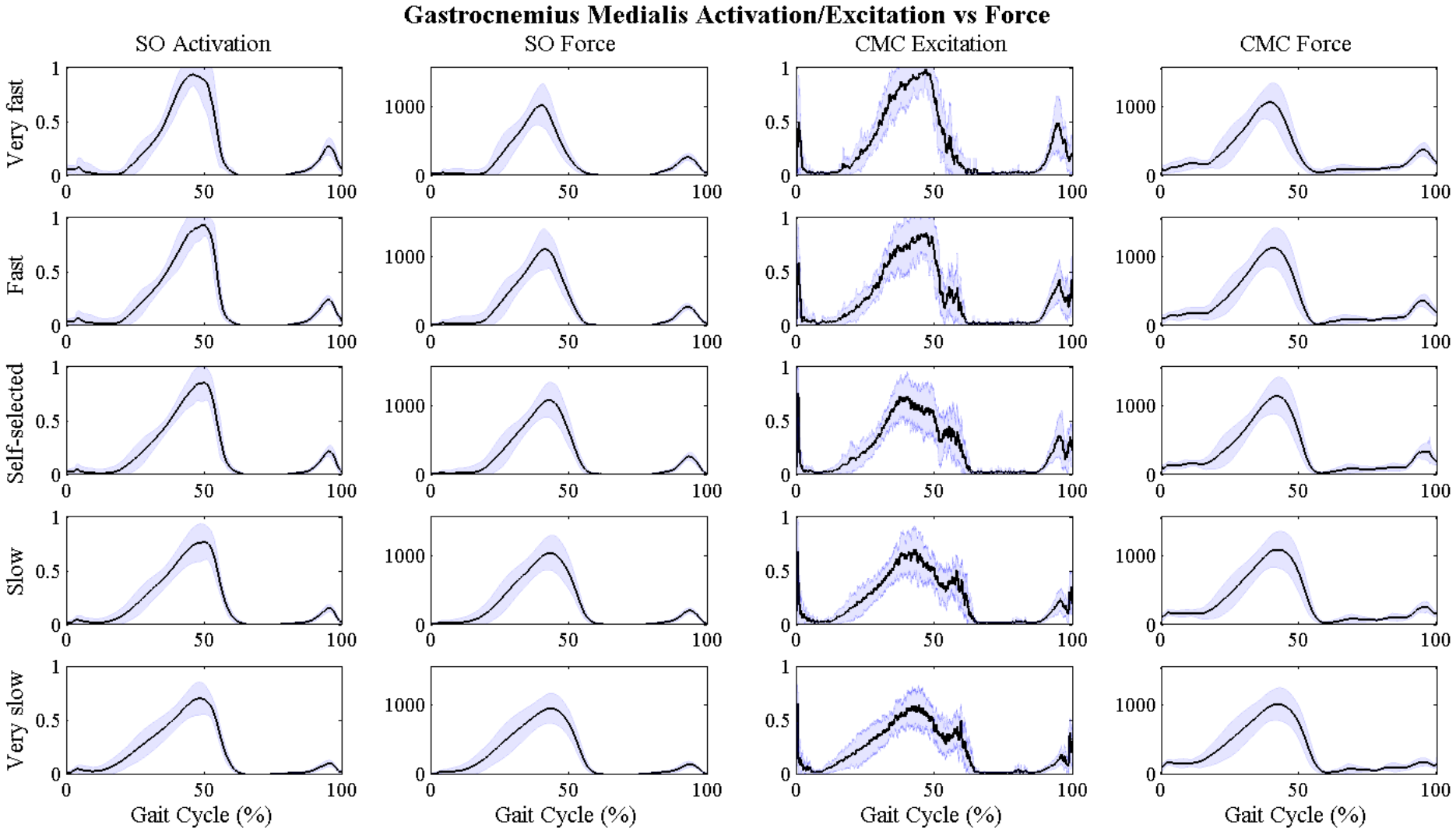

Figure 5.25. Static optimisation's and CMC's muscle force production of the gastrocnemius medialis compared to estimated activations of static optimisation and excitations of CMC.

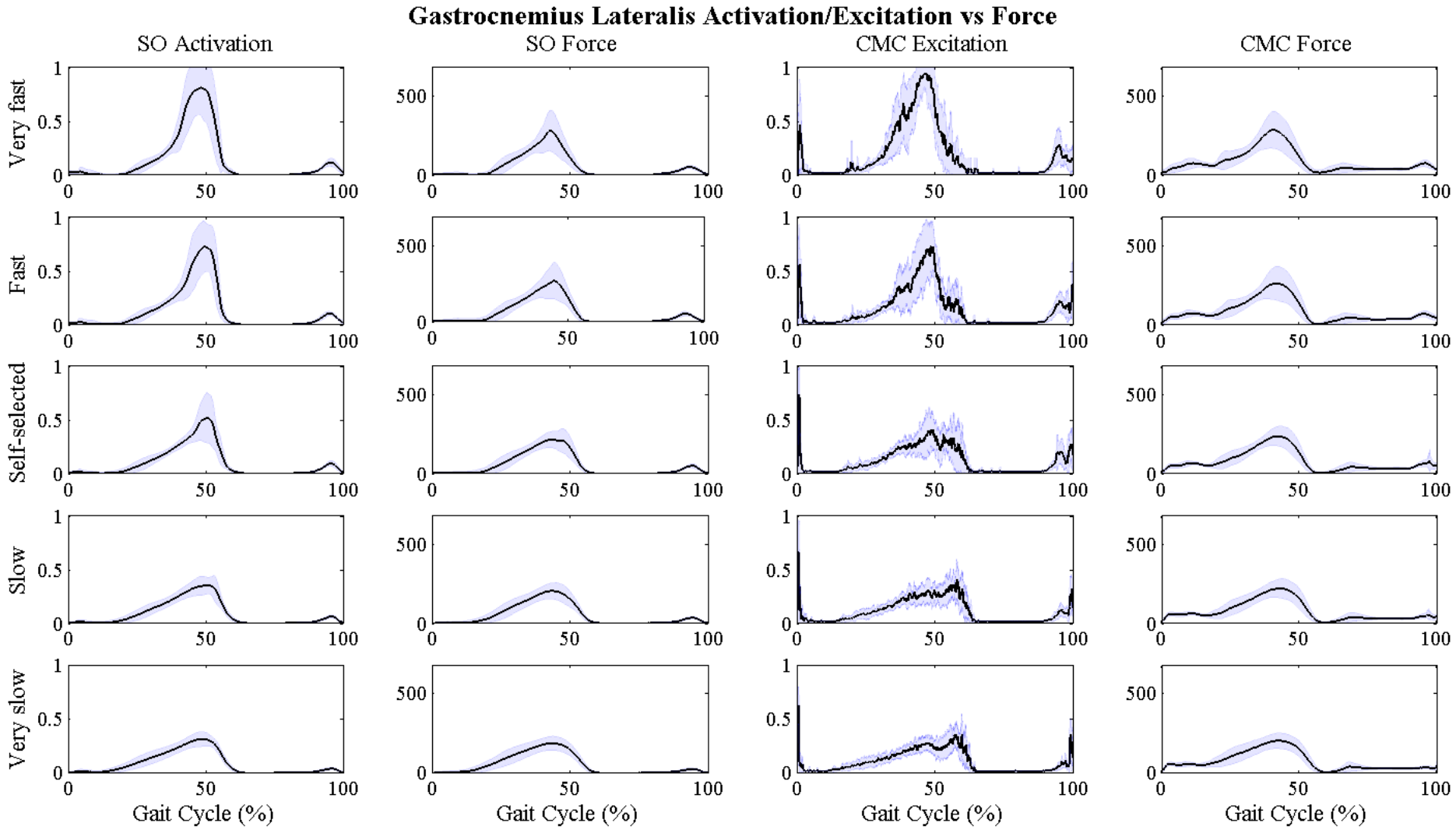

Figure 5.26. Static optimisation's and CMC's muscle force production of the gastrocnemius lateralis compared to estimated activations of static optimisation and excitations of CMC.

Soleus

Contrary to the estimated activations and excitations, the soleus has nearly no change in muscle force production across different walking speeds (Figure 5.27). The static optimisation's force production shows the same change in the first 50% of the gait cycle compared to its activations: with increasing walking speed the small plateau at the start develops to a small peak and the maximal peak slightly shifts to an earlier stage in the gait cycle. Like the gastrocnemius, the raw CMC excitations show spiky patterns at initial foot contact which disappear with the force estimation. The raw CMC excitations show additionally a smaller peak after the maximal peak at about 60% of the gait cycle which is for the force estimations slightly shifted to a later stage in the gait cycle. The standard deviations of soleus muscle forces do not change greatly between walking speeds.

Semitendinosus

For both static optimisation and CMC activation/excitation and force production behave similar in relation to different walking speeds (Figure 5.28). Force estimations with static optimisation increase with faster speeds and additionally present the third peak at about 45% of the gait cycle which has been shown for the static optimisation's activation. Highest standard deviation can be seen during very fast walking. This is similar with CMC estimations of the semitendinosus. However, both excitations and forces of CMC do not change with walking speeds, except a slight higher first peak ending in a plateau with is also slightly higher during very fast walking.

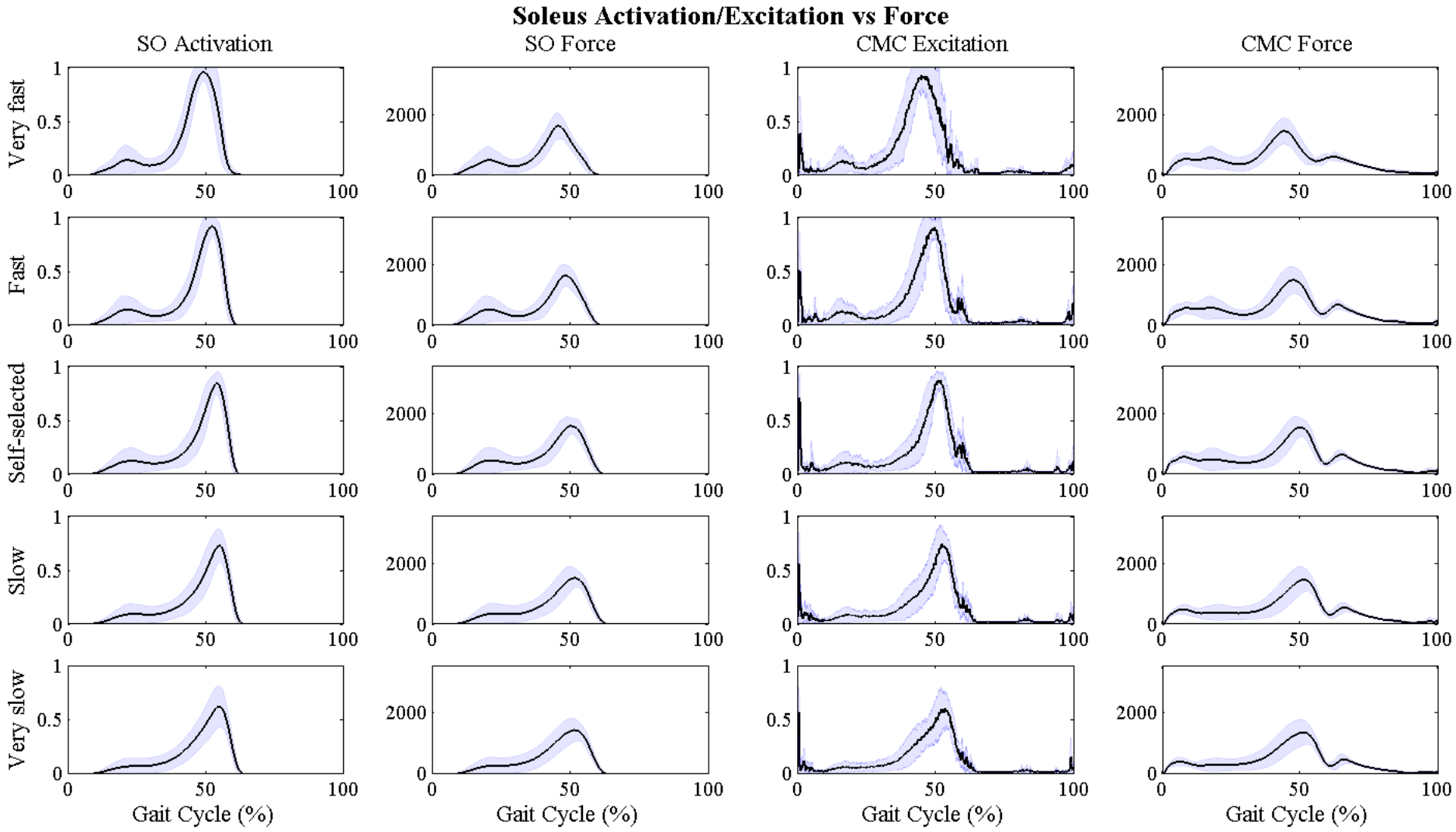

Figure 5.27. Static optimisation's and CMC's muscle force production of the soleus compared to estimated activations of static optimisation and excitations of CMC.

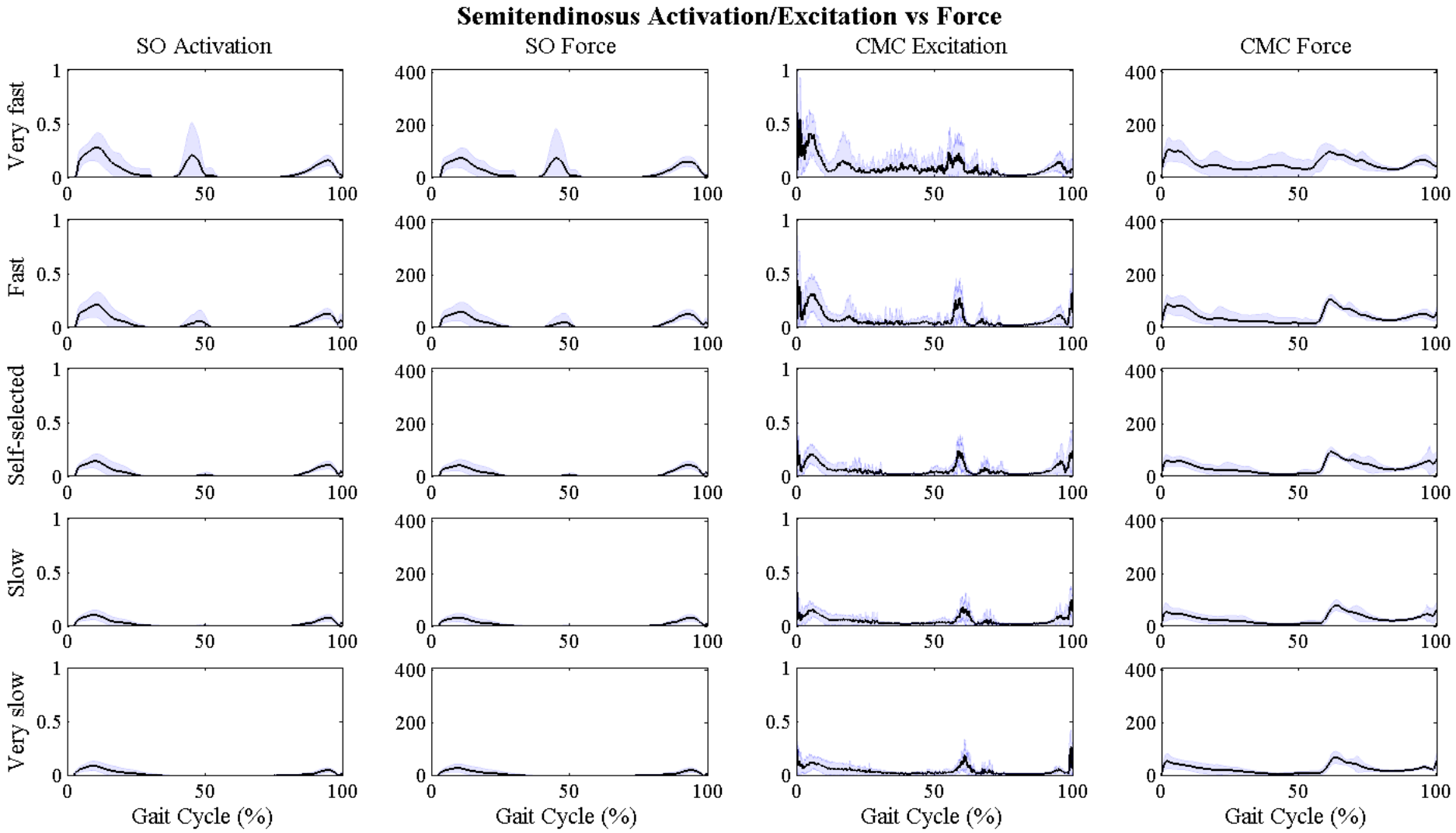

Figure 5.28. Static optimisation's and CMC's muscle force production of the semitendinosus compared to estimated activations of static optimisation and excitations of CMC.

Rectus femoris

The estimated muscle of the rectus femoris is presented in Figure 5.29. This muscle shows a great speed-dependence for both static optimisation and CMC which is comparable with corresponding activations/excitations. The shape between estimated activations and forces of static optimisation does not change, compared to the magnitude which is slightly higher in average for the force production compared to the activations. During very fast walking the rectus femoris force estimated with static optimisation reaches forces up to the maximal isometric force the muscle can produce. This is not the case for CMC muscle forces which are slightly lower than for static optimisation. The estimated muscle forces of CMC look, however, much similar to the forces of static optimisation than the unfiltered CMC excitations.

Vastus medialis and lateralis

Both estimated muscle forces of the vastus medialis and lateralis show an increase in force production with increasing walking speeds (Figure 5.30 and Figure 5.31). These changes are comparable to the corresponding activations/excitations in shape and magnitude. Vastus medialis produces in general less force than vastus lateralis for all walking speeds. Static optimisation's peak at about 15% of the gait cycle rises in average up to 300N and 700N for vastus medialis and lateralis, respectively, which is similar with the force estimation results of CMC. The standard deviation bands increase more for static optimisation and CMC.

As described for the self-selected walking speed, the second peak around 80% of the gait cycle which is shown for the estimations of CMC disappears for the muscle force estimation of CMC, however, a very small force appears with faster walking speeds around 65% of the gait cycle. Here, CMC forces show small spikes which are not shown for static optimisation.

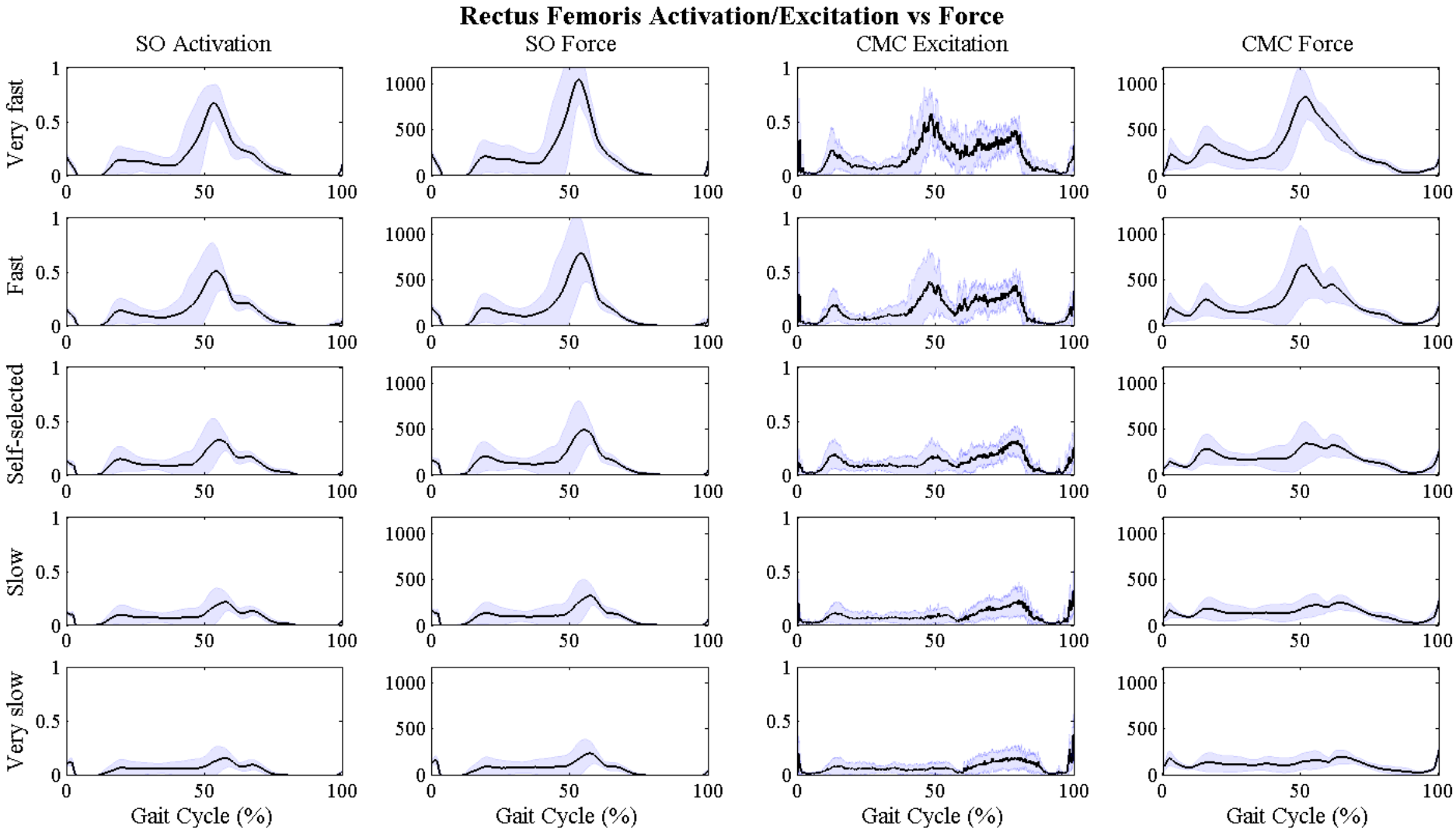

Figure 5.29. Static optimisation's and CMC's muscle force production of the rectus femoris compared to estimated activations of static optimisation and excitations of CMC.

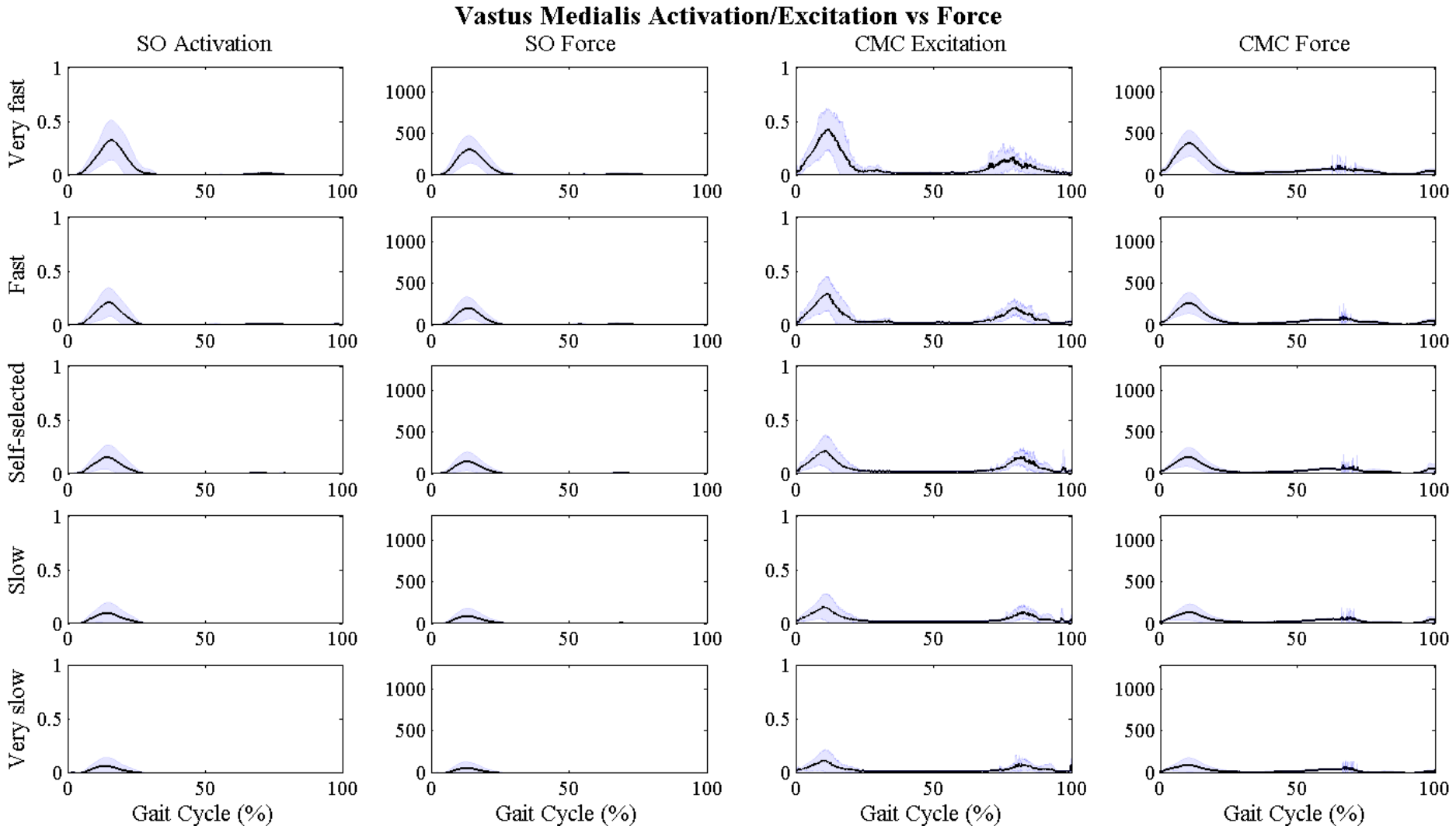

Figure 5.30. Static optimisation's and CMC's muscle force production of the vastus medialis compared to estimated activations of static optimisation and excitations of CMC.

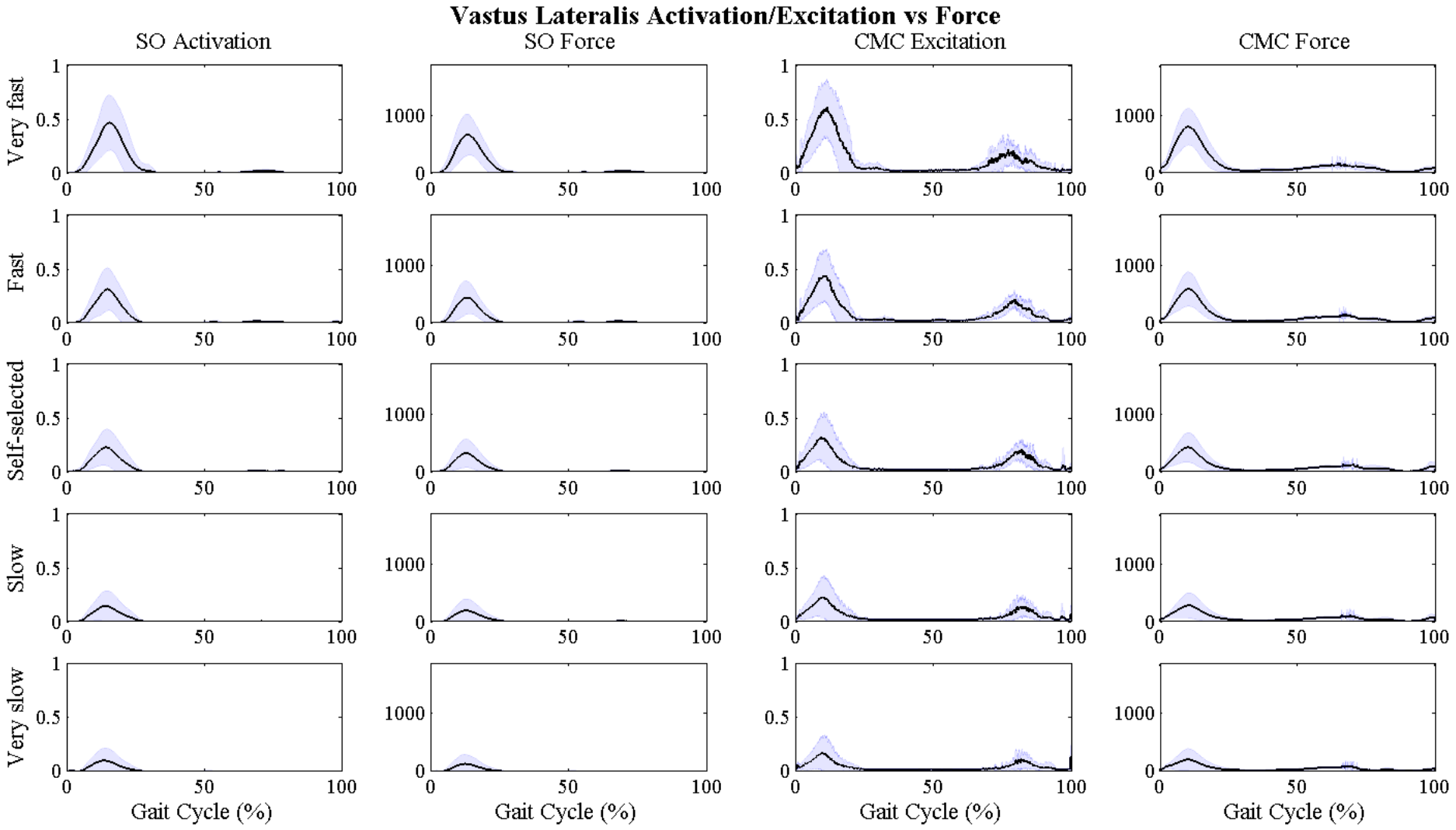

Figure 5.31. Static optimisation's and CMC's muscle force production of the vastus lateralis compared to estimated activations of static optimisation and excitations of CMC.

Figure 5.32 to Figure 5.34 present participant specific results (P02, P04, P08) for muscle force estimation with static optimisation and CMC compared to corresponding activations/excitations for all five walking speeds. Dark blue presents very fast walking down to light blue which presents very slow walking speed.

Participant P02

Estimated muscle forces of participant P02 are presented in Figure 5.32. For most of the muscles, P02 shows a speed-dependence in estimated forces, especially for the triceps surae muscles and the muscles of the quadriceps. Semitendinosus and tibialis anterior, however, do not change with walking speed.

The really high CMC excitations and maximal static optimisation activations of P02 during very fast walking for the gastrocnemius lateralis, medialis and soleus transform into relative smaller forces. The peak forces during very fast walking are still greater than self-selected and slower walking speeds but with much less difference to each other. The high CMC excitations at the end of swing are much smaller for CMC forces of the soleus, gastrocnemius and lateralis. Rectus femoris estimated muscle force for very fast walking speeds is with static optimisation slightly higher in its magnitude than the corresponding activations. However, this is only true for the faster walking speeds.

Estimated muscle forces of CMC of the vastus medialis and lateralis show a spiky peak around 70% of the gait cycle for very fast walking speeds which is not shown for static optimisation. However, only slightly later in swing about 80% of the gait cycle the excitations of CMC show a second peak.

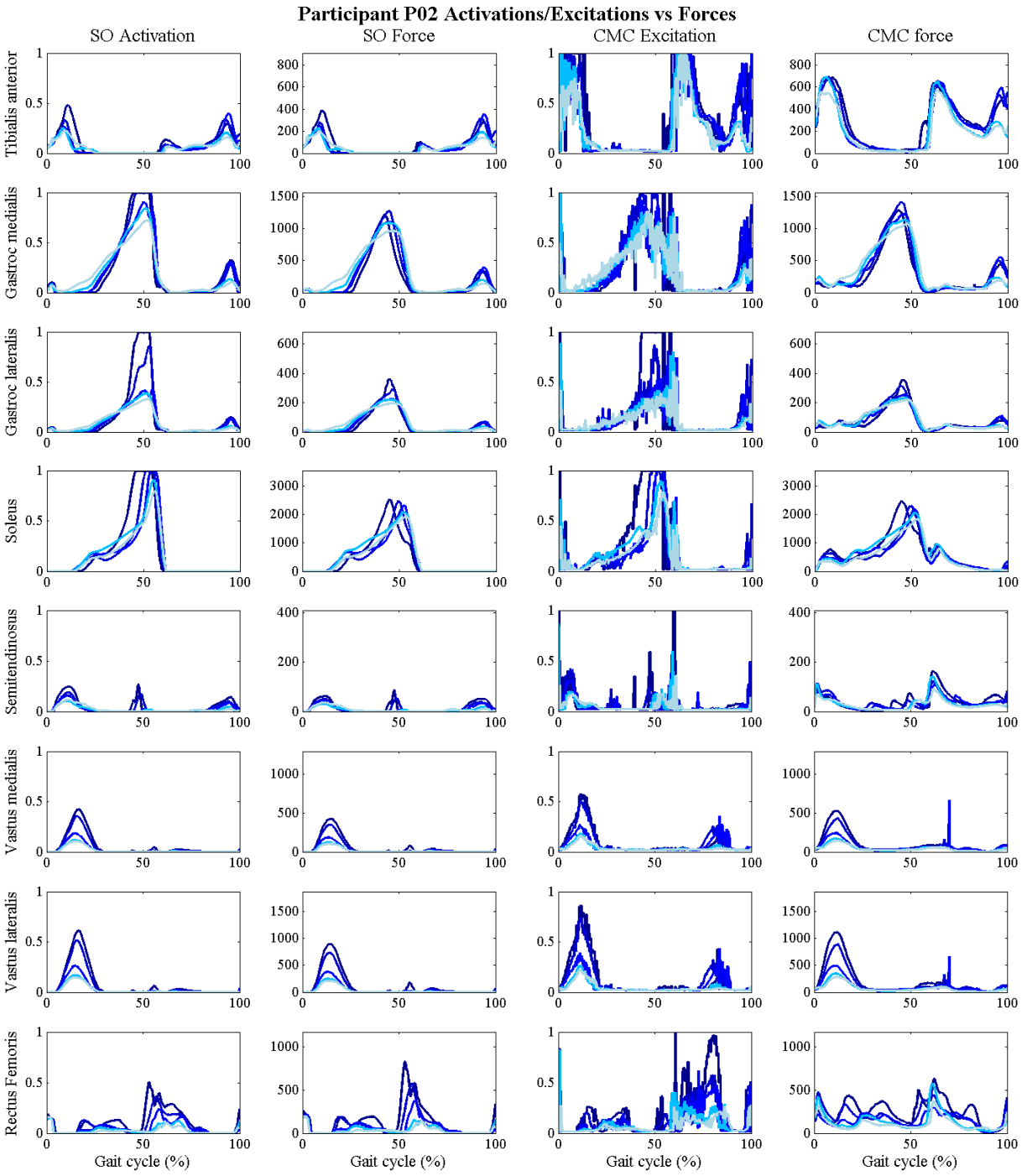

Figure 5.32. Single graphs of participant P02 (95.21kg) showing static optimisation's and CMC's muscle forces compared to surface EMG excitations for five different walking speeds.

Participant P04

Similar changes from P02 excitons/activations to muscle force can be found for P04 as well. Like P02, forces decreasing slightly for the muscles of the triceps surae for fast and very fast walking speeds, however, not to such an extent on the gastrocnemius medialis (Figure 5.33). Raw CMC excitations of the semitendinosus reveal really high activations for fast and very fast walking speeds at 35-40% of the gait cycle which is reflected by the much higher force production around 40% of the gait cycle. This is not shown for static optimisation. Same behaviour is present at the rectus femoris at about 50-60% of the gait cycle, this time also for fast and very fast walking speeds of static optimisation.

Unlikely participant P02, participant P04 has no CMC force production in the second half of the gait cycle for vastus lateralis and medialis and is very similar in the shape and magnitude to the results of static optimisation. Both static optimisation and CMC also show two different patterns between fast and very fast compared to the other speeds for the soleus muscle forces, which is also shown for the corresponding activations/excitations.

Participant P08

Muscle forces of participant P08 are in general smaller than the forces of participant P02 and P04 (Figure 5.34). The only muscle excitation which reaches 1 is the tibialis anterior. Gastrocnemius medialis and lateralis show an increased activation peak for very fast walking which, however, is not represented by the muscle force estimation of both static optimisation and CMC as the force peak is similar between walking speeds. A small difference between fast and very fast walking for the gastrocnemius medialis can be seen in the first 20% of the gait cycle where the slower walking speeds already start to produce force which is not shown for faster walking. The different patterns between speeds can also be found at the soleus between fast walking and slow walking. The maximal force occurs here a bit earlier with faster walking speeds than with slower walking speeds.

Static optimisation shows no force production for the semitendinosus in the middle of the gait cycle which is different to the results of CMC. The semitendinosus, in general, does no change greatly with walking speeds, which is also true for the vastus medialis and lateralis. Rectus femoris has, like with P04, much higher and slight earlier forces for very fast walking than for the rest of the walking speeds at around 50-60% of the gait cycle.

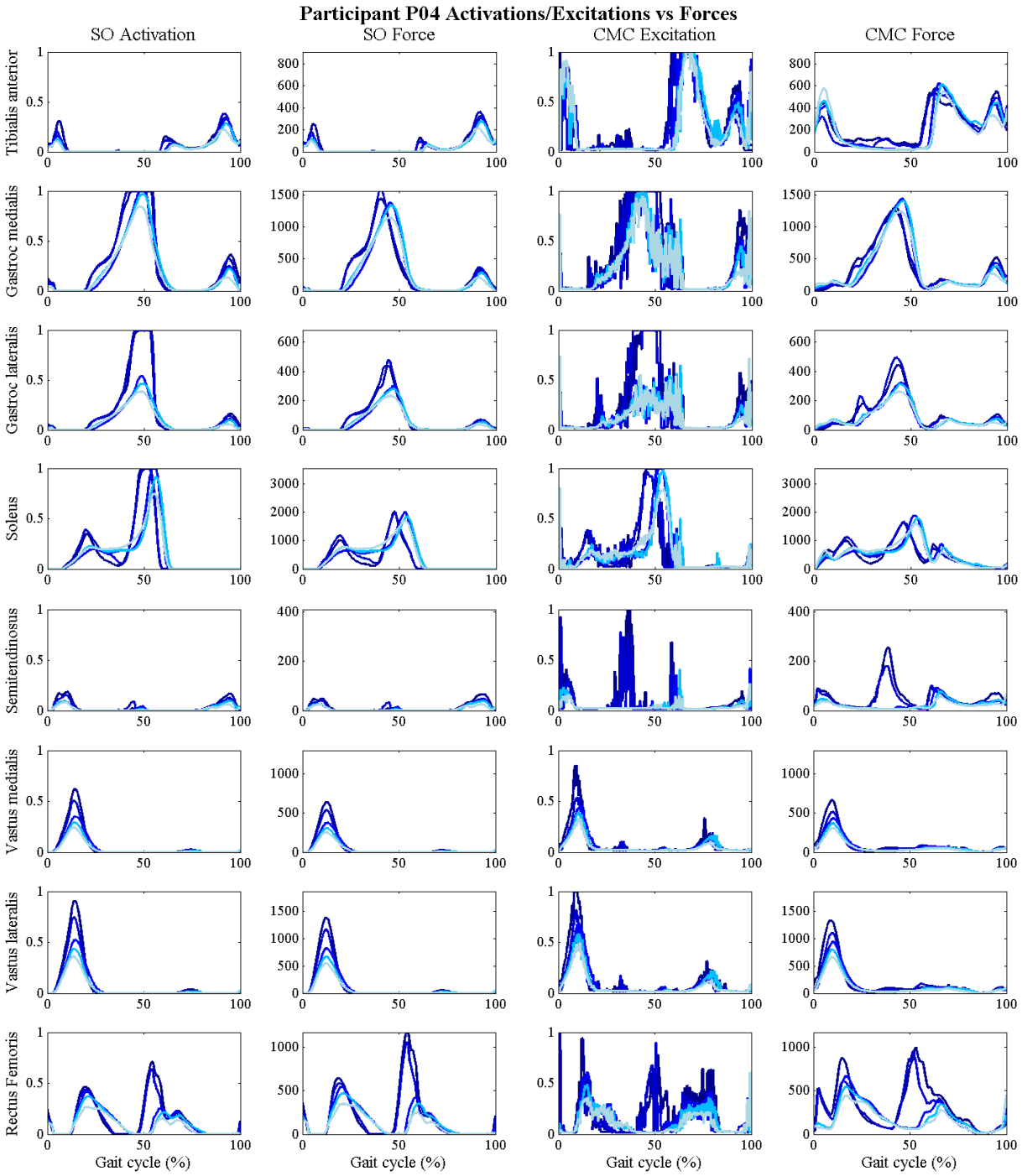

Figure 5.33. Single graphs of participant P04 (74.31kg) showing static optimisation's and CMC's muscle forces compared to surface EMG excitations for five different walking speeds.

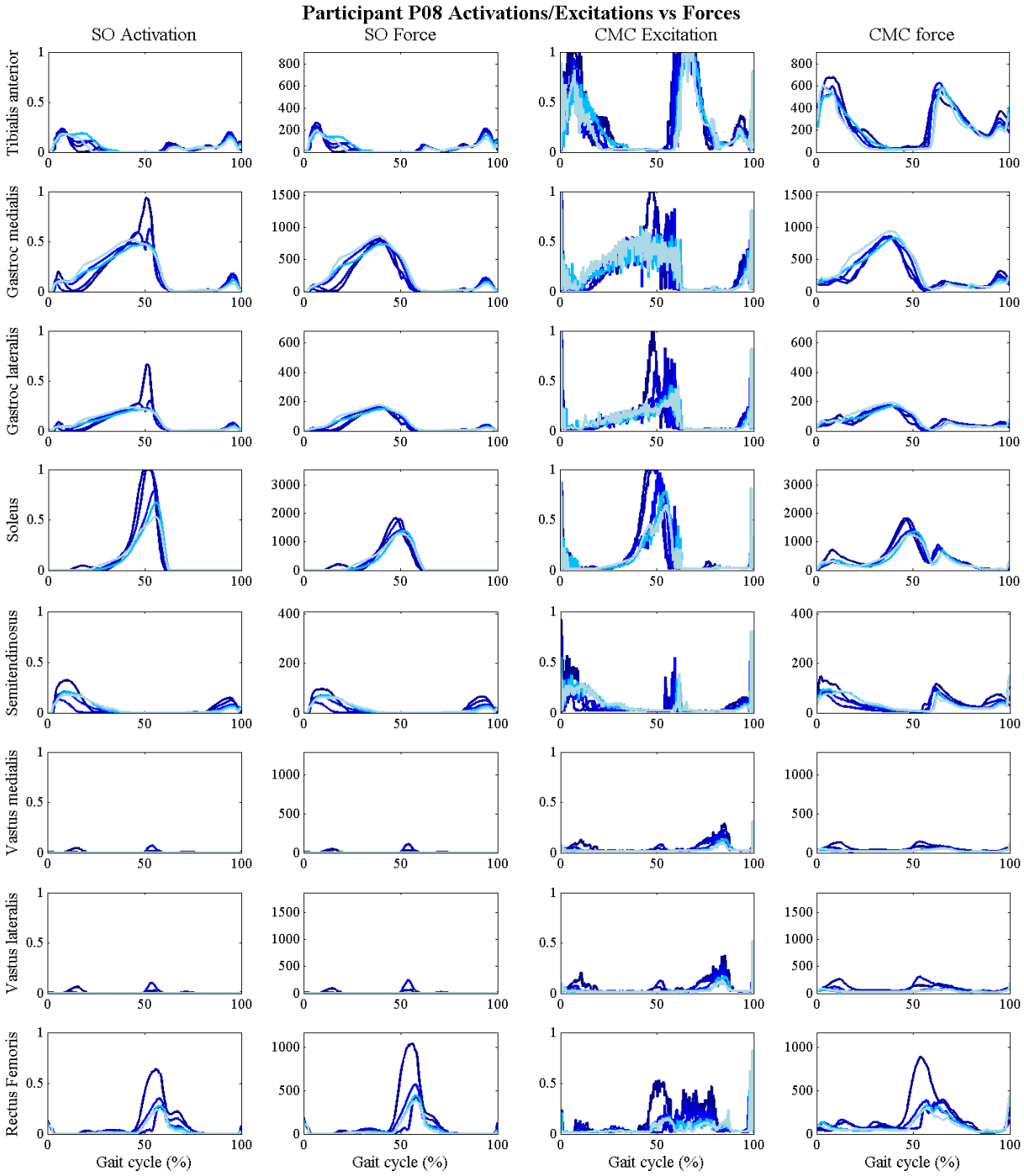

Figure 5.34. Single graphs of participant P08 (57.8kg) showing static optimisation's and CMC's muscle forces compared to surface EMG excitations for five different walking speeds.

5.4 Discussion

This is the first standardised approach to estimate muscle forces for different walking speeds in a healthy population. Also, it is to date the first time that static optimisation is compared to computed muscle control in such an environment. The developed standardised protocol (chapter IV) ran in general successfully, although some problems were detected especially with the RRA Tool. A broad agreement exists between mathematical models and surface EMG, however, not to the same extent for all muscles. In the next sections of this chapter, the results of the experimental study to estimate muscle forces will be discussed and conclusions about the practicality and validity related to implementation within clinical gait analysis will be given.

5.4.1 Discussion of Scaling, Joint Angles and Joint Moments

The scaling tool resulted in good results as most of the marker fitting errors, the difference between experimental and virtual marker, stayed under the recommendation of OpenSim. However, both lateral epicondyles and one of the fifth metatarsal markers are over the recommendations which could be due to the fact that the OpenSim knee and ankle represents a one-degree-of freedom joint and only accounts for the flexion-extension movements of the knee and plantar-dorsiflexion of the ankle. Furthermore, these errors may reflect individual variations of the foot-toes length relationship which have not been accounted for in the scaling of the model as all foot segments are scaled the same and relatively to each other. Studies which focus on the foot segment in more detail should scale the different segments separately; however, for this study and for the use in the clinic, the developed pipeline is sufficient enough as long as no additional information about foot segments movement are needed.

Similar marker fitting errors were detected for the dynamic inverse kinematics solution which indicates the influence of the same limiting factors as for the static trial: the limitation of the degrees-of-freedom on knee and ankle and participant specific anatomical features of the foot. In the OpenSim user guides maximal marker errors for a dynamic trial were valued as good when they ranged under 4cm. However, depending on the marker a 4cm difference between the experimental and the virtual marker could cause a significant difference in resulting joint angles as anatomical reference frames do change with different marker placements and therefore the orientation of the segments (Della Croce, Leardini, Chiari, & Cappozzo, 2005). Caution is advised when using these recommendations, especially for clinical studies and decision makings. It may even be helpful to adapt the recommendations according to the clinic.

Comparing the lower limb joint angles of OpenSim with the ones calculated by the Conventional Gait Model (PlugInGait) some small differences could be detected. These may result from the fact that the PlugInGait model includes a 3-degree-of-freedom knee and ankle joint, whereas OpenSim uses a slight different marker-set with the knee and ankle restricted to a 1-degree-of-freedom joint. This may have led to the small offset at the knee and ankle angle in the sagittal plane. Also, Vicon uses a direct kinematics technique, whereas OpenSim has inverse kinematics included in the SimTrack pipeline. Kainz and colleagues (2014) have shown that this can lead to different kinematic model outputs although they matched the definition of the joint centre locations and number of degree-of-freedoms.

The local reference frame of the pelvis is defined differently between both techniques. OpenSim does not account for the pelvis tilt in neutral position which explains the small offset between OpenSim's and PlugInGait's pelvic tilt. This may also explain the greater hip flexion angle with the PlugInGait model as the pelvis has a greater inclination. Furthermore, the raw trajectory data were filtered in Vicon, while OpenSim uses the raw marker trajectories without filtering. This is in general in discussion in the literature and needs to be taken into account when different laboratories are compared to each other (Gorton, Hebert, & Gannotti, 2009; McGinley et al., 2009). However, the overall similarity between OpenSim and the PlugInGait model and the high consistency between participants while using OpenSim shows that the OpenSim inverse kinematics pipeline is applicable. The functionality of the Inverse Kinematics Tool, however, must be carefully analysed and the pattern compared to other model approaches must be discussed. Further studies could expand the work of Kainz and colleagues to investigate the muscle force estimations' outcome using different kinematics data as an input into the estimation process.

The differences in joint moments which were detected between OpenSim and the Conventional Gait Model (PlugInGait) may have occurred out of two reasons. Either because the ground reaction force data was filtered for OpenSim compared to Vicon which uses raw ground reaction force data to calculate joint moments, or through the differences found at the joint angles. Especially the knee flexion moment at about 50% of the gait cycle is much greater with OpenSim than with the PlugInGait model. Although no big differences have been shown for the knee flexion angle at this point of the gait cycle, it could be a result from the different hip flexion angle between OpenSim and the PlugInGait model. The calculated joint moments of OpenSim as well as the results with the Concentional Gait Model are in range with the joint moments summarised in chapter III and compare, therefore, well with the literature.

5.4.2 Discussion of the Pre-Step Residual Reduction Algorithm

Computed muscle control is in need of a pre-step, where applied residuals are minimised while adjusting the joint kinematics to the ground reaction forces to be more dynamically consistent. This step is questionable for the clinic as the body mass and the centre of mass of the torso are adjusted. Also, this may result in greater differences to the real kinematics of the participant's gait as the error may have resulted out of an error in the ground reaction forces. The joint angles are adjusted to the ground reaction forces to account for experimental measurement errors, however, if the error of the ground reaction forces is higher than the error of the kinematics, the joint angles are changed in the wrong direction. Therefore, although computed muscle control does account for the muscle activation-contraction cycle may be more advanced than static optimisation, the adjustment made through the RRA tool makes computed muscle control less attractive for the clinic than static optimisation.

Another factor may question the OpenSim Tool RRA. The overall mass of the participant gets adjusted but not equally across trials and walking speeds. If RRA really adjusts the joint angles to the GRFs to minimise experimental errors, then this adjustment should be similar between walking trials of the same measurement session. However, for this study this is not the case, especially very slow and very fast walking speeds have much greater adjustments compared to self-selected walking speeds. For very fast walking the average body mass adjustments increase up to -1.69kg (˜2.5% of the average body weight), which makes the application into the clinic questionable. This suggests other factors which may affect the RRA output. It might be, however, that the adjustments are small enough to not affect the overall results, but further analysis are needed to understand the underlying mechanisms of RRA better that it can be used in a clinical setting.

Although the mean residual moments lie in the recommendations of OpenSim, attention must be drawn on the actual numbers the recommendations give. The "good" threshold ends with 30Nm which would be equivalent to around 30kg being placed 10cm from the centre of mass of the torso. This means that although the results of the study seem to be within a correct range, it might be that for clinical purposes these threshold are too high and adjustments need to be made. Another issue are the peak residual forces of this study. Some of the residual force outliers came up to 80N. This means a big additional force equivalent to the weight of a 8kg mass. Therefore, although the overall results seem to be good, it may not yet be applicable into a clinical gait analysis. Also, the population group of this study are healthy adults. It needs to

be further analysed how this pipeline behaves with participants with neuro-musculoskeletal disorders which might even result in greater residuals.

Some of the experimental trials during the RRA did not run successfully. OpenSim suggested three possible reasons for failing. However, all three reasons can be neglected as all model degree-of-freedoms are actuated, there are no tracking tasks for locked coordinates, and there are no unnecessary control constraints or residual actuators as the standard settings of the RRA pipeline were chosen, which was designed for gait analysis in human walking. Other trials with the exact same process ran successfully which additionally suggest another explanation for the failing of RRA. Therefore, alternative solutions were searched in preliminary studies but to-date no plausible explanation could be found. The online OpenSim user guides suggest to increase the maximum excitations for residuals and minimise tracking weights on coordinates. Though, this study does keep most parameters in the standard settings and it was not the intention to change the musculoskeletal model in such an extent. This may be material for another study, which would implement a standardised protocol how to adjust these parameters systematically.

5.4.3 Estimations of Static Optimisation vs Computed Muscle Control

The results of estimating muscle activations/excitations and muscle forces suggest that static optimisation is preferable to computed muscle control, because static optimisation results in more robust and physiological correct estimations of muscle activations and forces when comparing averaged traces. Firstly, the tibialis anterior excitation of CMC is far too high for self-selected walking speed which does not change for the other walking speeds. Secondly, the late stance – early swing activation for the semitendinosus is much smaller and only occur during faster walking speeds using static optimisation, while CMC experience much higher excitations around stance-to swing transition which are present across all walking speeds. Thirdly, Nene and colleagues (2004) have shown for self-selected walking that when measuring the rectus femoris with fine wire EMG electrodes that the muscle is only active during the transition from stance to swing with smaller activations around 30% of the gait cycle. This pattern is accurately reproduced by the estimated activations of static optimisation. CMC, however, shows a prolonged excitation from early stance to mid-swing which is difficult to believe to be physiologically correct. Fourthly, the estimated excitations and forces of CMC

present spiky patterns of vastus medialis and lateralis during swing which seem to be non-physiological, too, and may reflect some uncertainties of CMC.

Other issues and uncertainties were detected analysing individual results of specific participants, especially the spikiness and activity profiles of the unfiltered CMC excitations are conspicuous. Participant P02 shows considerably more activity in their plantarflexors in very late swing and early stance with CMC than static optimisation. Furthermore, participant P02 shows large spikes of semitendinosus activity in late stance which is also not present with static optimisation, too. Participant P02 shows also very high excitations and forces in early swing accomplished with some spiky activity at initial foot contact which do not seem physiologically correct and are also not shown for static optimisation. Compared to participant P02, participant P04 shows an earlier activity around mid-stance which is also much greater than with s static optimisation. P04's rectus femoris of CMC is less active in swing than P02, however, produces forces at initial contact for all walking speeds which stay nearly active until the end of the gait cycle.

Not all of the participants have such great discrepancies between CMC and static optimisation. Participant P08, much lighter than P02 and P04, experience less evidence of differences between the two mathematical approaches. However, CMC still shows the main issues of extensively activated tibialis anterior, spiky excitation and force production at stance-swing transition, and spiky excitation patterns of rectus femoris throughout swing.

Two other factors make static optimisation preferable to computed muscle control. In a clinical gait analysis routine time efficient data processing is crucial to be able to analyse and evaluate the patient's case. Static optimisation is more computational efficient and, therefore, faster in executing than forward dynamics (Anderson & Pandy, 2001b) and as computed muscle control which has been shown in this study. With up to 30 minutes of processing time of CMC compared to about one minute for static optimisation CMC is not practical for the clinic. This problem may be resolved by more powerful computers, however, these are not always available in clinical gait analysis. Furthermore, static optimisation had a 100% success rate, whereas computed muscle control could not be run successfully for some of the trials which makes CMC less stable than static optimisation. Especially during very fast walking CMC experienced a lot of unsuccessful trials which suggest that quicker walking speeds may not result in adequate results. This may result out of too weak muscle actuators which are not anymore able to account for the accelerations of the segments. This limitation, however, may be less pertinent in clinical

gait analysis where lower walking speeds can be anticipated in patients. Also, it may be worth following the development of CMC, as this pipeline has several advantages compared to other dynamic optimisations (e.g., computational time) and, compared to static optimisation, includes the activation-contraction cycle which might result in better results for patient groups with neurological disorders.

Comparing the results of this study to the results found in the systematic review (chapter III), static optimisation and CMC are much better in alignment and show a smaller variability to each other than the results found in the literature. This gives a hint that a lot of parameters which have been kept homogeneous between static optimisation and CMC in this study (e.g. experimental input, cost function…) might be the reason for the huge variability in the literature. Especially factors related to the experimental protocol and the musculoskeletal model might be triggering differences between studies.

5.4.4 Mathematical Models vs Experimental Surface EMG

Static optimisation and CMC showed a broad agreement with both the simultaneously measured surface EMG and the general accepted understanding of how muscles function during walking. The EMG results of this study are in agreement with known EMG studies from Winter (2009) and Perry (2010). However, there are unexplained and worrying discrepancies between modelling techniques and captured EMG when looking closely at the average muscle activation/excitation traces.

Firstly, there is a general estimation of gastrocnemius activity during late swing, which is not shown for EMG. In this phase the foot prepares for the initial foot contact phase which suggests more tibialis anterior activation and a relaxation of the plantarflexors. These gastrocnemius activations are not shown in EMG studies of Perry (2010) or Winter (Winter, 1990). Tibialis anterior is, on the other side, activated because of toe clearance at the end of swing (Winter, 1990).

Secondly, the prolonged rectus femoris activation especially with CMC is not comparable with experimental EMG measurements as surface EMG shows only activation at initial foot contact and at the end of stance. This difference between estimation and EMG may be an error of the EMG data and highlight the limitation of surface EMG. The study of Nene and colleagues (2004) has undertaken an in more depths analysis of the rectus femoris and its role in the

quadriceps. With fine-wire EMG inserted into the muscle they could show that recuts femoris is only active during the stance-to-swing transition and that the excitations recorded with surface EMG at the start and at the end of the gait cycle are cross talk from the vastii muscles. Still, the prolonged activation and force production with mathematical estimations throughout the gait cycle is physiological not correct and also not fully confirmed by the work of Nene and colleagues. This alludes to both the estimations (especially the one of CMC) and experimental data not reflecting the true activation of this muscle.

Thirdly, both mathematical models (static optimisation to a lesser extent) suggest a semitendinosus activity in late stance, which is not comparable with captured surface EMG and not physiological explainable as the semitendinosus is mainly extending the hip. During this phase of the gait cycle the foot gets plantar-flexed but the knee also starts to be in flexion again after being in nearly full extension. Both gastrocnemii are responsible for both movements as they are bi-articular muscles running over the knee and ankle joint. However, semitendinosus is also involved in the knee flexion. Depending on the moment arm semitendinosus could be chosen over the gastrocnemii as an additional activation of the semitendinosus could be more energy efficient than activating the gastrocnemii fully to 100%. This may result out of a slight misplacement of origin and insertion of the muscle-tendon actuators. Interestingly, the paper of Thelen and Anderson (2006) who investigated computed muscle control for experimental walking data show a similar peak for the hamstring muscles, although already at 40-50% of the gait cycle. They use a similar musculoskeletal model, an adaption of Delp's model (1990), with the same optimisation criterion (minimisation of the sum of squared muscle activation), but showed the activations and not the excitations of the estimated muscles. Unfortunately, they do not respond to the differences between their estimations and surface EMG and only comment that the timing of the computed muscle activations "correspond closely to published EMG activities".

Fourthly, the estimations of vastus lateralis and medialis, two other muscles of the quadriceps, are also slightly different compared to surface EMG. The second peak at the end of the gait cycle which is shown with surface EMG is missing in both estimation techniques. Same patterns of CMC vastus lateralis and medialis were shown in the work of Thelen and Anderson (2006), however, they did not discuss the different behaviour of these muscles compared to the surface EMG pattern. This activity which is seen solely for EMG may reflect the vastii to control knee flexion during push-off and "break" the leg from further swinging backward (Winter, 1990). Winter also describes in his work (1990) that the EMG activities in late swing did not occur for

all participants. This may give more evidence that the geometry of the muscles (e.g. origin and insertion) of the musculoskeletal model to estimate muscle forces may be not exact enough to represent the actual force which is produced.

Besides this, the dependence of walking speeds is in general similar between estimated activation/excitation of mathematical models and surface EMG. For some of the muscles, modelling techniques show differences in the shape or a big jump in magnitude between very fast and fast waling compared to very slow, slow and self-selected walking speeds (e.g. rectus femoris (CMC), gastrocnemius lateralis (static optimisation, CMC)). This is not shown to such an extent with corresponding EMG data, which may again suggest that the musculoskeletal model is too weak for faster walking speeds. EMG, on the other side, has for some of the muscles (vastus medialis and lateralis, soleus, gastrocnemius lateralis) extended increase in activity during very fast walking compared to the other walking speeds and additionally big wavy mid-stance activities for very fast walking (semitendinosus, rectus femoris, vastus medialis and lateralis), which may represent movement-artefacts. This may also suggest that the very fast walking speed was too quick for a normal walking pattern and already in a range where the participants would have naturally fallen into a jogging gait pattern.

5.4.5 Concerning Issues with Processing Steps of SimTrack

There are a number of concerning issues with the standardised protocol and included processing steps. Although RRA residuals and CMC reserve actuators are mostly lying within the recommendations of OpenSim some outliers were detected which exceeded these recommended values. Also, the limits of acceptable residuals appear too generous which demands stricter limitations for the implementation into clinical gait analysis. It is, however, not very clear why these high residuals and reserve actuators exist. OpenSim suggest that there may be issues with the scaled model, the inverse kinematics solution or the applied GRF's. However, the Scaling Tool was adapted to result in better physiological data which is confirmed by small scaling errors and extra care has been taken to collect good quality GRF's. The errors may result from the inverse kinematics solution, however, these were comparable with the solution of a standard Conventional Gait Model and also similar to the literature. In the case that the RRA residuals exceed the recommendations or RRA is failing, OpenSim suggests increasing the maximum excitation for residuals until the simulation runs. This, however, is not justifiable in a clinical setting, firstly, because residuals and reserve actuators may be

unrealistically high, and secondly, subjective changes on the pipeline need to be undertaken which is against the repeatability of a standardised process. The same applies for the reserve actuators of CMC.

Another issue may suggest the uncertainty which exists at the moment with mathematical models to estimate muscle forces may have a general impact on mathematical modelling. In this study, RRA and CMC had the tendency to fail for some of the trials, especially during fast and very fast walking speeds. Whilst this has been presented as a disadvantage over static optimisation, it may be also an indicator of underlying dynamic inconsistencies that are hidden in the static optimisation approach, which is less sensitive to such errors. This may explain the non-physiological activations which occurred for static optimisation and may confirm the need of such adjustments to be made with the RRA Tool. On the other side, it seems that RRA may not account correctly for these dynamic inconsistencies as some non-physiological excitations and forces appear with CMC even to a greater extent. This definitely suggests that before mathematical modelling may be routinely applied into a clinical gait analysis more research needs to be undertaken to understand the processes of mathematical modelling more extensively.

Reserve actuators make up for strength deficiencies which occur on the muscle actuators. They are an indicator of a too weak musculoskeletal model or an unbalanced agonist-antagonist relationship. OpenSim recommends to either reduce the passive muscle stiffness property of the muscle (Hicks & Uchida, 2013a) or, in case the muscle works at abnormal fibre lengths (see chapter II), to modify the tendon slack length or/and the muscle fibre length such that the muscle complex is in a more efficient length range and can generate more force. In a clinical setting, this may only be possible with a systematic pipeline to adjust these parameters according to the participant. In this study, however, the musculoskeletal model has only been adjusted according to the participants' anthropometrics and not to the individual muscular-tendon properties, for example the maximal isometric force or the origin and insertion of the muscle. It is possible to estimate the maximum isometric force by using a hand-held dynamometer or to calculate it through the knowledge of the physiological cross sectional area. Also, the origin and insertion of the muscles can be individualised by using MRI data (A. S. Arnold, Salinas, Asakawa, & Delp, 2000). However, both techniques are either time intensive, have other limitations or need more investigations to find a solution for these problems. One may use isometric contractions or reference data corresponding to the age and sex as well as the condition of the participant. However, the variability which may be present in patients with specific disabilities may make

this approach hard to be applied. The development of such a pipeline to include participant specific muscular-tendon properties could be one of the following works which will be undertaken to make the pipeline with CMC more robust.

5.4.6 Limitations

Although the calibration of the system showed adequate results, a systematic error was detected running RRA as the centre of mass of the torso was constantly shifted lateral in direction to the right. The error was independent of testing session and trial and ranged around two to three centimetres. Therefore, it was suspected that this error resulted out of a measurement error which could not be detected. Analysis in more depth revealed that the calibration wand was misplaced for about 1-2mm and less than 1° rotated around the origin of the global measurement volume. This occurred because the wand was orientated on the floor which was placed on top on the force plate and inhibited a direct view of the force plate. A small offset between floor and force plate provoke the wand being misplaced. This means that the force plates were with a small rotational angle misplaced to the camera system which caused an offset between marker trajectories and ground reaction forces.

One would think that a small offset of 1-2mm would not have such a great effect on the measurement outcomes including the fact that the CalTester revealed adequate calibration errors. However, because the laboratory was equipped with four force plates placed behind each other this error did add up and a rotational error of about 1° resulted in a much higher error on force plate 4 (Passmore & Sangeux, 2014). To analyse the effect on the results all ten walking trials of the participant with the greatest centre of mass torso shift (P02) were manually corrected by aligning the trajectories of the sacrum marker with the centre of pressures of the force plates. These results showed that small changes could be detected on the hip adduction moment as well as on muscles responsible for producing this moment (all three actuators of gluteus medius, appendix A9). However, because the muscles of interest did not change in magnitude or pattern this error has been accepted for this study. In general, small errors in experimental data represent a realistic problem in a clinical gait analysis laboratory and would not be massively out of the ordinary. These results show that the setup of the laboratories to appropriate standards is essential to enable the mathematical models to be adapted in such a clinical environment.

Another limitation of the standardised protocol is that in the current settings it is only tested with the use of the OpenSim marker-set. It is similar to the CAST marker-set (A. Leardini et al., 2007) with some differences of the thigh and shank markers, and is quite different to the PlugInGait marker set. Therefore, this protocol needs to be tested for other marker-sets (chapter III), too, to make it more attractive for the clinical use. However, it may not be as easy as additional bony landmarks and joint centres are calculated by relying on the experimentally placed markers. Another factor which limits the implementation of this protocol into the clinic is that the enhanced scaling tool needs the foot flat on the floor. This means that for patients not being able to bring their heel onto the floor for the static calibration the protocol needs to be adjusted. Further work needs to be done to refine the scaling tool so that it may be used for all kinds of disabilities.

5.5 Conclusion

This experimental study tested the standardised protocol which has been developed to estimate muscle activations and forces during walking. Overall, whilst on balance, the overall averaged results show general agreement between model estimates and EMG measurements, however, more detailed examination suggest differences that are difficult to explain and undermine confidence in the modelling approach for clinical work. This work is based on the analysis of healthy adult walking and these issues are likely to be exacerbated in clinical work for patients with a range of different pathologies. However, in clinical use and with patients, the walking speeds might be slower than the fast walking speeds where errors seem to be greater than with slower walking speeds. This suggests as well that focusing on slower speeds might result in better results.

Static optimisation seems, in general, more robust and stable than computed muscle control, is more computational efficient, and results in similar results than computed muscle control. Although computed muscle control does include the activation-contraction cycle it shows no additional features compared to static optimisation. This may suggest that static optimisation seems to be to-date the estimation method most suitable for the clinical gait analysis and is recommended to be chosen. Computed muscle control including its pre-step residual reduction algorithm revealed a lot of uncertainties which need to be investigated to be sure about how the process may influence the estimations outcome. Furthermore, these uncertainties may reveal underlying dynamic inconsistencies which are hidden within the static optimisation approach which may also suggest a general uncertainty with the estimation of muscle activation and forces. Anyhow, a further development of CMC might result in better results for patients as the activation-contraction cycle is included and might reveal deficits in patients with neurological diseases which static optimisation is not able to do.

The results of this study also suggest that the musculoskeletal model gait2392 may be too weak or may not be an appropriate level of specificity to an individual participant's (e.g. muscle-tendon length, maximum isometric force…). Muscles' origin and insertion which are defined in the musculoskeletal muscle for each muscle-tendon unit may not correlate well to the anthropometrics of the participant. Also muscle-tendon characteristics like the maximal isometric force may not be the true values of each participant as they do not get automatically adjusted in OpenSim. Increased efforts need to be undertaken to include a better individualisation of the model into the protocol. This protocol has already shown quite close

kinematic and kinetic results to a standard approach with a Conventional Gait Model as well as resulted in similar muscle activation and force estimations compared to surface EMG which indicates that the protocol is on a good way to be implemented into a clinical routine processing. Even individual differences between participants could often be confirmed by the surface EMG pattern. However, to be able to be sure about the quality and reliability of this protocol it needs to be further tested and limitations need to be either eliminated or better understood.

CHAPTER VI

6 Overall Conclusion and Future Work

This PhD thesis was conducted to analyse the state-of-the-art of musculoskeletal modelling and muscle force estimations related to clinical gait analysis and to further contribute to the current literature by developing a standardised protocol to estimate muscle forces suitable for the clinical gait analysis routine. The following sections, firstly, summarise the findings of the thesis according to the research questions which have been established in chapter II, secondly, discuss original contributions and the wider impact of this work, thirdly, will critically challenge the research design and results, and fourthly, define future work which may be undertaken to accomplish the research of this thesis.

6.1 Summary of the Thesis' Findings according to the Research Questions

The findings of this PhD project could answer the research questions of chapter II to following extent:

1. *What is the state-of-the-art in movement science to estimate muscle forces and joint moments which act on the lower limb joints during walking?*

The systematic review could identify in total 19 studies which investigated muscle force estimation in gait analysis of healthy human adults (chapter 3.3). These studies used in nearly all of the cases one or more of three main mathematical models to estimate muscle forces (static optimisation, forward dynamics, EMG-driven, table 3.4 and chapter 3.3.6). Two studies compared a static optimisation approach to a new developed technique which included an additional step, the incorporation of the activation-contraction cycle of the muscle. One of them is called computed muscle control, and developed by Thelen and Anderson (Thelen et al., 2003; Thelen & Anderson, 2006).

The musculoskeletal models which were used to simulate human walking were mainly a variation of two models developed from Delp and colleagues (1990) and Anderson and Pandy

(1999) (chapter 3.3.4). Anderson and Pandy's model, however, used the defined muscle-tendon paths of the Delp model. Both models are Hill-type muscle models, adapted from the work of Zajac (Zajac, 1989). Although the origin of the musculoskeletal models used in identified studies were mostly the same, they differed in the number of muscle-tendon actuators, in the source of geometry of muscles and segments (chapter 3.3.5), as well as in the included segments and degrees of freedom.

In general, the results of the systematic review showed a high variation in shape and magnitude of extracted and digitised muscle force profiles, especially compared to the digitised joint moment profiles (chapter 3.3.8.2). This variation varied, however, between muscles. Muscles on the shank were in average more consistent in their shapes than muscles on the thigh or hip.

A direct validation method of estimated muscle forces has not yet been developed or are not feasible in a clinical gait analysis routine. EMG measurements, however, have been widely included to serve as an indirect validation tool and a first indication of muscles coordination throughout a gait cycle (chapter 3.3.7). Often, however, this validation was lacking in quality. Either, studies did not capture own EMG data of the same participant and trial to reduce intra- and inter-subject variability, or EMG signals were additionally used as an input into the estimation process which biased the validation process.

2. *Are there experimental parameters and/or parameters related to modelling and simulation which may affect the estimation's outcome? Which parameters need to be taken into consideration to create a standardised protocol which implements the estimation of muscle forces in the clinical gait analysis?*

Several parameters related to the experimental conditions or the modelling and simulation process which can have an effect on the estimation's outcome (chapter 3.4.1.1 and chapter 3.4.1.2). This included the walking speed, the filtering of experimental data, the reference frame, the biomechanical model, or body segments' parameter as well as the mathematical model used to estimate muscle forces, the musculoskeletal model including the muscular-tendon properties, or the cost functions.

It is important to know the influence of walking speed on the estimations' output. In cases, where a patient group is compared to a healthy control group, walking speed on its own may influence the results as patients mainly walk slower than healthy participants. It has been shown

before that walking speed has an influence on experimental data (kinematics, kinetics, EMG, see chapter 2.4.1.1), however, the influence of walking speed on muscle force estimation has not yet been widely analysed.

Some other factors have already been tested according to their influence on the estimation's outcome. Some studies compared mathematical models with each other (e.g., Anderson & Pandy, 2001b; Lin et al., 2012), analysed the differences of a musculoskeletal model in two different simulation environments (Lin et al., 2012), or investigated the changes caused by different cost functions (Collins, 1995; Monaco et al., 2011). These studies showed, that it is important to keep the modelling and simulation protocol consistent to be able to compare different participants group or results of different laboratories with each other. Also, a detailed documentation of each step of the protocol is needed to understand the estimations' output and the limitations the applied estimation process may have caused.

3. *Which mathematical model, musculoskeletal model, and simulation environment to estimate muscle forces are the one most suitable for the clinical routine according to the literature?*

Two main mathematical models to estimate muscle forces have been found to be most practicable in a clinical gait analysis routine, static optimisation and computed muscle control (chapter 3.4.1.4). Static optimisation has been chosen due to its time efficiency compared to forward dynamic models, its robustness, and dominance in the literature. It resulted in at least as good results in chapter III compared to the other methods. The disadvantage of static optimisation may be the neglecting of the muscle activation-contraction dynamics which would be crucial for patients with neurological conditions. Computed muscle control claims to be time efficient, too, while including the activation-contraction cycle into the estimation process. Both models are also independent of EMG measurements which makes them most attractive for the clinical gait analysis routine.

Delp and colleagues model (1990) has been widely used and tested for modelling and simulation purposes in gait analysis. It makes it, therefore, attractive to be used for these purposes. SimTrack within OpenSim has been chosen to be the pipeline most suitable for the clinical purposes as this pipeline is straight forward and OpenSim a free available tool offering both mathematical models including the musculoskeletal model of Delp and colleagues (model gait2392 in OpenSim, chapter IV).

The cost function which was implemented in both mathematical models in OpenSim's standard settings was the sum of muscle activations squared. Monaco and colleagues (2011) found that the power of the cost function has an influence on the estimation's outcome and recommend values with range from 2.75 to 4. They only, however, used the performance criterion sum of muscle stresses. Collins (1995) compared different cost functions with each other. However, they did not include the sum of muscle activations. Therefore, it has been decided to use the standard settings OpenSim provides in the experimental study to estimate muscle forces during health human adult walking.

It was also decided to use the musculoskeletal model (e.g. muscle-tendon characteristics, degrees of freedom) in its standard settings, as it was important to understand first its usability in its default settings to then be able to systematically change the parameters of the model in case estimated results were physiologically incorrect. However, some changes needed to be undertaken which were the marker set of model gait2392, the placement of the markers on the model and the Scaling Tool of SimTrack (chapter 4.4.7).

4. *Is it possible with the current facilities to estimate individual muscle forces on a human healthy population on the lower limb during and are the results comparable to parallel captured surface EMG?*

The results of the experimental study (chapter V) which implemented the developed protocol of chapter IV showed that this developed protocol is on a good way. Compared to the findings in the literature (chapter III) the study shows a good consistency between participants and compared to surface EMG excitations, by limiting the influencing factors and keeping experimental as well as several modelling parameters consistent. The standardised protocol, however, is not yet robust enough to be implemented into a routine clinical gait analysis. According to the results of the study, static optimisation seems preferable to CMC because of differences found in estimating muscle forces (chapter 5.4.3). Model estimations showed in general a board agreement with measured EMG. However, both mathematical models result in unexplained and worrying discrepancies when comparing them with EMG (e.g. gastrocnemius activity in late swing, semitendinosus activity in late stance, prolonged rectus femoris activation). Also, RRA and CMC have the tendency to fail during the estimation process. Whilst this may point out a disadvantage of CMC compared to static optimisation it may also be an

indication of underlying dynamic inconsistencies which are hidden in the static optimisation approach due to a lesser sensitivity to it.

Therefore, with this protocol it is not yet possible to estimate individual muscle forces on a human heathy population of the lower limb. However, the current facilities which are available may allow to reach this. To be able to do so, more research needs to be undertaken to understand existing uncertainties and limitations in more detail. Also, these analysis are based on a healthy population which indicates an exacerbating of these issues in clinical work for patients with a range of different pathologies. Therefore, the protocol needs also to be tested on patient groups to make a better statement about the validity of muscle force estimation in clinical gait analysis.

6.2 Critical Appraisal of Research Design

Some general limitations of the approach of this PhD thesis need to be pointed out.

When choosing OpenSim, the operator needs to accept to be bound to the limitations of this simulation environment. Although OpenSim has a big user community with which it is possible to discuss issues about the different tools and models on a provided internet platform, direct professional help is not provided from the developer. OpenSim is a free available tool, which may have its advantages as every movement laboratory is able to download the programme including various musculoskeletal models. However, it may also leave the operator sometimes in ignorance of important steps which need to be undertaken to run an estimation successfully. Although SimTrack seems straight forward and applicable without any deep knowledge about the modelling and simulation process, the operator may struggle to understand every step which needs to be undertaken to result in decent estimations. OpenSim lives, therefore, from the contribution of its users. The developer of OpenSim do their best to keep up with up-to-date user guidelines. A lot of work has been done in the last years to develop the project OpenSim to a professional tool. Despite the limitations to work with OpenSim it has great possibilities.

To be able to use these possibilities, straight forward protocols are needed which do not need any subjective interference of the operator. Furthermore, the collaboration with experts in the fields where the programme with be applied may help to integrate more knowledge about the need of this profession. This means that for the application into a clinical gait analysis routine, a close collaborations with clinicians and related researchers is needed. A first step has been undertaken with this PhD project as the Scaling Tool has been further developed (chapter 4.4.1). The generic model is scaled in a more anatomical and physiological correct way so that joint centres and anatomical landmarks are aligned with the skeleton. However, it is to date only applicable for participants who are able to have their foot flat on the floor during the static standing trial. This means that this protocol is not suitable for patients like children with cerebral palsy who are not able to bring their heel down to the floor. Also, the protocol has only been tested on healthy adults. The results of this thesis are, therefore, only valid for this specific population group. More research is needed to open this pipeline to a broader population group.

The musculoskeletal model gait2392 has been used in its standard settings (chapter 4.2). One limitation of this model is that the maximum isometric force defined for each muscle is not scaled automatically to the participant's characteristics. It was decided that these standard settings were accepted for this study. Automatic changes to other muscle-tendon properties

have not been explored further. Muscle-tendons' origin and insertion are based on cadaver studies and, when using the Scaling Tool, are only scaled according to the length of the segments. This means that moment arms of specific muscles are not adjusted according to the individual participant. For healthy participants this all may not be from major issue, however, for patients with restricted neuromuscular functions this presents a major limitation.

One limitation of the mathematical model static optimisation is that it does not include the activation-contraction cycle. This means that all neurological processes which are involved in muscle force production are not incorporated. Therefore, static optimisation has its limitations when estimating muscle forces of patients with neurological diseases (e.g. cerebral palsy, stroke, or Parkinson's). However, for musculoskeletal diseases (joint replacements, prosthesis, and sport injuries) static optimisation may be sufficient. For further studies it may be in general useful to look first on musculoskeletal diseases before to be able to apply a protocol on neurological disorders.

The pre-step RRA which needs to be successfully undertaken before CMC is discussable. Joint angles as well as the centre of mass of the participant's torso are adjusted to be more consistent with the experimental GRFs. OpenSim justifies this step to minimise experimental errors between the camera and the force plate system (which may arise out of slight differences between the coordinate systems of both measurement systems). However, it is unclear if this adaptation of joint angles and centre of mass of the torso are physiologically correct or if the detected error may result out of GRF errors which may change the data in the wrong direction when applying RRA. Contrary to this, static optimisation may not be sensitive enough to detect dynamic inconsistencies.

6.3 Original Contributions and Wider Impact

The novel work within this PhD thesis can be summarised as follows:

1. The systematic review is the first in biomechanical modelling focussing on muscle forces and joint moments in human healthy walking and summarising graphical material together in one normalised graph. The review analysed successfully the variability between muscle force and joint moment profiles across a gait cycle which were presented in relevant studies. Also, the focus lied on comparing the three main mathematical models with each other which were used to estimate muscle forces.

   The results highlighted a diversity of approaches and results and a need for further harmonisation and validation. This attributes and adds knowledge to the study of Hicks and colleagues (2015) who summarised best practise for verification and validation of musculoskeletal models and simulations of movements. Additionally to the study of Hicks and colleagues this systematic review could summarise potential influencing factors on the estimation's outcome. Therefore, this systematic review could contribute to the current knowledge of muscle force estimation in clinical movement analysis which shows the usefulness of such approaches in biomechanical modelling.

2. This study is one of the very few works using recent technology in mathematical modelling to estimate muscle forces independently of EMG measurements, specifically in order to be able to validate the shape and speed-dependence with EMG without bias. This is important as EMG measurements are the only validation tool so far which is able to present muscle coordination non-invasively. Also, this study used simultaneously captured EMG data parallel to the kinematics and ground reaction forces which were used in the modelling process. This ensured a minimal intra- and inter-subject variability. Most studies which estimated muscle forces and validated the results to EMG used EMG data also in their estimation process. Furthermore, some studies did not collect their own EMG data and used available EMG profiles from the literature or only presented an on-off pattern of captured EMG data (chapter III and chapter V). As an example, the study of Neptune and colleagues (2008), one of the only studies to analyse the dependence of walking speed on some of the muscles of the lower limb, compared the estimated muscle forces to EMG. However, they used these EMG data into their estimation process, too, to define the muscle excitation patters. Therefore, this

study could increase the quality of the results compared to other studies by using independent and simultaneously captured EMG data.

3. This study could contribute to the knowledge of validating two different mathematical models in terms of whether the simulations show similar changes in activation/excitation with walking speed as measured EMG at different walking speeds. The wide and substantial approach of this study is novel compared to existing studies as it includes more muscles of the lower limb related to walking and compared to participant-specific EMG measurements. Neptune and colleagues (2008) used an EMG-driven mathematical model and only present the EMG speed-dependent changes of the soleus and gastrocnemius which were averaged across all participants included into the study. Liu and colleagues (2008) used CMC to estimate speed-dependent muscle forces on children and used averaged EMG standard deviation bands to validate the estimates muscle forces. Thus, this PhD study could enhance the knowledge about speed-dependent muscle force estimations by comparing them to independent and participant-specific EMG and between two mathematical models.

4. Developing the Scaling Tool in the SimTrack pipeline of OpenSim was the first approach to propose a technique for model scaling and calibration which requires no intervention from the operator. Also, its marker set definition was adjusted to make it suitable for clinical purposes. The standard Scaling Tool in OpenSim recommends the user subjective adjustment of the markers in case scaling errors are too high (Hicks & Dunne, 2012):

   > "Frequently, it is helpful to preview the inverse kinematic solution for the static pose before adjusting the positions of the model markers. This can be useful for identifying markers that are poorly placed on the model that you may need to manually adjust or may decide not to include in the inverse kinematic problem."

   To be able to include such a tool into the clinical gait analysis it is important that the operator does not need to subjectively interfere into the calculation process as the repeatability is not given. Therefore, this developed Scaling Tool for the use in OpenSim could resolve this issue and adjusted the SimTrack pipeline to the needs of the clinical gait analysis.

5. This study could develop a small normative data pool of muscle force estimation for ten healthy adults during different walking speeds while systematically comparing the

mathematical models static optimisation and computed muscle control with each other. The results will be made available on the OpenSim web-site to enable other OpenSim users to compare their data with this study. This is very important to motivate the interaction between different movement laboratories and encourage them to up-load their data which will develop a big community for estimating muscle forces in clinical gait analysis.

6. Through conducting this study, important limitations and uncertainties of the current approaches to estimate muscle activations and forces could be uncovered. These results showed that this protocol to estimate muscle forces in clinical gait analysis is not yet at the stage to be implemented into a clinical routine processing. However, the results which have been found can help to guide future work to be able to make modelling and simulation accessible for the implementation into the clinical gait analysis. Also, for slower walking speeds, the results showed better results for both mathematical models, which might point out that these models are suitable for the purpose of measuring patients as this population group mostly walks slower than a healthy population.

6.4 Future Work

One of the major research questions which may be performed to bring the protocol another step forward is to understand the musculoskeletal model gait2392 in more detail. Standardised settings like the characteristics of each muscle-tendon complex should be able to be adjusted to each participant and, especially, to each patient with different disorders. The recent study of Arnold and colleagues (2013) tested the influence of the muscle-fibre-length and -velocity's influence on muscle force estimations at different walking and running speeds, but especially focused on the walking-to-running transition. They used a musculoskeletal model (A. S. Arnold et al., 2000) implemented in OpenSim. Their findings suggested for some of the muscles an increase, but, interestingly, for other muscles a decrease of muscle force generation ability especially for the plantarflexors. They conclude that the muscle-tendon architecture of these muscles may not reach the demand for higher walking speeds. There findings show some limitations of available musculoskeletal models and the need of muscular-tendon characteristics more adapted to the anthropometrics of the participant.

This means that more studies need to be undertaken to understand if participant specific muscle-tendon properties may enhance the estimation's output. Firstly, muscle-tendon settings need to be systematically changed to understand the behaviour of these and, secondly, a standardised and straight forward way to adjust muscle-tendons properties automatically need to be developed. One solution may be magnetic resonance imaging (MRI) with which it is possible to define the orientation of the muscles to the segments and to calculate the maximum isometric force a muscle can exert (A. S. Arnold et al., 2000). Some of the muscle-tendon properties have already been analysed with the help of MRI imaging. Bolsterlee and colleagues (2015) used MRI to scale physiological cross-sectional area of muscles of the upper limb to analyse the influence on musculoskeletal model estimations who, however, only showed marginal differences in the estimation's output. Bosmans and colleagues (2015) determined individual origins and insertions of 33 lower limb muscles to analyse the influence on estimated muscle forces during walking compared to a generic model and found significant changes on the estimation's output.

The implementation of MRI scans has already been used in OpenSim as an option for the scaling of the segments. The disadvantage of this method, however, is that it is not available for every clinical gait analysis laboratory and is expensive to run. This may suggest two solutions, either to develop a database for different demographical and physiological

characteristics (e.g. gender, age, body height, condition of the patient), or to use methods like a standardised MVC test to account for individual maximal isometric forces.

It is highly important to test the robustness of the study by evaluating the sensibility of the protocol step by step (Hicks et al., 2015). Some first stage improvements have been done in this work, especially on the scaling routine of the musculoskeletal model. Influencing factors in the estimation's outcome need to be known, understood and controlled. Speed-dependent differences have been analysed in this study, but other factors can have an influence on the estimations outcome like other experimental conditions or processing steps of the estimation routine. These factors need to be analysed in detail to understand their influence on the estimations' outcome and to take them if applicable into account. Especially the uncertainties and limitations which have been detected through the experimental study to estimate muscle activations and forces need to be analysed to be able to make modelling and simulation tools more robust for a clinical use.

If the standardised pipeline is developed to a point that uncertainties are understood and limitations can be taken into account for interpretation purposes, the standardised pipeline needs to be tested with different marker sets to account for the Conventional Gait Model but also the 6-degree-of-freedom models frequently used in clinical gait analysis, which are slightly different to the OpenSim marker-set (A. Leardini et al., 2007). Important is as well that the protocol is tested on a group of participants, and not on single individuals. This is however, to date rarely the case in the literature, many modelling studies focus on one participant only. Recent studies like the work of Pinzone and colleagues (Pinzone, Schwartz, & Baker, 2016) pointed out the high kinematic and kinetic variability which exists between individual participants during walking. This confirms the need of studies on bigger cohort groups. Furthermore, this standardised protocol needs to be tested on patients with various conditions as this work is only based on healthy adult walking which may exacerbate detected issues with modelling and simulation routines.

APPENDICIES

A.1 OpenSim: muscle-Tendon Actuators of model gait2392

Table A.1. Muscle tendon actuators of OpenSim model gait2392.

Muscle actuator	Max iso force	Abbrevation right	Abbrevation left	Muscle actuator	Max iso force	Abbrevation right	Abbrevation left
Gluteus Medius 1	819	glut_med1_r	glut_med1_l	Psoas Major	1113	psoas_r	psoas_l
Gluteus Medius 2	573	glut_med2_r	glut_med2_l	Quadratus Femoris	381	quad_fem_r	quad_fem_l
Gluteus Medius 3	653	glut_med3_r	glut_med3_l	Gemellus	164	gem_r	gem_l
Gluteus Minimus 1	270	glut_min1_r	glut_min1_l	Piriformis	444	peri_r	peri_l
Gluteus Minimus 2	285	glut_min2_r	glut_min2_l	Rectus Femoris	1169	rect_fem_r	rect_fem_l
Gluteus Minimus 3	323	glut_min3_r	glut_min3_l	Vastus Medialis	1294	vas_med_r	vas_med_l
Semimembranosus	1288	semimem_r	semimem_l	Vastus Intermedius	1365	vas_int_r	vas_int_l
Semitendinosus	410	semiten_r	semiten_l	Vastus Lateralis	1871	vas_lat_r	vas_lat_l
Biceps Femoris Long Head	896	bifemlh_r	bifemlh_l	Medial Gastrocnemius	1558	med_gas_r	med_gas_l
Biceps Femoris Short Head	804	bifemsh_r	bifemsh_l	Lateral Gastrocnemius	683	lat_gas_r	lat_gas_l
Sartorius	156	sar_r	sar_l	Soleus	3549	soleus_r	soleus_l
Adductor Longus	627	add_long_r	add_long_l	Tibialis Posterior	1588	tib_post_r	tib_post_l
Adductor Brevis	429	add_brev_r	add_brev_l	Flexor Digitorum Longus	310	flex_dig_r	flex_dig_l
Adductor Magnus 1	381	add_mag1_r	add_mag1_l	Flexor Hallucis Longus	322	flex_hal_r	flex_hal_l
Adductor Magnus 2	343	add_mag2_r	add_mag2_l	Tbibialis Anterior	905	tib_ant_r	tib_ant_l
Adductor Magnus 3	488	add_mag3_r	add_mag3_l	Peroneus Brevis	435	per_brev_r	per_brev_l
Tensor Fasciae Latae	233	tfl_r	tfl_l	Peroneus Longus	943	per_long_r	per_long_l
Pectineus	266	pect_r	pect_l	Peroneus Tertius	180	per_tert_r	per_tert_l
Gracilis	162	grac_r	grac_l	Extensor Digitorum Longus	512	ext_dig_r	ext_dig_l
Gluteus Maximus 1	573	glut_max1_r	glut_max1_l	Extensor Hallucis Longus	162	ext_hal_r	ext_hal_l
Gluteus Maximus 2	819	glut_max2_r	glut_max2_l	Erector Spinae	2500	ercspn_r	ercspn_l
Gluteus Maximus 3	552	glut_max3_r	glut_max3_l	Internal Oblique	900	intobl_r	intobl_l
Iliacus	1073	iliacus_r	iliacus_l	External Oblique	900	extobl_r	extobl_l

A.2 OpenSim: mass and Inertia of gait2392 Segments

Table A.2. Mass and inertia of gait2392 segments.

Body Segment	Mass (kg)	Moments of Inertia		
		xx	yy	zz
Torso	34.3266	1.4745	0.7555	1.4314
Pelvis	11.777	0.1028	0.0871	0.0579
Femur	9.3014	0.1339	0.0351	0.1412
Tibia	3.7075	0.0504	0.0051	0.0511
Talus	0.1	0.001	0.001	0.001
Calcaneus	1.25	0.0014	0.0039	0.0041
Toe	0.2166	0.0001	0.0002	0.001

A.3 A Typical .osim File Format for Musculoskeletal Models in OpenSim

```
<?xml version="1.0" encoding="UTF-8" ?>
<OpenSimDocument Version="20303">
        <Model name="3DGaitModel2392">
        <length_units>meters</length_units>
                <force_units>N</force_units>
                <!--Acceleration due to gravity.-->
                <gravity> 0 -9.80665 0</gravity>
                <!--Bodies in the model.-->
                <BodySet>
                        <objects>
                                <Body name="ground">
                                        <mass>0</mass>
                                        <mass_center> 0 0 0</mass_center>
                                        <inertia_xx>0</inertia_xx>
                                        <inertia_yy>0</inertia_yy>
                                        <inertia_zz>0</inertia_zz>
                                        <inertia_xy>0</inertia_xy>
                                        <inertia_xz>0</inertia_xz>
                                        <inertia_yz>0</inertia_yz>
                                        <!--Joint that connects this body with the parent body.-->
                                        <Joint />
                                        <VisibleObject>
                                                <!--Set of geometry files and associated attributes, allow .vtp, .stl, .obj-->
                                                <GeometrySet>
                                                        <objects>
                                                                <DisplayGeometry>
                                                                        <!--Name of geometry file .vtp, .stl, .obj-->
                                                                        <geometry_file>treadmill.vtp</geometry_file>
                                                                        <!--Color used to display the geometry when visible-->
                                                                        <color> 1 1 1</color>
```

```
                                                <!--Name of texture file .jpg, .bmp-->
                                                <texture_file />
                                                <!--in body transform specified as 3 rotations (rad) followed by 3 translations rX rY rZ tx ty tz-
                                                ->
                                                <transform> -0 0 -0 0 0 0</transform>
                                                <!--Three scale factors for display purposes: scaleX scaleY scaleZ-->
                                                <scale_factors> 1 1 1</scale_factors>
                                                <!--Display Pref. 0:Hide 1:Wire 3:Flat 4:Shaded-->
                                                <display_preference>0</display_preference>
                                                <!--Display opacity between 0.0 and 1.0-->
                                                <opacity>1</opacity>
                                        </DisplayGeometry>
                                </objects>
                                <groups />
                        </GeometrySet>
                        <!--Three scale factors for display purposes: scaleX scaleY scaleZ-->
                        <scale_factors> 1 1 1</scale_factors>
                        <!--transform relative to owner specified as 3 rotations (rad) followed by 3 translations rX rY rZ tx ty tz-->
                        <transform> -0 0 -0 0 0 0</transform>
                        <!--Whether to show a coordinate frame-->
                        <show_axes>false</show_axes>
                        <!--Display Pref. 0:Hide 1:Wire 3:Flat 4:Shaded Can be overriden for individual geometries-->
                        <display_preference>4</display_preference>
                </VisibleObject>
                <WrapObjectSet>
                        <objects />
                        <groups />
                </WrapObjectSet>
        </Body>
        …
    </objects>
    <groups />
</BodySet>
<ForceSet>
```

```
<objects>
	<Thelen2003Muscle name="glut_med1_r">
		<!--Flag indicating whether the force is disabled or not. Disabled means that the force is not active in subsequent dynamics realizations.-->
		<isDisabled>false</isDisabled>
		<!--Minimum allowed value for control signal. Used primarily when solving for control values.-->
		<min_control>0</min_control>
		<!--Maximum allowed value for control signal. Used primarily when solving for control values.-->
		<max_control>1</max_control>
		<!--The set of points defining the path of the muscle.-->
		<GeometryPath>
			<PathPointSet>
				<objects>
					<PathPoint name="glut_med1_r-P1">
						<location> -0.0408 0.0304 0.1209</location>
						<body>pelvis</body>
					</PathPoint>
					<PathPoint name="glut_med1_r-P2">
						<location> -0.0218 -0.0117 0.0555</location>
						<body>femur_r</body>
					</PathPoint>
				</objects>
				<groups />
			</PathPointSet>
			<VisibleObject>
				<!--Set of geometry files and associated attributes, allow .vtp, .stl, .obj-->
				<GeometrySet>
					<objects />
					<groups />
				</GeometrySet>
				<!--Three scale factors for display purposes: scaleX scaleY scaleZ-->
				<scale_factors> 1 1 1</scale_factors>
				<!--transform relative to owner specified as 3 rotations (rad) followed by 3 translations rX rY rZ tx ty tz-->
				<transform> -0 0 -0 0 0 0</transform>
```

```
                    <!--Whether to show a coordinate frame-->
                    <show_axes>false</show_axes>
                    <!--Display Pref. 0:Hide 1:Wire 3:Flat 4:Shaded Can be overriden for individual geometries-->
                    <display_preference>4</display_preference>
                </VisibleObject>
                <PathWrapSet>
                    <objects />
                    <groups />
                </PathWrapSet>
            </GeometryPath>
            <!--The maximum force this actuator can produce.-->
            <optimal_force>1</optimal_force>
            <!--Maximum isometric force that the fibers can generate-->
            <max_isometric_force>819</max_isometric_force>
            <!--Optimal length of the muscle fibers-->
            <optimal_fiber_length>0.0535</optimal_fiber_length>
            <!--Resting length of the tendon-->
            <tendon_slack_length>0.078</tendon_slack_length>
            <!--Angle between tendon and fibers at optimal fiber length expressed in radians-->
            <pennation_angle_at_optimal>0.13962634</pennation_angle_at_optimal>
            <!--Maximum contraction velocity of the fibers, in optimal fiberlengths/second-->
            <max_contraction_velocity>10</max_contraction_velocity>
            <!--time constant for ramping up muscle activation-->
            <activation_time_constant>0.01</activation_time_constant>
            <!--time constant for ramping down of muscle activation-->
            <deactivation_time_constant>0.04</deactivation_time_constant>
            <!--tendon strain at maximum isometric muscle force-->
            <FmaxTendonStrain>0.033</FmaxTendonStrain>
            <!--passive muscle strain at maximum isometric muscle force-->
            <FmaxMuscleStrain>0.6</FmaxMuscleStrain>
            <!--shape factor for Gaussian active muscle force-length relationship-->
            <KshapeActive>0.5</KshapeActive>
            <!--exponential shape factor for passive force-length relationship-->
            <KshapePassive>4</KshapePassive>
```

```
                        <!--force-velocity shape factor-->
                        <Af>0.3</Af>
                        <!--maximum normalized lengthening force-->
                        <Flen>1.8</Flen>
                    </Thelen2003Muscle>
                    …
                </groups>
            </ForceSet>
        </Model>
</OpenSimDocument>
```

A.4 Developed Vicon BodyLanguage model to calculate anatomical landmarks and joint centres.

```
{* Adjust pelvic landmarks *}

PelO = (LASIS + RASIS)/2
PelAPUnit = (PelO - VSacral)/dist(PelO,VSacral)

LeftASIS = LASIS - ($MarkerRadius + $ASISstt)*PelAPUnit
RightASIS = RASIS - ($MarkerRadius + $ASISstt)*PelAPUnit

Sacrum = VSacral + ($MarkerRadius + $PSISstt)*PelAPUnit
output(LeftASIS,RightASIS,Sacrum)

PelvisOrigin = (LeftASIS + RightASIS)/2
output(PelvisOrigin)


{* Calculate Hip joint centres *}

PelvisBB = [PelvisOrigin,(LeftASIS-RightASIS),(PelvisOrigin-Sacrum),yzx]

PX = dist(PelvisOrigin,Sacrum)
PZ = dist(LeftASIS,RightASIS)

RightHipJointCentre = {-0.352*PX,-0.350*PZ,-0.561*PX}*PelvisBB
Output(RightHipJointCentre)

LeftHipJointCentre = {-0.352*PX,0.350*PZ,-0.561*PX}*PelvisBB
Output(LeftHipJointCentre)


{* Calculate midpoint of L and R Acromium *}

MidAcromionPoint = (LAcromium + RAcromium)/2
output(MidAcromionPoint)
```

```
{* Calculate lumbar sacral joint centre *}

LumbarSacralJoint = {-0.808*PX,-0,0.363*PX}*PelvisBB
output(LumbarSacralJoint)


{* Adjust knee landmarks *}

RMKnee = (RKneeLat + RKneeMed)/2
LMKnee = (LKneeLat + LKneeMed)/2

LKneeAxis = (LKneeLat - LKneeMed)/dist(LKneeLat,LKneeMed)
LeftMedialEpicondyle = LKneeMed + ($MarkerRadius + $Kneestt)*LKneeAxis
LeftLateralEpicondyle = LKneeLat - ($MarkerRadius + $Kneestt)*LKneeAxis
Output(LeftMedialEpicondyle,LeftLateralEpicondyle)

RKneeAxis = (RKneeLat - RKneeMed)/dist(RKneeLat,RKneeMed)
RightMedialEpicondyle = RKneeMed + ($MarkerRadius + $Kneestt)*RKneeAxis
RightLateralEpicondyle = RKneeLat - ($MarkerRadius + $Kneestt)*RKneeAxis
Output(RightMedialEpicondyle,RightLateralEpicondyle)


{* Calculate knee joint *}

RightKneeMid = (RightMedialEpicondyle + RightLateralEpicondyle)/2
LeftKneeMid = (LeftMedialEpicondyle + LeftLateralEpicondyle)/2

RightKneeWidth = RightLateralEpicondyle(2) - RightMedialEpicondyle(2)
LeftKneeWidth = LeftLateralEpicondyle(2) - LeftMedialEpicondyle(2)

RightKneeJointFactorX = 100/RightKneeWidth*13
LeftKneeJointFactorX = 100/LeftKneeWidth*13

RightKneeCentreX = RightKneeMid(1)+RightKneeJointFactorX
LeftKneeCentreX = LeftKneeMid(1)-LeftKneeJointFactorX

RightKneeJointCentre = {RightKneeCentreX,RightKneeMid(2),RightKneeMid(3)}
LeftKneeJointCentre = {LeftKneeCentreX,LeftKneeMid(2),LeftKneeMid(3)}
Output(RightKneeJointCentre,LeftKneeJointCentre)
```

```
{* Adjust ankle landmarks *}

RMAnkle = (RAnkleLat + RAnkleMed)/2
LMAnkle = (LAnkleLat + LAnkleMed)/2

LAnkleAxis = (LAnkleLat - LAnkleMed)/dist(LAnkleLat,LAnkleMed)
LeftMedialMalleolus = LAnkleMed + ($MarkerRadius + $Anklestt)*LAnkleAxis
LeftLateralMalleolus = LAnkleLat - ($MarkerRadius + $Anklestt)*LAnkleAxis
Output(LeftMedialMalleolus,LeftLateralMalleolus)

RAnkleAxis = (RAnkleLat - RAnkleMed)/dist(RAnkleLat,RAnkleMed)
RightMedialMalleolus = RAnkleMed + ($MarkerRadius + $Anklestt)*RAnkleAxis
RightLateralMalleolus = RAnkleLat - ($MarkerRadius + $Anklestt)*RAnkleAxis
Output(RightMedialMalleolus,RightLateralMalleolus)


{* Calculate ankle joint *}

RightMidMallPoint = (RightMedialMalleolus + RightLateralMalleolus)/2
LeftMidMallPoint = (LeftMedialMalleolus + LeftLateralMalleolus)/2

RightAnkleJointCentre=RightKneeJointCentre + 1.053*(RightMidMallPoint-RightKneeJointCentre)
LeftAnkleJointCentre=LeftKneeJointCentre + 1.053*(LeftMidMallPoint-LeftKneeJointCentre)
Output(RightAnkleJointCentre,LeftAnkleJointCentre)


{* Calculate ankle joint on ground *}

RightAnkleOnFloor = {RightAnkleJointCentre(1),RightAnkleJointCentre(2),$FloorHeight}
LeftAnkleOnFloor = {LeftAnkleJointCentre(1),LeftAnkleJointCentre(2),$FloorHeight}
Output(RightAnkleOnFloor,LeftAnkleOnFloor)


{* Adjust foot markers on level ground *}

LeftHalluxOnFloor = {LToeTip(1),LToeTip(2),$FloorHeight}
Output(LeftHalluxOnFloor)

RightHalluxOnFloor = {RToeTip(1),RToeTip(2),$FloorHeight}
Output(RightHalluxOnFloor)
```

```
Left5MTPJointOnFloor = {LToeLat(1),LToeLat(2),$FloorHeight}
Output(Left5MTPJointOnFloor)
Right5MTPJointOnFloor = {RToeLat(1),RToeLat(2),$FloorHeight}
Output(Right5MTPJointOnFloor)

Left1MTPJointOnFloor = {LToeMed(1),LToeMed(2),$FloorHeight}
Output(Left1MTPJointOnFloor)
Right1MTPJointOnFloor = {RToeMed(1),RToeMed(2),$FloorHeight}
Output(Right1MTPJointOnFloor)

LeftPosteriorCalcaneusOnFloor = {LHeel(1),LHeel(2),$FloorHeight}
Output(LeftPosteriorCalcaneusOnFloor)

RightPosteriorCalcaneusOnFloor = {RHeel(1),RHeel(2),$FloorHeight}
Output(RightPosteriorCalcaneusOnFloor)
```

A.5 Technical Development of the Scaling in OpenSim

Estimated landmark calibration of biomechanical models for inverse kinematics

Trinler U.[1] & Baker R.[1]

[1]School of Health Science, University of Salford, United Kingdom

Abstract- Inverse kinematics is emerging as the optimal method in movement analysis to match a multi-segment biomechanical model to experimental marker positions. Little consideration exists in the literature for the best approach of this modelling approach. The aim for this study is to propose a generic rational technique consisting of automated three steps model scaling, static pose estimation and marker calibration being driven by inverse dynamics. A standard musculoskeletal model of OpenSim has been adapted based on a process of estimating the position of anatomical landmarks from markers placed on a person during a static calibration trial. 10 healthy participants were captured in static position and normal walking. Results showed good results with a mean static and dynamic fitting error of 0.83cm and 0.91cm respectively. All fitting errors lied under the recommended range except the lateral epicondyle in static pose with a 2.05cm error. Highest fitting errors were found on the epicondyle (static), feet (static, dynamic) and on the thigh (dynamic). These may result out of the knee and ankle being designed as a one degree of freedom joint and, therefore, not being able to account for tibia torsion, and a foot segment without a separate toe segment. This approach makes it possible to use inverse kinematics in an automated pipeline resulting in good results for a healthy population. More investigations have to be undertaken for participants outside the normal range.

Keywords- Inverse kinematics, biomechanical modelling, human movement analysis.

Introduction

Inverse kinematics [1], also known as global optimisation [2] and kinematic fitting, is emerging as the optimal method for matching a multi-segment biomechanical model to a set of experimental marker positions measured during movement analysis. The quality of the kinematic fit is dependent on how a generic model of the skeletal system and the locations of markers upon it is adapted to reflect the anthropometry of the person being measured and the actual positions of those markers. It involves three interacting processes; scaling (adjusting the dimensions of the model segments to correspond to those of the person being analysed), fitting (adjusting the pose of the model to that in which the person is standing) and model marker alignment (specifying the position of markers within the model to correspond to the measured position of actual markers).

The calibrated anatomical systems technique (CAST) [3] proposed a method for calibrating a six degree of freedom model of the lower limbs. It only defined segment origins and co-ordinate systems and thus the primary additional requirement for contemporary biomechanical modelling is to include segment scaling. Most contemporary

musculoskeletal models are linked segment models requiring further adaptations to the CAST. Currently available software packages have thus implemented calibration of linked segment models in a number of different ways (e.g. Visual3d, C-motion Inc, Germantown, MD, USA [4]; OpenSim [5]). OpenSim [5] is becoming more and more widely used for musculoskeletal modelling and although it includes a Scaling Tool this requires interaction from the operator to complete full model calibration. Thus a subjective and hence variable process is introduced into a processing pathway which is otherwise objective and standardised. The paper will thus present an implementation of the generic technique within OpenSim which using the Scaling Tool in such a way that operator interaction is not required.

Material and Methods

This is a three stage process operating on data captured during a static calibration trial. In the first the positions of a number of anatomical landmarks and joint centres are estimated based on the positions of skin mounted calibration markers. It uses marker locations to estimate the position of bony anatomical landmarks and joint centres in such a way that scaling and fitting can be performed simultaneously in a manner that is consistent with the biomechanical model. Anatomical landmarks are estimated on the basis of the measured calibration marker position, the known dimensions of the marker and an estimate of the soft tissue thickness (STT). In the second the model is scaled and fitted to the participant to ensure that the anatomical landmarks and joint centres defined within the model are registered to those estimated from experimental data. Each segment was scaled separately along its principal axis [6] (longitudinal axis for foot, tibia, femur, thorax and medio-lateral axis for pelvis) and in the plane perpendicular to that (equally in both directions). Once the model has been scaled it is to minimise a weighted root mean square of the distances between modelled and measured landmarks and joint centres. The weighted sum is used to bias the fit in favour of the joint centres. Once the fit has been performed the position of the tracking markers within the corresponding segment coordinate system as specified in the model is set to match the measured position of the markers. The process is structured in such a way that the interacting elements of scaling, fitting and model marker alignment are automatically satisfied without the requirement for any interaction from the operator.

A convenience sample of ten healthy adult volunteers with no history of neuro-musculoskeletal impairments was recruited from the university community (28±5 years old, 1.72±0.08m, 69±12kg). 38 markers were placed (Table A.3). A 16 infra-red camera motion capture system (Nexus 1.8.5, Vicon, T40S cameras) was used to capture data from a static calibration trial (standing upright with feet flat on the floor) and then from several walks at self-selected walking speed over a walkway with four force plates (Kistler, 2x 9286A, 2x 9253A). The estimated anatomical landmarks and joint centres for static trial data were calculated using a BodyLanguage model (Vicon, Oxford, UK) running within Nexus. The hip and lumbar sacral joint centres are estimated to be in a position consistent with the pelvic segment when scaled along the medio-lateral and anterior-posterior axes to fit the estimated positions of the *ASIS* and *Sacrum* landmarks. Knee and ankle joint centres are estimated to be halfway between the medial and lateral femoral epicondyle and malleolus landmarks respectively.

Scaling, fitting and model marker alignment was implemented using the OpenSim Scaling Tool and model 3DGaitModel2392 (as distributed with OpenSim 3.2). The location of the key anatomical landmarks within their respective coordinate systems were estimated from the bone meshes and of the joint centres from the model file and added to the model as additional markers. Only the estimated landmarks and joint centres (not the original

marker positions) were used for scaling and fitting. Segments were scaled separately along the principal axis to fit to joint centres and in the plane perpendicular to this to fit landmark pairs. The only exception to this was at the foot which was scaled vertically to fit the distance between the ankle joint centre and the floor and in the horizontal plane to fit the distance between the heel and toe markers. A weighting of 3:1 in favour of the joint centres biased the fitting of the principal axes to the joint centres leaving the landmark information to determine the rotation of segments about those axes.

Table A.3 Physical markers used (as listed within GaitModel2392).

Position on body	**Description**
Sternum	Placed on the thorax frontal on the sternum.
Acromion	Representing the shoulder; placed on the most prominent bony process of the scapular.
ASIS	Anterior superior iliac spine.
VSacral	Midpoint between both posterior superior iliac spines.
ThighUpper ThighFront ThighRear	Three tracking markers on the thigh, two lateral (upper, rear) and one frontal (front).
KneeLat	Placed on the lateral epicondyle of the femur.
KneeMed	Placed on the medial epicondyle of the femur.
ShankUpper ShankFront ShankRear	Three tracking markers placed on the shank, two lateral (upper, rear) and one frontal (front).
AnkleLat	Placed on the lateral malleolus.
AnkleMed	Placed on the medial malleolus.
Heel	Placed on the posterior calcaneus.
MidfootLat MidfootSup ToeLat ToeMed	Four tracking markers placed on the medial and lateral side of the midfoot, and two markers placed on the medial and lateral side of the forefoot (metatarsophalangeal joint).
ToeTip	Placed on top of the hallux.

Once the model had been scaled the Inverse Kinematics tool was used to fit it to one of the walking trials for each volunteer. The mean and maximum RMS fitting error calculated across the trial was recorded for both the static

and walking trials as a measure of the quality of fit of the model to the measurements. For the dynamic trials, skin mounted markers were used for the kinematic fitting.

Results

Scaling factors for different segments differ slightly between each other as well as between the three directional scaling axes of some of the segments. Especially on the thigh, the primary axis (y) has been scaled with much smaller scaling factors compared to the axes normal to the primary axis (x,z). Mean static and dynamic fitting errors of single relevant joint centres, bony landmarks and skin mounted markers as well as maximum errors averaged across participants are presented in Table A.4. Overall RMS fitting errors are 0.83cm and 0.91cm for static and dynamic trials respectively. These values lie in the recommended error range of less than 1cm for static and 2cm for dynamic trials [7]. Mean RMS fitting errors for the static trial are the lowest at the pelvis, at the joint centres and at the ankles, which do not exceed 1cm. Fitting errors for the epicondyle landmarks at the knee range between 1.17 and 2.05cm, with one landmark just over the recommended limit of 2cm (lateral left epicondyle, 2.05cm). Both landmarks on the fifth metatarsal are approximately double as high as the average but still in the 2cm range.

Dynamic RMS fitting errors are in average slightly greater than averaged static errors but the range between 0.65 and 1.14cm is smaller than 0.15 and 2.05cm for the static fitting. Highest mean fitting errors are found at the thighs and at the tip toes with slightly greater errors than 1cm. RMS maximal fitting errors for the dynamic trials ranging between 1.37 and 3.02cm, which are all in the recommended maximal value of 2-4cm [7]. Greatest maximal errors can be found as well at the feet and the thighs.

Table A.4. Mean fitting errors for relevant bony landmarks, joint centres and skin mounted markers of static and dynamic trials and maximum marker error for the dynamic trial in cm across ten participants.

Static Trial (overall RMS error = 1.06)							
	MidAcromium	LASIS	RASIS	Sacrum	LHJC	RHJC	LKJC
Mean	0.15	0.27	0.27	0.32	0.21	0.22	0.78
	RKLC	LEpiconL	REpiconL	LEpiconM	REpiconM	LAJC	RAJC
Mean	0.65	2.05	1.95	1.35	1.17	0.43	0.46
	LMalleoL	RMalleoL	LMalleoM	RMalleoM	L5MTP	R5MTP	
Mean	0.98	0.78	0.66	0.61	1.65	1.49	

Dynamic Trial (overall RMS error = 0.91)							
	LAcromium	RAcromium	Sternum	LASIS	RASIS	VSacral	RThighF
Mean	0.82	0.75	0.85	0.86	0.81	0.65	1.07
Max	1.57	1.41	1.37	1.49	1.57	1.33	1.93
	RThighU	RThighR	RShankF	RShankU	RShankR	LThighF	LThighU
Mean	1.15	1.00	0.76	0.87	0.79	1.14	1.19
Max	2.05	2.30	1.87	2.14	2.00	1.82	2.08
	LThighR	LShankR	LShankU	LShankR	LHeel	RHeel	LToeTip
Mean	1.02	0.82	0.88	0.75	0.85	0.82	1.12
Max	1.78	1.66	2.10	1.82	2.16	2.34	3.02
	RToeTip	LToeLat	RToeLat	LToeMed	RToeMed		
Mean	1.14	1.01	0.98	0.76	0.83		
Max	2.95	2.66	2.44	1.66	2.71		

Discussion

This approach provides a generic and objective technique for the model scaling, static pose estimation and marker calibration of advanced musculoskeletal models which are driven by inverse kinematics. An automated pipeline has been conducted consisting of one main algorithm to define the estimated bony landmark and joint centre positions which then are used in the scaling tool of OpenSim [8].

The more conventional approach to this problem incorporates marker positions instead of landmarks as part of the model and fits these directly to the measured marker positions. Whilst estimating landmark positions and joint centres and fitting the model to these appears to introduce an extra step to the process it allows much more control over exactly how the model is scaled and the static pose determined. The precise method chosen ensures that model scaling and static pose estimation are mutually consistent.

The scaling factors for the primary axis have been found to be smaller especially for the thigh segment than scaling factors in both other planes. This may reflect the elderly cadavers on which the model is based on [9], having narrower bones than the healthy young adults from whom measurements were taken. Such scaling markedly increases the moment arms of several key muscles at a number of joints. These differences may explain the recurrent observation that current models do not have the moment generating capacity expected. Moreover, the visual STT estimation between bones and skin mounted markers could have influenced the scaling in x and z direction, especially with participants of greater muscle and fatty tissue. With a thicker STT the marker used for calculating bony landmarks in these both directions would have lied more far away from the bone than expected.

Including landmark estimation as a separate stage of the process makes the process much more explicit and gives a clear indication of how methods might need to be adapted in measurements of people where such estimation is challenging, e.g. such participants with significant soft tissue. Relatively simple measurements of soft tissue thickness from ultrasound or other approaches, could easily be factored into the algorithms for landmark estimation. Equally techniques based on indicating landmarks with a wand rather than directly by markers could also easily be incorporated.

Some marker experienced greater fitting errors than others. The greater RMS fitting errors on the feet may reflect individual variations of the foot-toe length relation. The musculoskeletal model chosen for this study defined the foot as one segment and markers placed on the fore foot may be placed on a slight different anatomical landmark than on the participant when the participant has a different relative length of the toes to the rest of the foot than the virtual model. The additional higher fitting errors on the epicondyles (static) and on the thighs (dynamic) may result out of the knee and the ankle being modelled as a single degree of freedom angle. This means, that the model cannot account for a possible tibia torsion in transversal plane [9].

Although the general principles underlying this approach are applicable to any other study the specific implementation has limitations. It should only be used for people who are able to stand with their feet flat on the floor and for whom the required landmarks can be reliably palpated. Modifications to the technique will be required to make similar measurements for people for whom this is not the case. Further studies may analyse the application of the proposed technique on other populations than healthy young adults. In conclusion, the presented generic approach could successfully include a systematic pipeline with which the operator can scale and calibrate the musculoskeletal model for inverse kinematics automatically.

References

[1] Reinbolt JA, Schutte JF, Fregly BJ, Koh BI, Haftka RT, George AD, et al. Determination of patient-specific multi-joint kinematic models through two-level optimization. J Biomech. 2005;38:621-6.

[2] Lu TW, O'Connor JJ. Bone postion estimation from skin marker co-ordinates using global optimisation with joint constraints. Jounrnal of Biomechanics. 1999;32:129-34.

[3] Cappozzo A, Catani F, Croce UD, Leardini A. Position and Orientation in space of bones during movement, anatomical frame definition and determination. Clinical Biomechanics. 1995;10:171-8.

[4] Hamill J, Selbie WS, Kepple TM. Three-dimensional kinematics. In: Robertson DGE, Caldwell GE, Hamill J, Kamen G, Whittlesey SN, editors. Research Methods in Biomechanics. Champaign, Il: Human kinetics; 2014.

[5] Delp SL, Anderson FC, Arnold AS, Loen P, Habib A, John CT, et al. OpenSim: Open-Source Software to Create and Analyze Dynamic Simulations of Movement. IEEE Trans Biomed Eng. 2007;54:1940-50.

[6] Baker R. Globographic visualisation of three dimensional joint angles. J Biomech. 2011;44:1885-91.

[7] OpenSim. OpenSim Support. 2013.

[8] Hicks J, Dunne J. How Scaling Works. OpenSim Documentation2012.

[9] Delp SL, Loan P, Hoy MG, Zajac FE, Topp EL, Rosen JM. An interactive graphics-based model of the lower extremtiy to study orhtopaedics surgical procedures. IEEE transactions on bio-medical engineering. 1990;37:757-67.

A.6 Ethical Approval

University of Salford MANCHESTER

Research, Innovation and Academic Engagement Ethical Approval Panel

College of Health & Social Care
AD 101 Allerton Building
University of Salford
M6 6PU

T +44(0)161 295 7016
r.shuttleworth@salford.ac.uk

www.salford.ac.uk/

18 September 2013

Dear Ursula,

RE: ETHICS APPLICATION HSCR13/45 – Muscle activity in human movement analysis: mathematical modelling vs. surface EMG

Based on the information you provided, I am pleased to inform you that application HSCR13/45 has now been approved. However, please ensure that you review the participant information letter thoroughly with your supervisor to amend the typographical errors before it is used for any recruitment.

If there are any changes to the project and/ or its methodology, please inform the Panel as soon as possible.

Yours sincerely,

Rachel Shuttleworth

Rachel Shuttleworth
College Support Officer (R&I)

A.7 Participant Information Sheet

Study title

Muscle activity in human movement analysis: Mathematical modelling vs. surface EMG

This is an invitation to take part in a movement analysis study. Please take time to read this information sheet thoroughly. If you have any questions, or if you think you might like to take part in, please do not hesitate to contact me (details below).

If, after reading all the information below, speaking to the researchers, you will be asked to sign a participant consent form before the measurement. After you have signed the consent form, you may withdraw from the study at any time, without giving the investigator any reason. In addition, after the measurement procedure, you can choose to have your data deleted. Your data will, of course, be handled in confidence.

What is the purpose of this study?

The main purpose of the study is to collect data, which will be used to compare two different measurement methods during five different movement tasks: a simple movement of one leg while standing on the other, bending over in standing position, a squat, a vertical jump, and normal walking. Two different variation factors will be embedded into the measurement tasks: we will vary the movement tasks in their speed and/ or ask you to wear a weight jacket (which will be 10% of your body weight) or an ankle weight (one kg heavy) to analyse if speed or weight have an influence on the measurements.

The measurements taken are, firstly, surface electromyography of the legs (EMG – which measures whether a muscle is active or not by recording the electrical impulses, sent through nerves to turn the muscle on) and, secondly, a measures of your movement position and forces acting on your joints during the movements (via force plates). This will be compared to mathematical model predictions, where dynamic measured data of the movements will be used as input.

Am I eligible to take part?

We are inviting all adults who are a staff member or a student at the University of Salford, aged 18 and older, and have no neurological, orthopaedic disease/ injury or other health issues affecting their legs.

What do I have to do?

If you choose to take part in this study, we will arrange an appointment at the University of Salford gait laboratory. The measurement will be a single session of approximately 2 1/2 hours.

During the session, you will be asked to wear shorts and a t-shirt, and to be barefooted. In the beginning, the researcher will make some anthropometric measurements of you (body height, weight, length of your legs and the width of your knees and ankles).

The next step will be, to place surface EMG electrodes with a medical tape on your legs, and, in addition, get them fixed with a bandage. This procedure is painless and the medial tape is easy to remove later. After this, the electrodes will be tested through maximal voluntary contractions of your muscles against a resistance, where you will be seated on a chair.

After placing the electrodes, retro-reflective markers will be put on specific positions at your hip, thigh, shank and feet with medical tape as well. Infra-red cameras positioned around the room record the position of the reflective markers as you perform the movement tasks (walking, squatting, vertical jumping, bending forward and knee extension). Force plates (similar to weight scales), embedded in the floor, will also be used to measure the forces acting on your body as you perform the movement tasks. We will ask you to repeat each of the movement three to ten times. If you need a break during the measurement, do not hesitate to ask. During the different movement tasks there will be brakes anyway.

All the collected data of you will be handled in confidence; none of the camera data records your personal image. The cameras only record positions of the markers on your body and data will be labelled with a study ID number and not your name. In this way no one can identify you or connect your data with your identity. Digital images may be taken from you during standing or during the exercises, without any identifying features visible, for checking the marker and electrode placement.

Participating in the measurement is voluntary; you can withdraw without giving us any reason at any time.

What are the disadvantages or risks of taking part in?

The test only involves walking on an even ground as well as easy exercises, where the risk of injury is, realistically, very low. The weights, which we will use to modify the movement tasks, will be fixed safely onto your body. You may become tired during the exercises. Rest brakes can be taken at any point during the measurement procedure. Should either you or the researcher have any indication that you may not be able to perform any more movement trials, the study will be stopped without any consequence to you whatsoever.

What are the advantages in taking part?

We hope that the study will improve our understanding of how muscle activation can be measured in a patient friendly way and, therefore, how mathematical models can be accurately used to predict muscle activation without the use of EMG. This information may help clinicians as well as sport scientists to analyse specific disease pattern or sport movements and develop new knowledge.

Will my taking part in this study be kept confidential?

As mentioned above, the acquired data will be kept strictly confidential, no one, except the investigator and her supervisors, will have access to your data. The data will be stored in a password protected computer, or will be locked away with no identifying markers whatsoever. The data will only be used by the primary researcher for her PhD studies.

What will happen to the results of this study?

The results of this study will be used for the PhD work of the investigator and may be used for presentations at conferences. Neither the presentations nor publications (dissertation, articles…) will identify individuals who participated in the study.

Contact for problems and questions

If you have any questions or problems about any aspect of this study, contact the researchers at any time, and they will do their best to answer your questions. You can contact them under the email address u.k.trinler@edu.salford.ac.uk.

If you still have concerns or complaints you can use the formally way through contacting the supervisors of the primary researcher, who will follow the University Procedure for Allegations of Scientific or Ethical Misconduct.

Thank you for reading this!

Ursula Kathinka Trinler, principal investigator

Contact details

Primary researcher: Ursula Trinler (u.k.trinler@edu.salford.ac.uk)

Supervisors: Prof. Richard Baker, Dr. Richard Jones, Dr. Kris Hollands

Information Sheet based on: COREC/NHS National Patient Safety Agency. *Information Sheets and Consent Forms – Guidance for Researcher and Reviewers'* Version 3.0 Dec 2006.

Link to IRAS website - IRAS

A.8 Research Participant Consent Form

Title of Project: Muscle activity in human movement analysis: Mathematic modelling vs. surface EMG

Ethics Ref No: HSCR13/45

Name of Researcher: Ursula Trinler

(Delete as appropriate)

➢ I confirm that I have read and understood the information sheet for the above study (version x- date) and what my contribution will be.	**Yes**	**No**
➢ I have been given the opportunity to ask questions (face to face, via telephone and e-mail)	**Yes**	**No**
➢ I agree to digital images being taken during the research exercises	**Yes**	**No**
➢ I understand that my participation is voluntary and that I can withdraw from the research at any time **without giving any reason**	**Yes**	**No**
➢ I understand how the researcher will use my responses, who will see them and how the data will be stored.	**Yes**	**No**
➢ I agree to take part in the above study	**Yes**	**No**

Name of participant ……

Signature ……

Date …….

Name of researcher taking consent Ursula Trinler

A.9 Results of correcting the Force Plate to the Camera System

A systematic error was detected: the calibration wand was misplaced for about 1-2mm and, therefore, less than 1° rotated around the origin of the global measurement volume. To analyse the effect on the results all ten walking trials during self-selected walking speed of the participant with the greatest centre of mass torso shift (P02) were manually corrected by aligning the trajectories of the sacrum marker with the centre of pressures of the force plates. Following figures show the joint moments (Figure A.1), muscle forces estimated with static optimisation (Figure A.2) and computed muscle control (Figure A.3) of the right leg (left side resulted in similar results). Figures affected are the hip abduction moment, as well as parts of the gluteus medius.

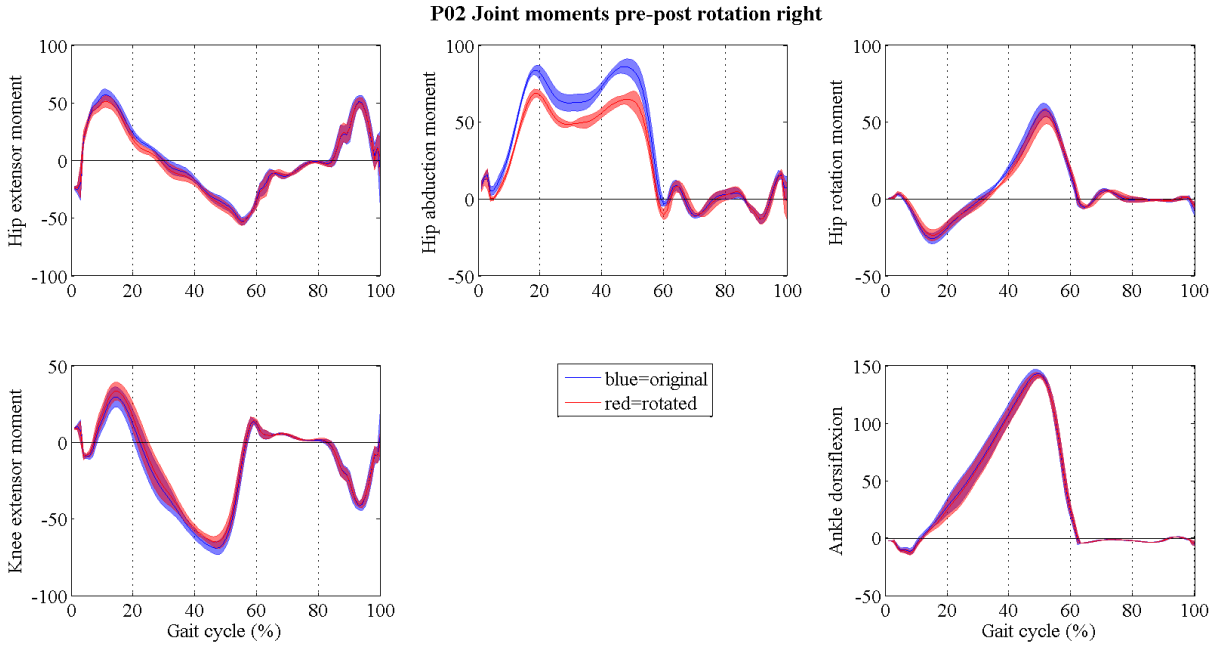

Figure A.1. Joint moments of participant P02 before (blue) and after rotating the force plates (red).

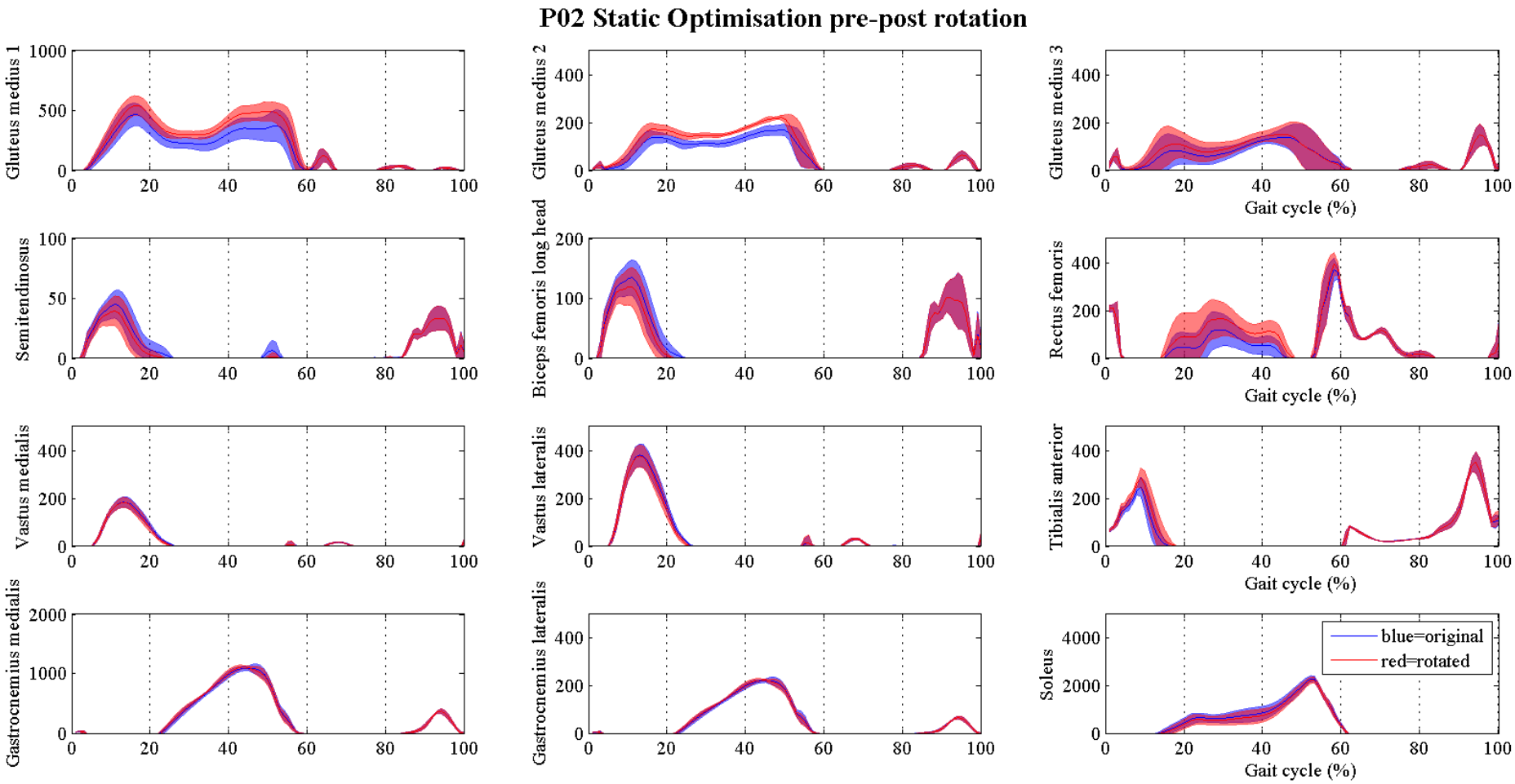

Figure A.2. Static optimisation's estimated muscle forces of participant P02 before (blue) and after rotating the force plates (red).

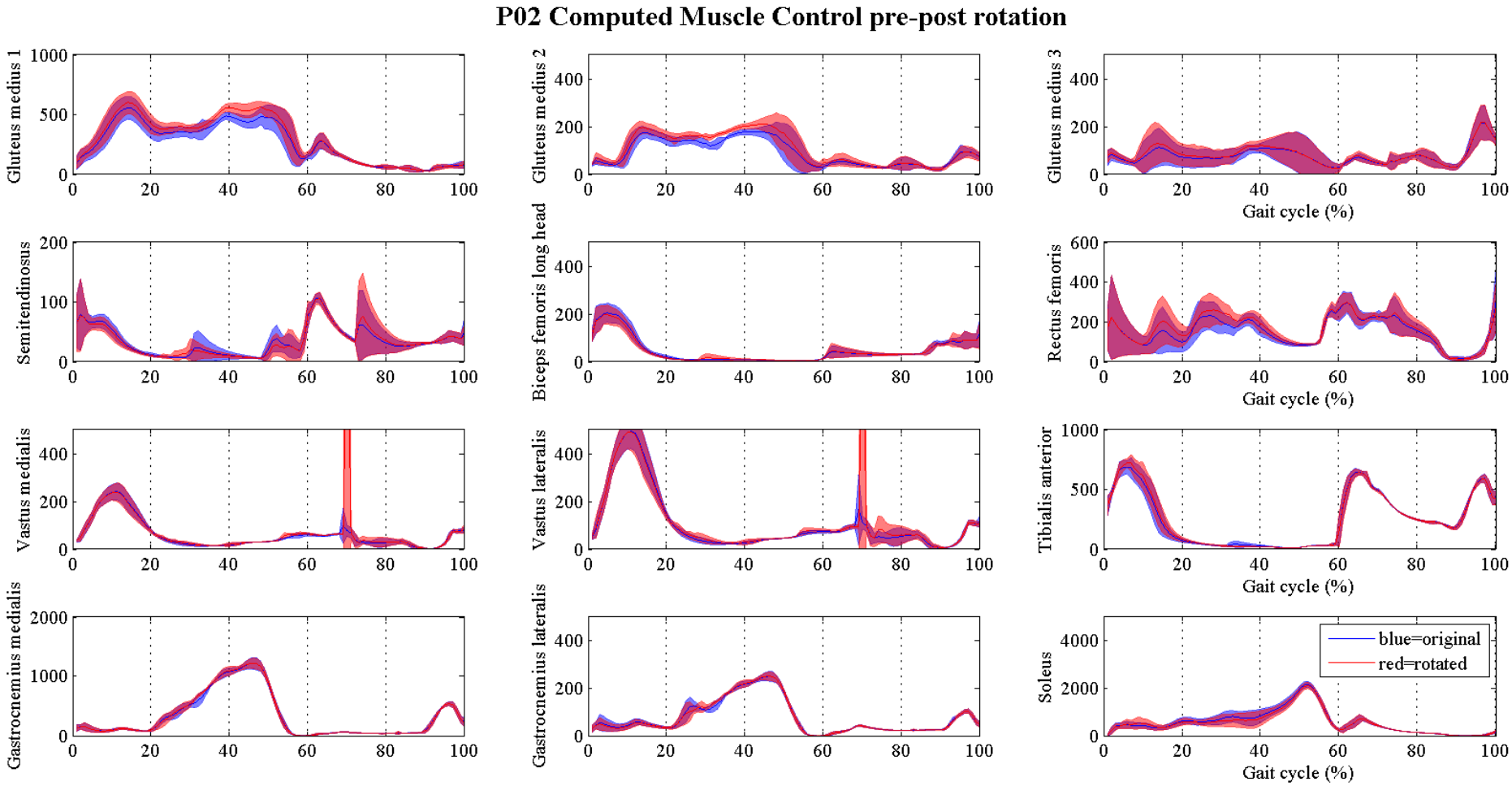

Figure A.3. Computed muscle control's estimated muscle forces of participant P02 before (blue) and after rotating the force plates (red).

List of References

Ackland, D. C., Lin, Y. C., & Pandy, M. G. (2012). Sensitivity of model predictions of muscle function to changes in moment arms and muscle-tendon properties: a Monte-Carlo analysis. *Journal of Biomechanics, 45*(8), 1463-1471.

Alkjaer, T., Simonsen, E., & Dyhre-Poulsen, P. (2001). Comparison of inverse dynamics calculated by two- and three-dimensional models during walking. *Gait and Posture, 13*(2), 73-77.

Alkner, B. A., Tesch, P. A., & Berg, H. E. (2000). Quadriceps EMG/force relationship in knee extension and leg press. *Medicine & Science in Sports & Exercise, 32*(2), 459-463.

Anderson, F. C., & Pandy, M. G. (1999). A dynamic optimization solution for vertical jumping in three dimensions. *Comput. Meth. Biomech. Biomed. Eng., 2*, 201-231.

Anderson, F. C., & Pandy, M. G. (2001a). Dynamic optimization of human walking. *J Biomech Eng, 123*(5), 381-390.

Anderson, F. C., & Pandy, M. G. (2001b). Static and dynamic optimization solutions for gait are practically equivalent. *Journal of Biomechanics, 34*(2), 153-161. doi: 10.1016/S0021-9290(00)00155-X.

Andriacchi, T. P. (1988). Biomechanics and gait analysis in total knee replacement. *Orthop Rev, 17*(5), 470-473.

Andriacchi, T. P., & Alexander, E. J. (2000). Studies of human locomotion: past, present, future. *Journal of Biomechanics, 33*(10), 1217-1224.

Arch, E. S., Stanhope, S. J., & Higginson, J. S. (2015). Passive-dynamic ankle-foot orthosis replicates soleus but not gastrocnemius muscle function during stance in gait: Insights for orthosis prescription. *Prosthet Orthot Int*. doi: 10.1177/0309364615592693.

Arnold, A. S., Anderson, F. C., Pandy, M. G., & Delp, S. L. (2005). Muscular contributions to hip and knee extension during the single limb stance phase of normal gait: a framework for investigating the causes of crouch gait. *Journal of Biomechanics, 38*(11), 2181-2189.

Arnold, A. S., Salinas, S., Asakawa, D. J., & Delp, D. (2000). Accuracy of Muscle Moment Arms Estimated from MRI-Based Musculoskeletal Models of the Lower Extremity. *Computer Aided Surgery, 5*, 108-119.

Arnold, E. M., Hamner, S. R., Seth, A., Millard, M., & Delp, S. L. (2013). How muscle fiber lengths and velocities affect muscle force generation as humans walk and run at different speeds. *J Exp Biol, 216*(Pt 11), 2150-2160. doi: 10.1242/jeb.075697.

Arnold, E. M., Ward, S. R., Lieber, R. L., & Delp, S. L. (2010). A Model of the Lower Limb for Analysis of Human Movement. *Annals of Biomedical Engineering, 38*(2), 269-279.

Au, C., & Dunne, J. (2012, 09.08.2013). Gait 2392 and 2354 Models. *OpenSim Documentation.* Retrieved 08.02.2015, from http://simtk-confluence.stanford.edu:8080/display/OpenSim/Gait+2392+and+2354+Models.

Baker, R. (2007). The history of gait analysis before the advent of modern computers. *Gait & Posture, 26*(3), 331-342. doi: 10.1016/j.gaitpost.2006.10.014.

Baker, R. (2011). Globographic visualisation of three dimensional joint angles. *J Biomech, 44*(10), 1885-1891. doi: 10.1016/j.jbiomech.2011.04.031.

Baker, R. (2013). *Measuring Malking: A Handbook of Clinical Gait Analysis*. London: MacKeith Press.

Basmajian, J. V., & De Luca, C. J. (1985). *Muscles Alive. Their Functions Revealed by Electromyography* (5th ed.). Baltimore, USA: Williams & Wilkins.

Bazett-Jones, D. M., Cobb, S. C., Joshi, M. N., Cashin, S. E., & Earl, J. E. (2011). Normalizing hip muscle strength: establishing body-size-independent measurements. *Arch Phys Med Rehabil, 92*(1), 76-82. doi: 10.1016/j.apmr.2010.08.020.

Besier, T., Fredericson, M., Gold, C., Beaupre, G., & Delp, S. L. (2009). Knee muscle forces during walking and running in patellofemoral pain patients and pain-free controls. *Journal of Biomechanics, 42*(7), 898-905.

Bigland, B., & Lippold, O. C. J. (1954). The relation between force, velocity and integrated electrical activity in human muscles. *Journal of Physiology, 123*, 214-224.

Blackburn, J. T., Bell, D. R., Norcross, M. F., Hudson, J. D., & Engstrom, L. A. (2009). Comparison of hamstring neuromechanical properties between healthy males and

females and the influence of musculotendinous stiffness. *J Electromyogr Kinesiol, 19*(5), e362-369. doi: 10.1016/j.jelekin.2008.08.005.

Bogey, R. A., Cerny, K., & Mohammed, O. (2003). Repeatability of wire and surface electrodes in gait. *Am J Phys Med Rehabil, 82*(5), 338-344. doi: 10.1097/01.PHM.0000064717.90796.7A.

Bogey, R. A., Gitter, A. J., & Barnes, L. A. (2010). Determination of ankle muscle power in normal gait using an EMG-to-force processing approach. *Journal of Electromyography and Kinesiology, 20*(1), 46-54. doi: http://dx.doi.org/10.1016/j.jelekin.2008.09.013.

Bogey, R. A., Perry, J., & Gitter, A. J. (2005). An EMG-to-Force Processing Approach for Determining Ankle Muscle Forces During Normal Human Gait. *IEEE Transactions on Neural Systems and Rehabilitation Engineering, 13*(3), 302-310.

Bohannon, R. W., & Williams Andrews, A. (2011). Normal walking speed: a descriptive meta-analysis. *Physiotherapy, 97*(3), 182-189. doi: 10.1016/j.physio.2010.12.004.

Bolsterlee, B., Vardy, A. N., van der Helm, F. C., & Veeger, H. E. (2015). The effect of scaling physiological cross-sectional area on musculoskeletal model predictions. *J Biomech, 48*(10), 1760-1768. doi: 10.1016/j.jbiomech.2015.05.005.

Bosmans, L., Valente, G., Wesseling, M., Van Campen, A., De Groote, F., De Schutter, J., & Jonkers, I. (2015). Sensitivity of predicted muscle forces during gait to anatomical variability in musculotendon geometry. *J Biomech, 48*(10), 2116-2123. doi: 10.1016/j.jbiomech.2015.02.052.

Bowsher, K. A., & Vaughan, C. L. (1995). Effect of foot-progression angle on hip joint moments during gait. *Journal of Biomechanics, 28*(6), 759-762.

Brand, R. A., Crowninshield, R., Wittstock, C., Pedersen, D., Clark, C., & van Krieken, F. (1982). A Model of Lower Extremity Muscular Anatomy. *JOurnal of Biomechanical Engineering, 104*, 304-310.

Brand, R. A., Pedersen, D. R., & Friedrich, J. A. (1986). The Sensitivity of Muscle Force Predictions to Changes in Physiologic Cross-Sectional Area. *Journal of Biomechanics, 19*(8), 589-596.

Bresler, B., & Frankel, J. P. (1950). The forces and Moments in the Leg During Level Walking. *Trans. ASME, 72*, 27-36.

Buchanan, T. S., Lloyd, D. G., Manal, K., & Besier, T. F. (2005). Estimation of Muscle Forces and Joint Moments Using a Forward-Inverse Dynamics Model. *Medicine & Science in Sports & Exercise, 37*(11), 1911-1916.

Burden, A. (2010). How should we normalize electromyograms obtained from healthy participants? What we have learned from over 25 years of research. *J Electromyogr Kinesiol, 20*(6), 1023-1035. doi: 10.1016/j.jelekin.2010.07.004.

Cappozzo, A., Catani, F., Croce, U. D., & Leardini, A. (1995). Position and Orientation in space of bones during movement, anatomical frame definition and determination. *Clinical Biomechanics, 10*, 171-178.

Chand, J., Hammer, S., & Hicks, J. (2012, 14.11.2014). Collecting Experiemntal Data. *OpenSim Documentation.* Retrieved 11.02.2015, from http://simtk-confluence.stanford.edu:8080/display/OpenSim/Collecting+Experimental+Data.

Chandler, R., Clauser, C., McConville, J., Reynolds, H., & Young, J. (1975). Investigation of the inertial properties of the human body. Springfield, Virgina.

Chow, C. K., & Jacobson, D. H. (1971). Human Locomotion via Optimal Programming. *Mathemactical Bioscience, 10*, 239-306.

Clarys, J. (2000). Electromyography in sports and occupational settings: an update of its limits and possibilities. *Ergonomics, 43*, 1750-1762.

Collins, J. J. (1995). The redundant nature of locomotor optimization laws. *Journal of Biomechanics, 28*(3), 251-267.

Crowninshield, R. D., & Brand, R. A. (1981). A physiologically based criterion of muscle force prediction in locomotion. *Journal of Biomechanics, 14*(11), 793-801. doi: 10.1016/0021-9290(81)90035-X.

Davis III, R. B., Õunpuu, S., Tyburski, D., & Gage, J. R. (1991). A gait analysis data collection and reduction technique. *Human Movement Science, 10*(5), 575-587. doi: 10.1016/0167-9457(91)90046-Z.

De Groote, F., Pipeleers, G., Jonkers, I., Demeulenaere, B., Patten, C., Swevers, J., & De Schutter, J. (2009). A physiology based inverse dynamic analysis of human gait: potential and perspectives. *Computer Methods in Biomechanics & Biomedical Engineering, 12*(5), 563-574.

De Leva, P. (1996). Adjustments to Zatsiorsky-Seluyanov's segment intertia parameters. *Journal of Biomechanics, 29*(9), 1223-1230.

De Luca, C. J. (1997). The Use of Surface Electromyography in Biomechanics. *Journal of Applied Biomechanics, 13*(2), 135-163.

Della Croce, U., Leardini, A., Chiari, L., & Cappozzo, A. (2005). Human movement analysis using stereophotogrammetry. Part 4: assessment of anatomical landmark misplacement and its effects on joint kinematics. *Gait Posture, 21*(2), 226-237. doi: 10.1016/j.gaitpost.2004.05.003.

Delp, S. L. (1990). *Surgery Simulation: A Computer Graphics System to Analyse and Design Musculoskeletal Reconstructions of the Lower Limb.* (Ph.D.), Standford University, Stanford, CA.

Delp, S. L., Anderson, F. C., Arnold, A. S., Loen, P., Habib, A., John, C. T., . . . Thelen, D. G. (2007). OpenSim: Open-Source Software to Create and Analyze Dynamic Simulations of Movement. *IEEE Trans Biomed Eng, 54*(11), 1940-1950.

Delp, S. L., Arnold, A. A., Speers, R. A., & Moore, C. (1996). Hamstrings and psoas lenths during normal and crouch gait: implications for muscle-tendon surgery. *Journal of Orthopaedic Research, 14*, 144-151.

Delp, S. L., Loan, P., Hoy, M. G., Zajac, F. E., Topp, E. L., & Rosen, J. M. (1990). An interactive graphics-based model of the lower extremtiy to study orhtopaedics surgical procedures. *IEEE transactions on bio-medical engineering, 37*, 757-767.

Delp, S. L., & Maloney, W. (1993). Effects of Hip Center Location on the Moment-Generating Capacity of the Muscles. *Journal of Biomechanics, 26*(4/5), 485-499.

Dempster, W. (1955). Space Requirements of the Seated Operator. Geometrical, Kinematic, and Mechanical Aspects of the BodyWith Special Reference to the Limbs. Wright-Patterson Air Force Base, OH: Wright Air Development Center, Air Research and Development Command.

DeVita, P. (2005). Musculoskeletal Modeling and the Prediction of In Vivo Muscle and Joint Forces. *Medicine & Science in Sports & Exercise, 37*(11), 1909-1910.

Dixon, P. C., Böhm, H., & Döderlein, L. (2012). Ankle and midfoot kinetics during normal gait: A multi-segment approach. *Journal of Biomechanics, 45*(6), 1011-1016.

Downs, S. H., & Black, N. (1998). The feasibility of creating a checklist for the assessment of the methodological quality both of randomised and non-randomised studies of health care interventions. *J Epidemiol Community Health, 52*, 377-284.

Eng, J. J., & Winter, D. A. (1995). Kinetic analysis of the lower limbs during walking: what information can be gained from a three-dimensional model? *Journal of Biomechanics, 28*(6), 753-758.

Erdemir, A., McLean, S., Herzog, W., & van den Bogert, A. J. (2007). Model-based estimation of muscle forces exerted during movements. *Clinical Biomechanics, 22*(2), 131-154.

Faber, G. S., Kingma, I., Martin Schepers, H., Veltink, P. H., & van Dieen, J. H. (2010). Determination of joint moments with instrumented force shoes in a variety of tasks. *Journal of Biomechanics, 43*(14), 2848-2854.

Ferrari, A., Benedetti, M., Pavan, E., Frigo, C., Bettinelli, D., Rabuffetti, M., . . . Leardini, A. (2008). Quantitative comparison of five current protocols in gait analysis. *Gait and Posture, 28*(2), 207-216.

Finni, T., Komi, P. V., & Lukkarimiemi, J. (1998). Achulles tendon loading during walking: application of a novel optic ffiber technique. *Eur J Appl Physiol, 77*, 289-291.

Fluit, R., van der Krogt, M. M., van der Kooij, H., Verdonschot, N., & Koopman, H. F. (2012). A simple controller for the prediction of three-dimensional gait. *J Biomech, 45*(15), 2610-2617. doi: 10.1016/j.jbiomech.2012.08.019.

Fraysse, F., Dumas, R., Cheze, L., & Wang, X. (2009). Comparison of global and joint-to-joint methods for estimating the hip joint load and the muscle forces during walking. *Journal of Biomechanics, 42*(14), 2357-2362.

Friederich, J. A., & Brand, R. A. (1990). Muscle fiber architecture in the human lower limb. *Journal of Biomechanics, 23*(1), 91-95.

Gage, J. R. (1994). The role of gait analysis in the treatment of cerebral palsy. *J Pediatr Orthop, 14*(6), 701-702.

Ganley, K., & Powers, C. (2004). Determination of lower extremity anthropometric parameters using dual energy X-ray absorptiometry: the influence on net joint moments during gait. *Clin Biomech (Bristol, Avon), 19*(1), 50-56.

Glitsch, U., & Baumann, W. (1997). The three-dimensional determination of internal loads in the lower extremity. *Journal of Biomechanics, 30*(11–12), 1123-1131. doi: 10.1016/S0021-9290(97)00089-4.

Goldberg, S. R., Kepple, T. M., & Stanhope, S. J. (2009). In Situ Calibration and Motion Capture Transformation Optimization Improve Instrumented Treadmill Measurements. *Journal of Applied Biomechanics, 25*, 401-446.

Gonzales, R., Buchanan, T., & Delp, S. (1997). How muscles architecture and moment arms affect wrist flexion-extension moments. *Jounral of Biomechanics, 30*(7), 705-712.

Gordon, A., Huxley, A., & Julian, F. (1966). the variation in isometric tension with sarcomere length in vertebrate muscle fibres. *Jounral of Physiology, 184*, 170-192.

Gorton, G. E., 3rd, Hebert, D. A., & Gannotti, M. E. (2009). Assessment of the kinematic variability among 12 motion analysis laboratories. *Gait Posture, 29*(3), 398-402. doi: 10.1016/j.gaitpost.2008.10.060.

Grabiner, M., Feuerbach, J., Lundin, T., & Davis, B. (1995). Visual guidance to force plates does not influence ground reaction froce variability. *Journal of Biomechanics, 28*(9), 1115-1117.

Grosset, J. F., Piscione, J., Lambertz, D., & Perot, C. (2009). Paired changes in electromechanical delay and musculo-tendinous stiffness after endurance or plyometric training. *Eur J Appl Physiol, 105*(1), 131-139. doi: 10.1007/s00421-008-0882-8.

Hase, K., & Yamazaki, N. (1997). Development of a Three-Dimensional Whole Body Musculoskeletal Model for Various Motion Analysis. *Jsme International Journal Series C-Dynamics Control Robotics Design and Manufacturing, 40*(1), 25-32.

Havanan, E. (1964). A Mathematical Model of the Human Body (pp. 64-102). Ohio: Aerospace Medical Division.

Heintz, S., & Gutierrez-Farewik, E. M. (2007). Static optimization of muscle forces during gait in comparison to EMG-to-force processing approach. *Gait and Posture, 26*(2), 279-288.

Hermens, H., & Freriks, B. Retrieved 25.09.2015, from http://www.seniam.org/.

Hermens, H., Freriks, B., Disselhorst-Klug, C., & Rau, G. (2000). Development of recommendations for SEMG sensors and sensor placement procedures. *Journal of Electromyographyand Kinesiology, 10*, 361-374.

Herzog, W. (1998). Muscle. In B. M. Nigg & W. Herzog (Eds.), *Biomechanics of the Musculo-skeletal System* (Vol. 2nd, pp. 148-188). West Sussex, UK: John Wiley & Sons Ltd.

Hicks, J. (2012a). How Inverse Dynamics Works. Retrieved 13.09.2015, from http://simtk-confluence.stanford.edu:8080/display/OpenSim/How+Inverse+Dynamics+Works.

Hicks, J. (2012b). Model Editing. *OpenSim Support.* Retrieved 18.08.2015, 2015, from http://simtk-confluence.stanford.edu:8080/x/S4Qz.

Hicks, J. (2013, 22.07.2013). OpenSim's Capabilities. *OpenSim Documentation.* Retrieved 11.02.2015, from http://simtk-confluence.stanford.edu:8080/display/OpenSim/OpenSim%27s+Capabilities.

Hicks, J., & Dembia, C. (2012, 17.07.2013). How Inverse Kinematics Works. *OpenSim Documentation.* Retrieved 11.02.2015, from http://simtk-confluence.stanford.edu:8080/display/OpenSim/How+Inverse+Kinematics+Works.

Hicks, J., & Dembia, C. (2014). How Static Optimisation Works. Retrieved 13.09.2015, from http://simtk-confluence.stanford.edu:8080/display/OpenSim/How+Static+Optimization+Works.

Hicks, J., & Dunne, J. (2012, 14.02.2014). How Scaling Works. *OpenSim Documentation.* Retrieved 08.02.2015, from http://simtk-confluence.stanford.edu:8080/pages/viewinfo.action?pageId=3376178.

Hicks, J., & Uchida, T. (2013a). How CMC Works. Retrieved 15.09.2015, from http://simtk-confluence.stanford.edu:8080/display/OpenSim/How+CMC+Works.

Hicks, J., & Uchida, T. (2013b). How RRA works. Retrieved 14.09.2015, from http://simtk-confluence.stanford.edu:8080/display/OpenSim/How+RRA+Works.

Hicks, J., Uchida, T. K., Seth, A., Rajagopal, A., & Delp, S. L. (2015). Is my model good enough? Best practices for verification and validation of musculoskeletal models and simulations of movement. *J Biomech Eng, 137*(2), 020905. doi: 10.1115/1.4029304

Higgins, J., & Green, S. (2011). *Cochrane Handbook for Systematic Reviews of Interventions* Retrieved from Available from www.cochrane-handbook.org.

Hill, A. V. (1938). The heat of shortening and the dynamic constrants of muscle. *Proceedings of The Royal Society of London. Series B, 76*, 136-195.

Hill, A. V. (1952). The mechanics of active muscle. *Proceedings of the Royal Society of London - Series B, 141*(902), 104-117.

Hof, A. L., Elzinga, H., Grimmius, W., & Halbertsma, J. P. K. (2002). Speed dependence of averaged EMG profiles in walking. *Gait & Posture, 16*, 78-86.

Hof, A. L., & van den Berg, J. (1977). Linearity between the weighted sum of the EMGs of the human triceps surae and the total torque. *Journal of Biomechanics, 10*, 529-539.

Hollands, K. L., Pelton, T. A., Tyson, A. F., Hollands, M. A., & van Vliet, P. M. (2012). interventions for coordination of walking following stroke: systematic review. *Gait & Posture, 35*, 349-359.

Holloway, C. S., Symonds, A., Suzuki, T., Gall, A., Smitham, P., & Taylor, S. (2015). Linking wheelchair kinetics to glenohumeral joint demand during everyday accessibility activities. *Conf Proc IEEE Eng Med Biol Soc*, 2478-2481.

Hoy, M. G., Zajac, F. E., & Gordon, M. E. (1990). A musculoskeletal model of the human lower extremity: the effect of muscle, tendon, and moment arm on the moment.angle relationship of musculotendon actuators at the hip, knee, and ankle. *Journal of Biomechanics, 23*(2), 157-169.

Hug, F., Hodges, P. W., & Tucker, K. (2015). Muscle force cannot be directly inferred from muscle activation: illustrated by the proposed imbalance of force between the vastus medialis and vastus lateralis in people with patellofemoral pain. *J Orthop Sports Phys Ther, 45*(5), 360-365. doi: 10.2519/jospt.2015.5905.

Hughes, V. A., Frontera, W. R., Wood, M., Evans, W. J., Dallal, G. E., Roubenoff, R., & Fiatarone Singh, M. A. (2001). Longitudinal Muscle Strength Changes in Older Adults: Influence of Muscle Mass, Physical Activity, and Health. *Journal of Gerontology, 56A*(5), B209-B217.

Inman, V. (1953). The Pattern of Muscular Activity in the Lower Extremity during Walking: University of California.

Ivanenko, Y., Dominici, N., & Lacquaniti, F. (2007). Development of Independent Walking in Toddlers. *Exercise and Sport Sciences Reviews, 35*(2), 67-73.

Izquierdo, M., Aguado, X., Gonzalez, R. V., López, J. L., & Häkkinen, K. (1999). Maximal and explosive force production capacity and balance performance in men of different ages. *Eur J Appl Physiol, 79*, 260-267.

Johnson, J. C. (1978). Comparison of analysis techniques for electromyographic data. *Aviation Space & Environmental Medicine, 49*, 14-18.

Judge, J. O., Ounpuu, S., & Davis, R. B., 3rd. (1996). Effects of age on the biomechanics and physiology of gait. *Clin Geriatr Med, 12*(4), 659-678.

Kadaba, M. P., Ramakrishnan, H. K., & Wootten, M. E. (1990). Measurement of Lower Extremity Kinematics During Level Walking. *Journal Of Orthopaedic Research, 8*, 383-392.

Kadaba, M. P., Ramakrishnen, H. K., Wootten, J. G., Gainey, J., Gorton, G., & Cochran, G. V. B. (1989). Repeatability of Kinematic, Kinetic, and Electromyographic Data in Normal Adult Gait. *Journal Of Orthopaedic Research, 7*, 849-860.

Kainz, H., Modenese, L., Carty, C., & Lloyd, D. (2014). *Direct kinematics versus inverse kinematics: Kinematic modelling approach alters lower limb joint kinematics, muscle moment arm and muscle-tendon length estimates in children with cerebral palsy.* Paper presented at the Congress of the International Society of Electrophysiology and Kinesiology, Rome, Italy.

Kerrigan, D. C., Todd, M. K., & Della Croce, U. (1998). Gender differences in joint biomechanics during walking - Normative study in young adults. *American Journal of Physical Medicine & Rehabilitation, 77*(1), 2-7. doi: 10.1097/00002060-199801000-00002.

Kirtley, C. (2006). *Clinical gait analysis: theory and practise*: Churchill Livingstone, ELSEVIER.

Kirtley, C., Whittle, M. W., & Jefferson, R. J. (1985). Influence of walking speed on gait parameters. *Journal of Biomedical Engineering, 7*, 282-288.

Knutson, D. (2007). Mechanics of the Musculoskeletal System. In D. Knutson (Ed.), *Fundamentals of Biomechanics* (pp. 69-103). New York, USA: Springer.

Komi, P. V. (1990). Relevance of *in-vivo* force measurements to human biomechanics. *Journal of Biomechanics, 23 (Suppl. 1)*, 23-34.

Komi, P. V., & Viitasalo, J. T. (1967). Signal characteristics of EMG at different levels of muscle tensions. *Acta Physiol Scand, 96*, 267-276.

Komura, T., & Nagano, A. (2004). Evaluation of the influence of muscle deactivation on other muscles and joints during gait motion. *Journal of Biomechanics, 37*(4), 425-436. doi: 10.1016/j.jbiomech.2003.09.022.

Komura, T., Nagano, A., Leung, H., & Shinagawa, Y. (2005). Simulating pathological gait using the enhanced linear inverted pendulum model. *IEEE Transactions on Biomedical Engineering, 52*(9), 1502-1513.

Koopman, B., Grootenboer, H. J., & de Jongh, H. J. (1995). An inverse dynamics model for the analysis, reconstruction and prediction of bipedal walking. *Journal of Biomechanics, 28*(11), 1369-1376.

Leardini, A., & O'Connor, J. J. (2002). A model for lever-arm length calculation of the flexor and extensor muscles at the ankle. *Gait & Posture, 15*(3), 220.

Leardini, A., Sawacha, Z., Paolini, G., Ingrosso, S., Nativo, R., & Benedetti, M. G. (2007). A new anatomically based protocol for gait analysis in children. *Gait Posture, 26*(4), 560-571. doi: 10.1016/j.gaitpost.2006.12.018.

Lee, S., & Son, J. (Producer). (2010, 07.02.2015). Lee-Son's Toolbox: a Toolbox that Converts VICON Mocap Data into OpenSim Inputs. Retrieved from https://simtk.org/home/lee-son/.

Lee, S. J., & Hidler, J. (2008). Biomechanics of overground vs. treadmill walking in healthy individuals. *J Appl Physiol, 104*, 747-755. doi: 10.1152/japplphysiol.01380.2006.

Lelas, J. L., Merriman, G. J., Riley, P. O., & Kerrigan, D. C. (2003). Predicting peak kinematic and kinetic parameters from gait speed. *Gait & Posture, 17*(2), 106-112. doi: 10.1016/s0966-6362(02)00060-7.

Lerner, Z. F., Board, W. J., & Browning, R. C. (2015). Pediatric obesity and walking duration increase medial tibiofemoral compartment contact forces. *J Orthop Res*. doi: 10.1002/jor.23028.

Lieber, R. L. (2010). *Skeletal Muscle Structure, Function, and Plasticity. The Physiological Basis of Rehabilitation.* (Vol. 3). Philadelphia, USA: Lippincott Williams & Williams.

Lin, Y. C., Dorn, T. W., Schache, A. G., & Pandy, M. G. (2012). Comparison of different methods for estimating muscle forces in human movement. *Proceedings of the Institution of Mechanical Engineers. Part H - Journal of Engineering in Medicine, 226*(2), 103-112.

Lippold, O. C. J. (1952). The relation between integrated action potentials in a human muscle and its isometric tension. *Journal of Physiology, 117*, 492-499.

Liu, J., & Lockhart, T. (2006). Comparison of 3D joint moments using local and global inverse dynamics approaches among three different age groups. *Gait and Posture, 23*(4), 480-485.

Liu, M. Q., Anderson, F. C., Pandy, M. G., & Delp, S. L. (2006). Muscles that support the body also modulate forward progression during walking. *Journal of Biomechanics, 39*(14), 2623-2630. doi: 10.1016/j.jbiomech.2005.08.017.

Liu, M. Q., Anderson, F. C., Schwartz, M. H., & Delp, S. L. (2008). Muscle contributions to support and progression over a range of walking speeds. *Journal of Biomechanics, 41*(15), 3243-3252. doi: 10.1016/j.jbiomech.2008.07.031.

Lloyd, D. G., & Besier, T. F. (2003). An EMG-driven musculoskeletal model to estimate muscle forces and knee joint moments in vivo. *J Biomech, 36*(6), 765-776. doi: 10.1016/s0021-9290(03)00010-1.

Lund, K., & Hicks, J. (2013). Getting Started with RRA. Retrieved 09.10.2015, from http://simtk-confluence.stanford.edu:8080/display/OpenSim/Getting+Started+with+RRA.

MacIntosh, B. J., Gardiner, P. F., & MacComas, A. J. (2006). *Skeletal Muslce: Form and Function* (2nd ed.): Human Kinetics.

Mahlknecht, P., Kiechl, S., Bloem, B. R., Willeit, J., Scherfler, C., Gasperi, A., . . . Seppi, K. (2013). Prevalence and burden of gait disorders in elderly men and women aged 60-97 years: a population-based study. *PLoS One, 8*(7), e69627. doi: 10.1371/journal.pone.0069627.

McConville, J., Clauser, C., Churchill, T., Cuzzi, J. R., & Kaleps, I. (1980). Anthropometric relationships of bod yand body segment moments of inertia. Wright-Patterson AFB, Ohio: Air Force Aerospace Medical Research Laboratory.

McGinley, J. L., Baker, R., Wolfe, R., & Morris, M. E. (2009). The reliability of the three-dimensional kinematic gait measurements: A systematic review. *Gait & Posture, 29*, 360-369.

McGinley, J. L., Wolfe, R., Morris, M., Pandy, M., & Baker, R. (2014). Variability of Walking in Able-Bodied Adults Across Different Time Intervals. *Journal of Physical Medicine and Rehabilitation Sciences, 17*, 6-10.

Merletti, R., & Hermens, H. (2000). Introduction to the special issue on the SENIAM European Concerted Action. *Journal of Electromyography and Kinesiology, 10*(5), 283-286.

Miller Buffinton, C., Buffinton, E. M., Bieryla, K. A., & Pratt, J. E. (2016). Biomechanics of Step Initiation After Balance Recovery With Implications for Humanoid Robot Locomotion. *Journal of Biomechanical Engineering, 138*(3).

Monaco, V., Coscia, M., & Micera, S. (2011). Cost function tuning improves muscle force estimation computed by static optimization during walking *33rd Annual International Conference of the IEEE EMBS*, 8263 - 8266.

Murray, M. P., Drought, A. B., & Kory, R. C. (1964). Walking Patterns of Normal Men. *Journal of Bone and Joint Surgery, 46A*, 335-360.

Muybridge, E. (1907). *The Human Figure In Motion 1907* (third ed. Vol. 3rd impression): Chapman and Hall.

Nene, A., Byrne, C., & Hermens, H. (2004). Is rectus femoris really a part of quadriceps?: Assessment of rectus femoris function during gait in able-bodied adults. *Gait & Posture, 20*(1), 1-13. doi: 10.1016/s0966-6362(03)00074-2.

Neptune, R. R., & Hull, M. L. (1999). A theoretical analysis of preferred pedaling rate selection in endurance cycling. *Journal of Biomechanics, 32*, 409-415.

Neptune, R. R., Kautz, S. A., & Zajac, F. E. (2001). Contributions of the individual ankle plantar flexors to support, forward progression and swing initiation during walking. *Journal of Biomechanics, 34*, 1387-1398.

Neptune, R. R., Sasaki, K., & Kautz, S. A. (2008). The effect of walking speed on muscle function and mechanical erergetics. *Gait & Posture, 28*, 135-143.

Nisell, R., Németh, G., & Ohlsén, H. (1986). Joint forces in extension of the knee. Analysis of a mechanical model. *Acta Orthop Scand, 57*, 41-46.

Nordez, A., Gallot, T., Catheline, S., Guével, A., Cornu, C., & Hug, F. (2009). Electromechanical delay revised using very high frame rate ultrasound. *J Appl Physiol, 106*, 1970-1975. doi: 10.1152/japplphysiol.00221.2009.

Oggero, E., Pagnacco, G., Morr, D., Simon, S., & Berme, N. (1998). PProbability od valid gait data acquisition using currently available force plates. *Biomedical Sciences Instrumentation, 34*, 392-397.

OpenSim. (2013, 24th of July, 2013). OpenSim Support. 2013, from http://simtk-confluence.stanford.edu:8080/display/OpenSim/OpenSim+Support.

Pandy, M. G., & Andriacchi, T. P. (2010). Muscle and Joint Function in Human Locomotion. In M. L. Yarmush, J. S. Duncan & M. L. Gray (Eds.), *Annual review of biomedical engineering* (Vol. 12, pp. 401-433).

Pandy, M. G., & Berme, N. (1988a). A numerical method for simulating the dynamics of human walking. *Journal of Biomechancis, 21*(12), 1043-1051.

Pandy, M. G., & Berme, N. (1988b). Synthesis of human walking: a planar model for single support. *Journal of Biomechanics, 21*(12), 1053-1060.

Pandy, M. G., Zajac, F. E., Sim, E., & Levine, W. S. (1990). An optimal control model for maximum-height human jumping. *Journal of Biomechanics, 23*(12), 1185-1198.

Passmore, E., & Sangeux, M. (2014). Improving repeatability of setting volume origin and coordinate system for 3D gait analysis. *Gait Posture, 39*(2), 831-833. doi: 10.1016/j.gaitpost.2013.11.002

Perry, J. (1992). *Gait nalysis: Normal and Pathological Function*. Thorofare, NJ: SLACK Incorporated.

Perry, J., & Burnfield, J. M. (2010). *Gait Analysis: Normal and Pathological Function. 2nd edition*: SLACK incorporated.

Peters, A., Galna, B., Sangeux, M., Morris, M., & Baker, R. (2010). Quantification of soft tissue artifact in lower limb human motion analysis: A systematic review. *Gait & Posture, 31*, 1-8.

Piazza, S., & Delp, S. L. (1996). The influence of muscles on the knee flexion during the swing phase of gait. *Journal of Biomechanics, 29*(6), 723-733.

Pinzone, O., Schwartz, M. H., & Baker, R. (2016). Comprehensive non-dimensional normalization of gait data. *Gait & Posture, 44*, 68-73. doi: 10.1016/j.gaitpost.2015.11.013.

Prince, F., Corriveau, H., Hébert, R., & Winter, D. A. (1997). Gait in elderly. *Gait and Posture, 5*, 128-135.

Rabuffetti, M., & Crenna, P. (2004). A modular protocol for the analysis of movement in children. *Gait & Posture ESMAC Abstracts 2004, 20S*, S61-S112.

Rampichini, S., Ce, E., Limonta, E., & Esposito, F. (2013). Effects of fatigue on the electromechanical delay components in gastrocnemius medialis muscle. *Eur J Appl Physiol*. doi: 10.1007/s00421-013-2790-9.

Rao, G., Amarantini, D., Berton, E., & Favier, D. (2006). Influence of body segments' parameters estimation models on inverse dynamics solutions during gait. *Journal of Biomechanics, 39*(8), 1531-1536.

Ren, L., Jones, R. K., & Howard, D. (2008). Whole body inverse dynamics over a complete gait cycle based only on measured kinematics. *J Biomech, 41*(12), 2750-2759. doi: 10.1016/j.jbiomech.2008.06.001.

Ridgewell, E., Dobson, F., Bach, T. M., & Baker, R. (2010). A systematic review to determine best practice reporting guidelines for AFO interventions in studies involving children with cerebral palsy. *Prothetics and Orthotics International, 34*(2), 129-145.

Rodrigo, S. E., Ambrósio, J. A. C., Tavares da Silva, M. P., & Penisi, O. H. (2008). Analysis of Human Gait Based on Multibody Formulations and Optimization Tools. *Mechanics Based Design of Structures and Machines, 36*(4), 446-477. doi: 10.1080/15397730802425497.

Sartori, M., Reggiani, M., Farina, D., & Lloyd, D. G. (2012). EMG-driven forward-dynamic estimation of muscle force and joint moment about multiple degrees of freedom in the human lower extremity. *PLoS One, 7*(12), e52618. doi: 10.1371/journal.pone.0052618.

Schache, A. G., Baker, R., & Vaughan, C. L. (2007). Differences in lower limb transverse plane joint moments during gait when expressed in two alternative reference frames. *J Biomech, 40*(1), 9-19. doi: 10.1016/j.jbiomech.2005.12.003.

Schuenke, M., Schulte, E., Ross, L. M., Schumacher, U., & Lamperti, E. D. (2006). *Atlas of Anatomy: General Anatomy and Musculosceletal System*. Stuttgart: Georg Thieme Verlag.

Schwartz, M. H., Rozumalski, A., & Trost, J. P. (2008). The effect of walking speed on the gait of typically developing children. *Journal of Biomechanics, 41*, 1639-1650.

Schwartz, M. H., Trost, J. P., & Wervey, R. A. (2004). Measurement and management of errors in quantitative gait data. *Gait Posture, 20*(2), 196-203. doi: 10.1016/j.gaitpost.2003.09.011.

Seireg, A., & Arvikar, R. J. (1973). A mathematical model for evaluation of forces in lower extremities of the musculo-skeletal system. *Journal of Biomechanics, 6*, 313-326.

Seth, A., & Pandy, M. G. (2007). A neuromusculoskeletal tracking method for estimating individual muscle forces in human movement. *Journal of Biomechanics, 40*, 356-366.

Shewman, T., & Konrad, P. (2011). *Surface Electromyography (SEMG). Clinical Sequence assessments and SEMG feedback: A Beginner's Guide*. Scottsdale, Arizona USA: Noraxon U.S.A.

Silva, M. P. T., & Ambrosio, J. A. C. (2003). Solution of redundant muscle forces,in human locomotion with multibody dynamics and optimization tools. *Mechanics Based Design of Structures and Machines, 31*(3), 381-411. doi: 10.1081/sme-120022856.

Sinclair, J., Taylor, P. J., & Hobbs, S. J. (2013). Digital filtering of three-dimensional lower extremity kinematics: an assessment. *J Hum Kinet, 39*, 25-36. doi: 10.2478/hukin-2013-0065.

Skalshoi, O., Iversen, C. H., Nielsen, D. B., Jacobsen, J., Mechlenburg, I., Soballe, K., & Sorensen, H. (2015). Walking patterns and hip contact forces in patients with hip dysplasia. *Gait Posture, 42*(4), 529-533. doi: 10.1016/j.gaitpost.2015.08.008.

Soderberg, G. L., & Cook, T. M. (1984). Electromyography in Biomechanics. *Physical Therapy, 64*, 1813-1820.

Spector, S. A., Gardiner, P. F., Zernicke, R. F., Roy, R. R., & Edgerton, V. R. (1980). Muscle Architecture and Force-Velocity Characteristics of Cat Soleus and Medial Gastrocnemius: Implications for Motor Control. *Journal of Neurophysiology, 44*(5), 951-960.

Sutherland, D. H. (1978). Gait analysis in cerebral palsy. *Dev Med Child Neurol, 20*(6), 807-813.

Sutherland, D. H. (2001). The evolution of clinical gait analysis part l: kinesiological EMG. *Gait & Posture, 14*(1), 61-70. doi: 10.1016/S0966-6362(01)00100-X.

Szczerbik, E., & Kalinowska, M. (2011). The influence of knee marker placement error on evaluation of gait kinemaitc parameters. *Acta of BIomengineering and Biomechanics, 13*(3), 43-46.

Thacker, B. H. (2001). ASME Standards Comittee on Verification and Validation in Computational Solid Mechanisms *Technical Report*: ASME Council on Codes and Standards.

Thelen, D. G. (2003). Adjustment of Muscle Mechanics Model Parameters to Simulate Dynamic Contractions in Older Adults. *Journal of Biomechanical Engineering, 125*(1), 70. doi: 10.1115/1.1531112.

Thelen, D. G., Anderson, A. E., & Delp, S. L. (2003). Gererating dynamic simulations of movement using computed muscle control. *Journal of Biomechanics, 36*, 321-328.

Thelen, D. G., & Anderson, F. C. (2006). Using computed muscle control to generate forward dynamic simulations of human walking from experimental data. *J Biomech, 39*(6), 1107-1115. doi: 10.1016/j.jbiomech.2005.02.010.

Thelen, D. G., Chumanov, E. S., Hoerth, D. M., Best, T. M., Swanson, S. C., Li, L. I., . . . Heiderscheit, B. C. (2005). Hamstring Muscle Kinematics during Treadmill Sprinting. *Medicine & Science in Sports & Exercise, 37*(1), 108-114. doi: 10.1249/01.mss.0000150078.79120.c8.

Umberger, B. R. (2008). Effects of suppressing arm swing on kinematics, kinetics, and energetics of human walking. *J Biomech, 41*(11), 2575-2580. doi: 10.1016/j.jbiomech.2008.05.024.

van den Bogert, A. J., & De Koning, J. J. (1996). *On optimal filtering for inverse dynamics analysis*. Paper presented at the Proceedings of the IXth Biennial Conference of the Canadian Society for Biomechanics, Vancouver.

Vaughan, C., Davis, B., & O'Connor, J. (1992). *Dynamic of Human Gait.* . Champaign, Illinois: Human Kinetics Publishers.

Vaughan, C., Davis, B. L., & O'Connor, J. C. (1999). *Dynamics of Human Gait. Second edition*. Howard Place: Kiboho Publisher.

Verghese, J., LeValley, A., Hall, C. B., Katz, M. J., Ambrose, A. F., & Lipton, R. B. (2006). Epidemiology of Gait Disorders in Communitx-Residing Older Adults. *J Am Geriatric Soc, 54*(2), 255-261.

Verniba, D., Vergara, M. E., & Gage, W. H. (2015). Force plate targeting has no effect on spatiotemporal gait measures and their variability in young and healthy population. *Gait Posture, 41*(2), 551-556. doi: 10.1016/j.gaitpost.2014.12.015.

White, S. C., & Winter, D. A. (1993). Predicting Muscle Forces in Gait from EMG Signals and Musculotendon Kinematics. *Journal of Electromyography and Kinesiology, 2*(4), 217-231.

Whittle, M. W. (2001). *Gait analysis: an introduction* (3 ed.): Butterworth-Heinemann.

Wickiewicz, T. L., Roy, R. R., Powell, P. L., & Edgerton, V. R. (1983). Muscle architecture of the human lower limb. *Clin Orthop Relat Res, 179*, 275-283.

Winter, D. A. (1990). *The Biomechanics and Motor Control of Human Gait: Normal, Elderly and Pathological*: Waterloo Biomechanics.

Winter, D. A. (2009). Biomechanics and motor contral of human movement. 4th edition.

Winter, D. A., Patla, A. E., Frank, J. S., & Walt, S. E. (1990). Biomechanical walking pattern changes in the fit and healthy elderly. *Physical Therapy, 70*, 340-347.

Woods, J. J., & Bigland Ritchie, B. (1983). Linear and nonlinear surface EMF/ force relationships in human muscles: an anatomical/ functional argument for the existence of both. *American Journal of Physical Medicine, 62*, 287-299.

Woolf, A. D., Erwin, J., & March, L. (2012). The need to address the burden of musculoskeletal conditions. *Best Pract Res Clin Rheumatol, 26*(2), 183-224. doi: 10.1016/j.berh.2012.03.005.

Xu, H., Merryweather, A., Bloswick, D., Mao, Q., & Wang, T. (2015). The effect of toe marker placement error on joint kinematics and muscle forces using OpenSim gait simulation. *Biomed Mater Eng, 26 Suppl 1*, S685-691. doi: 10.3233/BME-151360.

Yamaguchi, G. T., & Zajac, F. E. (1989). A planar model of the knee joint to characterize the knee extensor mechanism. *Journal of Biomechanics, 22*(1), 1-10.

Yavuz, S. U., Sendemir-Urkmez, A., & Turker, K. S. (2010). Effect of gender, age, fatigue and contraction level on electromechanical delay. *Clin Neurophysiol, 121*(10), 1700-1706. doi: 10.1016/j.clinph.2009.10.039.

Zajac, F. E. (1989). Muscle and Tendon: Properties, Models, Scaling, and Application to Biomechanics and Motor Control. *Critical Reviews in Biotechnology, 17*, 359-411.

Zatsiorsky, V., Seluyanov, V., & Chugunova, L. (1990). Methonds of determining mass-inertia characteristics of human body segments. In G. Chernyi & S. Regirer (Eds.), *Contemporary Problems of Biomechanics* (pp. 272-291). Massachusetts: CRC Press.